Characterisation of the highly conserved CutRS two-component system in *Streptomyces* spp.

Thomas Cameron McLean

A thesis submitted in fulfilment of the requirements for the degree of

Doctor of Philosophy at the University of East Anglia

John Innes Centre

Department of Molecular Microbiology

&

University of East Anglia

School of Biological Sciences

September 2021

Abstract

Streptomyces spp. are filamentous Actinobacteria with the propensity to produce a wide range of specialised metabolites. Many of our current therapeutics originate from these bacteria but their effectiveness is dwindling due to antimicrobial resistance. The biosynthesis of specialised metabolites by streptomycetes is intimately linked to the extracellular environment, detected through stimulus-response mechanisms such as two-component systems (TCS). These systems consist of a membrane-bound sensor kinase (SK) and partner DNA-binding response regulator (RR), and they enable detection of, and response to, a multitude of signals. Previously to this work we identified 15 highly conserved TCS in the genus *Streptomyces*, including the first TCS ever described in *Streptomyces* spp., CutRS. During this work, I characterised CutRS in *S. venezuelae* and *S. coelicolor* using a combination of classical microbiology and cutting-edge molecular techniques. Deletion of the *cutRS* genes results in a distinct developmental phenotype in *S. venezuelae* and the overproduction of specialised metabolites in both species. Using a combination of ChIP-seq, ReDCaT SPR and quantitative proteomics I demonstrate that CutR regulates the expression of two serine protease encoding genes, *htrB* and *htrA3*, and hypothesise that this is in response to secretion stress. Investigation into the SK CutS reveals an unusual extracellular dual cysteine-containing sensory domain which we propose is key to a novel mechanism of signal detection. Furthermore, I describe the development of a novel SPR-based technique which we anticipate will vastly increase the discovery of SK ligands *in vitro*. Overall, this work demonstrates a novel mechanism of TCS signal detection and further expands our understanding of these complex signalling systems and with this we can begin to imitate and subvert these systems for our own benefit. Ultimately, we hope this work enables the discovery of new antimicrobials to combat the threat of global antimicrobial resistance.

This thesis is 314 pages and 79,535 words in length

Publications arising from the work in this thesis

Prudence SMM, Addington E, Castaño-Espriu L, Mark DR, Pintor-Escobar L, Russell AH, **McLean TC** (2020) Advances in actinomycete research: an ActinoBase review of 2019. *Microbiology*. 166(8):683-694

McLean TC, Lo R, Tschowri N, Hoskisson PA, Al Bassam MM, Hutchings MI, Som NF (2019) Sensing and responding to diverse extracellular signals: an updated analysis of the sensor kinases and response regulators of *Streptomyces* species. *Microbiology*. 165(9):929-952

McLean TC, Wilkinson B, Hutchings MI, Devine R (2019) Dissolution of the Disparate: Co-ordinate Regulation in Antibiotic Biosynthesis. *Antibiotics*. 8(2):83

McLean TC (2018) Cover image. *Journal of Bacteriology*. 200(22)

Table of Contents

Acknowledgements

I would like to thank my two supervisors Professor Matt Hutchings and Professor Barrie Wilkinson. I was desperate to work in this lab ever since I started my undergraduate degree, and every day has exceeded my wildest expectations. I will be eternally grateful for the freedom you gave me to explore and experiment whilst pushing me to challenge myself and become a better scientist.

I would also like to thank all the members of the Hutchings lab, both past and present. Dr Nicolle Som first introduced me to the wonderful world of two-component systems whilst Dr Neil Holmes was a fountain of knowledge on all things *Streptomyces* and bagel related. Sam Prudence and Dr Jake Newitt were a source of great happiness, support and also mess, getting soil into places I never thought possible. I would like to take this chance to apologise to Dr Rebecca Devine and Dr Sarah Worsley who endured a never-ending barrage of questions from me and were the most superb scientists I have ever had the pleasure to work with. Whilst Dr Ainsley Beaton has not been in our group for long, she has been essential in continuing the CutRS story and I wish her the best of luck.

I will never forget the members of the Pamela Salter office but in particular Greg Rix for his continued support, both mentally and scientifically, during these past four years. Also thank you to the amazing members of the Wilkinson group who were incredibly welcoming when we moved over to the JIC and have made the past year so enjoyable, despite the pandemic.

I would like to thank the numerous technicians at the JIC who's expertise has proven priceless. These include Dr Gerhard Saalbach and Dr Carlo de Oliveira Martins from the proteomics department, Kim Findlay from the bioimaging department, Dr Govind Chandra for his bioinformatics support and Dr Clare Stevenson and Julia Mundy from the biophysical department.

Thank you also to all the mentors and supporters I have had along the way up to and during my PhD. These include my first lab mentor Dr Liam Sharkey, the amazing Professor Nicole Stonehouse and Dr Morgan Herod and of course Dr Ryan Seipke for getting me interested in *Streptomyces* in the first place and has been a constant source of support these past years.

I would not be where, or who, I am without the help of my beautiful fiancée Stephanie. She has supported my scientific endeavours from the first day we met and followed me around the world on the craziest of adventures. She has been there for me on the toughest of days and helped me achieve things I never thought possible. She is my best friend and role model, and I can't wait to see what the future has in store for us. Thank you to my mother, sister and brother who keep me grounded and have supported me my entire life. Even pursuing a PhD has not been enough in the constant battle that is a healthy sibling rivalry.

Finally, I would like to dedicate this thesis to my father who passed away in 2018. He was a wonderful man who prioritised his children's education over everything else, even in his final days. I am the man I am today because of him and will forever enjoy learning new things just as he did.

This work was supported by the UKRI Biotechnology and Biological Sciences Research Council Norwich Research Park Biosciences Doctoral Training Partnership [Grant number BB/M011216/1]

Chapter 1. Introduction

1.1. A brief history of the genus *Streptomyces*

In 1875 the German biologist Ferdinand Cohn published a treatise in which he described a fascinating microorganism found in an infected human tear duct. Cohn compared it to Hansen's Bacillus*,* the etiological agent of leprosy now called *Mycobacterium leprae,* but far more complex, displaying "thicker thread resembling mycelium" (**Figure 1.1A**). Whilst it appeared fungal in appearance, it was too small to be a true fungus. Despite his best efforts, Cohn was never able to isolate and culture this complex microorganism from the surrounding mass of unicellular bacteria but named it *Streptothrix foersteri* after his medical friend R. Foerster who had given him the original sample. Despite the failure to isolate *S. foersteri* in pure culture, it was not obviously implicated in the infection of the tear duct and is likely to have been on a soil particle blown into the patient's eye. This is believed to be the first description of the soil-living actinomycetes we now term *Streptomyces* (Hopwood, 2007).

Forty one years later, in 1916, the order *Actinomycetales* was officially recognised but disputes over the classification of this group would continue for decades (Hopwood, 2007). It was not until 1943 that Selman Waksman and Arthur Henrici classified the actinomycetes by their ability to form branching cells and divided the genera by the degree of mycelial branching (Waksman and Henrici, 1943). The finalised genera were *Mycobacterium*, *Actinomyces*, *Nocardia*, *Micromonospora* and the group into which Cohn's *Streptothrix* fell (**Figure 1.1B**). This genus was classified by colonies consisting of coherent branching filaments which also produced chains of spores. However, it transpired that Cohn's use of the name *Streptothrix* was invalid, due to its earlier application to a completely different microorganism. Eventually Waksman and Henrici invented a new name for the genus, *Streptomyces* (Hopwood, 2007). The name derived from ancient Greek, *streptos* meaning twisted and *mukēs* for fungus, representing the characteristic appearance of this genus (O'Neill, Summers and Collins, 2015).

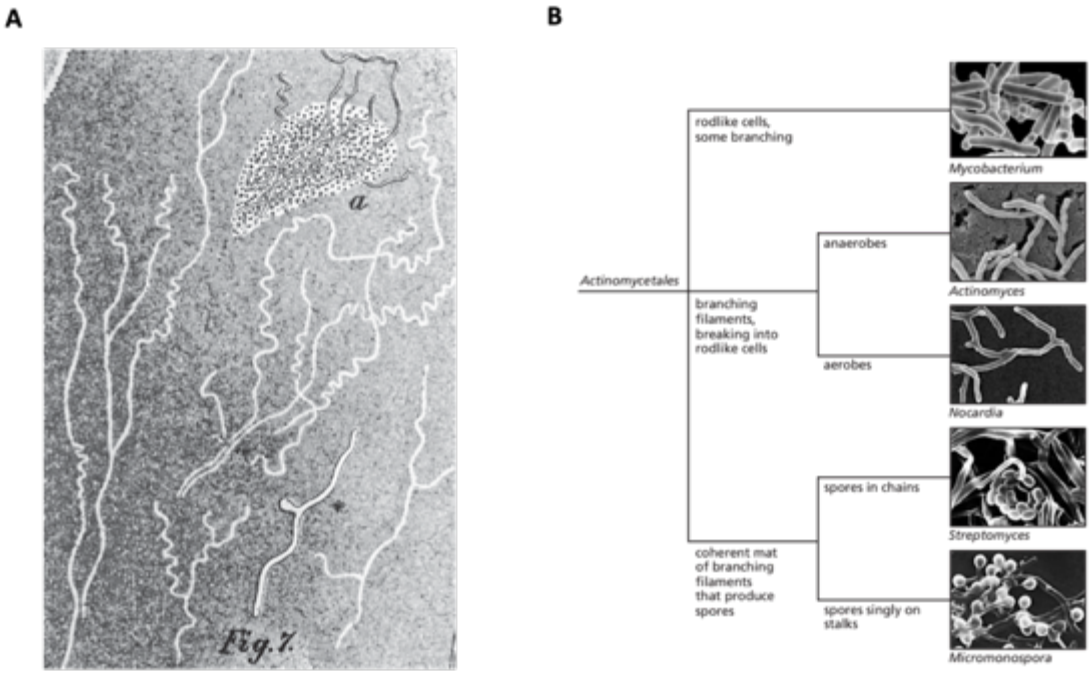

Figure 1.1. A) Ferdinand Cohn's drawings of the filamentous *Streptothrix foersteri* surrounded by unicellular bacteria from 1875. **B)** Classification of actinomycetes by Waksman and Henrici (1943) with modern scanning electron micrographs. Adapted from Hopwood, 2007.

Due to the filamentous nature of actinomycetes, Waksman thought these microbes fell between bacteria and fungi, bridging the evolutionary divide but lacked the instruments and data to definitively prove such a statement (Hopwood, 2007). It would not be until 1957 that the actinomycetes would begin to be classified correctly as bacteria when infections caused by actinomycetes were shown to be susceptible to penicillin. Dr John Harvey and colleagues at The John Hopkins Hospital studied and treated a rare actinomycete-caused infection, termed actinomycosis, and conducted a study on the fate of patients with differing treatments. Before 1945 there was no specific treatment, actinomycosis was tackled as any ordinary pyogenic infection; abscesses were drained surgically and patients treated with thymol, iodides or even irradiated, but with little success (Harvey, Cantrell and Fisher, 1957). Harvey *et al.* reported that of the 21 patients treated pre-1945 only 3 were cured, a survival rate of just 13%. However, since 1945 all patients had received antimicrobial therapy in the form of penicillin followed by surgical excision of infected tissues. Antibiotic treatment markedly increased survival rates, with survival rates rising to 75% post-1945. In their report, Harvey *et al.* described the causative agent as "a gram-positive, branching filamentous microorganism, related more to the true bacteria than to the fungi with which it is often classified.". The infectious bacterium was classified as

Actinomyces israelii and the suggested treatment was chronic penicillin therapy combined with surgical tissue removal (Harvey, Cantrell and Fisher, 1957). The susceptibility of this infectious actinomycete to antibacterial agents was key to the final classification of the *Actinomycetales* within the domain Bacteria. With modern capabilities it is clear that they are prokaryotic; they lack a distinct nucleus and nuclear membrane, encode 16S ribosomal RNA and have a cell wall composed of peptidoglycan rather than fungal chitin.

The order *Actinomycetales* falls within the phylum Actinobacteria, one of the largest phyla within the domain Bacteria (Ludwig *et al.*, 2015). Similar to *Streptomyces*, the name derives from Greek: *mukēs* again for fungus but *aktis* or *aktin* meaning ray due to their filamentous nature and growth via hyphal tip branching and extension. They are Gram-positive bacteria found both terrestrially and aquatically, generally free-living with high guanidine-plus-cytosine (G+C) content genomes (Barka *et al.*, 2015).

Members of the genus *Streptomyces* are ubiquitous in the global environment, and whilst there are exceptions, the vast majority are non-pathogenic to humans (Kapadia, Rolston and Han, 2007). However, it is not because of this rare disease actinomycosis, or their bizarre fungal attributes, that they have become the focus of generations of research. As discussed below, streptomycetes are prodigious producers of specialised metabolites, being responsible for providing around 50% of clinically applicable antibiotics (Hutchings, Truman and Wilkinson, 2019). Whilst Waksman and Henrici could be said to have founded the field of *Streptomyces* research, the vital genetics research underpinning so much contemporary work, was pioneered by Sir David Hopwood and his colleagues at the John Innes Centre (JIC) in Norwich, UK (Chater, 1999). Their work on *Streptomyces coelicolor* A3(2) established it as a model organism and was key to defining many of the paradigms of streptomycete research. Over five decades of work culminated in the publication of the first complete sequence of the 8 megabasepair (Mbp) *S. coelicolor* A3(2) genome (Bentley *et al.*, 2002).

1.2. The new model organism *Streptomyces venezuelae*

Whilst *S. coelicolor* was, and still is, a workhorse of streptomycete research a new model organism, *Streptomyces venezuelae*, has become favoured among laboratories worldwide (McCormick and Flärdh, 2012; Chater, 2016). Morphologically *S. venezuelae* presents as a typical streptomycete with green-pigmented spores and characteristic melanin production. It sporulates rapidly on solid media, within 3 days, and although not unique, it unusually is also able to sporulate in liquid culture (Glazebrook *et al.*, 1990; Bush *et al.*, 2019). Until recently the origin of the *S. venezuelae* type strain NRRL B-65442 was uncertain, but it must have been descended from one of two strains isolated from soil samples collected in the 1940s. The first sample, Burkholder no. A65, was taken from a mulched field near Caracas, Venezuela and the second, Gottlieb no. 8-44, from compost soil at the Illinois Agricultural Experiment Station at Urbana. The type strain, Burkholder no. A65, was proposed to be of a new species and named *Streptomyces venezuelae* due to the location from which it was originally collected (Ehrlich *et al.*, 1948). Recent evidence confirms that the NRRL B-65442 strain is descended from the Caracas strain rather than the Illinois strain. This work also reveals the FAD-dependant monooxygenase point mutation responsible for the green spore pigment seen in NRRL B-65442 contrasting its grey pigmented ancestors (Gomez-Escribano *et al.*, 2021). Both strains were shown to produce chloramphenicol, then known as chloromycetin, a new antibiotic that had been recently isolated from an unknown soil actinomycete isolated from the Caracas soil sample. Chloromycetin was shown to inhibit multiple species of bacteria including *Bacillus subtilis,* and *Brucella abortus* (Ehrlich *et al.*, 1947; Ehrlich *et al.*, 1948). Chloromycetin has since become the trade name of chloramphenicol, and is commonly used as an eye ointment to treat conjunctivitis (Sorsby, Ungar and Crick, 1953). Chloramphenicol is not the only antibiotic *S. venezuelae* is known to produce, it also produces the angucycline polyketide jadomycins when heat shocked or under ethanol stress (Ayer *et al.*, 1991; Doull *et al.*, 1994). Jadomycins are active against both Gram-positive and Gram-negative bacteria and exhibit anti-oncogenic activity (Sharif and O'Doherty, 2012).

As discussed later, most streptomycetes are only able to complete their full life cycle on solid agar media as they are unable to sporulate in liquid culture. *S. venezuelae* can complete its entire life cycle submerged, and this allows this species to be studied in ways others cannot. For example, tissue specific gene expression can only be carried out from liquid cultures as tissue separation (substrate and aerial hyphae and spores) cannot be achieved from agar grown cultures. Many assays are much easier in liquid culture and this not only unlocks a huge number of methodologies but also allows for a significant increase in through-put (McCormick and Flärdh, 2012). Because of its unusual ability to sporulate rapidly and synchronously in liquid, produce easily detectable antibiotics and be genetically tractable with contemporary molecular tools, *S. venezuelae* has become a modern laboratory workhorse, not only for developmental studies but also secondary metabolism and regulatory system research.

1.3. Antibiotics

Humanity has used antibiotics in one form or another to treat disease for millennia. Traces of tetracycline have been found in the bones of Nubian mummies dating back over 2500 years and the Papyrus Ebers was an ancient Egyptian medical document listing medicinal soil and mouldy bread among its remedies (Haas, 1999; Nelson *et al.*, 2010). However, the idea of modern antimicrobial therapy originated in 1900 with Paul Ehrlich, a German Nobel laureate who conceptualised *Zauberkugel*, a magic bullet to kill pathogens without harming the human body. Ehrlich went on to develop the synthetic organoarsenic compound arsphenamine, termed Salvarsan (salvation arsenic) or compound 606 in the 1910s. Salvarsan was the first chemotherapeutic agent, and used to treat syphilis the causative agent of which, *Treponema pallidum*, had been recently described in 1905 (Valent *et al.*, 2016). Another German scientist, Gerhard Domagk, took this idea a step further. Whilst working at Bayer in the 1920s Gerhard discovered the sulfa-drug Prontosil, which he used to save his daughter's arm from bacterial infection (Otten, 1986). The next great leap in antibiotic discovery, and perhaps the most famous, was taken by Alexander Fleming in 1928. When

returning from a holiday during the summer Fleming found a contaminated petri dish on which a fungus was inhibiting the growth of *Staphylococcus* bacteria (Fleming, 1929). With the help of Howard Florey, Ernst Chain and Norman Heatley, Fleming was able to purify the compound penicillin (Abraham *et al.*, 1941). It was later discovered to contain the signature β-lactam ring, when the structure was solved by Dorothy Hodgkin in 1945 (Hodgkin, 1949).

It was really from this point that the discovery of antibiotics exploded, aided by a discovery platform developed by Selman Waksman, who revealed the antimicrobial potential of actinomycetes including *Streptomyces* spp. Famously Waksman's graduate student Albert Schatz discovered the first anti-tuberculosis therapeutic, streptomycin, from *Streptomyces griseus* in 1943 (Schatz, Bugle and Waksman, 1944; Waksman, Schatz and Reynolds, 1946). This was the beginning of an era, during the 1940-60s, termed "The Golden Age of antibiotic discovery" where the majority of our clinical antibiotics were discovered. Over 12,000 antibiotics have been described, falling into 38 classes, with 200-300 discovered per year during the late 1970s (Demain, 2009). However, the increasingly frequent rediscovery of compounds has resulted in the antibiotic discovery and development pipeline "drying up". Since the turn of the millennium only one new class has reached the clinic, the proton pump inhibiting antimycobacterial diarylquinolines (Diacon *et al.*, 2009). This dearth of new bioactive compounds has led to a pressing global threat (Diacon *et al.*, 2009; O'Neill, 2016).

1.3.1 Antimicrobial Resistance

Antibiotics revolutionised the treatment of infectious diseases and during the mid-to-late 20th century were used relentlessly. Considering the plethora of compounds uncovered during this "Golden Age" the soil seemed to be full of antibiotics just waiting to be discovered and the idea of running out of effective antibiotics was generally dismissed. However, even in 1945 Fleming was acutely aware of the dangers of antibiotic misuse and, during his Nobel lecture, warned of the possibility of resistance to penicillin (Fleming, 1945). Whilst this is often thought as a prophetic

statement, Fleming was working off fact. Earlier, in 1942, four clinical strains of *Staphylococcus aureus* were found to resist penicillin therapy. Within 30 years over 80% of community and hospital-acquired *S. aureus* strains were penicillin-resistant (Lobanovska and Pilla, 2017). Penicillin resistance is narrow spectrum, resulting from the production of a plasmid-encoded β-lactamase, penicillinase, and does not inhibit treatment by other β-lactam antibiotics including methicillin (Bush, 2013). However, escalation of treatment resulted in a likewise escalation of resistance. In 1962, just a few years after the introduction of methicillin to the UK, the first case of methicillin-resistant *S. aureus* (MRSA) was reported (Aslam *et al.*, 2018). In comparison to penicillin resistance, methicillin resistance is broad spectrum, inhibiting the action of penicillins, carbapenems and cephalosporins. MRSA produce an altered penicillin-binding-protein (PBP), PBP2a, which is encoded by the plasmid transmissible *mecA* gene and is resistant to methicillin because it is still capable of cross-linking peptidoglycan via transpeptidation (Stapleton and Taylor, 2002). Vancomycin was first introduced in 1958 and initially used to treat enterococcal infections until resistance inevitably occurred (Levine, 2006). In 1972 vancomycin was repurposed as the solution to MRSA, targeting D-Ala-D-Ala peptides during peptidoglycan crosslinking. It was thought no clinical resistance would arise, however in 1997 a strain was reported from Japan displaying reduced vancomycin susceptibility. Since then both vancomycin-intermediate (VISA) and high level vancomycin-resistant *S. aureus* (VRSA) have become increasingly common (Loomba, Taneja and Mishra, 2010).

Penicillin, its use and the resulting resistance, it would transpire, was a microcosm reflecting the global use of antibiotics (**Figure 1.2**). In 2017 the WHO published the "priority pathogens" list. This list categorised pathogens based on the relative need to develop new therapeutics to treat their infections. MRSA, VISA and VRSA were categorised as priority 2, alongside multi-drug resistant (MDR) strains of *Neisseria gonorrhoeae* and vancomycin-resistant *Enterococcus faecium*, among others. Categorised as priority 1, and thus in critical need of research and development of new antibiotics, were carbapenem-resistant strains of *Acinetobacter baumannii, Pseudomonas aeruginosa* and extended spectrum β-lactamase (EBSL)-producing

Enterobacteriaceae (WHO, 2017). Worryingly there have been strains of MDR *P. aeruginosa* discovered that are resistant to almost every known antibiotic (Ventola, 2015).

AMR is not limited to bacteria. The yeast C*andida auris* emerged as an opportunistic human pathogen in Japan in 2009. *C. auris* has often been reported to be resistant to many azole antifungals including fluconazole and amphotericin B and, without early identification, has a high persistence and mortality (Osei Sekyere, 2018). This is particularly worrying as currently there are only three classes of antifungal for systemic fungal infections. New, safe antifungal drugs are notoriously difficult to develop due to the similarities between pathogen and host (Roemer and Krysan, 2014). Likewise there are pressing concerns with antiviral and antiparasitic resistance with examples including acyclovir resistant herpes simplex virus (Burns *et al.*, 1982) and artemisinin resistant *Plasmodium falciparum*, the parasite responsible for malaria (Fairhurst and Dondorp, 2016). A report published by Lord Jim O'Neill in 2016 highlighted the threat AMR poses both now and in the future. The report warned of a post-antibiotic era where common bacterial infections, currently easily treatable, could be untreatable and life-threatening. Beyond this, the scope for mortality could lead to over 10 million deaths per annum by 2050 and create a huge burden on the global economy in excess of 100 trillion USD (O'Neill, 2016). In short, we are in desperate need of new antibiotics to tackle AMR.

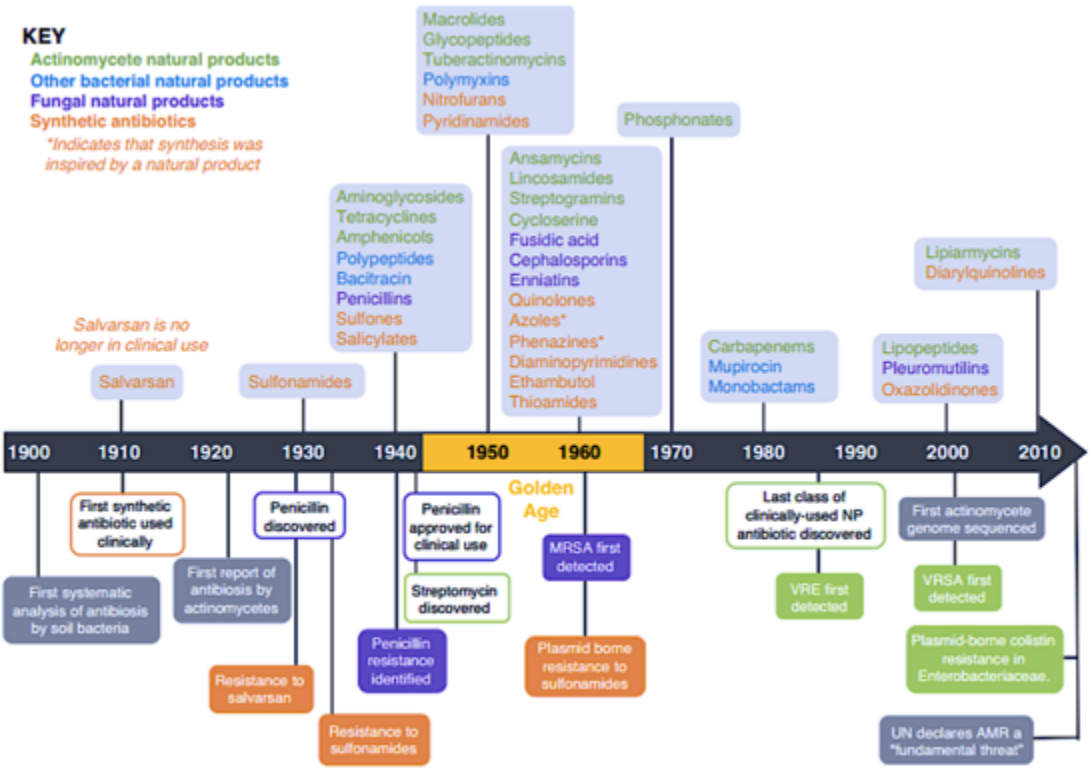

Figure 1.2. Timeline showing the clinical introduction of antibiotics by decade coloured by their source. Green: actinomycete; blue: other bacteria; purple: fungi and orange: synthetic with * indicating that synthesis was natural product inspired. The Golden Age is highlighted in yellow. Beneath the timeline are key dates for antibiotic discovery and resistance identification including the first reports of methicillin-resistance *Staphylococcus aureus* (MRSA), vancomycin-resistant *Enterococcus* (VRE) and plasmid-borne colistin resistance in Enterobacteriaceae. Adapted from Hutchings, Truman and Wilkinson, 2019.

1.3.2 *Streptomyces* and their specialised metabolites

Waksman was well aware that Actinobacteria, and in particular the streptomycetes, are gifted producers of specialised metabolites including antibiotics. Over two-thirds of all known antibiotics have been initially discovered in *Streptomyces* species (Antoraz *et al.*, 2015). In comparison to synthetic antibiotics, the natural products biosynthesised by streptomycetes, and other microbes, are relatively large, highly specialised compounds finely adapted over hundreds of millions of years of evolution (Demain, 2009). There is, and perhaps always will be, conflicting schools of thought to the primary purpose of natural products. Clearly, they play a role in chemical warfare, protecting the producing community from competition, enabling the safe collection of local resources and niche adaptation. However, there is evidence that antibiotics are signal molecules with many acting at sub-MIC levels as transcriptional

modulators (Yim, Huimi Wang and Davies, 2007). The aminoglycosides, for example, induce biofilm formation at sub-MIC levels (Hoffman *et al.*, 2005) whilst sub-MIC rifampicin, an RNA polymerase inhibitor, modulates the transcription of motility and virulence genes in *Salmonella enterica* serovar Typhimurium (Yim *et al.*, 2006). Regardless of the true purpose of antibiotics, the ubiquitous nature of streptomycetes results in continuous, complex interactions with a wide range of competitors and symbionts, microbial or otherwise (Seipke, Kaltenpoth and Hutchings, 2012). This undoubtably requires the production and secretion of a diversity of tailored compounds.

The biosynthesis of these molecules is generally encoded by self-contained biosynthetic gene clusters (BGCs). These can range from huge >100 kilobasepair (kbp) clusters to tiny BGCs of only a few kbp (Bibb, 2005). The distribution and diversity of BGCs is widespread among *Streptomyces* genomes with a weak, but significant, correlation between genome size and BGC prevalence. In a study of 1,110 streptomycete genomes the number of BGCs encoded was found to range anywhere from 8 BGCs (*Streptomyces gilvigriseus* MUSC 26) up to 83 BGCs (*Streptomyces rhizosphaericus*). The mean was ~40 BGCs per genome (s.d. 11.40), although this is likely to slightly overestimate the total number with hybrid BGCs under-represented of their true number within some of the draft genomes included. There are 34 major classes detected to date and within this study the five most prevalent BGC classes found were: non-ribosomal peptide synthetases (NRPS), type 1 polyketide synthases (PKS), terpenes, other ketide synthases and lantipeptides. Overall around half the BGCs identified belong to those five classes (Belknap *et al.*, 2020).

NRPS are large, multi-enzyme complexes that assemble proteins with a vast array of structural and functional diversity. Many clinical antibiotics are biosynthesised by NRPS BGCs. Famously penicillin (**Figure 1.3A**) results from a *Penicillium* spp. NRPS BGC whilst glycopeptides such as vancomycin (**Figure 1.3B**) and teicoplanin are NRPS antibiotics produced by streptomycetes. Assembly is co-ordinated by highly organised complexes controlling the systematic incorporation and modification of amino acids onto a growing peptide chain (Süssmuth and Mainz, 2017).

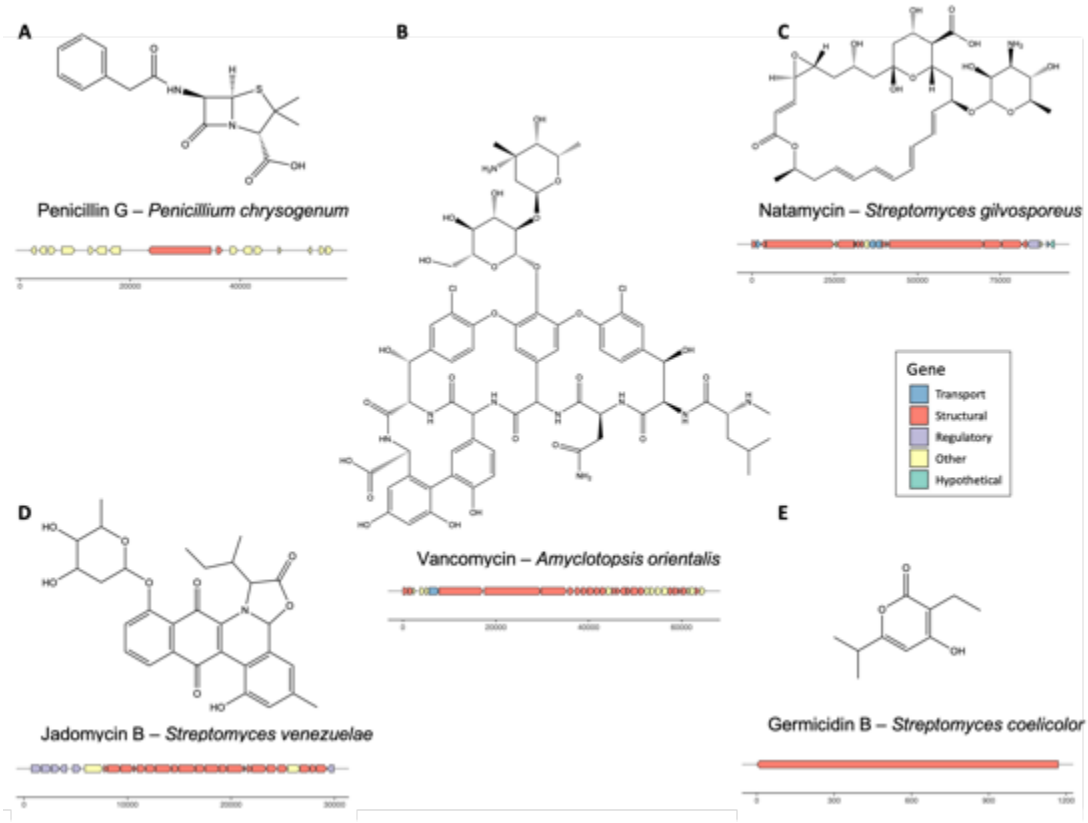

Figure 1.3. Chemical structure, producing organism and schematic representation of the encoding biosynthetic gene cluster (BGC) for: **A)** Penicillin G; **B)** Vancomycin; **C)** Natamycin; **D)** Jadomycin B; **E)** Germicidin B. Roles of BGC genes are colour coded. Blue: transport, red: structural, lilac: regulatory, yellow: other and green: hypothetical.

PKS natural products are assembled in a similarly gradual process however the extender units are organic acids, usually malonyl-CoA, instead of amino acids. These extend from a starter unit by sequential decarboxylation condensation reactions catalysed by the PKS enzymes. A huge range of diversity is generated dependant on the starter and extender units, final chain length and modifications. There are three groups of PKS enzymes, type 1, type 2 and type 3. As previously mentioned, type 1 PKS BGCs are one of the most abundant BGCs in *Streptomyces* spp. being responsible for antibiotics such as the antifungal drug natamycin (**Figure 1.3C**) and anthelmintic avermectins. Type 2 antibiotics include aromatic polyketides such as actinorhodin (ACT) and jadomycin B (**Figure 1.3D**) whilst type 3 includes the germicidins (**Figure 1.3E**) and pyrone-derived spore germination inhibitors (Risdian, Mozef and Wink, 2019).

Despite such an abundance and diversity of BGCs encoded by *Streptomyces* spp., and other actinomycetes, rediscovery is still a huge problem. This is mainly due to two reasons. The first reason is that biochemical structural diversity may be linked to biological habitat diversity (Silver, 2011). Historically the Waksman platform relied on the isolation of actinomycetes from soil, a relatively homogenous environment worldwide (Waksman and Woodruff, 1940). Recent efforts have turned to the isolation of actinomycetes from novel, more specialist niches. These include extreme environments such as the polar regions (Millán-Aguiñaga *et al.*, 2019), hyper-arid deserts (Carro *et al.*, 2019) and higher-organism symbionts (Qin *et al.*, 2017).

The second reason behind rediscovery is that under normal laboratory conditions most clusters remain silent or are only expressed at very low levels. Often very distantly related species will express the same clusters under laboratory conditions despite each harbouring an array of different BGCs (Chen, Wong and Burns, 2019). The expression of silent BGCs has been tackled from a multitude of angles but ultimately there is no universal solution. Common techniques focus on heterologous expression in "superhosts" or *in vivo* manipulation of regulatory elements (Baral, Akhgari and Metsä-Ketelä, 2018). Another technique relies on the intricate link between the expression of specialised metabolites and life cycle progression. Specifically, the transition from vegetative to aerial hyphal growth is when the majority of bioactivity is expressed by the streptomycete colony (Gallagher *et al.*, 2020). Due to this link, there has been considerable efforts made to better understand the complex *Streptomyces* life cycle.

1.4. The *Streptomyces* lifecycle

The classical model of *Streptomyces* development is unusual for bacteria, closer to that of moulds. The life cycle begins with a dormant haploid spore, specialised to survive inhospitable environments until nutrients become available, or dispersal lands the spore in a more favourable niche. Several bacterial clades produce spores to guard their genetic material including other actinomycetes, Bacilli and Clostridia. They are capable of surviving in this state for years even under some of the harshest

conditions (Bobek, Šmídová and Čihák, 2017). Remarkably, bacterial spores have been revived from the abdominal contents of an extinct bee species embedded in 25-40 million year old Dominican amber (Cano and Borucki, 1995) and from within a 250 million year old primary salt crystal (Vreeland, Rosenzweig and Powers, 2000), although there remains some controversy regarding the techniques used within these studies. To protect from abiotic factors such as thermal or osmotic stress, spores feature a thickened cell wall and substitute water for trehalose which stabilises the stored macromolecules pre-synthesised before dormancy. Due to the unique α, α-1,1-glycosidic bonding the trehalose is unreactive making it the perfect protective sugar. It also forms continuous aggregates which congeal under desiccating conditions preventing macromolecule aggregation (Bobek, Šmídová and Čihák, 2017). Whilst dormant, spores are far from inactive. Mature *Streptomyces avermitilis* spores have been shown to maintain energy supplies by oxidising atmospheric H_2 (Liot and Constant, 2016). The *Actinoplanes*, another genus of Actinobacteria, produce motile spores known as zoospores which are capable of chemotaxis-guided swimming via flagella (Palleroni, 1976).

Once a hospitable environment has been encountered germination can occur. Spores contain all the necessary constituents requiring only aqueous conditions, however other stimuli and nutrients accelerate the germination procedure (Hirsch and Ensign, 1976; Paredes-Sabja, Setlow and Sarker, 2011). The formation of germ tubes occurs over a number of hours and varies greatly even within a single population with the rate decreasing in less favourable conditions. However, heat shock, mechanical disruption and the presence of peptidoglycan residues can lead to germination synchronicity (Bobek, Šmídová and Čihák, 2017). Peptidoglycan fragments result from the partial digestion of mature peptidoglycan by hydrolases and amidase during cell growth. Unlike Gram-negatives, Gram-positive bacteria are unable to efficiently recycle these fragments, resulting in the release of peptidoglycan fragments into the surrounding environment (Shah *et al.*, 2008).

Germination occurs in three distinctive steps: darkening, swelling and germ tube emergence. During darkening spores lose their hydrophobic coating, water diffuses in, and metabolism is re-activated. The cells uncoat, using lysozyme-like hydrolases

such as the Rpf proteins to remodel the cell wall, increasing nutrient influx (Bobek, Šmídová and Čihák, 2017). Rpf transglycosylases cleave *N*-acetylglucosamine (GlcNAc) and *N*-acetylmuramic acid (MurNAc) at the β-(1,4)-glycosidic bond. Rpf mutants of *S. coelicolor* result in delayed germination, with germination taking up to 12 hours (Sexton *et al.*, 2015). It is likely that this muralytic system is regulated by Crp, a cAMP-receptor protein. The signal molecule of Crp, cyclic AMP, accumulates during germination and is derived from ATP, a reaction catalysed by the adenylate cyclase Cya. Crp or Cya mutants display dramatic germination defects and it is likely that the Cya-cAMP-Crp system is crucial in the control of cell wall remodelling (Piette *et al.*, 2005).

As the spores continue to swell with the influx of water, the trehalose is hydrolysed resulting in elevated intracellular glucose. This provides the cell with an energy source to power germination. The removal of trehalose also removes its protective properties, allowing stored proteins to refold and the ribosomes to re-activate. Within the first few minutes of germination, translation from stored mRNA commences and proteosynthesis is shortly followed by DNA replication. This is still using the internal energy sources such as trehalose-derived glucose (Bobek, Šmídová and Čihák, 2017).

Finally, one or two germ tubes emerge roughly 3 hours after the initiation of germination, with the site of emergence defined by the localisation of SsgA, a chaperonin-like protein. Primarily the germ tube elongates via apical tip extension, coordinated by DivIVA, FilP and FtsZ (Bobek, Šmídová and Čihák, 2017). DivIVA is essential for polar growth, localising to the hyphal tip and forming a major part of the polarisome to direct polar cell wall synthesis. Similar to eukaryotic intermediate filaments, FilP provides elasticity and rigidity to the hyphae and whilst not essential, mutants present with dysfunctional hyphae (Fröjd and Flärdh, 2019). Finally, FtsZ is the bacterial tubulin homologue required to form the hyphal cross walls (Grantcharova, Lustig and Flärdh, 2005).

As previously mentioned, specialised metabolism generally occurs during the transition from vegetative to aerial growth, however there are some interesting

specialised metabolites produced during germination. These include germination inhibitors such as the germicidins, hypnosin and gramicidine S. These act to control the germination rate when spore densities are high in order to prevent over-depletion of environmental nutrients thus increasing the chances of survival (Bobek, Šmídová and Čihák, 2017). During sporulation various streptomycetes produce antibiotics such as actinorhodin, neomycin or streptomycin (Barabás and Szabó, 1968; Bobek, Šmídová and Čihák, 2017). These bind the spore envelope, clinging to the spore during dispersal before being released upon germination. Once released these antibiotics protect the vulnerable germinating spores before BGCs can be activated. This generally occurs later during development but in *Streptomyces clavuligerus* both cephamycin C and clavulanic acid are produced early after germination (Sánchez and Braña, 1996).

As the germ tube(s) extend they begin to expand, resulting in a mat of vegetative mycelium. The divergence of hyphae requires a change in cell polarity. The coiled-coil DivIVA localises to the lateral cell wall of hyphae and it is from this point that outgrowth occurs (Flärdh and Buttner, 2009). The first stage of this process is the production of primary compartmentalized mycelium (MI). MI septa are curved, bending under osmotic pressure due to thinner cell walls. This substrate mycelium expands into the surrounding environment in the search of nutrients, secreting hydrolytic enzymes to break down polymeric substrates and sequester vital elements such as iron using siderophores.

At this point programmed cell death (PGD) occurs, localised towards the centre of the colony. The surviving MI become multinucleated hyphae (MII) whilst the dead hyphae are recycled. Finally a SapB-chaplin-rodlin layer is produced, covering the MII in a protective hydrophobic layer (Yagüe *et al.*, 2013). SapB is a hydrophobic lantibiotic-like protein that lacks antimicrobial activity and is required for the formation of aerial mycelium under certain conditions. The chaplins are necessary for the construction of the aerial fibrous sheath and provide redundancy when SapB is not produced. Rodlins organise the chaplins into rodlets, structures which give the characteristic pattern present on the surface of aerial hyphae (McCormick and Flärdh, 2012).

Once aerial hyphae are erected, chromosome replication commences creating long 'sporogenic cells' each containing up to 100 chromosome copies (Ruban-Ośmiałowska *et al.*, 2006). This is controlled by AdpA, a developmental regulator whose transcription is repressed by c-di-GMP bound BldD. AdpA can be found in many Gram-positive bacteria including *B. subtilis* where the homologue is named YvcL. AdpA acts to reduce DNA replication by sequestering *oriC* from DnaA, slowing the formation of aerial hyphae. At this point the proteins WhiA and WhiB come into play, cooperatively controlling the transition from aerial hyphae to septation and sporulation. WhiA directly activates sporulation septation proteins including FtsZ, FtsK and FtsW whilst directly repressing transcription of *filP* whose role was mentioned above (Bush *et al.*, 2015). FtsZ is required to form septation rings within the sporogenic cells whilst FtsK is a DNA translocase and FtsW a putative lipid II flippase (Bush *et al.*, 2013). Similarly to *adpA, ftsZ* is repressed by c-di-GMP-BldD. Finally, WhiA activates σ^{WhiG} which in turn activates the transcription of *whiH* and *whiI*. WhiH is a GntR transcription factor and is required for the mass conversion of sporogenic cells into spores (Flärdh, Findlay and Chater, 1999). WhiI is an orphan response regulator, lacking a cognate sensor kinase or indeed the key residues required for phosphorylation to occur (Aínsa, Parry and Chater, 1999). Whilst WhiI is not an active transcriptional regulator as a homodimer it does form a heterodimer with the response regulator BldM and activates a set of genes distinct to the BldM homodimer. These include the *smeA-sffA* operon and the *whiE* locus, all of which are responsible for controlling the later stages of sporulation. The *whiE* locus encodes seven genes required for the biosynthesis of the polyketide spore pigment whilst SmeA is a small membrane protein which targets SffA, a DNA translocase, to sporulation septa (Bush *et al.*, 2015).

Together these septation and sporulation regulators and effectors act to arrange FtsZ in sporogenic hyphae; first into helical filaments, before forming Z rings, directing septation and producing prespores. The ATPase ParA forms helices akin to FtsZ whilst the centromere-binding ParB binds chromosomal *parS* sites clustered around *oriC,* forming nucleoprotein complexes at loci defined by ParA. FtsK is located to sites of septation and ensures separation of chromosomes in the septa. Once septated these

prespores are unigenomic and produce thickened cell walls, requiring MreB, the bacterial actin homologue (Flärdh and Buttner, 2009). Ultimately each aerial hypha can result in chains containing dozens of mature, fully septated and unigenomic spores ready for dispersal into the environment to begin the life cycle once again.

1.5. *Streptomyces* exploration

More recently a new developmental mode of growth was discovered in *Streptomyces venezuelae*, termed 'exploratory growth' after their ability to rapidly transverse both biotic and abiotic surfaces. In contrast to the classical life cycle, exploration is independent of the *bld* or *whi* genes and features some curious hallmarks phenotypically represented as an unstoppable, rapidly expanding, vegetative colony (**Figure 1.4**) (Jones *et al.*, 2017). The exploratory growth of *S. venezuelae* is estimated to be ~90 μm/hour, an order of magnitude faster than regular hyphal tip expansion (Jones and Elliot, 2017). Exploring streptomycetes produce non-branching horizontal hyphae akin to aerial hyphae, spreading rapidly across the media. They display very little sporulation when induced abiotically via glucose depletion or alkaline pH and also have the fascinating ability to induce exploration distally via the microbial volatile organic compound (mVOC) trimethylamine (TMA) (Jones *et al.*, 2017).

Exploration was discovered during the co-culturing of *Streptomyces* species in an effort to better understand the interactions occurring in polymicrobial communities reminiscent of soil ecosystems. Roughly 10% of *Streptomyces* species were shown to display exploratory development when co-cultured with a diversity of yeasts including *Saccharomyces cerevisiae*, *Candida albicans* and *Pichia fermentans*. The model organism *S. venezuelae* was able to explore, as could 19 of 200 wild streptomycete strains tested. Interestingly many of the popular laboratory *Streptomyces* strains were unable to explore including *S. coelicolor*, *S. avermitilis, S. griseus* and *Streptomyces lividans*. Exploratory-capable streptomycetes do not form a monophyletic group suggesting the capacity is wide-spread but uncommon, at least under the tested conditions (Jones *et al.*, 2017).

Whilst a yeast co-culture is capable of triggering exploration, biotic factors are far from necessary. Yeast extract-Peptone-Dextrose (YPD) is a common growth media for the propagation of yeast and used in the original exploration co-culture experiments. However, it is actually the glucose-depletion of YPD media that induces exploratory behaviour in the co-cultured streptomycete. *S. venezuelae* cultured on YP agar (YPD without glucose) exhibits a similar phenotype, with glucose acting as a repressor. Glucose is the preferred carbon source for many bacteria and as such it appears explorative behaviour acts to rapidly divert *Streptomyces* colonies away from areas of glucose depletion in search of richer pastures. Interestingly *S. cerevisiae* strains with disrupted tricarboxylic acid (TCA) cycles are unable to induce exploration despite depleting glucose at rates equivalent to the wild-type strain. In contrast to the wild-type which raises agar pH from 7.0 to 7.5, the mutants lower it to a pH of 5.5. These TCA mutants are all blocked after the production of citrate and it is likely that the yeast is secreting accumulated organic acids into the surrounding environment to avoid an overly acidic intracellular pH (Jones *et al.*, 2017). Whilst an acidic pH does repress exploration, it transpires that highly alkaline conditions are a requirement. During exploration the five gene clusters most highly upregulated in comparison to non-explorers are the ATP synthase complex, two cation/proton complexes and two peptide transporters. Increased proton and peptide uptake are common responses to alkaline stress among bacteria. Another operon, the *cydABCD* operon encoding the cytochrome *bd* oxidase complex, also plays a role in the alkaline stress response. Deletion of *cydABCD* in *S. venezuelae* renders the colony incapable of exploration. This requirement of an alkaline pH suggests that exploration may result from the alkaline stress response and acts as a robust growth strategy under elevated pH (Jones *et al.*, 2017).

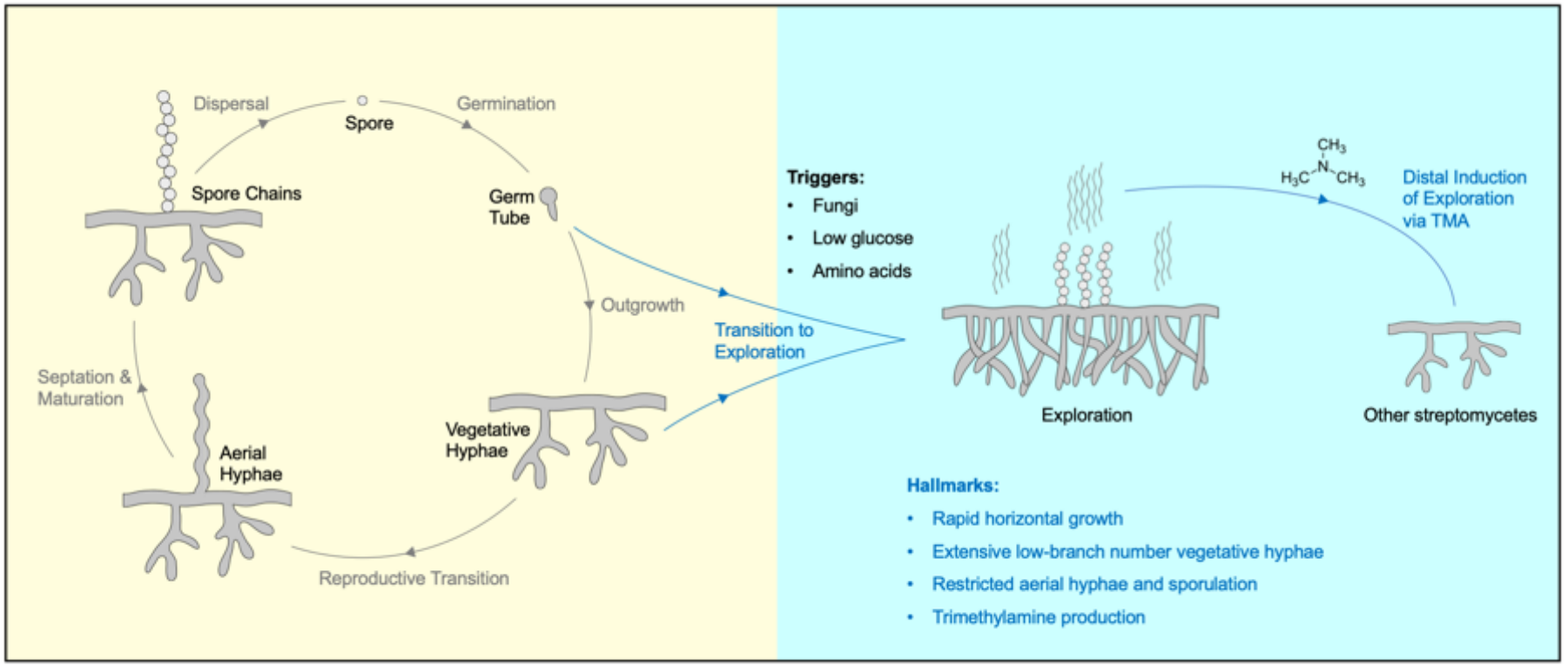

Figure 1.4. Left (yellow) schematically depicts the classical *Streptomyces* life cycle. A spore germinates forming one or two germ tubes eventually growing into vegetative mycelium. Reproductive aerial hyphae are erected which differentiate into chains of equally sized spores. These spores disperse, completing the life cycle. **Right (blue)** schematically depicts *Streptomyces* exploration. At some point early in the life cycle certain species of *Streptomyces* transition from the classical life cycle to exploration upon certain triggers including the presence of certain fungi, the depletion of local glucose or the abundance of certain amino acids. Exploration is hallmarked by certain features such as rapid vegetative growth with long, seldom-branching hyphae; restricted aerial hyphae production and sporulation and the ability to induce exploration in physically disconnected colonies via microbial volatile organic compounds such as trimethylamine.

Another hallmark of exploration is the ability to induce the same developmental phenotype in physically disconnected colonies, even cross-species, via mVOCs. Historically research into volatile organic compound signalling has focussed on interactions between plants and insects but microorganisms can produce a vast plethora of mVOCs and many of these have been implicated in bacterial communication (Schulz-Bohm, Martín-Sánchez and Garbeva, 2017). In *B. subtilis* and *S. aureus* volatile ammonia induces biofilm formation whilst 1-butanol and indole decrease *Escherichia coli* and *P. aeruginosa* motility (Audrain *et al.*, 2015). In streptomycetes, specialised metabolites, such as antibiotics, have long been implicated in signalling but have a short range of interaction (Yim, Huimi Wang and Davies FRS, 2007). Given the homogeny of soil environments mVOCs would be an ideal long-range messenger, capable of diffusing air-filled gaps and rapidly disseminating signals and TMA plays this role in *Streptomyces* exploration (Jones and Elliot, 2017). Almost all exploration-capable streptomycetes have been shown to produce these basic mVOCs during exploration and *S. venezuelae* produces TMA, however the biosynthetic pathway for this highly volatile amine has yet to be confirmed. These mVOCs act to raise the pH of the surrounding environment, inducing exploration via the alkaline stress response previously discussed (Jones *et al.*, 2017).

In addition to signalling, TMA can act offensively, reducing the survival of other microorganisms. Not only does a pH-elevated environment prove inhospitable but it reduces the availability of iron. Ferric iron (Fe^{3+}) is poorly soluble but also the most prevalent form of environmental iron (Ahmed and Holmström, 2014). Bacteria secrete siderophores, high-affinity iron-chelators, to bind and transport ferric iron back into the cytoplasm where the iron is reduced to its soluble ferrous state (Fe^{2+}). However, ferric iron forms a stable complex with hydroxide irons and for each unit the pH rises, iron solubility drops by roughly 1000-fold (Lindsay, 1991). In this way TMA acts to elevate the surrounding pH, reducing iron availability and inhibiting the growth of competing organisms. *Streptomyces* spp. respond when exploring, upregulating putative desferrioxamine transport systems and secreting siderophores (Jones *et al.*, 2019). Whilst many siderophores are biosynthesised by NRPS enzymes,

desferrioxamines are not peptides. Comprised of amide bond-linked alternating diamines and dicarboxylic acids, desferrioxamines belong to a family of nonpeptide hydroxamate siderophores used to treat iron overload in humans (Barona-Gómez *et al.*, 2004).

Beyond the production of iron-chelating agents to combat the reduced iron availability at elevated pH, exploration also acts to expand *Streptomyces* colonies into new regions in search of new iron sources. *S. venezuelae* mutants dysfunctional in ferrioxamine siderophore uptake display increased exploration as does the wild-type cultured on media containing the iron chelator 2,2'-dipyridyl. Low iron availability induces and enhance exploration, but a minimum iron cut-off exists. Deletion of the *desABCD* desferrioxamine gene cluster results in no extra explorative behaviour as the iron uptake likely falls below the cut-off level. Thus, explorer cells produce TMA, raising the pH and reducing iron availability. This in turn leads to increased exploration further raising TMA production and ultimately forming an incessant positive feedback loop, ending only perhaps when regions of irrepressibly low or neutral pH and high glucose concentration are encountered (Jones *et al.*, 2019).

Iron levels activate motility switches in many bacteria. In *P. aeruginosa* iron deficiency triggers motility with the increased production of surfactants and reduced biofilm structuring resulting in movement by sliding (Glick *et al.*, 2010). The production of surfactants in *P. aeruginosa* is partly controlled by the GacAS two-component system (Murray and Kazmierczak, 2008). Many other bacteria also slide, including *Salmonella, Bacillus* and *Mycobacterium* spp., but there is no conserved underlying mechanism (Hölscher and Kovács, 2017). Likewise, it appears that exploration is a form of passive motility similar to surfactant-driven sliding (Jones *et al.*, 2019). *Streptomyces* are known to produce the SapB and chaplin surfactants, and this is controlled by *bld* gene activity (Capstick *et al.*, 2007). However, it is likely alternative surfactants are produced during exploration as the *bld* genes are largely dispensable (Jones *et al.*, 2017).

In summary, *Streptomyces* exploration is a novel developmental phenotype triggered by a range of factors including glucose depletion, the unavailability of iron or an elevated pH. In response, a mass of non-branching vegetative hyphae is rapidly produced as is the mVOC trimethylamine and the colony induces motility akin to sliding. TMA acts to selfishly reduce the bioavailability of iron to inhibit the growth of local microorganisms and induces exploration in distal streptomycete colonies. All this has the ultimate goal of repositioning the bacteria to a more hospitable environment.

1.6. General regulatory mechanisms in *Streptomyces*

Development and the biosynthesis of specialised metabolites, along with a multitude of other bacterial processes, require precise and often complex regulatory control. Transcriptional modulation is the most common form of bacterial regulation with up to 1,101 transcription factors (TFs) predicted in the genome of *Streptomyces bingchenggensis* BCW-1. Of these 691 were transcriptional regulators, 229 were one-component systems, 105 DNA-binding response regulators and 76 sigma factors leaving 13 other DNA-binding proteins. Whilst this is an unusually large number of TFs, *S. avermitilis* and *S. griseus* were predicted to have 688 and 649 TFs respectively (Romero-Rodríguez, Robledo-Casados and Sánchez, 2015). *E. coli,* in comparison, has only 271 identified TFs (Madan Babu and Teichmann, 2003). This regulation occurs as a hierarchy, with high and low-level regulators effecting gene transcription to maintain a finely balanced homeostasis, or effect adjustments required for survival (McLean *et al.*, 2019). Global regulators include the important transcription factors BldD, Crp and the two-component system MtrAB which is discussed below. BldD sits above the rest of the *bld* regulators in the developmental cascade and, during vegetative growth, acts to repress the transcription of ~170 genes involved in sporulation. BldD activity is controlled by binding of the secondary messenger 3',5'-cyclic diguanylic acid (c-di-GMP) (Schumacher *et al.*, 2017). The Cyclic AMP receptor protein, Crp, is conserved among all bacterial phyla, excluding the Firmicutes (Körner, Sofia and Zumft, 2003). In *E. coli* Crp controls the general carbon catabolite repression (CCR) but this does not appear to be its role in *Streptomyces*, where it acts more as a global regulator of development and secondary metabolism (Derouaux *et al.*, 2004; Piette *et al.*, 2005). In *S. coelicolor* Crp not only regulates developmental homeostasis but also controls the biosynthesis of all four hallmark antibiotics: ACT, undecylprodigiosin (RED), calcium-dependent antibiotic (CDA) and yellow-pigmented polyketide (yCPK), in addition to the NRPS gene cluster *SCO6429-38* and the albaflavenone BGC (Gao *et al.*, 2012).

The exemplars of local regulators in *Streptomyces* are the cluster-situated regulators (CSRs). Initially mis-named as cluster-specific regulators these proteins were thought to control only the specific BGC in which they are located. This has since proved

untrue for many, with multiple examples of disparate regulation by CSRs being described in recent publications (McLean *et al.*, 2019). *Streptomyces albidoflavus* S4, isolated from leafcutter ants and previously names *Streptomyces albus* S4, encodes a BGC for the polyene antifungal candicidin which is regulated by four CSRs, FscRI, FscRII, FscRIII and FscRIV (Zhang *et al.*, 2015; Li *et al.*, 2019). These themselves form a fascinating hierarchy within the realm of localised BGC regulation with interconnecting activation and repression between the four regulators (Zhu *et al.*, 2020). The PimM-family PAS-LuxR regulator FscRI has been shown to be essential for the biosynthesis of the antimycins, broad-spectrum depsipeptides which inhibit cytochrome *c* reductase. FscRI activates transcription of part of the antimycin biosynthetic machinery and production of σ^{AntA}, the orphan ECF RNA polymerase sigma factor responsible for transcriptional activation of the remaining *ant* genes (McLean, Hoskisson and Seipke, 2016). Interestingly some two-component systems (TCS) act as CSRs adding a further layer of complexity to the regulation of BGCs. The formicamycin BGC of *Streptomyces formicae* KY5 encodes a TCS, *forGF*. The response regulator (RR) ForF binds within the divergent promoter activating expression of two operons*: forGF* and *forHI*. Both ForH and ForI are important formicamycin biosynthetic enzymes and deletion of *forGF* results in the complete abolishment of formicamycin production (Devine *et al.*, 2021). The activating signal must be intracellular due to the unusual lack of trans-membrane domains in the sensor kinase (SK) ForG (Qin *et al.*, 2017). Similarly, in the actinomycete *Nonomuraea gerenzanensis* the production of a precursor to the glycopeptide antibiotic dalbavancin, named A40926, is encoded by the *dbv* gene cluster. This cluster encodes the TCS Dbv6/22 which acts as a CSR, together directly negatively controlling A40926 production and increasing self-resistance. This system is slightly confusing because deletion of *dbv22* results in overproduction of A40926 and an increase in sensitivity to its own antibiotic (Alduina *et al.*, 2020). The work in this thesis focusses on TCS in *Streptomyces* which are further discussed below.

1.7. Two-component systems

Responding to stimuli or change is one of the seven criteria of life, and many organisms employ TCS as one of their mechanisms to do this (Koshland, 2002; Galperin, 2006). First described in 1986 by Nixon *et al.*, TCS are present throughout the Domains of life but are absent from humans and all other animals (Nixon, Ronson and Ausubel, 1986; Quon, Marczynski and Shapiro, 1996; Stock, Robinson and Goudreau, 2000). Whilst this absence makes them ideal targets for antibiotics, it is their role in stimuli response that has fascinated researchers for decades (Fol *et al.*, 2006). For bacteria, the number of TCS encoded in their genome is generally relative to the range of environments encountered. Intracellular pathogens encode very few TCSs as they inhabit a homeostatic environment whereas, due to their soil and sedimentary habitats, *Streptomyces* encode some of the highest numbers of TCSs found in bacteria (Galperin, 2006; Mclean *et al.*, 2019).

TCS fall into three classes: classical, hybrid and phosphorelay. The classical family consist of a dimeric transmembrane SK that typically senses a signal through binding of a ligand to an extracellular sensor domain. A resulting conformational change activates the intracellular kinase domain resulting in auto-phosphorylation, then the phosphate is transferred to a partner RR, which modulates the expression of target genes to bring about a response to the original signal (**Figure 1.5**) (Groisman, 2016). There are exceptions, for example the TCS ExaDE in *P. aeruginosa* controls expression of the quinoprotein ethanol dehydrogenase but the SK ExaD has no transmembrane domains and is located in the cytoplasm (Schobert and Görisch, 2001). As does the aforementioned ForGF TCS of *S. formicae* KY5. Nitrogen-regulated genes in enteric bacteria are, in part, controlled by the NtrBC two-component system. The NtrB sensor kinase lacks N-terminal transmembrane domains but unusually contains PAS domains instead, which also allow for dimerisation and signal detection (Martínez-Argudo *et al.,* 2002). A study by Ulrich *et al.* (2005) found that it was possible up to 27% of sensor histidine kinases did not contain any transmembrane domains and thus are likely cytoplasmic. In hybrid family TCSs the SK and RR are fused together and bound to the membrane. The final family, the phosphorelay TCSs, features additional phosphotransferases to form a phosphorelay to affect the transfer of the

phosphoryl group from the SK to its partner RR (Groisman, 2016). In addition to this, there are two further branched TCS architectures which can apply to any of the three families: convergent and divergent. Convergence occurs when multiple SKs modulate a single partner RR, as is discussed below about the AbrC1/2/3 TCSs (Rodríguez *et al.*, 2015). This allows a single RR to respond to multiple input signals. The opposite, whereby a single SK has multiple partner RRs, is defined as a divergent pathway and can generate a complexity of outputs through modulating the phosphorylation state of the RRs in response to a single signal (Groisman, 2016). This is the case in *E. coli* where the SK ArcB not only phosphorylates the partner RR ArcA but also the σ^S proteolytic targeting factor RssB, co-ordinating the synthesis and degradation of the general stress σ factor σ^S (Mika and Hengge, 2005).

A recent analysis of 93 high quality *Streptomyces* genomes identified 15 TCSs as being highly conserved throughout the genus. Below is an outline of the current knowledge of these 15 TCSs, excluding *vnz_07060/07065, vnz_08930/08935* and *vnz_24545/24550* (Mclean *et al.*, 2019). It is known that in *S. coelicolor* the homologues of the *vnz_07060/07065* TCS are upregulated in liquid culture and that *vnz_08930/08935* is not involved in antibiotic production (Yepes *et al.*, 2011; Yagüe *et al.*, 2014). Beyond this there has been no significant research, no name yet given to these systems and no characterised homologues from other species (Mclean *et al.*, 2019).

However, there are some slightly more specialist TCSs worth noting. The VanRS system detects the glycopeptide antibiotic vancomycin and induces expression of the *van* (vancomycin) resistance gene cluster (Hutchings, Hong and Buttner, 2006). Another TCS, which responds to cell wall damage, is the CseBC system. In *S. coelicolor* CseBC controls the expression of σ^E, with null mutants of either *cseBC* or *sigE* proving more susceptible to cell wall lytic enzymes (Paget *et al.*, 1999; Hong, Paget and Buttner, 2002; Tran *et al.*, 2019). Whilst the orphan RRs BldM and WhiI have already been mentioned, orphan SKs also play interesting roles in *Streptomyces* regulation. The OhkA orphan sensor kinase contains no transmembrane domains so is likely cytoplasmic sensing and is involved in late development and repression of ACT and CDA production in *S. coelicolor* (Lu *et al.*, 2011). It should be of no surprise that any

TCSs regulate development and secondary metabolism in streptomycetes but given the abundance of TCSs encoded it is curious that outcomes so often overlap with one another.

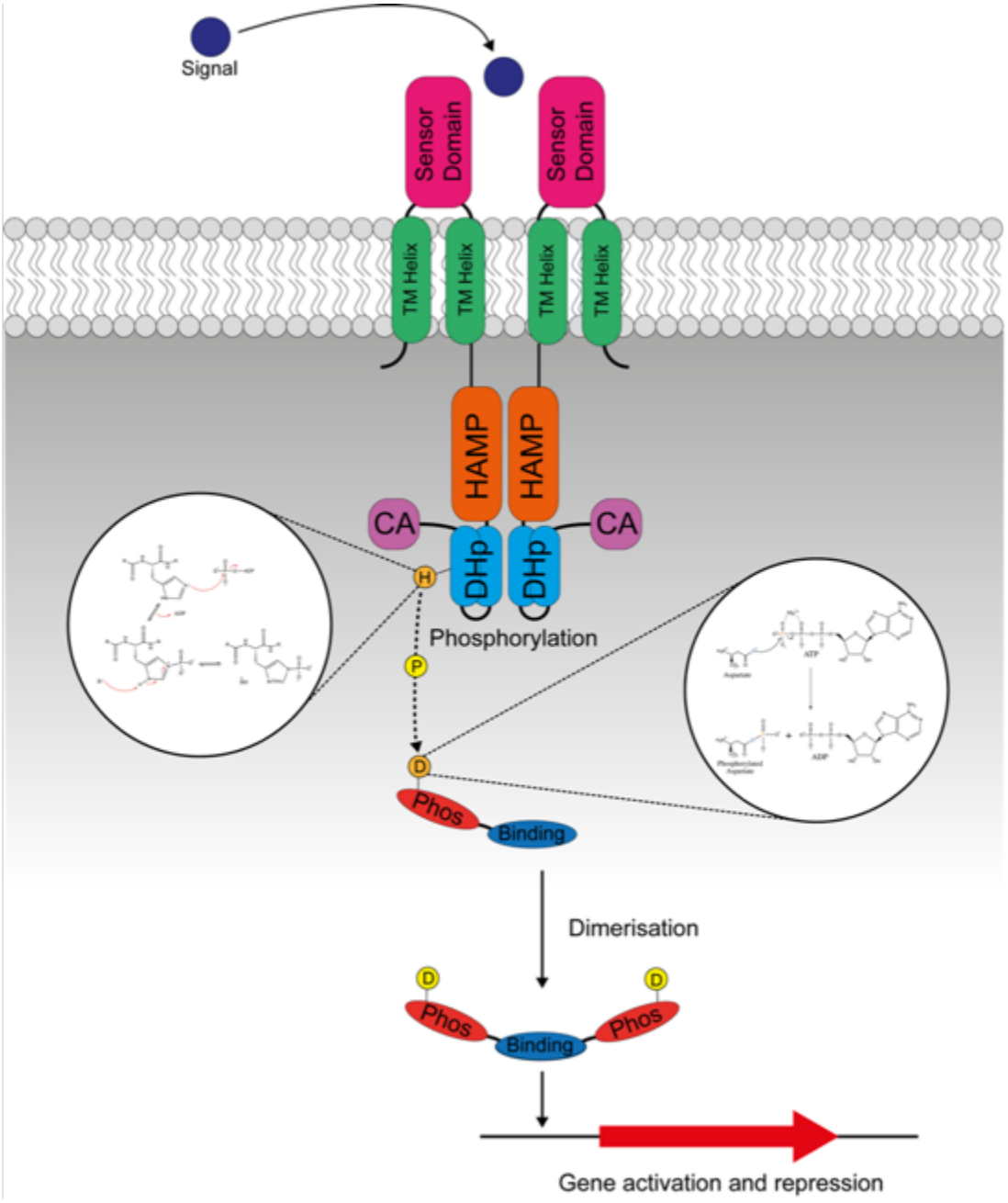

Figure 1.5. Diagrammatic representation of a two-component system. A homodimeric membrane-bound sensor kinase (SK) complex is activated by a signal. This causes a conformational change which is transduced through the SK via the HAMP domain resulting in the transfer of a phosphoryl group from the bound ATP substrate to the DHp-domain conserved histidine residue, a reaction catalysed by the catalytic/ATP-binding domain (CA). Kinase activity then transfers this phosphate from the SK to the conserved aspartate residue of the partner response regulator (RR) leading to homodimerization. Subsequently, the dimerised RR can bind DNA and affect gene activation or repression. Adapted from Mclean *et al.*, 2019**.**

1.7.1 Highly conserved two-component systems

1.7.1.1 MacRS

Transposon mutagenesis in *S. coelicolor* first uncovered the function of the TCS MacRS (SCO2120/21) with a *macRS* mutant strain showing enhanced aerial mycelium formation and inhibition of ACT biosynthesis (Xu *et al.*, 2017). Further studies by Lui *et al.* with the *S. coelicolor* Δ*macRS* strain led to the discovery that the NarL-type RR MacR modulates the transcription of genes, including *mmpABC*, encoding for six putative membrane proteins. MmpABC are novel morphogenic factors, as indicated by the fact that deletion of their coding genes leads to accelerated early aerial mycelium formation. The most substantial effect was seen in the Δ*mmpA* strain, reducing the onset of aerial hyphae from 60 hours in the wild-type to just 36 hours in the mutant. Comprehensive *in vivo, in vitro* and *in silico* analysis defined the MacR regulon but there was no evidence of any regulation of the ACT BGC. The reduction in ACT production in the Δ*macRS* strain is likely to be the result of indirect regulation by MacR. To highlight the conservation of MacRS, successful complementation of the *S. coelicolor* Δ*macRS* strain was achieved using homologues from several *Streptomyces* species including *S. venezuelae* and *S. avermitilis*. The activating signal of MacRS is still unknown although the six TM domains of MacS combined with the regulation of numerous membrane-associated proteins would suggest this TCS plays a role the detection and response to membrane disruption, perhaps during development and may interact with other TM proteins within the membrane (Liu *et al.*, 2019).

1.7.1.2 MtrAB

The MtrAB TCS (MtrA – RR, MtrB – SK) has been well-characterised in many members of the Actinobacteria phylum including the families Mycobacteriaceae, Corynebacteriaceae and Streptomycetaceae. Whilst essential in the facultative intracellular pathogen *Mycobacterium tuberculosis,* MtrAB has not proven indispensable to any other mycobacteria, streptomycetes or *Corynebacterium glutamicum* (Zahrt and Deretic, 2000; Möker *et al.*, 2004; Brocker and Bott, 2006). The name originates from *M. tuberculosis* regulator A, and in *M. tuberculosis* MtrA regulates expression of genes vital for DNA replication including the DNA replication

initiator *dnaA* and the DNA polymerase III stabilising protein *dnaN*. MtrA also binds and sequesters the chromosomal origin of DNA replication, *oriC.* After DNA replication, phosphorylated MtrA directly interacts with DnaA and this complex may instigate *oriC* sequestration, preventing unwarranted DNA replication (Purushotham *et al.*, 2015).

In *Streptomyces* species, MtrA is a regulator of development and antibiotic production. Deletion of *mtrA* in *S. venezuelae*, *S. coelicolor* and *S. lividans* leads to a media-dependant conditional bald phenotype, similar to that of *bld* or *sapB* mutants (Zhang *et al.*, 2017). *S. coelicolor* MtrA plays a role in nutrient uptake, regulating sterol uptake via Mce proteins. This system is important during the colonisation of plant roots with the rhizosphere being rich in steroid alcohols (Clark *et al.*, 2013). *S. venezuelae* MtrA directly binds within the chloramphenicol BGC and represses biosynthesis, whilst in *S. coelicolor* it directly represses ACT and RED production via *actII-ORF4* and *redZ* transcriptional repression (Som *et al.*, 2017b; Som *et al.*, 2017a; Zhu *et al.*, 2020). MtrA has also been shown to share core recognition sequences with the major nitrogen control regulator GlnR. The core of GlnR boxes are 16 nucleotides (gTnAc-n6-GaAAc) which are similar to the previously reported MtrA recognition sequence (GTnAcC-n5-GTnAcn). Indeed, MtrA binding of GlnR boxes has been confirmed experimentally under nutrient rich conditions where MtrA represses both *glnR* and GlnR-activated nitrogen genes via GlnR-box binding (Zhu *et al.*, 2019).

The operon encoding MtrAB contains a third gene, *lpqB*, which is also highly conserved and has been named as a signature protein of the Actinobacteria (Gao, Paramanathan and Gupta, 2006). LpqB is a lipoprotein which interacts with the sensor domain of MtrB in *M. smegmatis* to modulate its activity. Deletion or disruption of *M. smegmatis lpqB* results in developmental aberration by inducing filamentous growth and polyploidy that is akin to *Streptomyces* aerial hyphae (Nguyen *et al.*, 2010).

1.7.1.3 DraRK

An *S. coelicolor ΔdraRK* mutant grown on minimal media with excess nitrogen exhibits increased RED biosynthesis but decreased ACT biosynthesis. When supplemented with glutamate the same mutant overproduced yCPK, a yellow-pigmented type-I polyketide. The phosphorylated, active RR DraR directly binds the promoters of *actII-ORF4* and *cpkO* (previously *kasO*). Whilst it activates expression of *actII-ORF4*, DraR represses *cpkO* expression resulting in production of ACT and repression of Cpk biosynthesis. DraR does not directly modulate RED biosynthesis, with no evidence of binding to RED regulatory gene, *redZ* or *redD,* promoters. DraRK also plays a role in development, reducing *S. coelicolor* growth under high glutamine and glutamate conditions. This is likely through its regulation of primary metabolism genes including the putative enoyl-CoA hydratase (ECH) *SCO6748,* a pyruvate kinase, *SCO2014*, and the glutamate synthase gene *gltB*. A similar effect can be seen in *S. avermitilis* where DraRK was shown to indirectly repress avermectin B1a production and directly activate biosynthesis of the macrolide antibiotic oligomycin A. This functional conservation is due to a highly conserved DNA binding domain, nearly identical in *S. coelicolor*, *S. venezuelae, S. clavuligerus, S. scabies, S. avermitilis* and *S. griseus* (Yu *et al.*, 2012).

1.7.1.4 TunRS

The role of this TCS remains unknown but the operon is always found genetically linked to the *tmrB*-like gene, which in *S. venezuelae* is *vnz_15955*. In *Bacillus subtilis* TmrB is a membrane-associated ATP-binding protein responsible for resistance to the antibiotic tunicamycin. The mode of resistance has not been defined, but is likely through an efflux pump, or by blocking passive diffusion (Noda *et al.*, 1992). Originally isolated from *Streptom*yces *lysosuperificus* in 1971, the tunicamycins are fatty acyl nucleoside antibiotics. They inhibit the biosynthesis of a key peptidoglycan precursor, undecaprenyl-pyrophosphoryl-*N*-acetylmuramoyl pentapeptide, a reaction catalysed by MraY. This action ultimately results in the inhibition of bacterial cell wall biosynthesis. Whilst not all *Streptomyces* species can produce tunicamycin the resistance gene homologue, *tmrB*, is highly conserved and not located within the tunicamycin BGC. This would suggest that TmrB plays an additional role beyond that

of self-protection from tunicamycin production (Wyszynski *et al.*, 2010). Differential RNA-seq has shown that the gene encoding for the *S. coelicolor* TmrB homologue, SCO3388 (38.9% amino acid identity), is co-transcribed with *tunRS* (Munnoch *et al.*, 2016). SCO3388 is also suggested to be involved in *Streptomyces* cell wall metabolism as a spore cell-wall-remodelling factor with the *tmrB*-like *S. coelicolor* mutant producing spores defective in stress-survival and germination (Kwon and Kwon, 2013). In *S. venezuelae* the deletion of *tunRS* resulted in increased sensitivity to tunicamycin. However, further analysis suggests this is likely due to polar effects on the co-encoded *tmrB* gene (unpublished data).

1.7.1.5 CssRS

As saprophytes, streptomycetes secrete a plethora of soluble proteins into their surrounding environs. These include antibiotics, signalling molecules and also hydrolytic enzymes to deal with the vast number of insoluble polymers found in their natural environment. Misfolded proteins are inactive and not only a waste of energy and amino acids but can also possibly disrupt the activity of other correctly folded proteins, reducing the colony's ability to survive (Gilbert *et al.*, 1995). CssRS is one of 24 TCS homologues shared between *Streptomyces* and *B. subtilis,* where it was originally studied. In both bacteria CssRS activates HtrA-like proteases in response to extracellular misfolded protein. (Darmon *et al.*, 2002; Gullón, Vicente and Mellado, 2012). These proteases play a vital role in degrading misfolded extracellular proteins and also act as chaperones, ensuring protein solubility in the periplasm (Clausen, Southan and Ehrmann, 2002).

In *S. lividans*, secretion-stress induced CssRS activation can be achieved by high-level production of alpha-amylase via *amlB.* Under these conditions it directly activates the expression of three HtrA-like proteases: *htrB, htrA1* and *htrA2* with the expression of all three being significantly reduced in the Δ*cssS* and Δ*cssR* mutant strains. Indeed, it was shown that all three HtrA-like proteases were required for full alpha-amylase folding but also that overexpression of any one of these proteases resulted in incomplete alpha-amylase folding. This suggests CssRS finely controls the levels of HtrA-like proteases in *Streptomyces* spp. to combat secretion stress (Gullón, Vicente and Mellado, 2012; Vicente *et al.*, 2016)

1.7.1.6 PhoPR

Biological life is reliant on phosphorous, with genetic material and membrane phospholipids being just two vital phosphate containing molecules. In regard to TCS signalling, phosphate is the molecule responsible for transducing the message from SK to RR in response to signal activation. PhoPR is likely the best studied streptomycete TCS, responding to changes in inorganic phosphate levels in the surrounding environment (Allenby *et al.*, 2012). Genetically the SK gene *phoR* and the RR gene *phoP* form an operon with *phoU*, encoding another regulatory protein (Hutchings *et al.*, 2004; Sola-Landa *et al.*, 2005). PhoP is a master regulator, governing both primary and secondary metabolism in *Streptomyces* spp., binding to promoters containing PHO boxes. These comprise of at least two 11 nucleotide direct repeat units (DRUs) with a consensus sequence of GTTCACC, allowing the PhoP dimer to bind. In *S. coelicolor* the DNA-binding domain (DBD) of PhoP is only opened upon phosphorylation, tightly controlling the response. This is in contrast to the *E. coli* PhoP DBD which is permanently exposed, more likely controlling regulation through PhoP protein level rather than phosphorylation state (Sola-Landa *et al.*, 2005; Allenby *et al.*, 2012).

In general, when faced with phosphate-limiting conditions, PhoPR activates pathways to scavenge phosphate from both the extra- and intracellular environments. It also delays, or completely represses, morphological development until the stress has been removed (Allenby *et al.*, 2012). PhoP directly activates transcription of *phoA*, an alkaline phosphatase, *phoD*, a phospholipase, and *vnz_00450*, a phytase which act to scavenge and hydrolyse phytate and other sources of inorganic phosphate. Extracellular phosphate is then transported in via the phosphate-specific PstSCAB, a high-affinity transporter highly upregulated by PhoP (Apel *et al.*, 2007; Sola-Landa *et al.*, 2008; Boukhris *et al.*, 2016). Other direct targets of PhoP include the genes encoding for the phosphodiester phosphodiesterases GlpQ1 and GlpQ2 which hydrolyse membrane phospholipid glycerophosphodiesters. The resulting products are an alcohol and a cellular phosphate source, sn-glycerol-3-phosphate. This reaction allows recycling of cellular phosphate if extracellular sources are scarce (Brzoska and Boos, 1989; Santos-Beneit *et al.*, 2009b). The

divergently transcribed regulatory protein PhoU is activated by PhoP and acts as a feedback control mechanism, repressing the PHO regulon including the aforementioned *phoR, glpQ1* and *pstS* genes (Martín-Martín *et al.*, 2017).

As with many TCSs, PhoPR plays a role in regulating secondary metabolism. Excess phosphate generally represses specialised metabolism with PhoP repressing high-level regulators such as *afsS* and *scbR* (Santos-Beneit *et al.*, 2009a; Fernández-Martínez, Santos-Beneit and Martín, 2012). The small sigma factor-like protein AfsS activates ACT and RED biosynthesis via expression of *actII-ORF4* and *redD* whilst the γ-butyrolactone (GBL) receptor ScbR activates coelimycin P1 and CDA production, upregulating *cpkO* and *cdaR* (Allenby *et al.*, 2012). Interestingly the *actII-ORF4* and *redD* gene transcripts were under-represented in the *S. coelicolor phoU* mutant. Whether this is due to direct activation by PhoU or from the PHO regulon self-regulatory effect remains unclear (Martín-Martín *et al.*, 2017). The industrially important *Streptomyces natalensis* is particularly sensitive to the phosphate concentration in growth media. Disruption of *phoP* in *S. natalensis* increases the production of pimaricin (otherwise known as natamycin), a US-FDA approved macrolide tetraene antifungal used as a food preservative. The regulatory effect by PhoP is likely indirect as there are no PHO boxes present within the *pim* biosynthetic gene promoter regions (Mendes *et al.*, 2007).

1.7.1.7 AbrC1/2/3

The *abrC123* operon encodes one RR (AbrC3) and two SKs (AbrC1 and AbrC2). In *S. coelicolor* this branched TCS modulates antibiotic production and differentiation rates. Both deletion and overexpression of the operon led to a decrease in ACT, RED and CDA biosynthesis alongside delayed morphological differentiation (Yepes *et al.*, 2011). Whilst there is sufficient intergenic region for each to have their own promoters *abrC1* and abrC*2* are expressed together as one single transcript with only *abrC3* expressed independently (Rodríguez *et al.*, 2015; Jeong *et al.*, 2016). Despite this co-expression AbrC1 is the sole SK responsible for the antibiotic production phenotype, phosphorylating the RR AbrC3 which binds to its own promoter and that of the ACT CSR *actII-ORF4* (Rodríguez *et al.*, 2015). AbrC3 also binds to the promoters of developmental genes including the BldD-regulated transcription factor *bdtA*.

Interestingly overexpression of AbrC3 only leads to a 33% increase in ACT production, converse to the results of *abrC123* overexpression, highlighting the importance of the phosphorylation-based regulation played by SKs on partner RRs (Rico *et al.*, 2014).

1.7.1.8 EsrSR

EsrSR derives its name from homology to the envelope stress response TCS EsrSR in the industrial workhorse *C. glutamicum.* Both systems are related to the LiaFSR three-component system from *B. subtilis*, responsible for cell envelope stress-sensing. LiaFSR regulates the phage-shock-protein (Psp) response, a system widely distributed throughout bacteria, induced by extracytoplasmic stress generally in the form of disruption of cytoplasmic membrane integrity (Darwin, 2005; Joly *et al.*, 2010; Kleine *et al.*, 2017). Both the *Streptomyces* spp. and *C. glutamicum* EsrSR are divergently encoded from EsrI, an integral membrane protein which contains a PspC domain, as does the SK EsrS (Kleine *et al.*, 2017). Pneumococcal surface protein C (PspC) proteins are involved in invasion and adhesion and are part of the Psp response (van der Maten *et al.*, 2018). Whilst streptomycetes encode PspA, an essential protein for survival and growth under membrane attack, they do not encode any of the other components of the Psp response system (Vrancken, Van Mellaert and Anné, 2008). In *C. glutamicum*, transcription of *esrISR* can be induced with antibiotics which inhibit the lipid II cycle, including vancomycin and bacitracin, and this increases resistance to bacitracin via the ABC-transporter *cg3322-3320*. Deletion of either *esrSR* or *cg3322-3320* in *C. glutamicum* leads to increased susceptibility to bacitracin but had no effect on vancomycin resistance. EsrR regulates a large number of genes including *esrISR*, heat shock-responsive genes *clpB* and *dnaK* and the putative ABC-transporter systems genes *cg2812-2811* and *cg3322-3320* in *C. glutamicum*. EsrI however may act as a repressor with *esrSR* transcription increased two-fold in the *esrI* deletion mutant (Kleine *et al.*, 2017). In *S. coelicolor* bacitracin resistance has been attributed to two ABC-transport systems, encoded by *SCO3089-3090* and *SCO3010-3011* with the double mutant significantly susceptible to bacitracin (Hesketh *et al.*, 2011). Cg2811 and Cg3320 share 26.4% a.a. identity with SCO3090 whilst Cg2812 and Cg3321 share 58.4% a.a. identity with SCO3089

suggesting EsrISR function is conserved between *C. glutamicum* and *S. coelicolor*. That is, responding to cell envelope stress with a broad response that includes activation of the bacitracin resistance ABC-transporter systems.

1.7.1.9 AfsQ1/2

Similar to MtrAB and CseBC, the AfsQ1/2 (AfsQ1 – RR, AfsQ2 – SK) TCS is co-transcribed with a partner lipoprotein, AfsQ3. The *afsQ123* operon is divergent from the *sigQ* gene which encodes the ECF sigma factor, σ^{Q} (Wang *et al.*, 2013). Homologous genomic architecture can be seen in CseBC, a TCS involved in detecting and responding to peptidoglycan degradation or physical cell wall disruption. CseBC is encoded in the *sigE-cseABC* operon with its partner lipoprotein, CseA, and the ECF sigma factor σ^{E} (Hong, Paget and Buttner, 2002; Tran *et al.*, 2019). AfsQ1 was named after its regulation of A-factor synthesis in *S. lividans* and heterologous expression of the *S. coelicolor afsQ1* leads to activation of ACT and RED production in *S. lividans*. In *S. coelicolor* AfsQ1/2 activates ACT, RED and CDA biosynthesis and negatively regulates aerial hyphae production when cultured on glutamate supplemented minimal media (Ishizuka *et al.*, 1992; Wang *et al.*, 2013; Tran *et al.*, 2019). Whilst there is no evidence that AfsQ2 detects glutamine or glutamate, despite its response to glutamate supplementation, there is evidence of crosstalk with the orphan RR GlnR, which itself also cross-talks with MtrA. When excess nitrogen is present, AfsQ1 modulates nitrogen assimilation by competing with GlnR for the promoter regions of *nirB* and *glnA*, genes encoding for a nitrite reductase and glutamine synthase respectively. The AfsQ1 binding site (GTnAC-n_6-GTnAC) can be found throughout the genome and putatively includes important development genes such as *bldM* and *whiD* (Wang *et al.*, 2013). AfsQ1 has been shown to directly activate transcription of *actII-ORF4, redD* and *cdaR* to modulate antibiotic production, and it also activates expression of σ^{Q} . Interestingly σ^{Q} was shown to have antagonistic activity to AfsQ1, repressing ACT, RED and CDA expression but has no effect on the transcription of the *afsQ123* operon (Shu *et al.*, 2008). Constitutive heterologous production of phosphomimetic AfsQ1 in most streptomycetes leads to lethality, whilst over-expression of the wild-type version is not lethal. Using a thiostrepton-inducible promoter it is possible reach a safe level of phosphomimetic AfsQ1 expression. There

is potential, and indeed existing evidence, that this construct could be a useful tool for the discovery of novel antibiotics. The novel class-I lasso peptide siamycin-I was isolated from *Streptomyces* sp. WAC00263 via production of this altered AfsQ1 protein. This antibiotic has activity against both VRE and MRSA. A similar cluster from *Streptomyces nodosus* contains a TCS (SNOD34170-RR, SNOD34175-SK) suggesting overlap of the AfsQ1 and SNOD34170 RR regulons (Daniel-Ivad *et al.*, 2017).

1.7.1.10 OsaABC

Transposon mutagenesis in *S. coelicolor* and *S. lividans* first identified the function of the unusual TCS OsaABC, comprised of two hybrid SKs (OsaA and OsaC) with a single CheY-family RR, OsaB (Bishop *et al.*, 2004). OsaB is essential for aerial hyphae production under osmotic stress conditions; however, the hybrid SK OsaA is not, displaying only a delayed osmoadaptation phenotype. Disruption of *osaB* results in a three to five-fold increase in ACT and RED production in *S. coelicolor*, but this is most likely an indirect side-effect of the osmotic stress response (Bishop *et al.*, 2004). A similar phenotype is seen in *S. avermitilis* where disruption of *osaB* or *osaC* under osmotic stress resulted in the same lack of aerial hyphae and increased levels of the antimicrobials oligomycin and avermectin (Godinez *et al.*, 2015). The final component of the OsaABC TCS, the second hybrid SK *osaC,* is divergently transcribed from *osaAB.* OsaC, like OsaB, is essential for the osmoadaptation response with mutants unable to differentiate under osmotic stress. It acts to normalise the level of *osaB* transcription post osmoadaptation. OsaC also performs the same function on the sigma factor σ^B, a master regulator of both osmotic and oxidative stress response, sequestering σ^B, disrupting the σ^B-positive feedback loop. Homologous overexpression of OsaC also prevents osmoadaptation, highlighting the fine balancing act ongoing within the cell (Martinez *et al.*, 2009). In summary, OsaABC forms a tripartite TCS essential for cell differentiation under osmotic stress, and whilst its regulon remains undefined a vital, and intricate, feedback system has been demonstrated.

1.7.1.11 GluRK

The amino acid glutamate is important for all living organisms, linking nitrogen and carbon metabolism and playing a role in multiple fundamental processes including glycolysis, the TCA cycle and gluconeogenesis. Under acidic conditions bacteria have also been shown to utilise the proton consumption occurring during glutamate decarboxylation to reduce intracellular pH, helping to resist acid stress (Feehily and Karatzas, 2013). In Actinobacteria, the *gluRK* operon is divergently transcribed from the *gluABCD* operon, which encodes a glutamate uptake system. One curious exception to this is the industrial producer of glutamate *C. glutamicum*, which does not contain *gluRK* homologues. GluA is an ATP-binding protein and GluB a glutamate-binding protein whilst GluC and GluD are glutamate permeases. In *S. coelicolor* GluK binds glutamate and phosphorylates GluR, which then directly activates expression of the *gluABCD* operon resulting in glutamate uptake. On minimal media supplemented with low glutamate (10 mM) the *S. coelicolor* Δ*gluRK* mutant overproduced ACT and displayed reduced RED production. When supplemented with high glutamate (75 mM) the mutant overproduced ACT and had reduced yCPK production. It also showed significant developmental impairment. GluR does not bind the promoters of *actII-ORF4, redZ/redD* or *kasO* so the modulation of antibiotic biosynthesis must be either indirect or through a previously unreported mechanism such as direct RR-protein regulation (Li, Jiang and Lu, 2017).

1.8. The CutRS two-component system

In 1991 a study by Tseng *et al*. described a 1,687 basepair (bp) region of DNA isolated from *S. lividans* HT32 that appeared to phenotypically suppress *melC1* null-mutants (Tseng and Chen, 1991). MelC1 is a trans-activator of MelC2, the copper-containing monooxygenase tyrosinase catalysing the formation of melanin in *Streptomyces* species (Leu *et al.*, 1992). Using CodonPreference this region of DNA was shown to contain two coding sequences: a complete 217 amino acid protein and a truncated 190 amino acid open reading frame (ORF)(Gribskov, Devereux and Burgess, 1984; Tseng and Chen, 1991). The 217 amino acid protein was predicted to belong to the

OmpR RR family, sharing extensive homology with the exemplar OmpR from *E. coli*. The other, truncated, protein resembled the N-terminus of EnvZ, the partner histidine kinase of OmpR. A potential ribosome binding site (RBS) was identified (GGAGG) and using the location of this, in conjunction with the codon usage bias of streptomycetes, the start codons for the two proteins were assigned as GTG-458 and GTG-1118. The putative *melC1* suppressor gene was identified as the OmpR-family RR as the complete deletion of the truncated ORF had no effect on the suppressive phenotype whilst truncation of the RR eliminated the activity (Tseng and Chen, 1991). It was hypothesized that these proteins were akin to the *ompB* operon, acting together to detect and respond to environmental factors to regulate a copper transport protein. The proteins were named CutR (RR) and CutS (SK) to reflect their role in the regulation of cupric ion transport. When cloned it was thought to result in dysregulated copper uptake leading to restoration of melanin production in the *melC1* mutant. This *cutRS* sequence was identified to be conserved among streptomycetes with homologous sequences found in all 16 *Streptomyces* spp. tested by using high stringency DNA hybridization (Tseng and Chen, 1991). Eventually it would transpire that CutRS was the first two-component system to be described in *Streptomyces* spp., but this was not fully appreciated by Tseng *et al*. in 1991.

A follow-up publication was released in 1996 authored by Chang *et al*., again from Carton Chen's group in Taiwan. The full sequence of the 414 amino acid CutS SK was deduced, with significant similarity to the recently described AfsQ2 SK, confirming the suspicion that CutRS was a TCS (Ishizuka *et al.*, 1992; Chang *et al.*, 1996). However further attempts to identify the Δ*melC1* suppressor mutation in the partial *cutRS* clone proved futile. Comparison of the *cutRS* operon between *S. lividans* HT32 and wild-type *S. lividans* TK64 revealed no differences. Despite this, the same fragment from TK64 was phenotypically identical when cloned, supressing the melanin repression. Further investigation into the 457 bp region of DNA upstream of *cutRS* revealed divergent transcription. In the original cloning vector pLUS175 (**Figure 1.6**) this region would act as a *cis*-activating promoter for *melC1* effectively restoring wild-type phenotype with MelC1 complementation. Indeed, when the entire 1.69 kb region was inverted suppression was abolished. Ultimately, the promoter region

alone was sufficient for suppression and could be substituted by any strong constitutive promoter. Neither the *cutR* or *cutS* genes proved to have any effect on the production or suppression of melanin (Tseng and Chen, 1991; Chang *et al.*, 1996).

Whilst this invalidated the putative role played by CutRS the authors set out to identify the true function of the first identified streptomycete TCS. Single mutants of *cutR* and *cutS* were generated in *S. lividans* TK64 and subjugated to a wide range of assays: visible colony morphology, electron microscopy, metal ion resistance, expression and inducibility of alkaline phosphatase activity and osmotic stress. No phenotypic differences were detected in any of these assays. Both mutants did however display increased ACT production on a range of solid media including R5 and minimal media supplemented with proline. Additionally, whilst ACT biosynthesis is not usually noticeable in TK64 until day 7, both mutants secreted ACT after 3-4 days. The same was true in liquid culture, with an average of 3-fold greater ACT production and induction 15 hours earlier. Temporal mapping of the transcripts in the wild-type strain grown in liquid culture suggested that *cutRS* was transcribed during the transition phase at 19 hours, persisting throughout actinorhodin production at 40 hours. CutR therefore repressed the *act* BGC for 21 hours, after which it would appear repression was overridden. This confirmed CutR as a repressor of ACT biosynthesis and further introduction of *S. lividans cutR* into *S. coelicolor* M145 likewise resulted in reduced ACT production (Chang *et al.*, 1996). Based on published work, it was reported that a M145 *cutS::tsr* mutant overproduced ACT and that phosphorylation of CutR was essential for ACT repression, fitting the *modus operandi* of TCSs (H.M. Chang, unpublished). S1 nuclease mapping revealed protected sites 75 and 76 bp upstream of the putative *cutR* start codon and 4 bp beyond this was a sequence, CAGGAT, which resembles the -10-consensus sequence of streptomycete promoters, but no -35-consensus sequence could be identified. Additionally, ~180 bp upstream from the start site 8 bp inverted repeats were detected which could represent putative transcriptional regulator binding sites (Chang *et al.*, 1996). Whilst Chang *et al.* postulated that phospho-CutR acted as a repressor of actinorhodin biosynthesis in *S. lividans* and *S. coelicolor* they could not define it as direct or indirect

regulation. The role played by the SK was also left unexplored (Tseng and Chen, 1991; Chang *et al.*, 1996).

Despite being a highly conserved TCS in a genus with such biosynthetic potential, there has been no published research on CutRS since 1996. CutRS clearly plays some role in the regulation of ACT production however the *act* BGC is not conserved among all streptomycetes, unlike *cutRS* (Mclean *et al.*, 2019). Clearly CutRS has additional functions that have yet to be revealed.

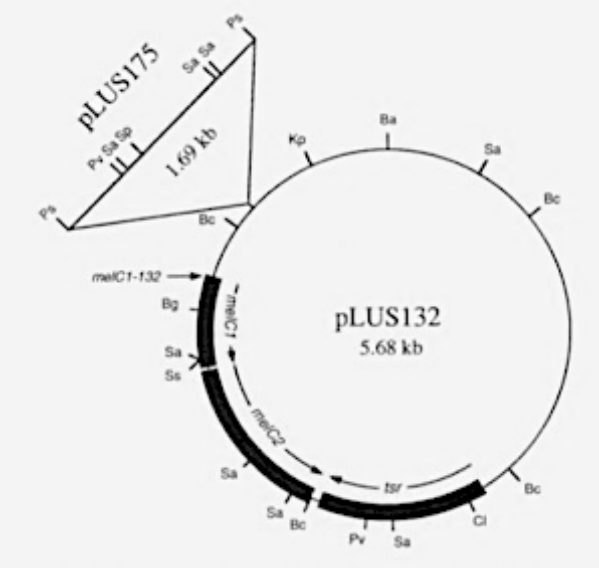

Figure 1.6. The plasmid pLUS175 containing the truncated *cutRS* operon-encoding 1.69 kb *PstI* fragment from *Streptomyces lividans* HT32 inserted into the backbone cloning vector *melC1*$^{-}$ pLUS132. The coding sequences and orientations of *tsr, melC1* and *melC2* are indicated via solid bars and arrows above. Restriction site abbreviations as follows: Ba: *BamHI;* Bc: *BclI;* Bg: *BglII;* Cl: *ClaI;* Kp: *KpnI;* Ps: *PstI;* Pv: *PvuII;* Sa: *SalI;* Sp: *SphI and* Ss: *SstI.* Adapted from Tseng and Chen, 1991.

1.9. Aims and objectives of this project

The aim of this project was to investigate the function of the highly conserved TCS CutRS within the genus *Streptomyces*. Building on previous work which generated deletion mutants in the 15 highly conserved TCS operons, wide ranging assays were conducted to determine the morphological and biochemical phenotypes of TCS mutants in the model organism *S. venezuelae*. The highly conserved CutRS TCS had the most striking phenotype and was determined to play a role in the newly described exploratory growth. The conservation of CutRS was confirmed *in vivo* and the CutR regulon was explored in *S. venezuelae* and *S. coelicolor*, alongside a more holistic approach looking at the whole cell proteome changes in *cutRS* mutants. Using this knowledge, we investigated the activating signal of the CutS sensor kinase and engineered strains, endeavouring to define the underlying mechanism the CutRS regulon plays in the observed phenotype. Further investigations into the secondary metabolome of the CutRS strains was undertaken and appears to link primary and secondary metabolism with the hypothesised mechanism of action. This work has expanded our knowledge of TCSs within streptomycetes and added to the broader knowledge of bacterial regulatory mechanisms. Greater understanding of the roles TCSs play in the regulation of development and secondary metabolism in *Streptomyces,* and the mechanisms by which they work, will enhance future research and expedite the discovery of antibiotics from these fascinating bacteria.

Chapter 2. Materials and methods

2.1. Chemicals and Reagents

Unless otherwise stated the chemicals and reagents used were purchased from Sigma Aldrich (UK) or Thermo Fisher Scientific (UK) and were of laboratory standard grade or above. All media and solutions were made using deionised water (dH_2O) unless otherwise stated.

2.2. Bacterial and yeast strains

A table of all bacterial and yeast strains used in this study can be found in the appendix of this thesis (**Table 8.1**). *E. coli* strains were routinely cultivated at 37°C on LB agar or in LB broth, with 220 rpm shaking, unless otherwise stated. *Streptomyces* spp. strains were routinely cultivated at 30°C on MYM + TE agar or SFM agar unless otherwise stated. The growth media used in this work are listed in **Table 2.1** whilst the antibiotics used for selection and their selective concentrations are listed in **Table 2.2**.

Table 2.1. Growth media and constituents used in this work

Media	Recipe (per litre)	Notes	Water	pH
SFM	20 g soy flour 20 g mannitol 20 g agar		Tap	
MYM + TE	4 g maltose 4 g yeast extract 10 g malt extract 2 ml trace element solution +/- 20 g agar	Added post-autoclaving	50:50 tap:deionised	7.3

LB / Soft LB	10 g tryptone 5 g yeast extract 10 g NaCl +/- 20 g agar	Exclude for hygromycin selection 5 g for Soft LB	Deionised	
YP / YPD	10 g yeast extract 20 g bacto-peptone 100 ml 40% filter-sterilised dextrose +/- 20 g agar	Added post-autoclaving for YPD, omit for YP	Deionised	
2xYT	16 g tryptone 10 g yeast extract 5 g NaCl		Deionised	
Minimal Media	0.5 g L-asparagine 0.5 g dipotassium phosphate 0.2 g magnesium sulfate heptahydrate 0.01 g iron (II) sulfate heptahydrate 10 g dextrose 10 g agar	Added post-autoclaving	Deionised	7.0

DNA	4 g Difco Nutrient Broth powder +/- 10 g agar		Deionised	
YBP	2 g yeast extract 2 g beef extract 4 g Bacto-peptone 1 g magnesium sulfate 15 g sodium chloride 10 g dextrose +/- 15 g agar	Added post-autoclaving	Deionised	

Table 2.2. Antibiotics used in this work and their final selective concentrations

Antibiotic	**Final selective concentration (µg/ml)**
Ampicillin	100
Apramycin	50
Carbenicillin	50
Chloramphenicol	50
Hygromycin	50
Kanamycin	50
Nalidixic Acid	25
Thiostrepton	30

2.3. Preparation of *Streptomyces* spores

A single colony of *Streptomyces* was resuspended in 100 µl sterile dH_2O with a sterile toothpick, plated onto MYM + TE or SFM agar and incubated at 30°C for 3-5 days until visibly sporulated. The plate was then flooded with 5 ml sterile dH_2O and spores resuspended using a sterile cotton bud. The spore resuspension was transferred to a 15 ml falcon tube and pelleted at 4000 rpm for 10 minutes at 4°C in a benchtop centrifuge. The supernatant was discarded, and the pellet resuspended in 1.5 ml 20% glycerol. The spore stock was stored at -20°C in a cryotube.

2.4. Glycerol stocks

For storage of *E. coli, B. subtilis, C. albicans* and *S. cerevisiae* 375 µl of overnight culture was mixed with 525 µl of 40% glycerol. The glycerol stock was stored at -80°C in a cryotube.

2.5. DNA extraction

Genomic *Streptomyces* spp. DNA was extracted from 10 ml overnight culture. The culture was pelleted at 4000 rpm for 10 minutes in a benchtop centrifuge before the supernatant was discarded and the pellet resuspended in 500 µl solution I (50 mM Tris-HCl pH 8.0, 10 mM EDTA, 100 µg/ml RNase A) with lysozyme added to 5 mg/ml. Solution was incubated at 37°C for one hour with regular inversions before adding SDS to 1% and placing on ice for 10 minutes. Equal volume phenol:chloroform:isoamyl alcohol was added, vortexed and centrifuged at 13000 rpm for 5 minutes. The upper layer was removed to a fresh microcentrifuge tube and the previous step was repeated twice more with phenol:chloroform:isoamyl alcohol and once with chloroform:isoamyl alcohol. With the final upper phase in a fresh microcentrifuge tube three volumes 100% ethanol was added and incubated at -20°C for 30 minutes. The samples were pelleted at 13000 rpm for 20 minutes before removing the supernatant and gently washing the DNA pellet with 500 µl 80%

ethanol. After a 1-minute spin at 13000 rpm, the supernatant was carefully aspirated and airdried for 5 minutes. The DNA pellet was then resuspended in sterile dH_2O overnight in the fridge.

2.6. DNA quantification

DNA concentration and purity were analysed using a Nanodrop™ 2000 UV-Vis Spectrophotometer.

2.7. Primers

Primers were either designed manually using ApE (A Plasmid Editor) or through Primer3web (version 4.1.0, primer3.ut.ee) and purchased from Integrated DNA Technologies (IDT). A table of all primers used in this work can be found in the thesis appendix (**Table 8.3**).

2.8. Polymerase Chain Reaction (PCR)

In this work PCRBIO® Taq DNA polymerase (Biotaq, PCR Biosystems) was used for diagnostic and colony PCRs whilst Phusion® High-Fidelity DNA Polymerase (NEB) was used for the amplification of DNA fragments for subsequent use in cloning. PCRs were conducted using a Techne® Prime thermocycler generally following mixtures and conditions outlined in **Table 2.3/Table 2.4** and **Table 2.5/Table 2.6**. The annealing temperature used for Biotaq and Phusion® PCRs were 55°C and 60°C respectively unless otherwise stated.

Table 2.3. PCRBIO® Taq DNA Polymerase PCR reaction mix

Reagent	20 µl reaction	Notes
2x PCRBIO Taq Mix Red	10 µl	Contains loading dye
50% DMSO	2 µl	Helps primer annealing
Forward Primer (10 µM)	1 µl	
Reverse Primer (10 µM)	1 µl	
Template DNA	1 µl	~30 ng plasmid or gDNA
Deionised water	5 µl	

Table 2.4. PCRBIO® Taq DNA Polymerase PCR thermocycler conditions

Cycles	Temperature	Time	Process
1	95°C	1 min	Initial denaturation
25	95°C	15 s	Denaturation
	55°C	15 s	Annealing
	72°C	15 s / kb	Extension
1	72°C	5 min	Final extension
1	10°C	Hold	Final hold

Table 2.5. Phusion® High-Fidelity DNA Polymerase PCR reaction mix

Reagent	20 µl reaction	Notes
5x Phusion GC Buffer	4 µl	Improves performance with GC-rich templates
50% DMSO	2 µl	Helps primer annealing
2 mM dNTPs	2 µl	
Forward Primer (10µM)	1 µl	
Reverse Primer (10 µM)	1 µl	
Template DNA	1 µl	~30 ng plasmid or gDNA
Deionised water	8.8 µl	
Phusion polymerase	0.2 µl	

Table 2.6. Phusion® High-Fidelity DNA Polymerase PCR thermocycler conditions

Cycles	Temperature	Time	Process
1	98°C	3 min	Initial denaturation
35	98°C	10 s	Denaturation
	60°C	10 s	Annealing
	72°C	15 s / kb	Extension
1	72°C	15 s / kb + 15 s	Final extension
1	10°C	Hold	Final hold

2.9. Agarose gel electrophoresis

Agarose gels were made with 1% agarose in TBE bugger (90 mM boric acid, 90 mM Tris-HCl, 2 mM EDTA) with ethidium bromide added to 2 µg/ml. DNA samples were loaded with a 10x gel-loading dye (3.9 ml glycerol, 500 µl 10% (w/v) SDS, 200 µl 0.5 M EDTA, 0.025 g bromophenol blue, 0.025 g xylene cyanol, dH_2O to 10 ml) alongside a 1 kb DNA ladder. The gels were run at 100 V (Sub-Cell GT electrophoresis system, BIOLINE) for 45-60 minutes dependant on fragment size. DNA was visualised with UV-light using a Molecular Gel Doc System (Bio-Rad).

2.10. Gene synthesis

Gene synthesis was performed by Genewiz (UK) and GenScript (US).

2.11. Plasmid preparation

E. coli plasmid DNA was purified from 10 ml overnight culture using a QIAprep Spin Miniprep Kit (QIAGEN) following the manufacturer's instructions. Plasmids were eluted in 50 µl Buffer EB (10 mM Tris-HCl pH 8.5). A table of all plasmids used or generated in this work can be found in the thesis appendix (**Table 8.2**).

2.12. Restriction digest

Single and double restriction digests were carried out in 50 or 100 µl reactions using both NEB and Roche restriction enzymes following the manufacturer's instructions using the most optimal buffer available. 1 µg of DNA was typically digested at 37°C for 4 hours in a 50 µl reaction containing 2 units of the required restriction enzyme. To prevent re-ligation in vectors to be used for classical ligation 1 µl of rapid shrimp alkaline phosphatase (rSAP, NEB) would be added for the final 30 minutes of the reaction. Digests were then analysed and purified using gel electrophoresis and subsequent extraction of desired products.

2.13. Gel extraction

Gel slices containing DNA fragments of interest were excised from agarose gels using a scalpel. DNA was extracted using a QiaQuick Gel Extraction Kit (QIAGEN) following the manufacturer's instructions. DNA was eluted in 30 µl Buffer EB (10 mM Tris-HCl pH 8.5).

2.14. Ligation

Ligations were performed in 15 µl reactions using T4 DNA Ligase (NEB) following manufacturer's instructions on ice overnight. A standard 3:1 ratio of insert to vector was used with required volumes calculated using the In.silico ligation calculator (http://www.insilico.uni-duesseldorf.de/Lig_Input.html).

2.15. Golden gate assembly

Constructs were assembled using the 20 µl reaction per **Table 2.7** and the golden gate program run in a thermocycler with the conditions outlined in **Table 2.8**.

Table 2.7. Golden gate assembly reaction mix

Reagent	20 µl reaction	Notes
T4 ligase buffer	2 µl	
T4 ligase	1 µl	Added last
BbsI	1 µl	
Insert	0.3 µl	
Vector backbone	X µl	100 ng
Deionised water	Y µl	

Table 2.8. Golden gate assembly thermocycler conditions

Cycles	Temperature	Time	Process
10	37°C	10 min	Digestion
	16°C	10 min	Ligation
1	50°C	5 min	Final digestion
1	65°C	20 min	Heat inactivation
1	10°C	Hold	Final hold

Completed 20 nucleotide synthetic protospacer insert constructs were transformed into chemically competent *E. coli* Top10 via heat shock, screened using blue/white X-Gal plates and confirmed by sequencing (**Chapter 2.23**).

2.16. Gibson Assembly®

Multiple DNA fragments containing 25-35 nucleotide overlapping regions were seamlessly assembled into digested DNA vectors using the exonuclease-based Gibson Assembly® (NEB). With the Gibson Assembly® Master Mix (NEB) a standard 3:1 ratio of insert to vector was used and assembly performed at 50°C for 1 hour in a thermocycler.

2.17. Preparation and transformation of chemically competent *E. coli*

E. coli Top10 were grown from single colonies in 10 ml selective LB overnight before being sub-cultured into 50 ml LB and grown until an OD_{600} of approximately 0.4 was reached. The cultures were centrifuged at 4000 rpm for 5 minutes at 4°C and the cell pellets washed with 20 ml ice-cold 100 mM $CaCl_2$ twice. The washed cell pellet was resuspended in 2 ml ice-cold 100 mM $CaCl_2$, flash frozen in liquid nitrogen, and stored at -80°C as 100 µl aliquots. For transformation aliquots were dethawed on ice for 20 minutes before adding approximately 2 µg of DNA and mixing gently. Following 30

minutes on ice the samples were heat-shocked at 42°C for 30 seconds and immediately placed back on ice for 5 minutes. 1 ml room temperature LB was added, and samples incubated at 37°C with shaking at 220 rpm for 1-2 hours. Recovered transformation mixture was plated on selective media and incubated overnight.

2.18. Preparation and transformation of electrocompetent E. coli

E. coli Top10 or ET12567/pUZ8002 were grown from single colonies in 10 ml selective LB overnight before being sub-cultured in 50 ml selective LB and grown until OD_{600} of 0.6. The cultured were centrifuged at 4000 rpm for 5 minutes at 4°C and the cell pellets washed with 20 ml ice-cold 10% glycerol twice. The washed cell pellet was resuspended in 1 ml ice-cold 10% glycerol, flash frozen in liquid nitrogen, and stored at -80°C as 50 µl aliquots. For transformation aliquots were dethawed on ice for 20 minutes before adding approximately 2 µg of DNA and mixing gently and transferred to an ice-cold electroporation cuvette. Using a MicroPulser Electroporator (Bio-Rad) set to 200 Ω, 25 µF and 2.5 kV electroporation was carried out on each sample with 1 ml ice-cold LB added immediately after electroporation and sample transferred to a 1.5 ml microcentrifuge tube. The samples were recovered at 37°C with shaking at 220 rpm for 1-2 hours before plating on selective media and incubated overnight.

2.19. Tri-parental mating

E. coli DH10β pESAC-13 215-G, Top10 pR9604 and ET12567 were cultured overnight in 10 ml selective LB at 37°C with shaking at 220 rpm. The cultures were then sub-cultured, grown to OD_{600} 0.6 and washed twice with LB via centrifugation. Each pellet was resuspended in 500 µl LB and subsequently 20 µl of each strain was spotted onto the same location on LB agar. Following overnight incubation, the culture spot was then re-streaked on LB selective for all three desired plasmids and incubated overnight. Colony PCR was used to confirm successful tri-parental mating.

2.20. *E. coli* colony PCR

Single colonies from overnight incubation plates were picked into 20 µl sterile dH_2O and resuspended. 6 µl of the colony resuspension was used in place of the 5 µl dH_2O and 1 µl template DNA for a Biotaq PCR as described above (**Chapter 2.8**) and analysed via gel electrophoresis. 10 µl of the remaining colony suspension from positive clones was used to inoculate 10 ml LB containing selective antibiotics and incubated overnight.

2.21. Lambda λ RED methodology (ReDIRECT) for gene deletion

This strategy for PCR-targeting *Streptomyces* spp. for mutagenesis uses a λ RED-based gene disruption methodology termed ReDIRECT as previously described (Gust, Kieser and Chater, 2002). 58 and 59 nucleotide primers were designed with 39 nucleotide 5' ends which overlap the sequence adjacent to the region to be disrupted. The 3' ends match the chosen disruption cassette, generally pIJ773 containing *aac(3)IV* for apramycin resistance. PCR amplification was then used to extend the resistance cassette. The *Streptomyces* sp. cosmid clone containing region of interest was introduced into electrocompetent *E. coli* BW25113/pIJ790 and incubated overnight at 30°C on selective LB. A single colony was picked into 10 ml selective LB and incubated overnight at 30°C with shaking at 220 rpm. This clone was then prepared for electroporation and transformed with 100 ng of PCR product. After recovery the mixture was plated on selective LB and incubated at 37°C to promote the loss of pIJ790 unless further mutations were required. The gene disruption was confirmed using diagnostic PCR. Cosmid DNA was isolated and transformed into *Streptomyces* via *E. coli* ET12567/pUZ8002 conjugations (**Chapter 2.24**). Desired double cross-over kanamycin sensitive strains were screened for using replica-plating before confirming mutations using diagnostic PCR.

2.22. CRISPR/Cas9 methodology for gene deletion and genome editing

This methodology for scar-less gene deletion and genome editing in *Streptomyces* uses a CRISPR/Cas9 as previously described (Cobb, Wang and Zhao, 2015). Using CRISPy-web (https://crispy.secondarymetabolites.org) a 20 nucleotide protospacer was designed to target the region of interest via a synthetic guide RNA (sgRNA). 24 nucleotide primers were designed to construct this protospacer containing 5' BbsI sticky ends. The pair of oligonucleotides were resuspended to 100 µM in dH_2O before 5 µl of both were mixed in 90 µl 30 mM HEPES pH 7.8. The mixture was heated to 95°C for 5 minutes before ramping to 4°C at a rate of 0.1°C per second. Golden gate assembly (**Chapter 2.15**) was used to insert the annealed protospacer into pCRISPomyces-2 at the BbsI site and the resulting vector heat shocked into chemically competent *E. coli* Top10 before plating on selective LB containing IPTG and X-Gal. White colonies were picked into 10 ml selective LB for overnight incubation. Following plasmid preparation vectors were sequence confirmed and digested with XbaI. Gibson Assembly (**Chapter 2.16**) was used to assemble two 1 kb PCR-amplified homology repair templates, matching regions adjacent to the target region, into the vector. The sequence-confirmed final vector was transformed into *Streptomyces* via *E. coli* ET12567/pUZ8002 conjugation (**Chapter 2.24**) and apramycin resistant colonies PCR-screened (**Chapter 2.25**) for desired mutations. Finally, the mutants were passaged for multiple generations at 37°C to facilitate the loss of the temperature sensitive pCRISPomyces-2.

2.23. Sequencing of plasmids and DNA fragments

Constructed DNA plasmids were sequenced confirmed using the Mix2Seq kit (Eurofins Genomics) following manufacturer's instructions, with the addition of DMSO to a final concentration of 5%.

2.24. Intergeneric conjugation

Single colonies of *E. coli* ET12567/pUZ8002 (or pR9604 from tri-parental mating) containing desired target vector were picked from selective LB plates and incubated overnight in 10 ml selective LB with shaking at 220 rpm. The overnight culture was subsequently sub-cultured in 50 ml selective LB and grown to OD_{600} 0.6. The cultures were washed with 10 ml ice-cold LB twice by centrifugation to remove the residual antibiotics and finally resuspended in 1 ml ice-cold LB. 20-50 µl of *Streptomyces* spp. spores were suspended in 500 µl 2xYT and heat shocked at 50°C for 10 minutes. Heat shocking was not required for *S. venezuelae*. 500 µl of the *E. coli* suspension was mixed with the spore suspension, mixed by inversion and pelleted at 13000 rpm for 2 minutes. The supernatant was removed, and the pellet resuspended in 150 µl residual supernatant. Serial dilutions were performed and plated on SFM + 10 mM $MgCl_2$ ($MgCl_2$ not required for *S. venezuelae*). Plates were incubated at 30°C (or room temperature for *S. venezuelae*) for 16-20 hours and subsequently overlaid with 1 ml sterile dH_2O containing 30 µl of each selective antibiotic required (including nalidixic acid). Once dried the plates were incubated at 30°C for 3-7 days until colonies appeared. Colonies were then re-streaked on SFM containing selective antibiotics (including nalidixic acid) at least once before being plated for spore preparation.

2.25. *Streptomyces* spp. colony PCR

Streptomyces spp. exconjugants were re-streaked on DNA agar and incubated for 2 days at 30°C. Single colonies were picked into 100 µl 50% DMSO and incubated at 50°C for 1 hour, vortexing every 10 minutes. 2 µl of colony suspension was used for a Biotaq colony PCR (**Chapter 2.8**) replacing the 2 µl 50% DMSO component for a 20 µl reaction. Primers were used at a final concentration of 5 µM.

2.26. Genetic complementation

Individual gene deletions were complemented using the native gene and promoter regions cloned into pSS170 or the native gene cloned downstream of the constitutive *ermE** promoter in pIJ10257 using ligation or Gibson Assembly. The complement construct was then conjugated into the corresponding wild-type and mutant strains as described (**Chapter 2.24**).

2.27. Antimicrobial bioactivity assay (Bioassay) on solid media

A 5 µl spot of *Streptomyces* spp. was inoculated onto the centre of an agar plate and incubated for 2-14 days at 30°C. *E. coli, B. subtilis* or *C. albicans* indicator strains were incubated in 10 ml LB at 37°C with 220 rpm shaking the night prior to desired assay date. After overnight incubation the indicator strains were sub-cultured into 50 ml LB and grown to OD_{600} 0.6. For *E. coli* and *B. subtilis* strains the sub-culture was then diluted 1:10 into 50°C Soft LB agar whilst *C. albicans* CA6 was diluted to 4:100 in 50°C Soft LB agar. 5 ml of the subsequent Soft LB agar was then pipetted over the *Streptomyces* plate and tapped to ensure complete coverage. Once dry the *E. coli* and *B. subtilis* indicator plates were incubated at 37°C overnight whilst the *C. albicans* CA6 plates were incubated at room temperature for 2 days.

2.28. Chemical extraction of chloramphenicol from solid media

Two 5 µl aliquots of spore stock were used to inoculate cellophane disc covered 30 ml agar plates with *Streptomyces* spp. before incubation at 30°C for 2 days. Subsequently the cellophane was removed, and colony biomass measured as described later in this thesis (**Chapter 2.50**). The remaining agar was cut into 1 cm^3 pieces using a sterile razor blade and transferred to a 100 ml Duran bottle. 30 ml of ethyl acetate was added to the agar, briefly shaken and left at room temperature for 1 hour. The top 25 ml of HPLC-grade ethyl acetate was then transferred to a sterile 50 ml falcon tube and the solvent removed using a Genevac EZ-2 Elite (Genevac). The

remaining residue was resuspended in 500 µl HPLC-grade methanol and transferred to a 1.5 ml microcentrifuge tube. Insoluble particulates were removed via centrifugation at 13000 rpm for 10 minutes with the uppermost 200 µl of solution transferred to a 2 ml screw thread autosampler vial containing a 200 µl glass insert for downstream chloramphenicol quantification (**Chapter 2.29**).

2.29. High-performance Liquid Chromatography (HPLC)

The HPLC and LC-MS experiments were run in collaboration with Dr Sibyl Batey from the John Innes Centre (JIC). First, a chloramphenicol standard curve was prepared in triplicate with serial dilutions of chloramphenicol in methanol from 1000 – 0.01 µg/ml. Analytical HPLC was performed on a 1290 Infinity II LC System (Agilent). Chloramphenicol standards and extracted samples were analysed using a Kinetex 2.6 µm XB-C18 110 Å, 100 x 4.6mm column (Phenomenex) with a gradient elution: MeCN/ 0.1% (v/v) TFA (H_2O) – 10/90 for 1 minute, gradient to 100/0 1–11 minutes, 100/0 for 11–13 minutes, gradient to 10/90 13–13.10 minutes and 10/90 for 13.10–15 minutes; flow rate 1 ml/min; injection volume 10 µL. The λ_{max} observed for chloramphenicol was 278 nm and peak area at this wavelength was quantified for analysis. The minimum concentration of chloramphenicol that could accurately be detected under these conditions was 0.5 µg/ml.

2.30. Heterologous protein overexpression and purification in *E. coli*

Small scale batch heterologous expression and purification of *Streptomyces* proteins was achieved using the pET28a vector. The target protein was cloned into the vector to create a N-terminal 6xHis-fusion protein. The sequence-confirmed vector was transformed into chemically competent *E. coli* BL21 pLysS via heat shock (**Chapter 2.17**) and single colonies selected for overnight incubation in 10 ml selective LB at 37°C with shaking at 220 rpm. Following sub-culturing into 50 ml LB the culture was grown under the same conditions until OD_{600} reached 0.6-0.8 and was induced with 1 mM IPTG. After a further 4 hours incubation cells were harvested by 4000 rpm

centrifugation for 30 minutes and pellets stored at -80°C for future purification. 1 ml of the supernatant was saved as the “insoluble fraction” sample.

Cell pellets were defrosted on ice and resuspended in 25 ml lysis buffer (20 mM Tris-HCl pH 8.0, 75 mM NaCl, 0.1% Triton X-100, 10 mg/ml lysozyme, EDTA-free protease inhibitor). Suspensions were sonicated on ice twice at 50 Hz for 40 seconds per cycle and 1 ml saved as “whole cell lysate” sample. The samples were pelleted by centrifugation at 4000 rpm for 20 minutes at 4°C and a 1 ml sample of supernatant saved as the “soluble fraction” sample. In a 50 ml falcon tube the sample was combined with 350 µl Ni-NTA Agarose (QIAGEN) and incubated for 1 hour at 4°C with gentle rocking. The samples were spun at 1200 rpm for 1 minute at 4°C, the supernatant carefully aspirated, and the agarose resuspended in 2 ml wash buffer (80 mM Tris-HCl pH 8.0, 200 mM NaCl, 10% glycerol, 10 mM $MgCl_2$, 0.1 mM DTT, 20 mM β-mercaptoethanol). The resuspension was transferred to a 1 ml polypropylene column (QIAGEN) and 1 ml of the flow through saved as “flow through” sample. The column was washed twice with 20 ml wash buffer with 1 ml saved each time as “wash sample 1/2”. Finally, the bound protein was eluted in 1 ml elution buffer (80 mM Tris-HCl pH 8.0, 200 mM NaCl, 10% glycerol, 10 mM $MgCl_2$, 0.1 mM DTT, 20 mM β-mercaptoethanol, 350 mM imidazole). All sample fractions collected were either stored on ice for immediate use or flash frozen in liquid nitrogen and stored at -80°C for future use.

2.31. Fast Protein Liquid Chromatography (FPLC) purification of heterologous protein overexpression in *E. coli*

For large scale protein expression following batch purification (**Chapter 2.30**) heterologous expression *E. coli* strains were treated in the same manner except 1 L LB cultures were used in place of the 50 ml for induction of protein expression. Once cell pellets were collected, as above, they were stored at -80°C for future purification. Cell pellets were defrosted on ice for 30 minutes before being resuspended in 25 ml lysis buffer (20 mM Tris-HCl pH 8.0, 75 mM NaCl, 0.1% Triton X-100, 10 mg/ml lysozyme, EDTA-free protease inhibitor) and incubated at room temperature for a

further 30 minutes. Suspensions were sonicated on ice 8 times at 50 Hz for 30 seconds per cycle with 1 minute off between each sonication cycle. Cell debris was removed by centrifugation at 15000 rpm for 30 minutes at 4°C and the supernatant filtered through a sterile 0.22 µm filter (Sartorius Stedim Biotech).

Using an ÄKTA pure protein purification system (Cytiva) the sample was then loaded onto a 1 mL HisTrap column (GE Healthcare) that had been pre-equilibrated with Nickel Buffer A (50 mM Tris-HCl pH 8.0, 200 mM NaCl, 5% glycerol). The loaded column was washed with increasing concentrations of imidazole (step 1: 10 mM; step 2: 20 mM; step 3: 30 mM) before the protein was eluted using 500 mM imidazole, all in the same buffer. Target protein fractions were pooled and loaded onto a Superdex 200 gel filtration column (GE Healthcare) via a 5 ml loop injection system for final purification. The gel filtration column was pre-equilibrated with gel filtration buffer (50 mM Tris-HCl pH 8.0, 200 mM NaCl, 10% glycerol, filtered). Final pure protein fractions were flash frozen and stored at -80°C

2.32. Circular Dichroism (CD) spectroscopy

Protein sample was diluted to a final concentration of 0.5 mg/ml and dialysed into 10 mM phosphate buffer overnight at 4°C. CD spectroscopy was performed by Julia Mundy from the JIC as follows. Spectra were recorded in 1 nm steps on a Chirascan Plus spectrophotometer (Applied Photophysics) at 20°C in a 0.5 mm quartz cuvette (Hellma). Measurements were collected in triplicate, averaged and background subtracted with matched buffer using Chirascan software. Data were exported to an excel file, and then plotted using Microsoft Excel.

2.33. Dynamic Light Scattering (DLS)

To prepare the protein sample for DLS it was centrifuged for 1 minute at 13000 rpm using a 0.1 µm centrifugal filter (Merck). DLS was performed on a Dynapro Titan DLS instrument (Wyatt). 13 µl of Milli-Q (MQ) H_2O was loaded into a 12 µl 8.5 mm quartz

cuvette (Wyatt) using a gel-loading tip and cuvette loaded into the machine. The laser power was adjusted to 100% and count rate confirmed. The cuvette was cleaned until a stable count rate of less than 40,000 was achieved. The cuvette was dried using compressed air and 13 µl filtered protein sample loaded. The cuvette was placed back in the machine and laser power adjusted until a stable count rate of less than 8 million was achieved. Measurements were taken using the default settings of 10 measurements of 10 seconds each. Data collected was analysed with DYNAMICS software v6 (Wyatt).

2.34. Small molecule - protein Surface Plasmon Resonance (SPR)

The Biolog phenotypic microarray for microbial cells plates PM01 – PM10 (Biolog) were used as a small molecular screening library for small molecule – protein interaction screening. Each 96-well Biolog plate was resuspended with 50 µl MQ H_2O to result in a rough concentration of 5-10 µM. Further 1 in 2000 dilutions were made using SPR running buffer (0.01 M HEPES pH 7.4, 0.15 M NaCl, 0.005% v/v Tween 20) into 2 ml 96-deepwell plates (Starlab). All SPR experiments were performed using a single Sensor Chip CM5 (Cytiva) on a Biacore 8K SPR system (Cytiva) in collaboration with Dr Clare Stevenson at the JIC. The CM5 chip used enabled 8 separate channels for use each with 2 flow cells (FCs). Each FC_1 was used as the reference FC (FC_{REF})with FC_2 used as the test FC (FC_{TEST}).

In order to amine couple the protein to the CM5 chip a type 2 amine coupling kit (Cytiva) was used following manufacturer's instructions. The protein sample was first diluted to 6 µM in 10 mM acetate pH 4.0. The surface of the chip was activated with a 420s injection of a 50% mix of N-hydroxysuccinimide (NHS) / 1-ethyl-3-(3-dimethylaminopropyl)carbodiimide hydrochloride (EDC) at a flow rate of 10 µl/min and then protein was injected over all channels (FC_{TEST} only) with a 420s injection at 10 µl/min. Covalent immobilisation was secured, and the remaining chip surface blocked with 420s of 1.0 M ethanolamine-HCl pH 8.5 at 10 µl/min. The final stable response rate was ∼1000 response units.

Two methods were written by Dr Clare Stevenson: the first to test binding of the compound library and the second to run each 96 well as a separate run. For each plate a start-up cycle consisting of a 60s injection of SPR running buffer at 30 µl/min was followed by a wash cycle with 1M NaCl for 60s at 30 µl/min. For analysis, sample was injected for 60s at 30ul/min and then switched to buffer only flow for dissociation for a further 60s. 1M NaCl was then injected for 60s at 30 µl/min to wash the chip before the next cycle commenced. A negative control of buffer only was run at the start, end and every 16 cycles. All ten 96-well plates were screened in triplicate with each plate replicate taking ~2 hours to complete. Data analysis was performed using the Biacore Insight Evaluation software (Cytiva). The full details of the Biolog PM1-PM10 screening plates can be found at the Biolog website (www.biolog.com).

2.35. Reusable DNA Capture Technology (ReDCaT) SPR

Protein-DNA binding site scanning and footprinting was performed using ReDCaT SPR as previously described (Stevenson *et al.*, 2013). For binding scanning target genomic promoter regions of interest were divided into a series of overlapping fragments by the program POOP (Stevenson *et al.*, 2013). The total length of each fragment was 40 nt with 15 nt overlaps. To be able to create double-stranded (ds) targets each fragment was also reverse-complimented and a ReDCaT biotinylated single-stranded (ss) linker added to the 3' end as an overhang. Fragments were purchased as DNA oligos from IDT and resuspended to 100 µM in dH_2O. For each fragment 55 µl forward oligo was mixed with 45 µl reverse oligo and annealed at 95°C for 5 minutes with slow ramping to 4°C. The ds DNA fragments were then diluted to a final concentration of 1 µM in HBS-EP+ buffer (150 mM NaCl, 3 mM EDTA, 0.05% v/v surfactant P20, 10 mM HEPES pH 7.4). All ReDCaT SPR experiments were performed using a single Sensor Chip SA (GE Healthcare) on a Biacore 8K SPR system (Cytiva) in collaboration with Dr Clare Stevenson at the JIC as follows.

The SA chip used enabled 8 channels for use each with 2 FCs. Each FC_1 was used as the FC_{REF} with FC_2 used as the FC_{TEST}. Binding of the DNA was initially tested to ensure a correct response (~400 response units) and sample protein was diluted to a range

found to also give a good response (2 µM, 1 µM and 500 nM) in HBS-EP+ buffer. DNA capture was achieved (FC_{TEST}) with a contact time of 60s at a flow rate of 10 µl/min. Protein analyte was then added over both FCs for 60s at a flow rate of 50 µl/min followed by a buffer only dissociation of 60s. Regeneration of the chip was achieved with 1 M NaCl, 50 mM NaOH injected for 60s at a flow rate of 10 µl/min over both FCs. All experiments were run in duplicate and data analysis was performed using the Biacore Insight Evaluation software (Cytiva) and Microsoft Excel.

Positive hits from site scanning were selected for footprinting. 2 nt truncations were made from the 3' end of the selected fragments and similarly from the 5' of the inverted fragment. For further footprinting single nucleotide mutations were made to the putative binding sites. Both sets of footprinting fragments underwent the same ReDCaT SPR in duplicate and were analysed as above.

2.36. Protein crystallisation trials

For crystallisation trials protein was dialysed into 50 mM Tris-HCl pH 8.0, 200 mM NaCl and concentrated to 14 mg/ml using an Amicon Ultra-15 3kDa cut-off spin filter (Merck). Trial plates were set-up using an Orxy8 crystallisation robot (Douglas Instruments Ltd) in sitting-drop vapour diffusion format in 96-well 2-drop MRC plates (Molecular Dimensions) using a combination of commercially available (Hampton Research and Molecular Dimensions) and bespoke screens. Drops consisted of 0.3 µl of precipitant solution mixed with 0.3 µl of protein solution with a reservoir volume of 50 µl. The screens were stored at a constant temperature of 18°C and regularly visualised for crystals over a time period of 6 months.

2.37. Protein analysis by SDS-Polyacrylamide Gel Electrophoresis (SDS-PAGE)

A standard 12% polyacrylamide resolving gel was made per **Table 2.9** and cast in 1 mm glass plates using the Mini-PROTEAN® Tetra Handcast System (Bio-Rad). Once

the resolving gel was fully polymerised a short 5% polyacrylamide stacking gel was prepared, per **Table 2.10**, and cast on top of the resolving gel and left to fully set at room temperature. The lanes were set using a 1 mm comb. Protein samples were defrosted on ice and 20 µl was mixed with 20 µl SDS loading buffer (950 µl Bio-Rad Laemmli Sample Buffer, 50 µl β-mercaptoethanol), boiled at 100°C for 10 minutes and pelleted by centrifugated at 13000 rpm for 5 minutes. 10-20 µl supernatant was loaded onto the prepared SDS-PAGE gels alongside 3 µl PageRuler™ Plus Prestained Protein Ladder (Thermo Fisher Scientific). Electrophoresis was carried out in TGS running buffer (25 mM Tris-HCl pH 8.3, 192 mM glycine, 0.1% SDS) at 100 V for 2 hours and stained with InstantBlue Protein Stain (Expedeon) for 1 hour. After de-staining overnight with dH_2O the gels were imaged on a Molecular Imager Gel Doc™ XR System (Bio-Rad). To confirm the presence of 6xHis-tagged protein following SDS-PAGE the InVision™ His-Tag In-Gel Stain (Thermo Fisher Scientific) was used following manufacturer's instructions.

Table 2.9. 12% polyacrylamide resolving gel constituents

Reagent	20 ml solution (4 gels)
1.5 M Tris-HCl pH 8.8	5 ml
40% (w/v) acrylamide	6 ml
10% SDS	200 µl
Tetramethylethylenediamine (TEMED)	10 µl
10% (w/v) ammonium persulfate (APS)	100 µl
Deionised water	8.7 ml

Table 2.10. 5% polyacrylamide stacking gel constituents

Reagent	10 ml solution (4 gels)
1.0 M Tris-HCl pH 6.8	2.5 ml
40% (w/v) acrylamide	1.26 ml
10% SDS	100 µl
TEMED	10 µl
10% (w/v) APS	50 µl
Deionised water	6.08 ml

2.38. Western blot

Following SDS-PAGE (**Chapter 2.37**) the protein samples in polyacrylamide gel were placed on top of a nitrocellulose Biodyne A membrane (Pall Life Sciences) and sandwiched between three layers of soaked blotting paper on either side. The membrane had been prepared by soaking in 100% methanol for 1 minute and washing in transfer buffer (25 mM Tris-HCl pH 8.3, 192 mM glycine, 0.1% SDS, 20% methanol) for 5 minutes. Likewise, the blotting paper had been prepared by soaking in transfer buffer for 5 minutes. The protein samples were transferred to the nitrocellulose membrane using a Trans-Blot SD Semi-Dry Transfer Cell (Bio-Rad) at 10 V for 1 hour. The membrane was then washed twice in TBS buffer (50 mM Tris-HCl pH 7.5, 150 mM NaCl) for 10 minutes and incubated at room temperature overnight in a blocking solution of 5% fat-free skimmed milk powder in TBST buffer (TBS, 1% Tween 20) with gentle rocking. The blocking solution was removed, and the membrane washed with TBST buffer twice for 10 minutes apiece and once with TBS buffer for a further 10 minutes. 20 ml of antibody solution (1:2000 dilution of primary antibody in TBST) was added and incubated at room temperature for 1 hour with gentle rocking. The membrane was washed with TSBT thrice for 1 minute and thrice for 10 minutes. The horseradish peroxidase (HRP) linked secondary antibody was diluted in 20 ml TBST to 1:12000 and incubated with the membrane for 1 hour at

room temperature with gentle rocking. The membrane was then washed with TBST as before (3x1 minute, 3x10 minutes). For development 10 ml developing solution A (100 mM Tris-HCl pH 8.5, 0.01% luminol, 0.0045% coumaric acid) and 10 ml developing solution B (100 mM Tris-HCl pH 8.5, 0.00018% hydrogen peroxide) were combined and added to the membrane. After incubation for 1 minute the fluorescence was detected using a Syngene G:BOX F3 gel doc system.

2.39. Bicinchoninic acid assay (BCA) for protein quantification

To quantify protein samples solutions containing SDS the Pierce™ BCA Protein Assay Kit (Thermo Fisher Scientific) was used following manufacturer's instructions.

2.40. *Streptomyces* whole cell (phospho)proteome extraction

Streptomyces colonies were grown on cellophane covered agar plates as triplicate spots from 5 µl spore spots all in duplicate. After 2- or 9-day incubation at 30°C the mycelium was scraped off the cellophanes into a 15 ml falcon and resuspended in 10 ml cell lysis buffer (50 mM TEAB buffer pH 8.0, 150mM NaCl, 2% SDS, EDTA-free protease inhibitor, PhosSTOP phosphatase inhibitor). The suspension was disrupted via French press 3 times before being boiled at 100°C for 10 minutes. Samples were sonicated at 50 Hz 4 times for 20 seconds per cycle and then pelleted at 4000 rpm for 30 minutes. Protein concentration was determined using the BCA assay (**Chapter 2.39**) and 1 mg of protein from each sample transferred to a fresh 15 ml falcon tube. 4 volumes of methanol were added and vortexed thoroughly before 1 volume chloroform was added and vortexed thoroughly. 3 volumes dH_2O was added, vortex thoroughly, and spun for 10 minutes at 4000 rpm. The upper layer was carefully discarded, 4 volumes of methanol added and vortex thoroughly. The samples were spun for 20 minutes at 4000 rpm before aspirating the supernatant. The pellets were then immediately taken to the JIC proteomics facility on ice.

Sample preparation, isobaric mass tagging, fractionation and subsequent mass spectrometry followed by data processing was all carried out by Dr Gerhard Saalbach and Dr Carlo de Oliveira Martins at the JIC.

2.41. Proteomics sample preparation and isobaric labelling

Pellets from the protein extraction were washed with acetone and dissolved in 50-100 µl of 2.5% sodium deoxycholate (SDC; Merck). After quantification by BCA assay (**Chapter 2.39**), 100 µg (or 75 µg in case of set 2) of protein was reduced, alkylated, and digested with trypsin in the presence of 0.2 M EPPS buffer (Merck) and 2.5% SDC according to standard procedures. After digestion, the SDC was precipitated by adjusting to 0.2% TFA, and the clarified supernatant subjected to C18 solid phase extraction (SPE; OMIX tips; Agilent). Tandem mass tagging (TMT) labelling was performed using Thermo TMT10plex™ kits (Lots TL279977 and TL274393) for set 1 and TMT16plex™ kits (Lot VI306840 and VK309613) for set 2 according to the manufacturer's instructions with slight modifications; the dried peptides were dissolved in 90 µl of 0.2 M EPPS buffer/10% acetonitrile, and 200 µg TMT10plex or 250 µg TMT16plex reagent dissolved in 22 µl of acetonitrile was added. Samples were assigned to the TMT channels in an order avoiding channel leakage between different samples if possible as detailed by Brenes *et al.*, 2019.

2.42. High pH fractionation and phosphopeptide enrichment

After labelling, aliquots of 1.7 µl from each sample were combined and analysed on the mass spectrometer (detailed below) to check labelling efficiency and estimate total sample abundances. The main sample aliquots were then combined correspondingly and desalted using a 50 mg C18 Sep-pak cartridge (Waters). The eluted peptides were dissolved in 500 µl of 25 mM NH_4HCO_3 and fractionated by high pH reversed phase HPLC. Using an ACQUITY Arc Bio System (Waters), the samples were loaded to a Kinetex® 5 µm EVO C18 100 Å LC Column 250 x 4.6 mm (Phenomenex). Fractionation was performed with the following gradient of solvents

A (water), B (acetonitrile), and C (25 mM NH_4HCO_3) at a flow rate of 1 ml/min: solvent C was kept at 10% throughout the gradient; solvent B: 0-5 min: 5%, 5-10 min: 5-13% curve 5, 10-70 min: 13-40%, 70-75 min: 40-50%, 75-80%: 50-80%; followed by 5 min at 80% B and re-equilibration to 5% for 24 minutes. Fractions of 1 ml were collected, dried down, and concatenated to produce on average 25 final fractions for MS analysis. For samples also required for phosphoproteome analysis aliquots of 30-40 µl were first removed and stored at -80 °C for global proteome quantification. The remaining major portions were dried down again and re-dissolved for phosphopeptide enrichment using the method as previously described by Fukuda *et al.*, 2013.

Briefly, 200 µl pipette tips were prepared with 1 mg TiO_2 (Titansphere, 10 µm) per tip suspended in wash buffer (80% acetonitrile, 5% TFA) over a plug of Empore C8 membrane (3M). The tips were washed twice by centrifugation at 3500 rpm for 3 minutes with wash buffer followed by 2 washes with sample buffer (60% acetonitrile, 5% TFA, 5% glycerol). The peptide samples were dissolved in 250 µl sample buffer and loaded to the TiO_2-prepared tips. They were centrifuged twice at 2500 rpm to pass the solution slowly through the TiO_2 tips. The peptide loaded tips were washed twice with 200 µl sample buffer, twice with wash buffer and once with water by centrifuging at 3500 rpm. The phosphopeptides were eluted with 2 portions of 100 µl 0.4 M ammonium hydroxide in 30% acetonitrile by centrifugation at 2500 rpm. The eluate was immediately neutralised by adding 20 µl of 5% formic acid. A final elution step was performed with 50 µl 1 M bis-tris propane (BTP). The BTP eluates from all fractions were combined and acidified with 100% TFA to pH <3.0 followed by desalting using OMIX C18 pipette tips (Agilent). All eluted phosphopeptide fractions were dried using a speedvac, resuspended in 50 µl of 3% acetonitrile/0.1% TFA, and stored at -80 °C.

2.43. Analysis of TMT-labelled samples by LC-MS on an Orbitrap Fusion Tribrid instrument.

Aliquots of all concatenated fractions were analysed by nanoLC-MS/MS on an Orbitrap Eclipse™ Tribrid™ mass spectrometer coupled to an UltiMate® 3000 RSLCnano LC system (Thermo Fisher Scientific). The samples were loaded onto a trap column (nanoEase M/Z Symmetry C18 Trap Column, Waters) with 0.1% TFA at 15 µl/min for 3 minutes. The trap column was then switched in-line with the analytical column (nanoEase M/Z column, HSS C18 T3, 1.8 µm, 100 Å, 250 mm x 0.75 µm, Waters) for separation using the following gradient of solvents A (water, 0.1% formic acid) and B (80% acetonitrile, 0.1% formic acid) at a flow rate of 0.2 µl/min: 0-3 min 3% B (parallel to trapping); 3-10 min increase B curve 4 to 12%; 10-105 min linear increase B to 47%; 105-113 min increase B curve 7 to 99%; followed 3 min at 99% B and re-equilibration to 3% B for 23 minutes. Data were acquired with the following parameters in positive ion mode: MS1/OT: resolution 120K, profile mode, mass range *m/z* 400-1800, AGC target 100%, max inject time 50 ms; MS2/IT: data dependent analysis with the following parameters: top10 in IT Turbo mode (for TMT10plex) or IT Rapid mode (for TMT16plex), centroid mode, quadrupole isolation window 0.7 Da, charge states 2-5, threshold $1.9e^4$, CE = 33 (TMT10plex) or CE=30 (TMT16plex), AGC target standard, max. inject time 50 ms, dynamic exclusion 1 count/15 s/±7 ppm; MS3 synchronous precursor selection (SPS): 10 SPS precursors, isolation window 0.7 Da, HCD fragmentation with CE=65 (TMT10plex) or CE=50 (TMT16plex), Orbitrap Turbo TMT and TMTpro resolution 30k, AGC target 200%, max inject time 105 ms, Real Time Search: protein database *S. coelicolor* A3(2) M145 (uniprot.org, 8126 entries), or protein database *S. venezuelae* (http://strepdb.streptomyces.org.uk/, 7420 entries) enzyme trypsin, 1 missed cleavage, oxidation (M) as variable, carbamidomethyl (C) and TMT6plex or TMTpro as fixed modifications, Xcorr = 1, dCn = 0.05.

2.44. Data processing and statistical analysis for protein and peptide quantification

The raw data were processed and quantified in Proteome Discoverer 2.4.1.15 (Thermo) using the incorporated search engine Sequest HT and the Mascot search engine (Matrix Science; Mascot version 2.7.0, in-house server). The processing workflow included recalibration of MS1 spectra (RC), precursor ion quantification by most confident centroid (20 ppm), fasta database *S. coelicolor* or *S. venezuelae* (as above) and common contaminants (MaxQuant 250 entries), enzyme trypsin, 1 missed cleavage, precursor/fragment tolerance 5 ppm/0.6 Da, variable/fixed modifications were oxidation (M)/carbamidomethyl (C) and TMT6plex or TMTpro. The consensus workflow included the following parameters: unique peptides (protein groups), intensity-based abundance, TMT channel correction values applied (according to Lot number), co-isolation/SPS matches thresholds 50%/80%, normalisation on total peptide abundances, protein abundance-based ratio calculation, missing values imputation by low abundance resampling, hypothesis testing by t-test (background based), adjusted p-value calculation by BH-method.

2.45. Chromatin Immuno-precipitation Sequencing (ChIP-Seq)

Streptomyces were inoculated onto cellophane covered agar plates as triplicate 5 µl colonies and grown for 5-10 days at 30°C. To cross-link proteins to DNA the cellophane disks were removed and submersed in 10 ml fresh 1% (v/v) formaldehyde solution at room temperature for 20 minutes. After a 5-minute incubation in 10 ml 0.5 M glycine the mycelium was harvested and washed twice with 25 ml ice-cold PBS pH 7.4 before being flash frozen in liquid nitrogen and stored at -80°C. For lysis the pellets were resuspended in 2 ml lysis buffer (10 mM Tris-HCl pH 8.0, 50 mM NaCl, 10 mg/ml lysozyme, EDTA-free protease inhibitor) before 750 µl was transferred to a 2 ml microcentrifuge and samples incubated at 37°C for 30minutes. For fragmentation 750 µl IP buffer (100 mM Tris-HCl pH 8.0, 250 mM NaCl, 0.5% v/v Triton X-100, 0.1% SDS, EDTA-free protease inhibitor) was added and samples

sonicated on ice at 50 Hz for 20 cycles of 10 seconds with at least 1 minute of rest between each cycle.

25 µl of the crude lysate was combined with 75 µl TE Buffer (10 mM Tris-HCl pH 8.0, 1 mM EDTA) and extracted with 100 µl phenol:chloroform. 2 µl 1mg/ml RNase A was mixed with 25 µl of the resulting extract, incubated at 37°C for 30 minutes and run on a 1% agarose gel to confirm a smear centred at 500 bp. The remaining crude lysate was centrifuged for 15 minutes at 13000 rpm, 4°C and supernatant saved. To prepare for binding 750 µl of Anti-FLAG M2 magnetic beads (Sigma Aldrich) were washed in 3.75 ml 0.5 IP buffer. The bead slurry was then mixed with 40 µl clarified lysate and incubated overnight on a vertical rotator.

The lysate was removed, and the beads washed 4 times with 500 µl 0.5 IP buffer including 10 minutes vertical rotation at 4°C each cycle. Washed beads were incubated in 100 µl elution buffer (50 mM Tris-HCl pH 7.6, 10 mM EDTA, 1% SDS) overnight at 65°C. Elutant was removed and saved before an additional 50 µl elution buffer was added and incubated at 65°C for a further 5 minutes. Once removed 3 µl 10mg/ml proteinase K was added to the combined eluants and incubated at 55°C for 2 hours. DNA was extracted with 200 µl phenol:chloroform and purified using a QIAquick PCR Purification Kit (QIAGEN) following the manufacturer's instructions. DNA was eluted in 50 µl Buffer EB (10 mM Tris-HCl pH 8.5) and 47 µl snap frozen in liquid nitrogen and stored at -80°C. The remaining 3 µl of sample was used to determine the DNA concentration and quality. The Qubit Fluorometer 2.0 with the high-sensitivity kit was used for DNA concentration whilst DNA purity was quantified using a Nanodrop™ 2000 UV-Vis Spectrophotometer. The stored DNA samples were the shipped to Novogene on dry ice for sequencing using the NovaSeq 6000 Sequencing System (Illumina).

2.46. Analysis of ChIP-Seq Data

Raw sequencing data were received as FASTQ files from Novogene and processed by Dr Govind Chandra (JIC). Raw files were aligned to the relevant reference genome and enrichment normalised to a moving window of 30 nucleotides compared to a region of the surrounding 3000 nucleotides with the window moving in steps of 15 nucleotides.

2.47. Co-immunoprecipitation (co-IP) sample preparation

Co-IP sample preparation followed the same methodology as ChIP-Seq sample preparation (**Chapter 2.45**) until elution from the Anti-FLAG M2 magnetic beads. Elution was instead performed using 30 µl SDS gel loading buffer (4% SDS, 20% glycerol, 200 mM DTT, trace bromophenol blue, and 0.1 M Tris-HCl, pH 6.8) with boiling at 100°C for 5 minutes before being pelleted at 13000 rpm for 1 minute. Samples were loaded onto an SDS-PAGE gel (**Chapter 2.37**), 10% throughout, which had been left overnight to completely polymerise. The samples were run a few millimetres into the gel at 150 V before the gel was removed from the cassette and thoroughly rinsed with dH_2O. The glass plates were opened, gel slices excised, and volumes measured.

The slices were de-stained with 1 ml 30% ethanol for 30 minutes at 65°C, repeating until clear. A wash was then carried out with 1 ml 50 mM TEAB, 50% acetonitrile with vigorous vortexing at room temperature for 20 minutes before incubation with 1 ml 10 mM DTT in 50 mM TEAB for 30 minutes at 55°C. The DTT solution was removed, 1 ml iodoacetamide (IAA) added and samples vigorously vortexed for 30 minutes at room temperature in the dark. The samples were then washed with 1 ml 50 mM TEAB, 50 % acetonitrile at room temperature with vigorous vortexing for 20 minutes followed by an identical wash with 1 ml 50 mM TEAB. The buffer was then removed, slice volume estimated, cut into 1x1 mm pieces using a sterile scalpel and pieces transferred into a fresh 1.5 ml protein LoBind® microcentrifuge tube (Eppendorf). Samples were then washed once with 50 mM TEAB, 50% acetonitrile and twice with

100% acetonitrile with each wash consisting of 20 minutes of vigorous vortexing at room temperature. The acetonitrile was removed, a small hole pierced in the lid and samples dried for 30 minutes in a Genevac miVac centrifugal concentrator (Genevac).

Sample processing, mass spectrometry and data processing was all carried out by Dr Gerhard Saalbach and Dr Carlo de Oliveira Martins at the JIC.

2.48. Co-IP sample mass spectrometry and data processing

Gel slices were prepared according to standard procedures adapted from Shevchenko *et al.*, 2006. Briefly, the slices were washed with 50 mM TEAB buffer pH 8.0 (Sigma), incubated with 10 mM DTT for 30 min at 65 °C followed by incubation with 30 mM IAA at room temperature (both in 50 mM TEAB). After washing and dehydration with acetonitrile, the gels were soaked with 50 mM TEAB containing 10 ng/µl Sequencing Grade Trypsin (Promega) and incubated at 50 °C for 8 hours. The extracted peptide solution was dried down, and the peptides dissolved in 0.1%TFA/3% acetonitrile. Aliquots were analysed by nanoLC-MS/MS on an Orbitrap Eclipse™ Tribrid™ mass spectrometer coupled to an UltiMate® 3000 RSLCnano LC system (Thermo Fisher Scientific). The samples were loaded and trapped using a pre-column with 0.1% TFA at 15 µl/min for 4 minutes. The trap column was then switched in-line with the analytical column (nanoEase M/Z column, HSS C18 T3, 100 Å, 1.8 µm; Waters) for separation using the following gradient of solvents A (dH_2O, 0.1% formic acid) and B (80% acetonitrile, 0.1% formic acid) at a flow rate of 0.2 µl/min : 0-4 min 3% B (parallel to trapping); 4-10 min linear increase B to 8%; 10-60 min increase B to 25%; 60-80 min increase B to 38%; 80-90 min increase B to 60%; followed by a ramp to 99% B and re-equilibration to 3% B. Data were acquired with the following mass spectrometer settings in positive ion mode: MS1/OT: resolution 120K, profile mode, mass range *m/z* 300-1800, AGC $2e^5$, fill time 50 ms; MS2/IT: data dependent analysis was performed using parallel CID and HCD fragmentation with the following parameters: top20 in IT turbo mode, centroid mode, isolation window 1.6 Da, charge states 2-5, threshold $1.9e^4$, CE = 30, AGC target $1e^4$, max. inject time 35 ms, dynamic exclusion 1 count, 15 s exclusion, exclusion mass window ±5 ppm.

Recalibrated peaklists were generated from the MS raw files with MaxQuant 1.6.10.43 (Tyanova, Temu and Cox, 2016) using the *S. venezuelae* protein sequence database (http://strepdb.streptomyces.org.uk/, 7420 entries) plus the MaxQuant contaminants database (250 entries). The final search was performed with the merged HCD and CID peaklists from MaxQuant using in-house Mascot Server 2.7.0 (Matrixscience) on the same databases. For this search a precursor tolerance of 6 ppm and a fragment tolerance of 0.6 Da was used. The enzyme was set to trypsin with a maximum of 1 allowed missed cleavage. Oxidation (M), deamidation (N/Q) and acetylation (protein N-terminus) were set as variable modifications and carbamido-methylation (CAM) of cysteine as fixed modification. The Mascot search results were imported into Scaffold 4.11.0 for visualisation and further analysis.

2.49. β-Glucuronidase activity assays

Streptomyces spp. β-glucuronidase reporter strains were incubated as triplicate 5 µl spots on cellophane covered agar plates for either 2 or 9 days at 30°C. After incubation the mycelium was scraped off into a 2 ml microcentrifuge tube and resuspended in 1 ml GUS dilution buffer (5 mM phosphate buffer pH 7.0, 0.001% (v/v) Triton X-100, 5mM DTT, 1 mg/ml lysozyme). Samples were sonicated 3 times at 50 Hz for 10 seconds per cycle on ice before being pelleted at 13000 rpm for 10 minutes at 4°C. 100 µl of the supernatant was plated in triplicate in a 96-well plate and the remainder used to ascertain sample protein concentration. GUS assay plates were stored at -80°C and dethawed for 30 minutes at 37°C before the addition of 4-Nitrophenyl β-D-glucopyranoside (PNPG) to a final concentration of 10mM. Immediately after the addition of PNPG the plate was incubated at 37°C in a Hidex Sense (Hidex) plate reader for an hour with 200 rpm shaking. Spectrophotometer readings were taken every 5 minutes at 415nm, 550nm and 600nm wavelengths. The data was analysed in Microsoft Excel and visualised in R.

2.50. Biomass and glucose quantification assay

Streptomyces spp. were cultured on cellophane-covered agar plates for 5-14 days at 30°C. Following incubation, the cellophane disks were removed, and mass measured using a Fisherbrand Precision FPRS423 analytical balance (Thermo Fisher Scientific). For extraction of glucose the underlying agar was chopped into small pieces using a sterile scalpel and transferred to a 250 ml conical flask. 20 ml dH_2O was added and samples incubated for 2 hours at 25°C with shaking at 220 rpm. The resulting liquid was aspirated from the flask and diluted 1:1000 with dH_2O before being assayed using the Glucose (GO) Assay Kit (Sigma Aldrich) following manufacturer's instructions.

2.51. Trimethylamine headspace Gas Chromatography-Mass Spectrometry (GC-MS)

Colonies of *Streptomyces* were grown on 5 ml agar slants in 20 ml headspace GC-MS vials (Gerstel) for 10 days at 30°C. Following incubation, the samples were sealed and equalised for 5 hours at room temperature before being transferred to the Molecular Analysis facility at the JIC.

GC-MS analysis and data processing was carried out by Paul Brett. In short, the headspace of samples and standards were injected into an Agilent GC-MS Quad (7890/5977) via a Gerstel MPS with the following settings: Inj. Volume: 250 µl; Inj. Speed: 1000 µl/s; Pullup Delay: 1 s; Fill Speed 200 µl /s, Pre Inj. Delay: 0 s; Post Inj. Delay: 5 s. The GC-MS conditions were as follows: Inlet temp: 250 °C; Inj mode: pulsed split 10:1 20psi until 0.75 min; Column: Zebron HP5-MS INFERNO 30 m + 5m guard, 0.25 mm ID x 0.1 µm; Carrier gas: Helium at constant flow of 1.0 ml/min; Oven temp: Initial – 30°C for 3.0 min, Ramp – 50°C/min 20 220°C, Hold – 10 min, Equilibration time – 0.5 min; Aux temp: 280°C, Acq mode: Scan/SIM; Scan: 45-300; SIM: m/z 58,59; MS temps: Source – 230°C, Quad – 150°C. The MS data was collected at values above m/z 45 to minimise interference from the air peak. Blanks were

analysed between each injection to determine and reduce carryover. The raw GC-MS data were analysed using MassHunter (Agilent).

2.52. Microscopy

Scanning electron microscopy (SEM) was conducted by Kim Findlay at the bioimaging facility at the JIC. Cryogenic sample preparation was performed using an ALTO 2500 cryo-transfer system (Gatan) as follows. *Streptomyces* colonies were excised form the agar plate, mounted on the cryo-holder using Tissue-Tek™ optimal cutting temperature compound (Agar Scientific) and immediately plunged into liquid slush at approximately -210°C to cryo-preserve the material. The sample was transferred onto the cryo-stage of the cryo-transfer system, attached to a FEI Nova NanoSEM 450 FEG scanning electron microscope (Thermo Fisher Scientific). After sublimation of surface frost at -95°C for 3 minutes, the sample was sputter coated with platinum for 2 minutes at 10 mA, at colder than -110°C. The sample was then moved onto the cryo-stage in the main chamber of the microscope, held at approximately -125°C and imaged at 3 kV with images stored as digital TIFF files. Time-lapse imaging was conducted by Dr Susan Schlimpert at the JIC using a Leica M205FA stereo microscope with a DFC310FX colour camera. Images were taken every 30 minutes during a 24-hour period at room temperature and collated using ImageJ. Standard light microscopy was used to check *Streptomyces* spp. cultures for sporulation.

Chapter 3. Identifying and describing the CutRS mutant phenotype in *S. venezuelae*

Identifying and understanding the roles played by TCSs in any organism can prove difficult. The challenge of studying large membrane proteins, such as SKs, combined with the phosphorylation-dependant regulatory effects of the RR results in a potential minefield for research (Tan, Tan and Chung, 2008; Gao and Stock, 2013). This is compounded by the complexity and diversity of TCS regulatory networks in Actinobacteria, such as *Streptomyces* species (Mclean *et al.*, 2019). Despite this, the significant roles these regulatory systems play within bacteria makes their study worthwhile and modern techniques have enabled the use of more systems biology-based approaches. One overarching goal is to create a library of mutant strains each lacking a single TCS to facilitate further study in *S. venezuelae*. To date 45 of the total 58 TCS mutant strains have been created, primarily by previous group members Dr Rebecca Lo and Dr Mahmoud M. Al-Bassam. This includes all 15 which were identified to be highly-conserved among streptomycetes (**Table 3.1**) (Mclean *et al.*, 2019). As outlined in **Chapter 1.9**, the work in this thesis is focussed on just one of these TCS, CutRS, investigating its role in *Streptomyces* development and metabolism, both primary and secondary, using *S. venezuelae* and *S. coelicolor* as model organisms. This chapter describes the *S. venezuelae* Δ*cutRS* mutant phenotype, its features and its limitations.

Table 3.1. Two-component systems in *S. venezuelae* NRRL B-65442 as predicted with P2RP software. Annotations are based on the Pfam database with transmembrane helices (TM) predicted by HMMTOP software. Row highlight colours correspond to status in TCS mutant library: Yellow: mutant created using the ReDIRECT system; Blue: mutant created using pCRISPOmyces-2; Red: mutant not yet available. Adapted from Mclean *et al.*, 2019.

Vnz gene no.	Name	Conserved	Component	Type	TM	Annotation	Function	SCO homologue	Reference
vnz_00735			SK	Classic	6	1 HisKA_3,1 HATPase_c	Under control of the SARP CSR CcaR in the cephamycin C-clavulanic acid BGC	-	Álvarez-Álvarez *et al.*, 2014
vnz_00740			RR	NarL		1 RR-N_rec ,1 HTH_LUXR		-	
vnz_02225			RR	OmpR		1 RR-N_rec,1 Trans_reg_C		-	
vnz_02230			SK	Classic	1	1 HAMP,1 HisKA,1 HATPase_c		-	
vnz_02755			RR	TrxB		1 RR-N_rec, 2 Pyr_redox, Thioredoxin reductase at C-terminus	Upregulated in response to pH shock in *S. coelicolor*	7298	Kim *et al.*, 2008
vnz_02760			SK	Classic	0	Possible incomplete, 1 cNMP_binding,1 HATPase_c		7297	
vnz_03370			RR	NarL		1 RR-N_rec,1 HTH_LUXR		1070	
vnz_03375			SK	Classic	5	1 HisKA_3,1 HATPase_c		1071	
vnz_07060		**yes**	RR	NarL		1 RR-N_rec,1 HTH_LUXR	Upregulated in liquid culture in *S. coelicolor*	1801	Yagüe *et al.*, 2014
vnz_07065			SK	Classic	0	1 GAF,1 HisKA_3,1 HATPase_c		1802	
vnz_07460			SK	Classic	4	1 HisKA_3, 1 HATPase_c		-	
vnz_07465			RR	NarL		1 RR-N_rec,1 HTH_LUXR		1260	

vnz_08725	MacR	**yes**	RR	NarL		1 RR-N_rec,1 HTH_LUXR	Activation of actinorhodin and repression of aerial hyphae formation in *S. coelicolor*	2120	Liu *et al.*, 2019
vnz_08730	MacS		SK	Classic	6	1 HisKA_3,1 HATPase_c		2121	
vnz_08930		**yes**	RR	NarL		1 RR-N_rec,1 HTH_LUXR	Not involved in antibiotic production in *S. coelicolor*	2165	Yepes *et al.*, 2011
vnz_08935			SK	Classic	4	1 HisKA_3,1 HATPase_c		2166	
vnz_09645			RR	NarL		1 RR-N_rec,1 HTH_LUXR		-	
vnz_09650			SK	Classic	4	1 HisKA_3,1 HATPase_c		1259	
vnz_09810			SK	Classic	6	1 HisKA_3,1 HATPase_c		2307	
vnz_09815			RR	NarL		1 RR-N_rec,1 HTH_LUXR		2308	
vnz_10715			SK	Classic	6	1 HisKA_3,1 HATPase_c		3757	
vnz_10720			RR	NarL		1 RR-N_rec,1 HTH_LUXR		3756	
vnz_10755			SK	Classic	0	1 HAMP,1 HisKA,1 HATPase_c	Upregulated in response to pH shock in *S. coelicolor*	7231	Kim *et al.*, 2008
vnz_10760			RR	OmpR		1 RR-N_rec,1 Trans_reg_C		7232	
vnz_11720			SK	Classic	5	1 HisKA_3,1 HATPase_c		-	
vnz_11725			SK	Classic	0	1 PAS_4,1 HisKA,1 HATPase_c		-	
vnz_11730			RR	OmpR		1 RR-N_rec,1 Trans_reg_C		-	
vnz_12685			SK	Classic	3	1 HAMP,1 HisKA,1 HATPase_c		2800	
vnz_12690			RR	OmpR		1 RR-N_rec,1 Trans_reg_C		2801	

vnz_12785			RR	NarL		1 RR-N_rec,1 HTH_LUXR	Upregulated in response to pH shock in *S. coelicolor*	4668	Kim *et al.*, 2008
vnz_12790			SK	Classic	3	1 HisKA_3,1 HATPase_c		4667	
vnz_13520	MtrB	**yes**	SK	Classic	2	1 HAMP,1 HisKA,1 HATPase_c	Life cycle and antibiotics	3012	Som *et al.*, 2017
vnz_13525	MtrA		RR	OmpR		1 RR-N_rec,1 Trans_reg_C		3013	
vnz_13755	DraK	**yes**	SK	Classic	2	1 HisKA,1 HATPase_c	Represses and activates secondary metabolites in response to pH stress	3062	Yu *et al.*, 2012; Yeo *et al.*, 2013
vnz_13760	DraR		RR	OmpR		1 RR-N_rec,1 Trans_reg_C		3063	
vnz_15850	CseB		RR	OmpR		1 RR-N_rec,1 Trans_reg_C	Envelope stress	3358	Paget, Leibovitz and Buttner, 1999
vnz_15855	CseC		SK	Classic	3	1 HAMP,1 HisKA,1 HATPase_c		3359	
vnz_15960	TunR	**yes**	RR	NarL		1 RR-N_rec,1 HTH_LUXR	Tunicamycin resistance	3389	Wyszynski *et al.*, 2010
vnz_15965	TunS		SK	Classic	4	1 HisKA_3,1 HATPase_c		3390	
vnz_16275			SK	Classic	2	1 HisKA_3,1 HATPase_c		3750	
vnz_16280			RR	NarL		1 RR-N_rec,1 HTH_LUXR		-	
vnz_16750			RR	NarL	0	1 RR-N_rec,1 HTH_LUXR		3638	
vnz_16755			SK	Classic	6	1 HisKA_3,1 HATPase_c		3639	
vnz_16940	EcrE2		RR	NarL		1 RR-N_rec,1 HTH_LUXR	Regulation of RED production in *S. coelicolor*	6422	Wang *et al.*, 2007
vnz_16945	EcrE1		SK	Classic	4	1 HisKA_3,1 HATPase_c		6421	
vnz_17085			RR	NarL		1 RR-N_rec,1 HTH_LUXR	Unique to *S. venezuelae* NRRL B-65442	-	
vnz_17090			SK	Classic	3	1 HisKA_3,1 HATPase_c		-	

vnz_17480			SK	Classic	2	1 HAMP,1 HisKA,1 HATPase_c		-	
vnz_17485			RR	OmpR		1 RR-N_rec,1 Trans_reg_C		-	
vnz_17825			RR	NarL		1 RR-N_rec,1 HTH_LUXR		-	
vnz_17830			SK	Classic	6	1 HisKA_3,1 HATPase_c		-	
vnz_18555	CagR		RR	OmpR		1 RR-N_rec,1 Trans_reg_C	Global regulator of clavulanic acid and primary metabolism in *S. clavuligerus*	4020	Song *et al.*, 2009; Fu *et al.*, 2019
vnz_18560	CagS		SK	Classic	1	1 HAMP,1 HisKA,1 HATPase_c		4021	
vnz_18845	RagR		RR	NarL		1 RR-N_rec,1 HTH_LUXR	Regulation of development	4072	Paolo *et al.*, 2006
vnz_18850	RagK		SK	Classic	6	1 HisKA_3,1 HATPase_c		4073	
vnz_19150			RR	NarL		1 RR-N_rec,1 HTH_LUXR		4123	
vnz_19155			SK	Classic	5	1 HisKA_3,1 HATPase_c		4124	
vnz_19330	CssS	**yes**	SK	Classic	2	1 HAMP,1 HisKA,1 HATPase_c	Misfolded protein stress	4155	Gullón, Vicente and Mellado, 2012
vnz_19335	CssR		RR	OmpR		1 RR-N_rec,1 Trans_reg_C		4156	
vnz_19580	PhoR	**yes**	SK	Classic	1	1 HisKA,1 HATPase_c	Phosphate limitation	4229	Sola-Landa, Moura and Martín, 2003
vnz_19585	PhoP		RR	OmpR		1 RR-N_rec,1 Trans_reg_C		4230	
vnz_19880	SenR		RR	NarL		1 RR-N_rec,1 HTH_LUXR		4276	Ortiz De Orué Lucana and Groves, 2009
vnz_19885	SenS		SK	Classic	5	1 HisKA_3,1 HATPase_c		4275	

vnz_21250	AbrC3		RR	NarL		1 RR-N_rec,1 HTH_LUXR		4596	
vnz_21255	AbrC2	**yes**	SK	Classic	4	1 HisKA_3,1 HATPase_c	Antibiotics	4597	Rodríguez *et al.*, 2015
vnz_21260	AbrC1		SK	Classic	4	1 HisKA_3,1 HATPase_c		4598	
vnz_22090	EsrS		SK	Classic	6	1 PspC,1 HATPase_c		4791	
vnz_22095	EsrR	**yes**	RR	NarL		1 RR-N_rec,1 HTH_LUXR	Envelope stress	4792	Kleine *et al.*, 2017
vnz_22600	AfsQ2		SK	Classic	2	1 HAMP,1 HisKA,1 HATPase_c		4906	
vnz_22605	AfsQ1	**yes**	RR	OmpR		1 RR-N_rec,1 Trans_reg_C	Nitrogen limitation	4907	Shu *et al.*, 2008
vnz_24545			SK	Classic	2	1 HAMP,1 HisKA,1 HATPase_c		5282	
vnz_24550		**yes**	RR	OmpR		1 RR-N_rec,1 Trans_reg_C		5283	
vnz_24860	ChiR		RR	NarL		1 RR-N_rec,1 HTH_LUXR		5377	
vnz_24865	ChiS		SK	Classic	5	1 HisKA_3,1 HATPase_c	Chitin utilisation	5378	Tsujibo *et al.*, 1999
vnz_25130			RR	CheY		1 RR-N_rec		5434	
vnz_25135			SK	Classic	0	Probable incomplete, 1 PAS, 1 HATPase_c		5435	
vnz_25235			SK	Classic	5	1 HisKA_3,1 HATPase_c		7711	
vnz_25240	AbsA2		RR	NarL		1 RR-N_rec,1 HTH_LUXR	Butyrolactone BGC	3226	Brian *et al.*, 1996
vnz_26330			RR	NarL		1 RR-N_rec,1 HTH_LUXR		6667	
vnz_26335			SK	Classic	6	1 HisKA_3,1 HATPase_c	Upregulated in response to pH shock in *S. coelicolor*	6668	Yagüe *et al.*, 2014

vnz_26705	OsaC	**yes**	SK	Hybrid	0	1 HATPase_c_2, 1 PAS, 2 GAF, 1 SpoIIE	Osmotic stress	5747	
vnz_26710	OsaA		SK	Hybrid	1	11 HAMP,1 GAF,1 HisKA,1 HATPase_c		5748	
vnz_26715	OsaB		RR	CheY		1 RR-N_rec		5749	
vnz_26805			RR	NarL		1 RR-N_rec,1 HTH_LUXR	Siderophore BGC	-	
vnz_26810			SK	Classic	5	1 HisKA_3,1 HATPase_c		-	
vnz_26890	GluR	**yes**	RR	OmpR		RR-N_rec,1 Trans_reg_C	Glutamate uptake	5778	Li, Jiang and Lu, 2017
vnz_26895	GluK		SK	Classic	2	1 HAMP,1 HisKA,1 HATPase_c		5779	
vnz_27015			RR	NarL		1 RR-N_rec,1 HTH_LUXR		2358	
vnz_27020			SK	Classic	2	1 HisKA_3,1 HATPase_c		2359	
vnz_27230			SK	Classic	4	1 HisKA_3,1 HATPase_c		5824	
vnz_27235			RR	NarL		1 RR-N_rec,1 HTH_LUXR		5825	
vnz_27250			RR	unclassified		1 RR-N_rec,1 HTH_11		5828	
vnz_27255			SK	Classic	1	Probable incomplete; 1 HATPase_c		5829	
vnz_27390	CutR	**yes**	RR	OmpR		1 RR-N_rec,1 Trans_reg_C	Antibiotic production	5862	Tseng and Chen, 1991
vnz_27395	CutS		SK	Classic	2	1 HAMP,1 HisKA,1 HATPase_c		5863	
vnz_27435	KdpD		SK	Classic	4	1 HisKA,1 HATPase_c	Potassium transport	5871	Heermann, Lippert and Jung, 2009
vnz_27440	KdpE		RR	OmpR		1 RR-N_rec,1 Trans_reg_C		5872	

vnz_28060	DegS	SK	Classic	2	1 HAMP,1 HisKA_3,1 HATPase_c	Antibiotics and secretion of proteins	5784	Rozas, Gullón and Mellado, 2012
vnz_28065		RR	NarL		1 RR-N_rec,1 HTH_LUXR			
vnz_28455		RR	NarL		1 RR-N_rec,1 HTH_LUXR		-	
vnz_28460		SK	Classic	4	1 HisKA_3,1 HATPase_c		-	
vnz_28510	DegU	RR	NarL		1 RR-N_rec,1 HTH_LUXR		5785	
vnz_28515		SK	Classic	4	1 HisKA_3,1 HATPase_c		-	
vnz_30150	HrrA	RR	NarL		1 RR-N_rec,1 HTH_LUXR	Haem dependent homolog of *Corynebacterium diphtheriae*	1370	Bibb, Kunkle and Schmitt, 2007
vnz_30155	HrrS	SK	Classic	4	1 HisKA_3,1 HATPase_c		1369	
vnz_30210		SK	Classic	4	1 HisKA_3,1 HATPase_c	Homologs in Polyenoyltetramic Acid α-Lipomycin BGC in *S. aureofaciens* Tü117	6253	Bihlmaier *et al.*, 2006
vnz_30215		RR	NarL		1 RR-N_rec,1 HTH_LUXR		6254	
vnz_30700		RR	NarL		1 RR-N_rec,1 HTH_LUXR		-	
vnz_30705		SK	Classic	4	1 HisKA_3,1 HATPase_c		-	
vnz_32125	ResD	RR	OmpR		RR-N	Homologs from *B. subtilis* possible involvement in anaerobic stress	3741	Van Keulen *et al.*, 2007
vnz_32130	ResE	SK	Classic	3	1 HisKA,1 HATPase_c		3740	
vnz_33685	VanR	RR	OmpR		1 RR-N_rec,1 Trans_reg_C	Vancomycin resistance but no vanJ, vanK or vanHAX genes in *S. venezuelae*	3590	Hong *et al.*, 2004
vnz_33690	VanS	SK	Classic	2	1 HAMP,1 HisKA,1 HATPase_c		3589	

vnz_35360	SK	Classic	2	1 HAMP,1 HisKA,1 HATPase_c	-
vnz_35365	RR	OmpR		1 RR-N_rec,1 Trans_reg_C	-
vnz_36030	SK	Classic	5	1 HisKA_3,1 HATPase_c	-
vnz_36035	RR	NarL		1 RR-N_rec,1 HTH_LUXR	-
vnz_36355	RR	OmpR		1 RR-N_rec,1 Trans_reg_C	-
vnz_36360	SK	Classic	2	1 HAMP,1 HisKA,1 HATPase_c	-

3.1. The *S. venezuelae* Δ*cutRS* mutant phenotype

The TCS mutant library was screened for phenotypic differences to the wild-type strain (WT) under a number of different growth conditions including base media and additives. Under most of these conditions there was no discernible visible differences between each mutant strain and the WT at a colony level. It is possible that there were molecular phenotypic differences incapable of being discerned by eye but due to the number of strains, range of screens and potential cost of sensitive molecular techniques it was deemed impractical to screen for these at the time. However, one condition that was screened was for changes to the *S. venezuelae* exploration phenotype discussed in **Chapter 1.5** (Jones *et al.*, 2017). All 45 *S. venezuelae* TCS mutant strains, as well as the *S. venezuelae* WT strain, were cultured on both YP and YPD agar plates (**Table 2.1**) for 14 days at 30°C before being observed. As previously mentioned, most strains showed no variation from the *S. venezuelae* WT strain however one strain displayed an obvious difference on YPD agar, the Δ*vnz_27390/95*

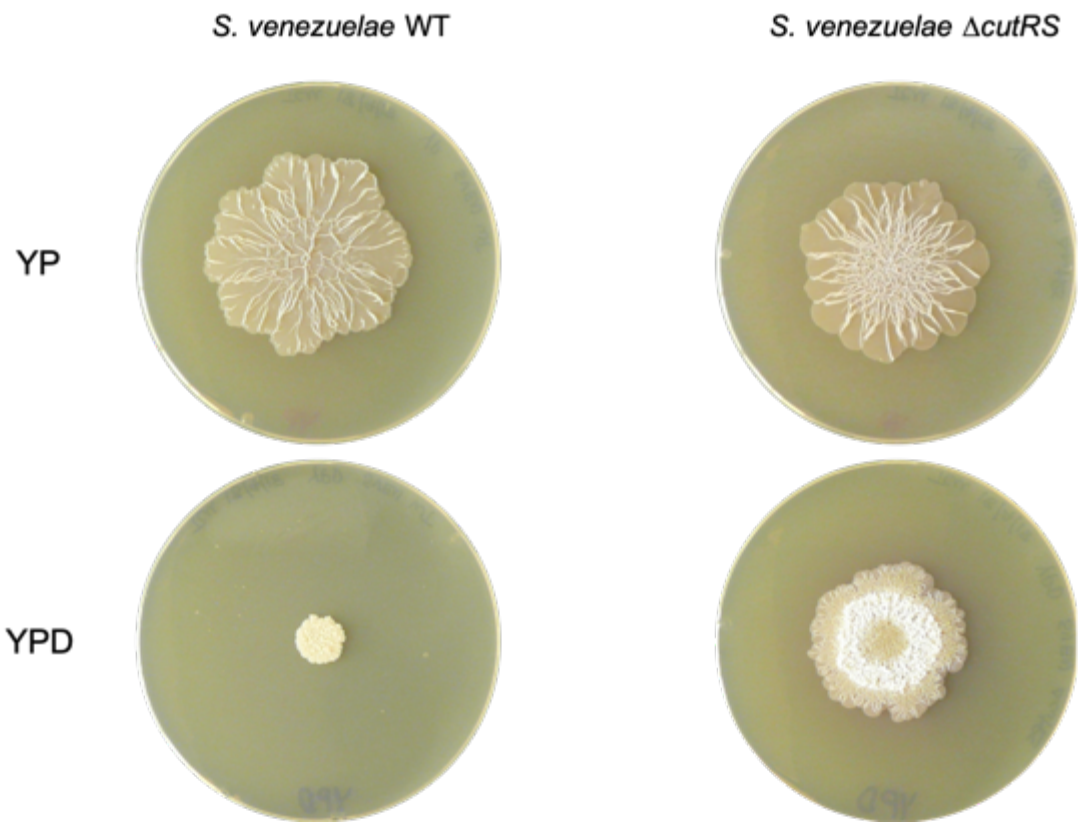

Figure 3.1. *S. venezuelae* WT and Δ*cutRS* strains cultured for 14 days on YP (- glucose) and YPD (+ glucose) solid media.

mutant strain (**Figure 3.1**). This operon encodes for a TCS homologous to the *cutRS* TCS identified in *S. lividans* and *S. coelicolor* discussed in **Chapter 1.8.**

Both the *S. venezuelae* WT and Δ*cutRS* strains appear to have a similar colony structure and are exploring on YP agar as would be expected, whilst exploration was inhibited in the WT strain by addition of glucose (YPD agar). However, with the addition of glucose the Δ*cutRS* mutant formed a much larger colony than the WT with stark phenotypic differences which could be split into three "zones". The central "zone" appears similar to the WT colony in its entirety and is surrounded by a white middle "zone" reminiscent of immature aerial hyphae production. Finally, the outside "zone" has an appearance similar to the exploration hyphal growth visible on the YP plates. Interestingly, whilst the WT colony on YPD would remain unchanged for any period after 14 days, the Δ*cutRS* colony would continue to expand but only as the outside "zone", with the middle and centre "zones" remaining unchanged.

To confirm the phenotype was due to deletion of the *cutRS* operon and not off-target genomic effects the mutant strain was complemented *in trans* with two plasmid constructs (**Figure 3.2**). The first, pSS170-*cutRS*, contained the *cutRS* operon and included 550 bp upstream of the translational start codon. This large region was chosen as a conservative comparison to the non-coding region found in the original *S. lividans* 1.69 kb *Pst*I fragment (Tseng and Chen, 1991). The aim was to be as confident as possible that the *cutRS* promoter had been included to allow for WT-level gene regulation and expression. The second construct, pIJ10257-*cutRS*, is a variant on the first with the native promoter replaced by the strong constitutive *ermE** promoter (Hong *et al.*, 2005).

As can be seen **in Figure 3.2** both constructs complemented the mutant phenotype fully. This confirms the phenotype seen in the Δ*cutRS* mutant results only from the deletion of the *cutRS* operon. The ability for full complementation to occur under *ermEp**, as well as the native promoter, suggests strong, constitutive expression, removing temporal or life cycle linked regulation, does not lead to any deleterious effects or other phenotypic changes. This is presumably due to the fact that, as with

other TCS RRs, activity is controlled post-translationally by the phosphorylation state of CutR.

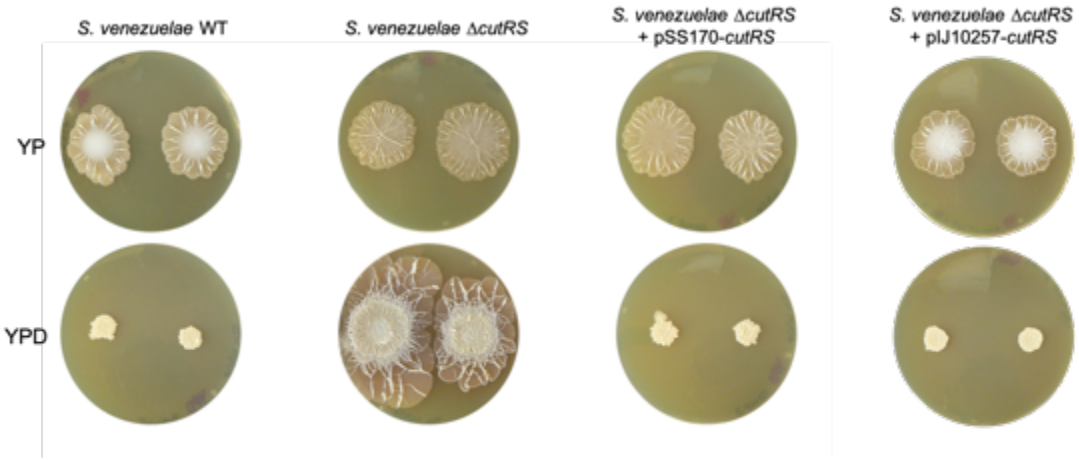

Figure 3.2. Complementation of the *S. venezuelae* Δ*cutRS* mutant phenotype *in trans* by both pSS170-vnz_*cutRS* and pIJ10257-vnz_*cutRS* on YP and YPD agar.

Streptomyces exploration can be identified by certain hallmark features, as discussed in **Chapter 1.5**. These include the presence of elongated vegetative hyphae with very few branches, rapid horizontal growth and the production of mVOCs, including TMA, capable of inducing exploration in physically disconnected streptomycete colonies. With the outer "zone" of the Δ*cutRS* mutant on YPD appearing exploration-like it seemed logical to test for these hallmarks.

The simplest test to begin with was to check the hydrophobic properties of the colonies. To enable escape from the aqueous environment of vegetative growth, aerial hyphae are coated in a hydrophobic sheathing of chaplin proteins (Elliot *et al.*, 2003). Lacking this coating, vegetative hyphae, and explorer cells, are hydrophilic (Jones *et al.*, 2017). Using droplets of dilute bromophenol blue, the hydrophobic properties of colony superstructure can be determined; if the droplet stays formed then the surface is hydrophobic and if it collapses the surface is hydrophilic. **Figure 3.3A** and **Figure 3.3B** show that, whilst the centre of YP-exploring colonies of *S. venezuelae* WT and Δ*cutRS* are hydrophobic, as you move towards the outer parts of the colony the explorer cells are more prevalent and hydrophilic properties appear. In contrast, the WT strain growing on YPD (**Figure 3.3C**) displayed a consistently

hydrophobic surface. The Δ*cutRS* mutant strain on YPD (**Figure 3.3D**) is tripartite, as discussed above. The central "zone" is similar to the WT on YPD with the middle "zone" showing even stronger hydrophobicity. However, as the outer "zone" of the colony is reached the surface properties change, becoming hydrophilic which is suggestive of explorer hyphae production.

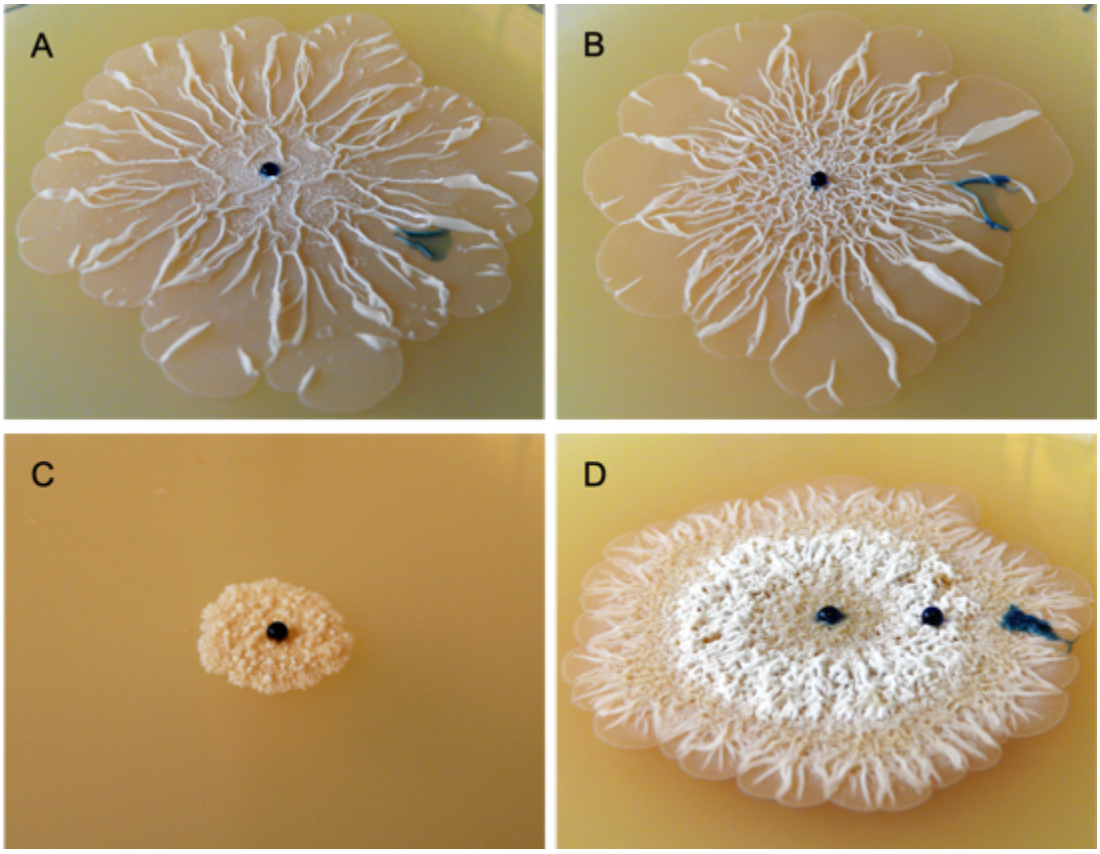

Figure 3.3. The hydrophobic properties of *S. venezuelae* colonies visualised using droplets of dilute bromophenol blue. **A)** *S. venezuelae* WT on YP. **B)** *S. venezuelae* Δ*cutRS* on YP. **C)** *S. venezuelae* WT on YPD. **D)** *S. venezuelae* Δ*cutRS* on YPD.

To observe the hyphae in more detail SEM was used (**Figure 3.4**). At 8000x magnification the hyphal superstructure can be clearly seen with the centre "zones" of both strains on YP showing evidence of septal formation, indicating the presence of maturing aerial hyphae. However, this is far more prominent in the YP cultured Δ*cutRS* sample with more vegetative hyphae present in the WT sample. The outer "zones" of the YP cultured strains appear to show distinct explorer hyphae;

elongated with few or no branches although this can be harder to discern in the Δ*cutRS* image as the hyphae are more tightly entwined. The central, and only, "zone" of the *S. venezuelae* WT colony on YPD reveals very short, stubby hyphae with multiple branches. At a microscopic level the central "zone" of the Δ*cutRS* colony on YPD appears more similar to that of the central "zones" of the mutant YP, rather than the WT on YPD, as indicated at macroscopic level. The vast majority of the middle "zone" is aerial hyphae with septal formation visible in many of the hyphae. Finally, the outer "zone" appears similar to both outer "zones" of *S. venezuelae* WT and Δ*cutRS* on YP suggesting the transition from aerial hyphae production to exploration has occurred in this part of the colony. However, it would be prudent to perform more SEM experiments to confirm these findings as some of these images are not fully conclusive. This poses some interesting questions as whilst *S. venezuelae* WT develops in an exploration-like style from the start on YP, the Δ*cutRS* mutant appears to transition from a classical lifestyle to exploratory development at some point during the 14-day culture time, and that this may occur at a distinct timepoint as indicated by the colony-level "zones".

To compare the growth rate of the strains stereo microscopy was used to create 24-hour time-lapse videos available at https://figshare.com/s/e86e6f7f0b60dbb559f7 (**Figure 3.O1)**. As previously discussed in **Chapter 1.5** exploratory hyphal tip extension is 10x faster than regular hyphal tip extension, reportedly 0.13 µm/min (Jones and Elliot, 2017). Whilst we are unable to determine accurate numbers for growth rate using the time-lapse microscopy, we are able to compare between the samples. When comparing both strains on YP to *S. venezuelae* WT on YPD growth is clearly much more rapid with analysis estimating it indeed to be around 10x faster, matching the reports by Jones and Elliot, 2017. By the same method we are able to estimate the growth rate of the Δ*cutRS* mutant on YPD to be even faster, roughly 1.7µm/min; 30% faster than the YP explorers and 13x faster than the WT control.

The final hallmark to check was for the production of mVOCs capable of inducing exploration in physically disconnected streptomycete colonies. We used a similar experimental procedure as used in the original exploration study (Jones *et al.*, 2017) but instead of using a single partitioned Petri dish we opted to use a combination of

small round (50 mm) and large square (100 mm) Petri dishes. The small Petri dish (P_{Small}) was placed without its lid inside the large Petri dish (P_{Large}) to allow for gas exchange whilst preventing diffusion through the solid media. P_{Small} always contained *S. venezuelae* WT on YPD, a combination that prevents exploration without external influence but is capable of being exploration-induced by mVOCs such as TMA. Meanwhile in P_{Large} we cultured *S. venezuelae* WT (**Figure 3.5A**) or Δ*cutRS* (**Figure 3.5B**) on YP or YPD for 20 days, imaging at both 10 and 20 days. In the top row of both **Figure 3.5A** and **Figure 3.5B** we can observe the expected induction of exploration in P_{Small} by both *S. venezuelae* WT and Δ*cutRS* exploring on YP, most obviously at 20 days but change can also be observed at the earlier 10-day timepoint.

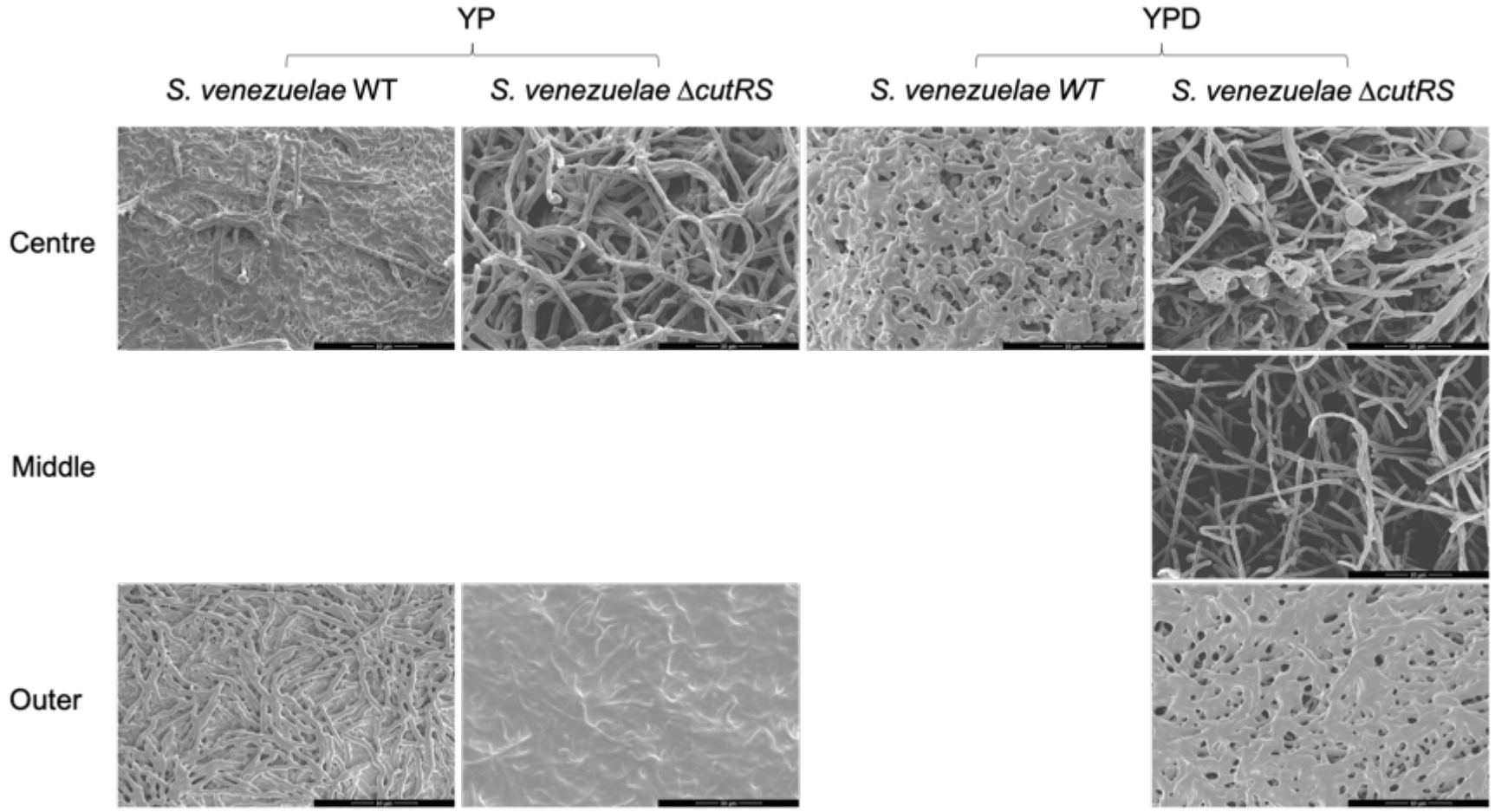

Figure 3.4. Scanning electron micrographs of *S. venezuelae* WT and Δ*cutRS* on YP and YPD at 8000x magnification separated by "zone". Where no image is present there was no biological "zone" to image.

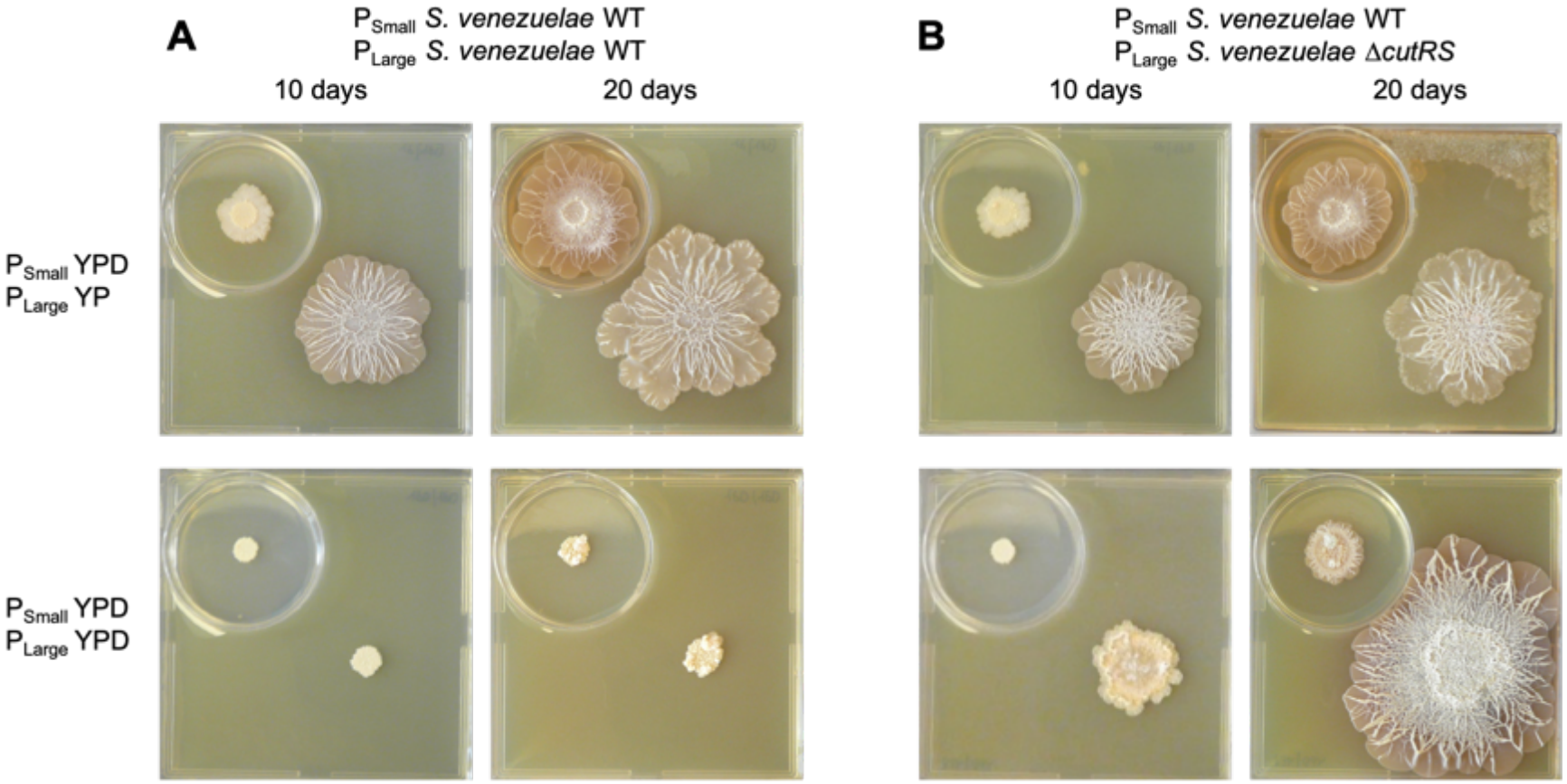

Figure 3.5. Induction of exploratory behaviour by microbial volatile organic compounds (mVOCs) imaged after 10- and 20-day incubation. The small (50 mm) Petri dishes contain *S. venezuelae* WT on YPD – P_{Small}. The large (100 mm) square Petri dishes contain the variable – P_{Large}. **A)** Top row P_{Large} : *S. venezuelae* WT – YP. Bottom row P_{Large} : *S. venezuelae* WT – YPD. **B)** Top row P_{Large} : *S. venezuelae* Δ*cutRS* – YP. Bottom row P_{Large} : *S. venezuelae* Δ*cutRS* – YPD

As expected, the inability of the WT on YPD to produce TMA results in an unchanging P_{Small} even after 20 days. The Δ*cutRS* mutant on YPD in the bottom row of **Figure 3.5B** is capable of inducing exploration in P_{Small} indicating the production of TMA, or similar mVOCs with the same effect. Interestingly the phenotypic change in P_{Small} was only observable at the 20-day timepoint, not after 10 days. This corresponds with the colony structure observed at 10 days which, whilst different to the WT strain, presents no obvious explorer hyphae i.e., no outer "zone". After 20 days that outer "zone" is present, and extensive, and it is likely that the developmental transition that occurs between 10 and 20 days also leads to the production of TMA.

We attempted to confirm the presence of TMA with GC-MS. Using agar slants in GC-MS vials we were able to culture the strains on solid YP and YPD, accumulating headspace for the final 5 hours before GC-MS analysis (**Figure 3.6A**). However, this analysis proved to be challenging; TMA is very small, volatile and was found to elute extremely early during gas chromatography, close to the air peak (oxygen/nitrogen). Using a 0.01% standard, TMA was found to elute at a retention time of 1.65 minutes however there was little evidence of the same peak in the test samples. Instead, we found a peak at 1.78 minutes with a similar but not identical m/z 59:58 ratio suggesting the presence of a different amine (m/z 58 = $C_3H_8N^+$). However, due to the very low abundance of this peak in scan mode it was unfortunately not possible to extract a useful mass spectrum (**Figure 3.6B**). This peak was greatly increased in the YP samples compared to the YP blank and the WT on YPD suggestive of an explorer-specific amine-based mVOC similar to TMA. Whilst the same compound was more abundant in the Δ*cutRS* YPD samples (mean peak area = 925, n=4) compared to the WT YPD samples (mean peak area = 381.5, n=4), both were fairly comparable to the blank samples.

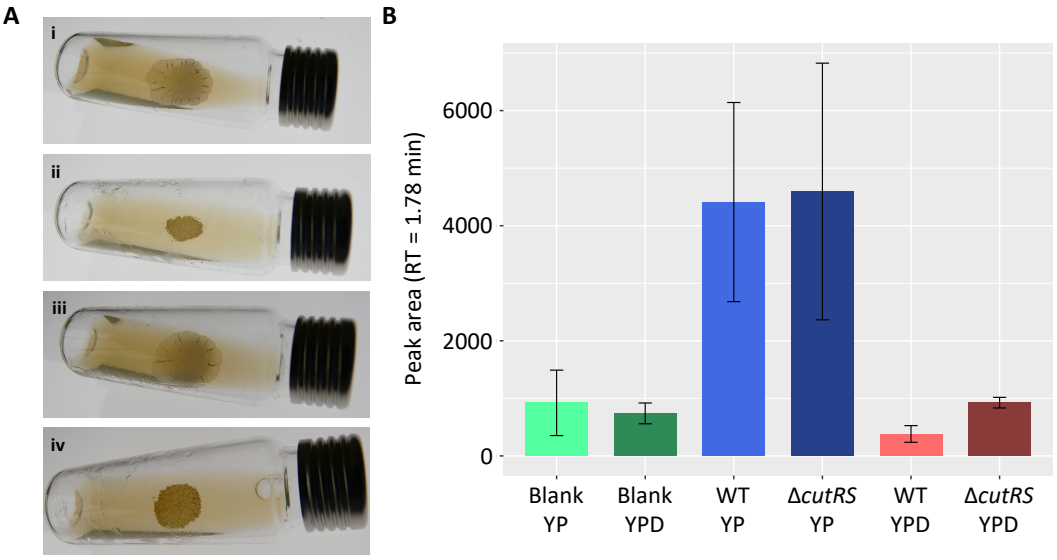

Figure 3.6. A) *Streptomyces* cultures growing on agar slants for GC-MS head-space analysis: i) *S. venezuelae* WT – YP; ii) *S. venezuelae* WT – YPD; iii) *S. venezuelae* Δ*cutRS* – YP; iv) *S. venezuelae* Δ*cutRS* – YPD. **B)** Bar graph showing the GC-MS recorded peak area for a retention time of 1.78 minutes comparing *S. venezuelae* WT and Δ*cutRS* on YP and YPD.

It has been previously shown that TMA is not the only mVOC capable of inducing exploration, indeed any volatile compound able to lower the pH of the growth media is able to induce exploration in physically separated colonies (Jones *et al.*, 2017). If the volatile amine detected by GC-MS is indeed a TMA-like mVOC then this would corroborate with the abundance in YP samples compared to YPD samples. However, as we have observed the Δ*cutRS* mutant inducing exploration when cultured on YPD (**Figure 3.5B**) it must produce alkaline mVOCs itself. Due to the size of the GC-MS vials we were limited to an incubation time of 10 days, after this the depth of the agar did not support growth as it would start to dry and crack. It is possible that the Δ*cutRS* mutant on YPD is producing a different alkaline mVOC to the strains grown on YP but it is more likely that due to the time restraint the mutant was unable undergo the phenotypic change as observed in **Figure 3.5B** where it took 20 days rather than 10 days to see induction of exploration in P_{Small}. If we were able to collect the headspace of the strains cultured for 20 days, it would be likely that the same compound detected in the GC-MS at 1.78 minutes would be present in the Δ*cutRS* YPD samples.

When we combine the results of all the experiments described above it seems most likely that the *S. venezuelae* Δ*cutRS* mutant is exploring when cultured on YPD, a growth medium which normally represses exploration. There appears to be an important developmental shift occurring during the long-term growth of the mutant, switching from one phenotype, still distinct to the WT, to a different phase where it explores, producing the elongated hydrophilic hyphae and exuding mVOCs capable of inducing exploration in distant colonies of *Streptomyces.*

3.2. Further microbiological characterisation of the *cutRS* mutant

The phenotypic changes described above are clearly a response to the presence of glucose, which raised the question: is it limited to solely glucose, or can other sugars induce the same effect? To test this, *S. venezuelae* WT and Δ*cutRS* were cultured on YP containing a range of sugars at the same concentrations (**Figure 3.7**). Glucose is the monosaccharide previously shown to repress exploration, whilst glycerol was included in the screen as it has been shown to exacerbate exploration (Elliot. M. A, unpublished work). The results of **Figure 3.7** show that glucose is the only sugar tested that is capable of repressing exploration on YP media and YP + glucose (YPD) is the only media where there is a phenotypic difference between the WT and Δ*cutRS* strains. It is possible other sugars not included in this screen could have an effect, or indeed the effects could be only evident at specific concentrations not assayed here.

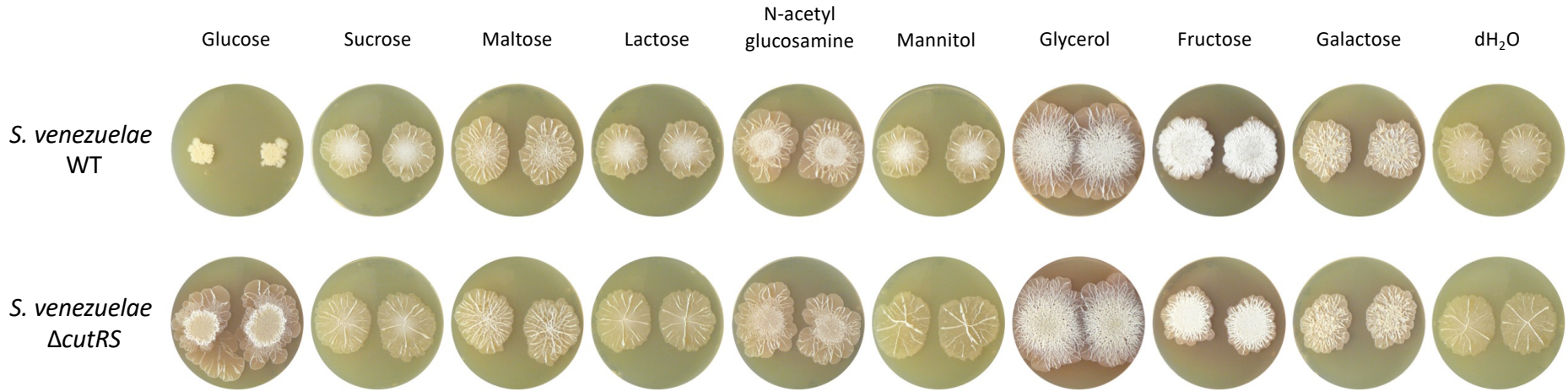

Figure 3.7. *S. venezuelae* WT and Δ*cutRS* cultured on YP media supplemented with various saccharides and glycerol with dH_2O as the negative control.

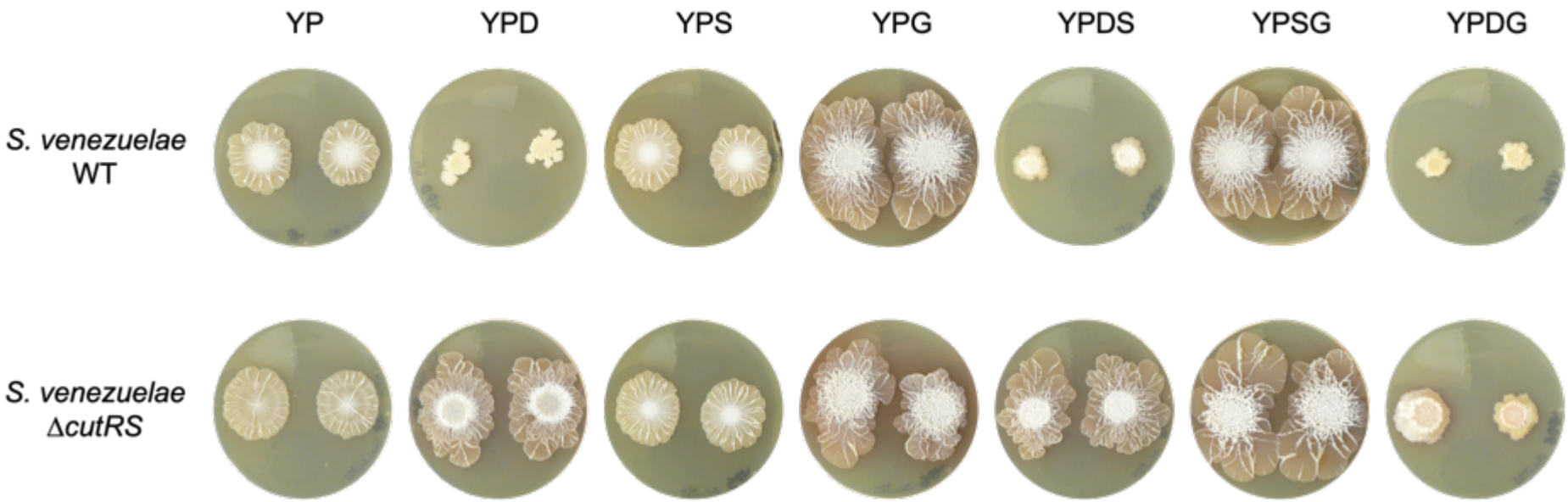

Figure 3.8. *S. venezuelae* WT and Δ*cutRS* strains cultured on YP supplemented with various sugars or combinations thereof. D: glucose; S: sucrose; G: glycerol.

To attempt to determine carbon source hierarchy between the exploration repressive glucose and exploration intensifying glycerol a simple combinatorial approach was undertaken using sucrose as the control sugar supplement (**Figure 3.8**). The combination of glucose and sucrose (YPDS) was unable to alter the regular YPD phenotype of either the WT or Δ*cutRS*. Combining sucrose and glycerol (YPSG) had a similar outcome, with no change from the YP with glycerol (YPG) plates. However, by combining glucose and glycerol (YPDG) we can observe a WT phenotype similar to YPD, suggesting that glucose is preferred as a carbon source to glycerol. Whilst the Δ*cutRS* mutant on YPDG does have a slightly different phenotype to YPD growth, it still displays the larger colonies with three "zones" – the outer "zone" is slightly underdeveloped at the timepoint, suggestive of glycerol perhaps delaying the phenotypic transition but not repressing it completely and certainly not exacerbating it as seen on YPG. Together this suggests that of these three compounds glucose is the preferred carbon source, followed by glycerol with sucrose the least preferential. Further experiments could be carried out to create a full YP sugar supplement hierarchy but the most important observation from **Figure 3.7** and **Figure 3.8** is that glucose is the only exploration-repressive sugar and also the only saccharide supplement on which a phenotypic difference is observed between *S. venezuelae* WT and Δ*cutRS*.

YP is a complex and rich growth medium that contains both yeast extract and Bacto-peptone. Whilst the previously discussed evidence suggests that glucose is the key component in the observed phenotype it was prudent to test this on other media starting with minimal medium (MM). MM simply contains trace amounts of select salts along with L-asparagine as a nitrogen source and agar added for solidity (**Table 2.1**). *S. venezuelae* WT and Δ*cutRS* were compared on MM with glucose as the sole carbon source (As expected, the strains grew very slowly and produced much smaller colonies on MM compared to more nutritious media such as YP and YPD. They also lacked much of the colouring making imaging difficult. To ease visualisation the colonies have been displayed in **Figure 3.9** against a black background, cropped and magnified at the same ratio. There is a distinct difference between the WT and Δ*cutRS* colonies, the latter being larger with a slight yellow colouring and two

different “zones” whilst the WT is unpigmented and uniform across its smaller colony.

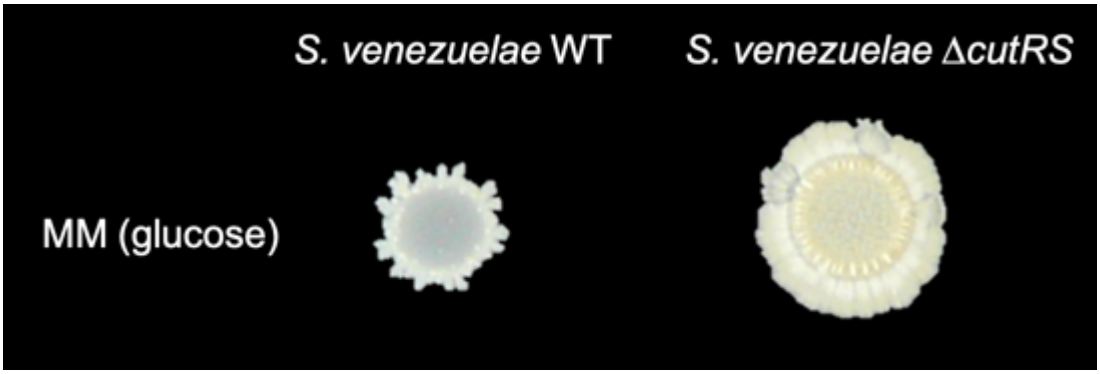

Figure 3.9. *S. venezuelae* WT and Δ*cutRS* grown for 14 days on minimal medium (MM) with glucose as the sole carbon source.

Two additional streptomycete media, MYM+TE and SFM (**Table 2.1**), were tested for a similar glucose-dependant Δ*cutRS* mutant phenotype (**Figure 3.10A**). There was no discernible phenotypic difference between the WT and Δ*cutRS* strains on either MYM+TE without glucose or SFM with or without glucose. However, on MYM+TE with glucose the Δ*cutRS* mutant formed much larger colonies that the WT with significant 3D structuring out from the plate surface. In an attempt to determine if there was a single media component responsible for the extreme YPD and MYM+TE+glucose phenotypes, further media breakdown experiments were performed. **Figure 3.10B** shows the results of culturing *S. venezuelae* WT and Δ*cutRS* strains on agar plates consisting of a single component of YP and MYM+TE with and without glucose. As observed in previous experiments there was no difference between the WT and Δ*cutRS* strains on any media without glucose. With glucose the Δ*cutRS* colonies grown solely on Bacto-peptone or malt extract were slightly larger but it was on yeast extract with glucose that the clearest phenotypic difference could be identified. On this, the mutant produced much larger colonies than the wild-type. Whilst it would have been enlightening to breakdown yeast extract into its constituent parts this would be extremely challenging as yeast extract is the complete cell contents of yeast without the cell walls. As such, efforts were focussed

elsewhere. However, the importance of the yeast extract constituent parts should not be ignored.

The *S. venezuelae* Δ*cutRS* strain produces much larger colonies than the WT on both YPD and MYM+TE with glucose. To quantify the difference in biomass, colonies were grown on these media on top of sterile cellophane discs. These discs allow uptake of nutrients whilst preventing the colony from embedding within the agar. After incubation, the discs can be removed, and the biomass of the attached colony weighed on an analytical balance (**Figure 3.11A**). Whilst in **Figure 3.1** and **Figure 3.10A** the colony size difference is clearly large, the quantification reveals the true extent of the change. The mean mass of the Δ*cutRS* mutant on YPD is over 19x greater than the WT (890 mg vs. 47 mg). On MYM+TE with glucose this is less extreme, but the fold change was still 5x (421 mg vs. 78 mg). Whilst the cellophane disks could be affecting the growth of the strains these biomass observations match clearly to the phenotypes observed on plates without cellophanes so this is unlikely.

As previously mentioned, glucose is exploration repressive and yet the Δ*cutRS* mutant is capable of exploring on YPD after around 10 days of outgrowth. This led us to question the fate of the glucose in the YPD medium and so a colorimetric glucose assay was used to test this on the same YPD plates used in **Figure 3.11A** (**Figure 3.11B**). Using a set of un-inoculated YPD plates as a glucose positive control we were able to compare between the *S. venezuelae* WT and Δ*cutRS* mutant. Interestingly whilst the WT uses little to no glucose in comparison to the blank YPD plates it appears that the Δ*cutRS* mutant uses far more glucose; in many of the samples there was almost no detectable glucose remaining. This is impressive given the final amount of glucose in each YPD plate is around 1.2 grams, a significant amount of carbon for the strain to metabolise.

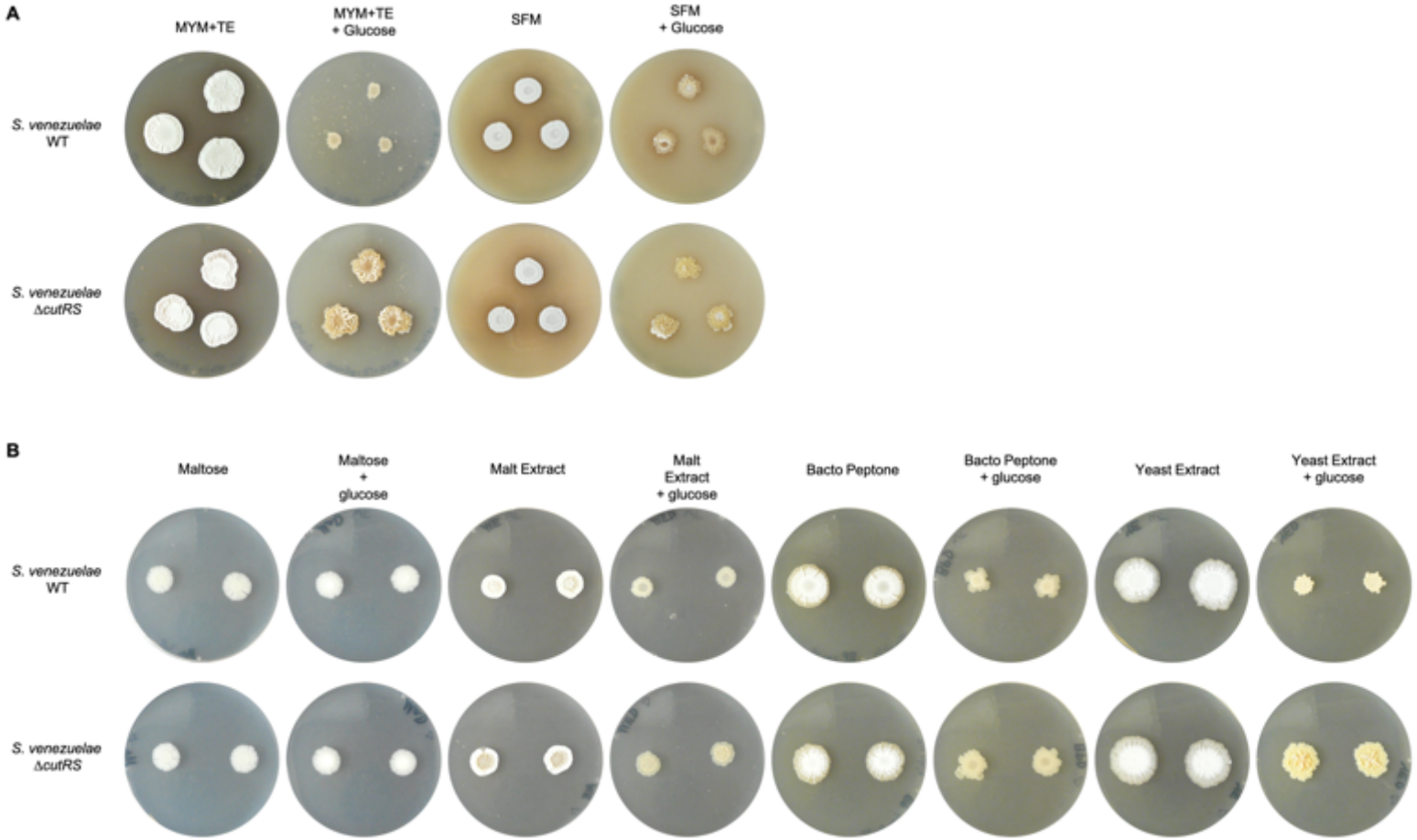

Figure 3.10. *S. venezuelae* WT and Δ*cutRS* cultured on various solid media. **A)** Common streptomycete culture media MYM+TE and SFM with and without glucose. **B)** The constituents of MYM+TE and YP broken down in individual plates, with and without glucose.

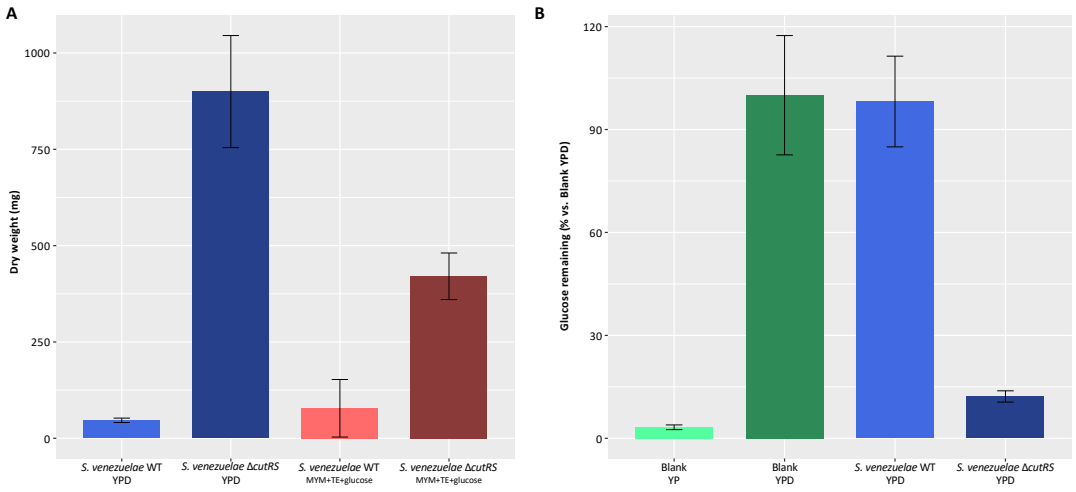

Figure 3.11. A) The dry biomass in milligrams of *S. venezuelae* WT and Δ*cutRS* cultured on YPD and MYM+TE with glucose. **B)** Glucose remaining within the solid media as a percentage compared to the blank YPD control.

It would appear that there are two distinct phases to the Δ*cutRS* phenotype with a significant biological shift between the first and second phase. The working hypothesis is that during the first phase (0-10 days) the *S. venezuelae* Δ*cutRS* mutant takes up and uses all the glucose in the underlying YPD medium. After which the absence of glucose removes repression of exploration, commencing the phenotypic shift resulting in the outer "zone" which consists of explorer hyphae. This would also explain the delayed production of exploration-inducing mVOCs observed in **Figure 3.5**; the mutant requires the depletion of glucose and resulting phenotypic shift to exploration before TMA-like mVOCs can be produced.

3.3. Biochemical characterisation of the *cutRS* mutant

As discussed in **Chapter 1.3.2** streptomycetes are prodigious producers of antibiotics and other natural products with wide-ranging medicinal and industrial uses. It is commonplace to screen novel *Streptomyces* strains for antimicrobial bioactivity in the hopes of discovering a new antibiotic compound. Overlay bioassays were conducted for *S. venezuelae* WT and Δ*cutRS* on YP and YPD using *E. coli, B. subtilis* and *C. albicans* as indicator strains for Gram-negative, Gram-positive and fungal organisms respectively (**Figure 3.12**). The first observation is that both *S. venezuelae* strains display broad-spectrum antimicrobial activity on YP, creating small zones of inhibition against all three indicator organisms, but most obviously against *B. subtilis* and *C. albicans*. This effect has been previously described and results from the production of aforementioned mVOCs such as TMA. As TMA increases the pH of the surrounding media iron availability is reduced with ferric iron forming complexes with hydroxide ions making it more inaccessible to microorganisms (Jones *et al.*, 2019). Whilst it was positive to see these results reproduced in **Figure 3.12** they were to be expected.

It was the results on YPD in **Figure 3.12** that proved more interesting. The WT strain displayed no bioactivity against any of the indicator organisms but the Δ*cutRS* mutant produced a large zone of inhibition when overlaid with *B. subtilis*. As discussed in **Chapter 1.2**, *S. venezuelae* is known to produce two antibiotics under laboratory conditions: chloramphenicol and jadomycin. A preliminary method of testing if the *ΔcutRS* mutant overproduces either of these antibiotics was to use an *S. venezuelae* strain deficient in both chloramphenicol and jadomycin production. *S. venezuelae* M1702 was created by Dr Neil Holmes (JIC) as a chloramphenicol and jadomycin BGC double mutant (unpublished). The original *cutRS*-targeting ReDIRECT construct was used to create Δ*cutRS* mutants in the M1702 background. These M1702 Δ*cutRS* mutants displayed the same developmental phenotype on YPD as the Δ*cutRS* mutant but displayed no bioactivity when overlaid with the *B. subtilis* indicator strain consistent with *ΔcutRS* inducing chloramphenicol and/or jadomycin overproduction (**Figure 3.13**).

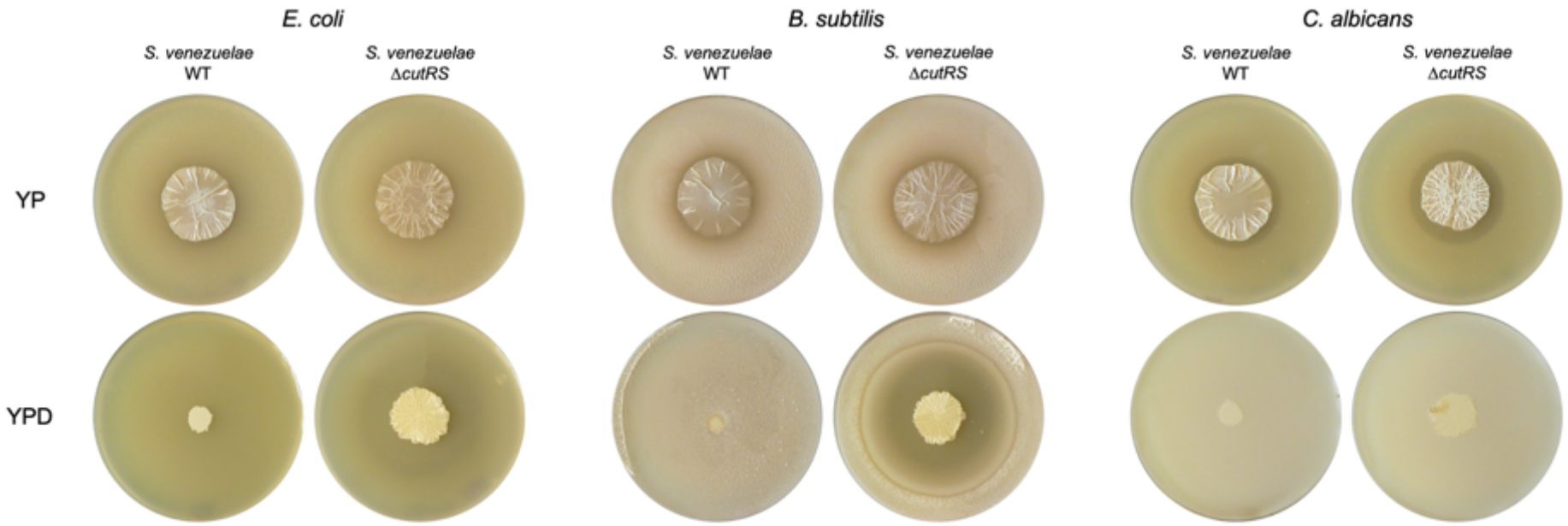

Figure 3.12. Bioassay results of *E. coli, B. subtilis* and *C. albicans* overlays of *S. venezuelae* WT and Δ*cutRS* strains cultured for 5 days on YP and YPD.

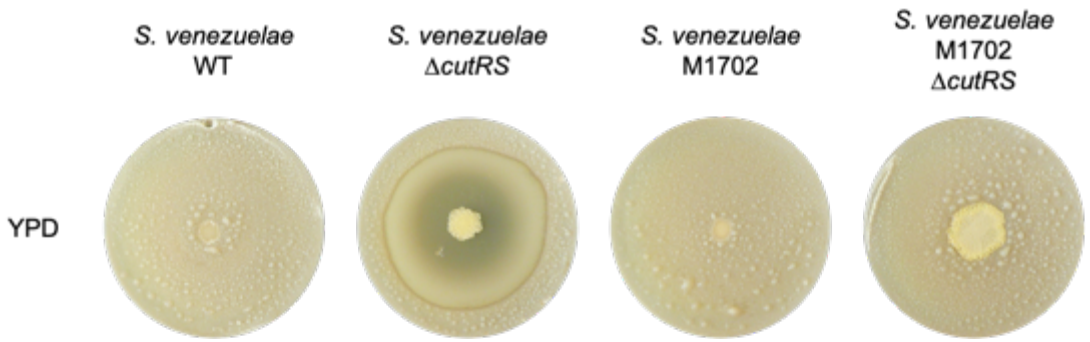

Figure 3.13. Bioassay results of *B. subtilis* overlays of *S. venezuelae* WT, Δ*cutRS,* M1702 (ΔChl ΔJad) and M1702 Δ*cutRS* stains cultured on YPD.

To further test whether the bioactivity was a result of chloramphenicol or jadomycin production by the Δ*cutRS* mutant we used a *B. subtilis* strain (NRS1112, JH642 *amyE*::Piptg-*gfp* [Cml]) with genome-encoded chloramphenicol resistance kindly provided by Prof. Nicola Stanley-Wall (University of Dundee). Overlaying with *B. subtilis* NRS1112 completely eliminated the zone of inhibition created by the Δ*cutRS* mutant, confirming activity was due to chloramphenicol overproduction on YPD (**Figure 3.14**).

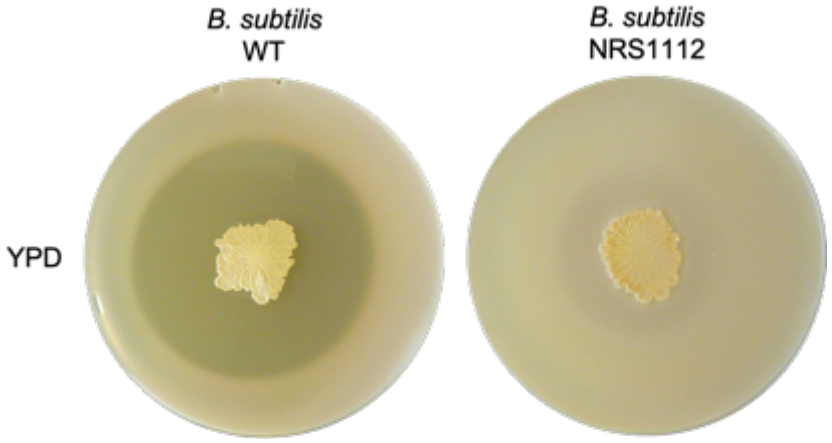

Figure 3.14. Bioassay results of *B. subtilis* WT and NRS1112 (chloramphenicol resistant) strain overlays of *S. venezuelae* Δ*cutRS* cultured on YPD.

To compare and quantify chloramphenicol production in the Δ*cutRS* strain, HPLC analysis of extracted metabolites was used. Previous work by our lab developed an extraction and quantification protocol for chloramphenicol from *S. venezuelae* cultured in liquid media (Som *et al.*, 2017a). To account for extraction from solid media and updated HPLC equipment, a new method was developed (**Chapter 2.28** and **Chapter 2.29**).

Preliminary experiments showed production of chloramphenicol by the Δ*cutRS* mutant was found to be independent of the bacterial overlay. That is, the overproduction is constitutive, not reliant on the presence of competing microorganisms. This made extraction from solid cultures less complex as no overlay was required. As such, *Streptomyces* strains were cultured on top of sterile cellophane discs allowing the removal of cells and the extraction of metabolites from agar. Whilst this only allows for the comparison of extracellular chloramphenicol this was deemed sufficient as that is the area in which the zone of inhibition is present, thus the biologically relevant region. It also allowed for a much cleaner final chromatogram, removing many of the background metabolites that would have been extracted from the colony itself. Additionally, it was found that streptomycetes develop faster on YP / YPD with cellophanes than without. As such a 2-day timepoint on cellophanes was considered equal to the 5-day timepoint without cellophanes used in the previous bioassay experiments. The same extraction procedure was performed on the agar underneath the cellophanes and likewise analysed by HPLC (**Figure 3.15A**). Using the information gained from the previous experiments we were able to quantify the chloramphenicol concentrations present in each sample (**Figure 3.15B**).

Very low levels of chloramphenicol production were detected in both the *S. venezuelae* WT and Δ*cutRS* strains on YP. Whilst we observe bioactivity on YP plates in **Figure 3.12**, as previously discussed this is due to the reduced bioavailability of iron and the zone of inhibition can be removed with the supplementation of $FeCl_3$. This also matches with previous reports of microarray data suggesting the chloramphenicol BGC is expressed at low levels under laboratory conditions despite bioactivity never being observed suggestive of biosynthesis too low to cause a zone

of inhibition (Bibb *et al.*, 2014). The YPD extracts also verify the results of **Figure 3.12** with more than twice the amount of chloramphenicol detected in the Δ*cutRS* samples compared to the WT samples. Interestingly there is more chloramphenicol detected in the WT samples than expected, although overlay bioassay data would suggest that this is not enough to elicit a biological response in *B. subtilis* when overlaid, this is curious and requires further investigation.

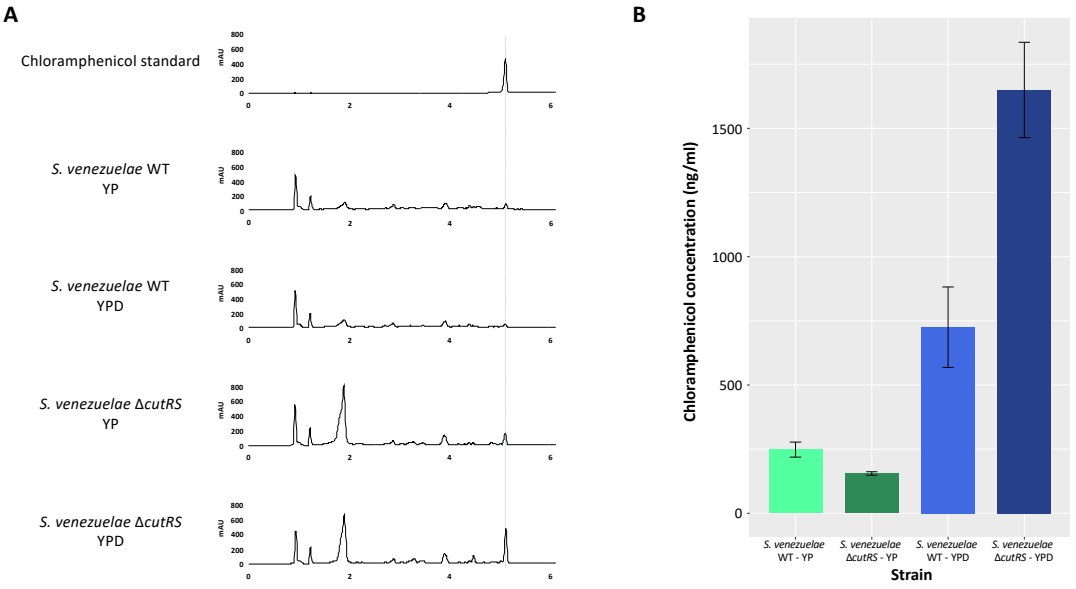

Figure 3.15. A) Representative chromatograms of chloramphenicol extractions from *S. venezuelae* WT and Δ*cutRS* on both YP and YPD compared to a standard control. Chloramphenicol peak indicated by the blue dotted line. **B)** Calculated chloramphenicol concentrations (ng/ml) from the *S. venezuelae* WT and Δ*cutRS* on both YP and YPD.

3.4. The curious case of *Streptomyces* Δ*cutRS* and redox-active phenazines

It was observed that streptomycete exploration is visually similar to the biofilms formed by many species of bacteria, but particularly those formed by a *P. aeruginosa* biofilm mutant described by Ramos *et al.*, 2010. This mutant was incapable of producing a family of redox-active antibiotics called the phenazines, specifically the blue-pigmented pyocyanin (PYO). This deletion resulted in thinner *P. aeruginosa* biofilm colonies with larger surface areas and increased surface folding known as wrinkling. The addition of exogenous phenazine-1-carboxylate (PCA), the precursor to PYO, was able to rescue the mutant phenotype in *P. aeruginosa* (Ramos *et al.*, 2010; Dietrich *et al.*, 2013).

If the observed phenotype was similar to that of *Streptomyces* exploration, we hypothesised that the addition of PYO and PCA would revert, or at least somewhat supress the explorer phenotype (**Figure 3.16A**). Whilst the addition of PYO perhaps reduced the colony size of both WT and Δ*cutRS* strains on YP, the other redox-active phenazine tested, PCA, had no such effect. However, when we repeated the experiment on YPD agar we observed intriguing results (**Figure 3.16B**). With the addition of PYO or PCA the WT strain on YPD produces similar colonies to the negative controls. The colonies are perhaps slightly smaller, and the edges are certainly more regular but otherwise phenotypically identical. However, the addition of the same compounds to the Δ*cutRS* mutant completely reverted the phenotype to that of the WT. The addition of redox-inactive phenazine had no effect, suggesting the phenotype reversion is wholly due to the redox activity.

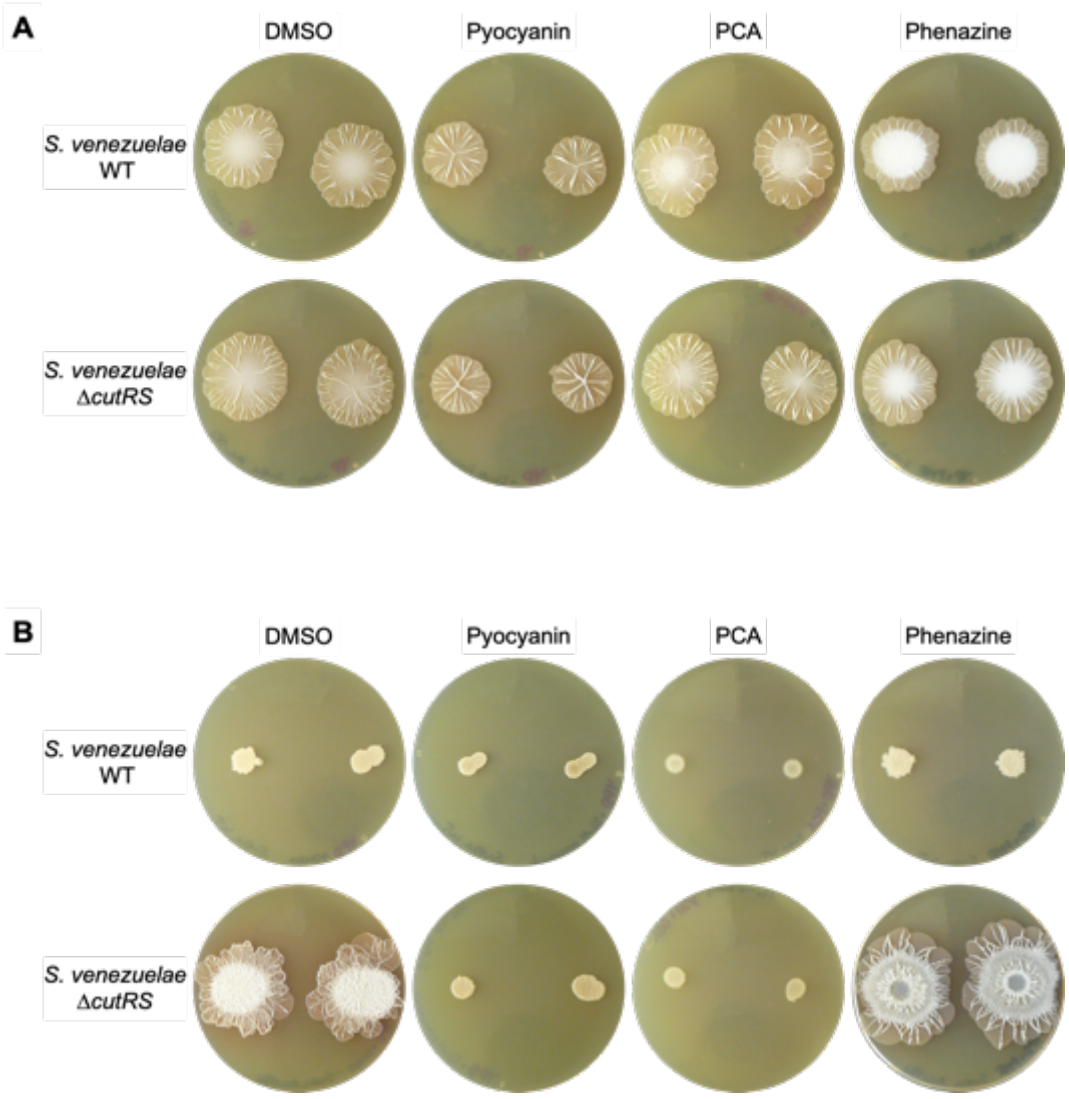

Figure 3.16. *S. venezuelae* WT and Δ*cutRS* strains cultured on **A)** YP and **B)** YPD; supplemented with DMSO (negative control), redox-active antibiotics 25 µM pyocyanin and phenazine-1-carboxylate (PCA) or non-redox-active phenazine.

3.5. Discussion

The results in this chapter describe a fascinating phenotype displayed by the *S. venezuelae* Δ*cutRS* mutant, defining its biological and biochemical properties in comparison to the wild-type strain. Deletion of this highly conserved streptomycete TCS reveals a phenotype limited, in our experience, to certain solid growth media which contain glucose including YPD, MM with glucose and MYM + TE with glucose. Genetic complementation of this mutant can be achieved irrespective of expression levels with the phenotype completely reverting to WT. Closer examination of the *Streptomyces* exploration hallmarks indicate that the mutant is indeed capable of exploring on YPD agar, a medium which represses exploration of the WT strain. These explorer cells are limited to an outside "zone" of the colony and appear only after approximately 10 days of incubation. Before this time, there is still significant biomass growth in comparison to the WT, and almost complete depletion of glucose from the growth medium. It is likely that this depletion causes the same effect as cultivation of *S. venezuelae* on YP, i.e., exploration, and this would explain the lag period. During this early period the mutant also overproduces a bioactive specialised metabolite identified as chloramphenicol. Finally, the addition of redox-active antibiotics such as PYO and PCA are capable of repressing the mutant phenotype completely, perhaps providing an intriguing insight into the cellular redox state of the Δ*cutRS* strain.

The depletion of glucose from within the media seems key to this phenotype and its apparent properties including biomass generation and chloramphenicol production. Glucose uptake in many bacteria is achieved by the phosphoenolpyruvate: glycose phosphotransferase system (PTS). This involves the concomitant phosphorylation and uptake of glucose. The phosphate group is derived from phosphoenolpyruvate (PEP) and, through a series of transfer proteins, is ultimately transferred to the carbohydrate molecule by the membrane-bound glucose permease $IICB^{Glc}$ (Rohwer *et al.*, 2000). However, the PTS in *S. coelicolor*, *S. lividans* and *S. griseofuscus* has been shown to be aligned towards fructose and N-acetylglucosamine phosphorylation and uptake, suggesting glucose uptake is likely effected through a different system (Titgemeyer *et al.*, 1995; Parche *et al.*, 2000; Nothaft *et al.*, 2003). In a search for

alternate glucose uptake systems, it was revealed that the major transporter in *S. coelicolor* is the high-affinity glucose transporter GlcP, not $IICB^{Glc}$. Whilst *Streptomyces* species, such as *S. coelicolor,* encode two copies of GlcP it appears that this has arisen through gene duplication with GlcP1 being responsible for the significant portion of glucose uptake. There also does not seem to be alternate transporters, with no glucose uptake being detectable in the *S. coelicolor* Δ*glcp1* Δ*glcp2* double mutant (Wezel *et al.*, 2005). *S. venezuelae* encodes just a single copy of *glcP* (*vnz_26080*) which might be the primary mechanism of glucose uptake in this organism, but this would need to be tested experimentally. Post-uptake, glucose must still undergo phosphorylation to glucose-6-phosphate (G6P) before it can enter the pathways described above, and this is achieved by the glucose kinase GlkA (Vnz_08755) which likely binds to GlcP, phosphorylating glucose as it is transported into the cell (Wezel *et al.*, 2007; Gubbens *et al.*, 2012). In contrast to the PTS, which relies on PEP as the phosphate source, Glk proteins utilise the hydrolysis of ATP to ADP. From here G6P is metabolised with the ultimate goal to generate cellular energy and reductive potential in the form of ATP and NADH / NADPH (Baron, 1996). This occurs via three pathways: glycolysis / the Embden-Meyerhof-Parnas (EMP) pathway, the pentose phosphate pathway (PPP) and the Entner-Doudoroff (ED) pathway (**Figure 3.17**). Whilst it is beyond the scope of this work to fully describe these pathways, it is important to summarise their activities and priorities in streptomycetes.

The EMP pathway is perhaps the most recognisable of the three glycolytic pathways and is the pathway commonly referred to when glycolysis is mentioned. It consists of 10 reactions starting with the phosphorylation of glucose by Glk as discussed above, and ends in the production of pyruvate which can enter the TCA cycle during aerobic respiration (Baron, 1996). Intermediates of the pathway can be used directly by the cell, such as PEP which is a precursor in the shikimate pathway discussed later (Bentley and Haslam, 1990). The first five stages of glycolysis are known as the preparatory phases, requiring energy input to catabolise glucose into two glyceraldehyde 3-phosphate molecules. After the preparatory phase comes the payoff phase resulting in the net gain of cellular energy in the form of 2 molecules of

both ATP and NADH. The final product, pyruvate, is then able to enter the TCA cycle where the majority of cellular energy is generated. Through the subsequential interconversion of organic acid, one molecule of pyruvate can generate 15 molecules of ATP through the TCA cycle (Baron, 1996).

The PPP runs parallel to EMP glycolysis and is the major source of cellular NADPH and pentose sugars, including ribose-5-phosphate (R5P), required for the synthesis of amino acids and nucleotides. It can also cross-feed with the EMP pathway via R5P-derived intermediates (Stincone *et al.*, 2015). NADPH is required for the production of many specialised metabolites including penicillin and methylenomycin with flux through the PPP appearing to be responsive to such requirements. During the PPP, NADPH is produced at two points: during the conversion of G6P to 6-phosphoglucono-D-lactone, and 6-phosphogluconate to R5P by glucose-6-phosphate dehydrogenase (G6PDH) and 6-phosphogluconate dehydrogenase (6PGDH) respectively (Xue-Mei *et al.*, 2017). Because the PPP is more active during the stationary growth phase and produces important intermediates for secondary metabolism it has been the focus of efforts in increasing specialised metabolite production in streptomycetes by directing glucose catabolism preferentially through the PPP over the EMP (Obanye *et al.*, 1996; Xue-Mei *et al.*, 2017).

The ED pathway is most commonly found in Gram-negative bacteria but has been reported in some actinomycetes such as *M. smegmatis* and *Nonomuraea* sp. ATCC 39727 (Gunnarsson *et al.*, 2004). The industrially important antibiotic producer *Streptomyces tenebrarius* has also been shown to have an active ED pathway. Key ED pathway genes such as *edd,* encoding 6-phosphogluconate dehydratase, were identified in the genome and even flux between EMP and ED was shown during exponential growth on glucose, with the PPP activity being relatively low (Borodina *et al.*, 2005). Homology searching and phylogenetic analysis has shown most actinomycetes, including *S. coelicolor* and *S. avermitilis,* do not encode genes such as *edd* (Gunnarsson *et al.*, 2004). Our own analysis supports this conclusion and also confirms that *S. venezuelae* does not encode ED-related genes. This suggests that in these streptomycetes the ED pathway is inactive and glucose catabolism proceeds through the EMP and PPP pathways.

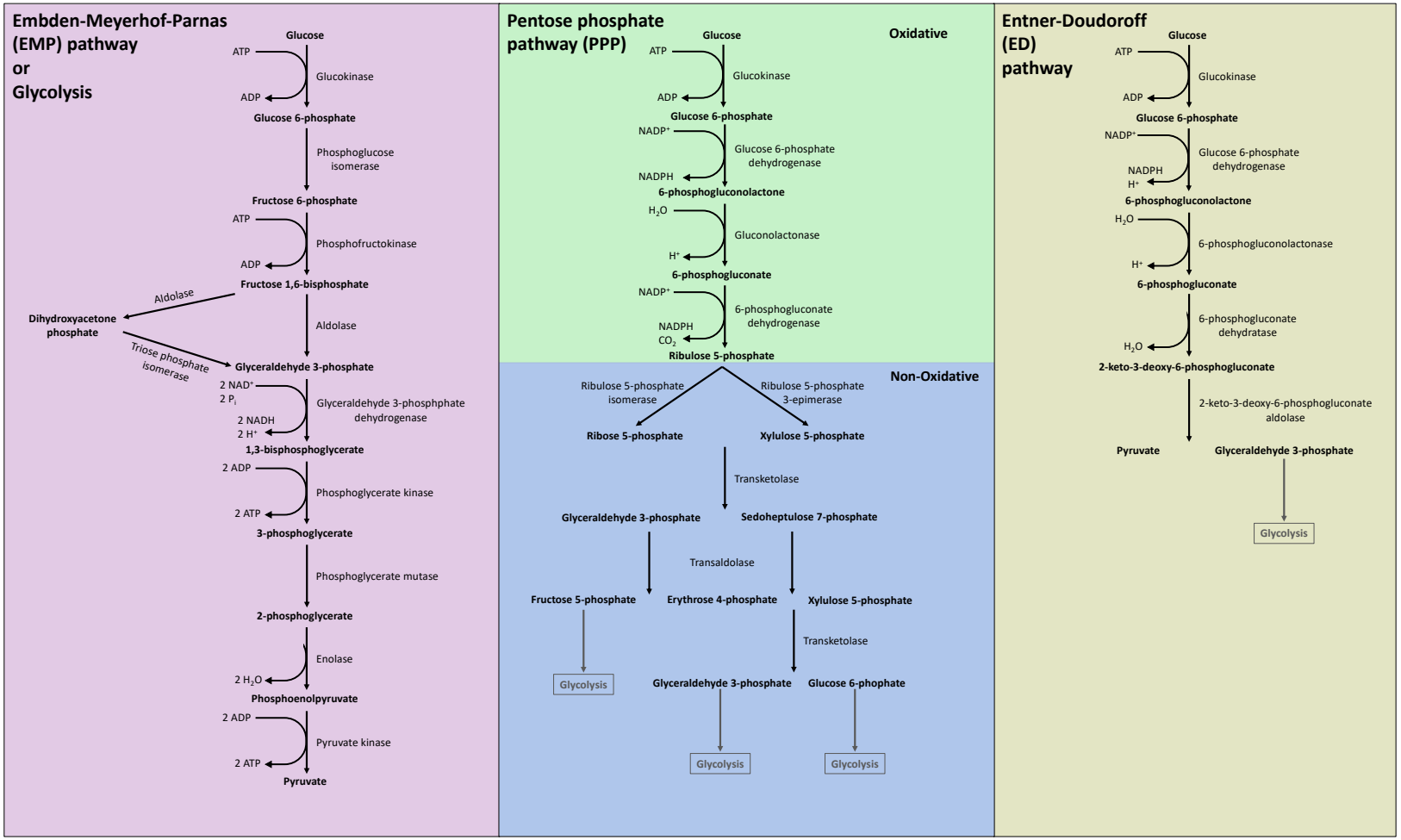

Figure 3.17. The three pathways of glucose catabolism in bacteria. The Embden-Meyerhof-Parnas (or Glycolysis) pathway is shown in purple, the pentose phosphate pathway in green (oxidative steps) and blue (non-oxidative) with the Entner-Doudoroff pathway in orange.

The Δ*cutRS* mutant clearly depletes glucose from the surrounding media, and rapidly. Presumably this glucose is then catabolised as described above by a combination of both the EMP and PPP routes. It is unclear whether the significant biomass generation we see in the mutant creates the requirement for glucose uptake and catabolism, or whether uncontrolled glucose uptake stimulates the significant colony growth. In adaptive laboratory evolutionary experiments using *E. coli* and glucose minimal media it was shown that despite a 1.6-fold growth increase in glucose-adapted strains, intracellular metabolic pathway usage remained relatively unchanged and the growth increase was purely resultant on an increased glucose uptake (Long *et al.*, 2017). So why then does the WT remain as a small, unchanging colony on YPD? Is exploratory growth so disadvantageous (and if it is disadvantageous, why?) that the colony would prefer to not use any of the available glucose to avoid the phenotypic shift we see in the mutant? These are just a few of the many questions regarding the extreme uptake of glucose by the Δ*cutRS* mutant that arise from the work described in **Chapter 3**. It is, however, important to remember cellular energy and metabolites are not just being used for biomass production. Specialised metabolism is reliant on primary metabolic precursors including for the production of chloramphenicol.

Biosynthesis of chloramphenicol in *S. venezuelae* (**Figure 3.18**) is intriguing because the initial stages utilise the shikimate pathway (Bibb *et al.*, 2014). The shikimate pathway is primarily used to biosynthesise chorismic acid, the direct precursor to aromatic compounds including the aromatic amino acids phenylalanine, tryptophan and tyrosine (Zucko *et al.*, 2010).

The precursors used by the shikimate pathway, PEP and erythrose-4-phosphate (E4P), originate from glycolysis and the PPP respectively (Sauer and Eikmanns, 2005). From chorismic acid the subsequent production of chloramphenicol is performed by enzymes encoded within the chloramphenicol biosynthetic gene cluster. Whilst we were able to detect chloramphenicol produced by both the mutant and WT grown on YP medium, there was no bioactivity. This low-level production matches the reports of constitutive low-level expression of the chloramphenicol BGC under most conditions (Bibb *et al.*, 2014). Much greater concentrations of the chloramphenicol

were detected in YPD agar used to grow both strains and, despite the mutant only producing roughly 2-fold more than the WT, this difference appears to be responsible for the large zone of inhibition observed in the Δ*cutRS* YPD overlays. This overexpression could be the result of regulatory repression relief by the deletion of CutR and this will be explored later in this thesis. However, it is also possible that with the pathway seemingly activated already, the shunt of metabolites from increased glycolysis through to the shikimate pathway to provide aromatic amino acids for growth could simply result in a greater flux of chorismic acid into the final stages of chloramphenicol biosynthesis.

Finally, the observation that exploring streptomycetes appear similar to *Pseudomonas* biofilms is intriguing. The study of *P. aeruginosa* colony biofilms, those grown on solid media, has revealed colony morphogenesis is highly dependent on phenazines, a group of endogenously produced specialised metabolites with redox activity. Whilst these are secreted into the environment and likely act as antibiotics against competing organisms, phenazines have also been shown to act as pseudomonad signalling molecules. The blue-pigmented phenazine PYO activates quorum sensing genes via the transcription factor SoxR (Dietrich *et al.*, 2006). SoxR binds DNA as a dimer, with each monomer containing a [2Fe-2S] cluster kept in the reduced state and only with oxidation of this cluster does SoxR become transcriptionally active (Ding, Hidalgo and Demple, 1996). In *E. coli* SoxR regulates the superoxide (O_2^-) response, detecting oxidative stress via its [2Fe-2S] cluster and activates another regulatory protein, SoxS, which in turn activates a regulon of superoxide response genes (Amábile-Cuevas and Demple, 1991; Pomposiello and Demple, 2001). However, despite SoxR being conserved among Proteo- and Actinobacteria, SoxS is found only in Enterobacteriaceae suggesting a different role in these other bacteria. In *P. aeruginosa* it appears that the primary function of SoxR is to mediate this pyocyanin response, and a similar mechanism has been shown in *S. coelicolor* with SoxR responding to extracellular ACT (Dietrich *et al.*, 2008; Shin *et al.*, 2011).

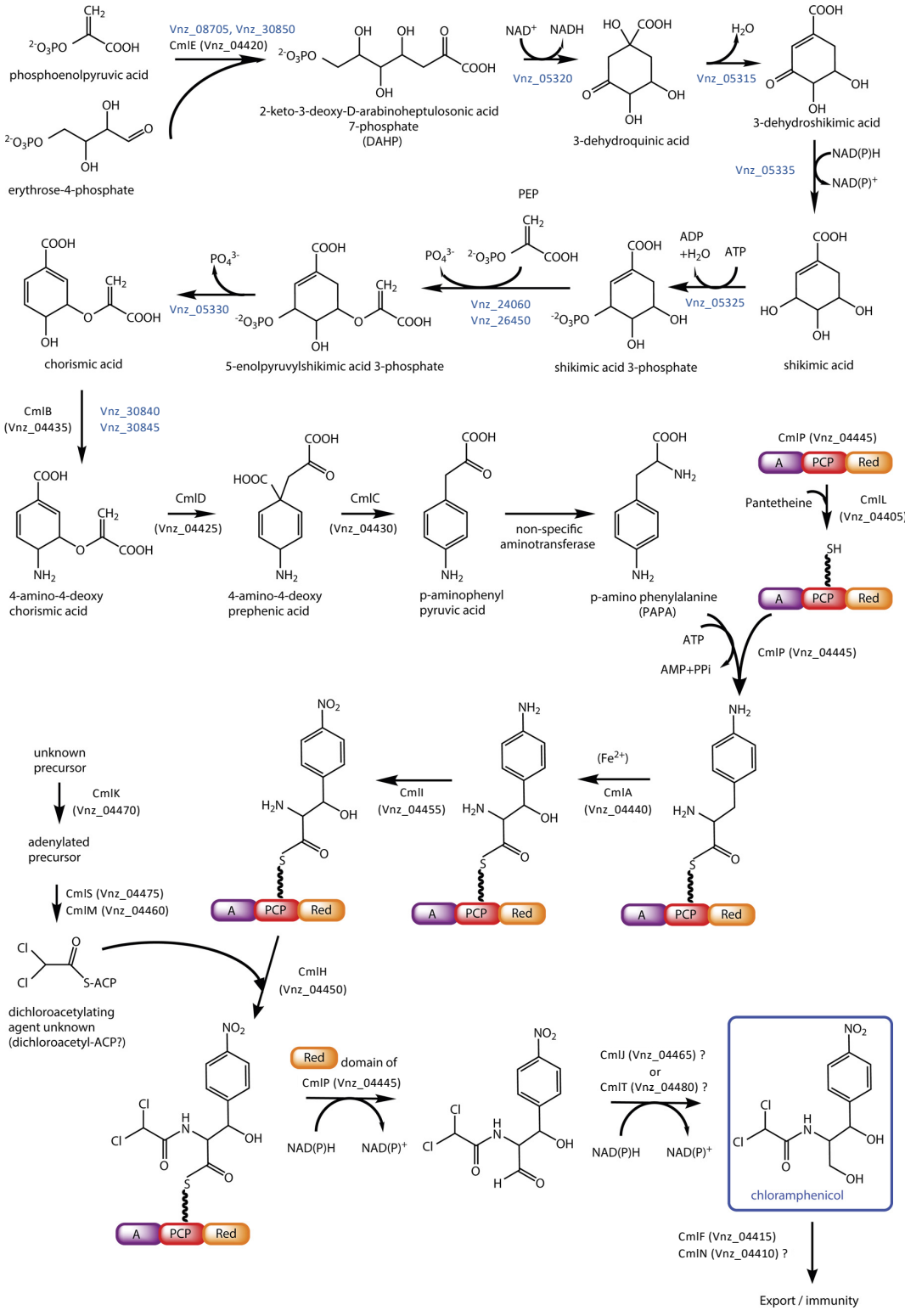

Figure 3.18. *S. venezuelae* chloramphenicol biosynthesis pathway updated to use Vnz protein numbering. Proteins involved in the shikimate pathway not encoded by the chloramphenicol BGC are shown in blue. Adapted from Bibb *et al.*, 2014.

However, whilst it is possible a pyocyanin-responsive effect in *S. venezuelae* Δ*cutRS* is played out through the regulation of SoxR, evidence presented later in this thesis would argue otherwise and perhaps relates more to the glucose uptake and catabolism described in earlier results. It is the biochemical role of phenazines in *P. aeruginosa* that is perhaps more relevant to the effects observed in **Figure 3.16B**. One major problem bacteria face in biofilms is distribution of nutrients across the multicellular colony including oxygen for aerobic respiration. Redox-active antibiotics, such as PYO, can act as alternate electron acceptors to oxygen and nitrate, maintaining the intracellular redox balance in oxygen limited conditions by reducing NADH to NAD^+ (Dietrich *et al.*, 2013). The addition of oxidised PYO or PCA to the Δ*cutRS* mutant could possibly be adding a pool of oxidising agents which maintain intracellular redox homeostasis. This might suggest there is an imbalanced intracellular redox state in the mutant likely caused by the excessive aerobic respiration linked to the increased glucose uptake. Experiments were attempted to determine the intracellular levels of NAD^+ and NADH but these proved difficult to adapt to *Streptomyces* spp. grown on solid medium as they were originally designed to assay *Pseudomonas* spp. grown in liquid media. With more time and access to an anaerobic cabinet these assays could be modified successfully. Comparison of NAD^+: NADH ratios between the WT and Δ*cutRS* strains on YPD with and without PYO / PCA would not only help uncover the mechanism by which redox-active phenazines revert the mutant phenotype but also reveal any differences between the intracellular redox states of the two strains.

Chapter 4. Molecular characterisation of CutRS in *S. venezuelae*

The results presented in **Chapter 3** identify CutRS as a TCS responsive to glucose, or a signal related to the presence of glucose. Deletion of *cutRS* results in distinct developmental defects and the overproduction of the antibiotic chloramphenicol. However, all the work to this point was performed at a colony level, leaving much to be uncovered at the genomic and molecular level. In general, work on TCSs focusses on the RR: identifying the DNA-binding regions, defining the regulon and describing the mechanism of action. *S. venezuelae* CutR is a 217 residue OmpR-family RR and neither its regulon nor its DNA recognition motif have been previously described. In this chapter we aim to identify these using a combination of *in vivo* and *in vitro* techniques with the aim of further understanding the mechanism of action of CutRS and explaining the Δ*cutRS* phenotype described in **Chapter 3**.

4.1. ChIP-Seq

The first step in defining the CutR regulon was to map the CutR binding sites to the *S. venezuelae* genome. Chromatin immunoprecipitation followed by sequencing is a common technique used to achieve this, for RRs as well as many other DNA-binding proteins. Following success with previous ChIP-seq experiments by our lab on MtrA (Som *et al.*, 2017a) and ForF (Devine *et al.*, 2021) a complement construct for the Δ*cutRS* mutant was designed containing the *S. venezuelae cutRS* operon under the expression of the native promoter. This operon was modified to fuse a 3xFLAG tag (DYKDHD-D-DYKDHD-I-DYKDDDDK) to CutR using a flexible linker sequence (GGGGSGGGGSGGGGS). A C-terminal 3xFLAG fusion of CutR was chosen over the N-terminus as historically the linker-3xFLAG peptide has not interfered with DNA-binding and it is thought best to avoid occluding the N-terminal receiver domain where the conserved aspartate required for phosphorylation, and therefore activation, is located. This construct was synthesized by Genewiz (UK) and shown to fully complement the mutant phenotype confirming the C-terminal tag does not

inhibit CutR-DNA binding (**Figure 4.1**). As can be seen in **Figure 4.1**, there were occasions where the Δ*cutRS* mutant phenotype was not as pronounced as was observed in previously discussed experiments. The colony is still larger, more yellow in colour and overproduces chloramphenicol but has simply not begun exploring at the time of imaging.

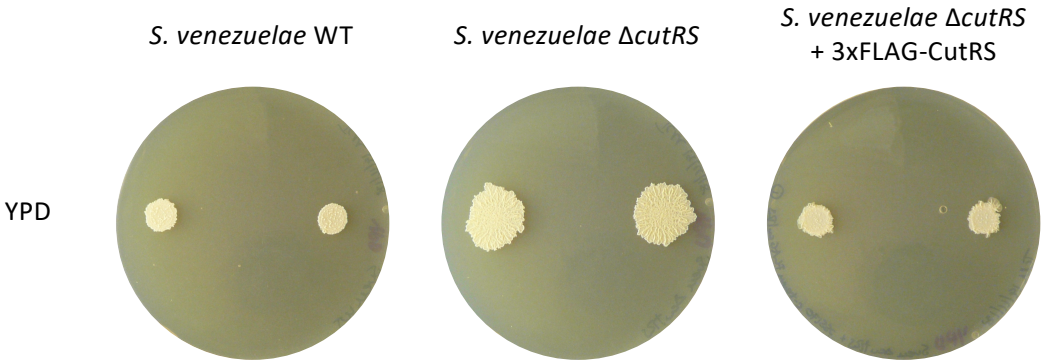

Figure 4.1. Complementation of the *S. venezuelae* Δ*cutRS* mutant phenotype by the CutR-3xFLAG construct on YPD agar.

Once the construct was confirmed as functional, ChIP-seq was performed and analysed as described in **Chapter 2.45** and **Chapter 2.46** on both YP and YPD agar after 5- and 10-days growth on top of cellophane disks, equivalent to 7 and 14 days on agar alone.

Preliminary analysis identified the 5-day timepoint as the most physiologically relevant for identifying the CutR regulon. The issue with the 10-day colony is that is not uniform, giving complex results with no way to deconvolute the data. If we only collected the outer exploring region of the Δ*cutRS* mutant on YPD it is possible the results would be comparable. However, the efficiency of ChIP-seq-ready DNA extraction from solid media proved to be very low, and the amount of pure outside "zone" biomaterial needed would have been difficult to procure.

From the 5-day timepoint samples three significant CutR-DNA binding regions were identified through ChIP-seq (**Figure 4.2**). RRs are commonly reported to bind to

regions of DNA upstream of their own TCS operon as a form of self-regulation. This proved to be the case for MtrA and ForF as well as many others (Som *et al.*, 2017a; Devine *et al.*, 2021). CutR is no exception, with significant enrichment upstream of its own operon (*vnz_27390/vnz*_27395) compared with the WT control. CutR was found to bind two other locations within the genome, upstream of *vnz_08815* and between the divergent genes *vnz_18425* and *vnz_18430*. Promisingly these peaks are only present in the YPD samples, suggesting CutR binds only when glucose is present. This fits with a model of glucose-mediated activation of CutS, resulting in the phosphorylation of CutR and subsequent DNA-binding; these genes could be classified as the putative CutR regulon.

The gene *vnz_08815* encodes a 349-residue putative cell wall hydrolase. According to the peptidase database MEROPS (https://www.ebi.ac.uk/merops/) Vnz_08815 belongs to the C40 endopeptidase family (Rawlings *et al.*, 2018). Further Interpro homology scanning (https://www.ebi.ac.uk/interpro/) identified an N-terminal signal peptide domain, confirmed by SignalP-5.0 (http://www.cbs.dtu.dk/services/SignalP-5.0/) and very likely (88.73%) to be a standard Sec/signal peptidase I domain.

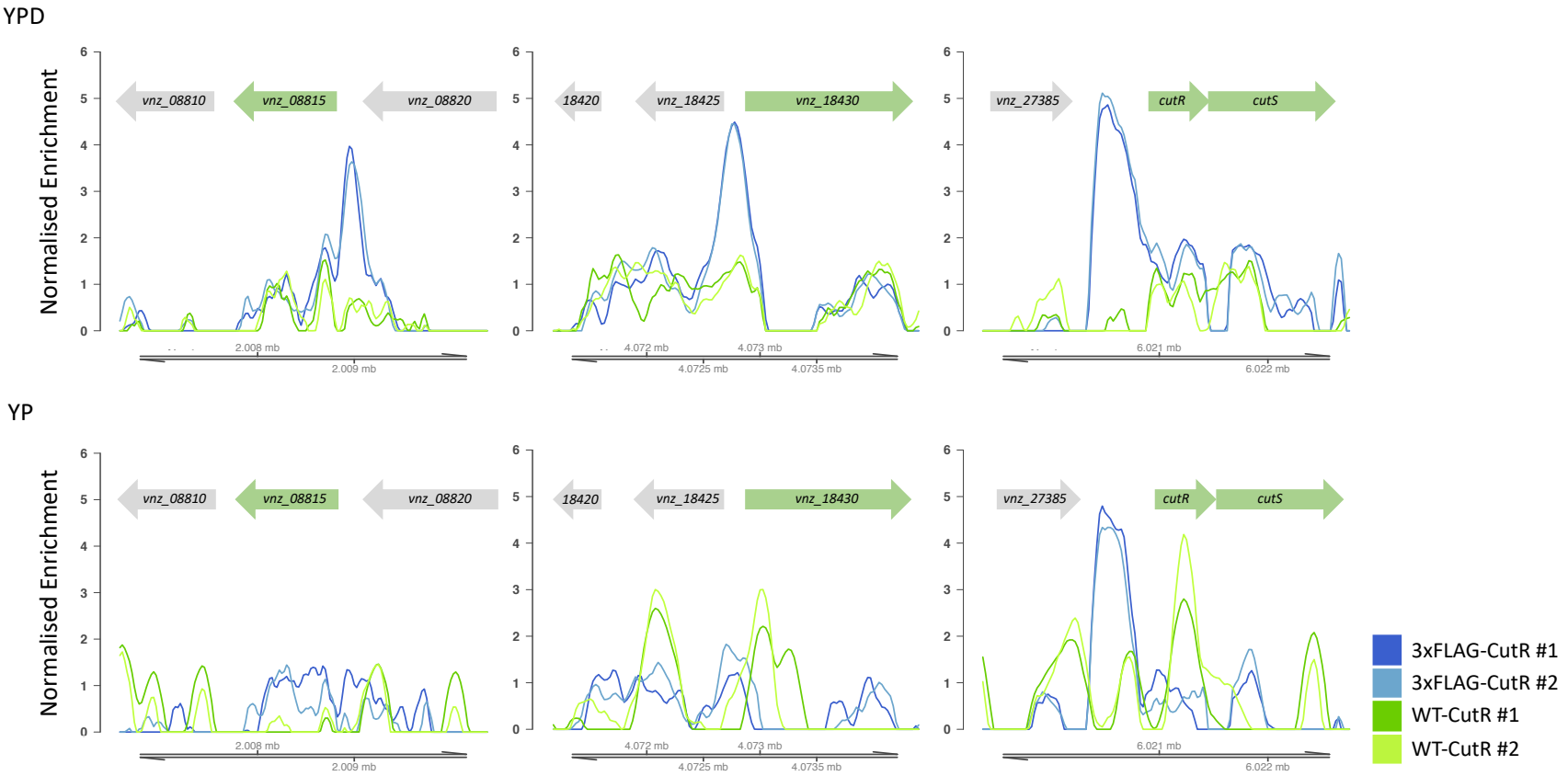

Figure 4.2. CutR binds to three locations within the *S. venezuelae* genome. The coloured lines show ChIP-seq data for CutR-3xFLAG (dark blue and light blue) and the WT control (green and yellow) at 5 days on YPD and YP. Genome locations are displayed below the relevant graphs with gene schematics above. Genes of interest are highlighted in green.

This suggests Vnz_08815 is exported out of the cell which matches with the function of a cell wall hydrolase. The C-terminal region was also identified to contain a NlpC/P60 domain. The NlpC/P60 superfamily, defined by a C-terminal catalytic triad of a cysteine, histidine and a polar residue, contains the aforementioned C40 endopeptidases in which that final polar residue is often a histidine (Anantharaman and Aravind, 2003). Amino acid alignment confirms this to be the case with Vnz_08815. These endopeptidases often cleave the D-glutamine-LL-diaminopimelic acid linkage, and in *Streptomyces* spp. this would occur within the lipid II building block: GlcNAc-MurNAc-L-Ala-D-Glu-LL-diaminopimelate(Gly)-D-Ala-D-Ala (Aart *et al.*, 2018). Further investigation revealed significant homology (45% identity) of Vnz_08815 to CgR_2070 from *C. glutamicum* which appears to be involved in cell separation (**Figure 4.3**). Whilst deletion of *cgR_2070* in *C. glutamicum* resulted in no obvious morphological defects, the same gene deletion in a strain deficient in another NlpC/P60 protein, CgR_1596, exacerbated the growth defects caused by the single *cgR_1596* deletion. Septum formation was complete in the double mutant, suggesting that the two proteins are more likely responsible for cell separation, with multiple septa observed within individual cells (Tsuge *et al.*, 2008). Cell replication in *C. glutamicum* is significantly different to the sporogenic streptomycete life cycle however cell separation still occurs during streptomycete development, especially during spore maturation (Aart *et al.*, 2018).

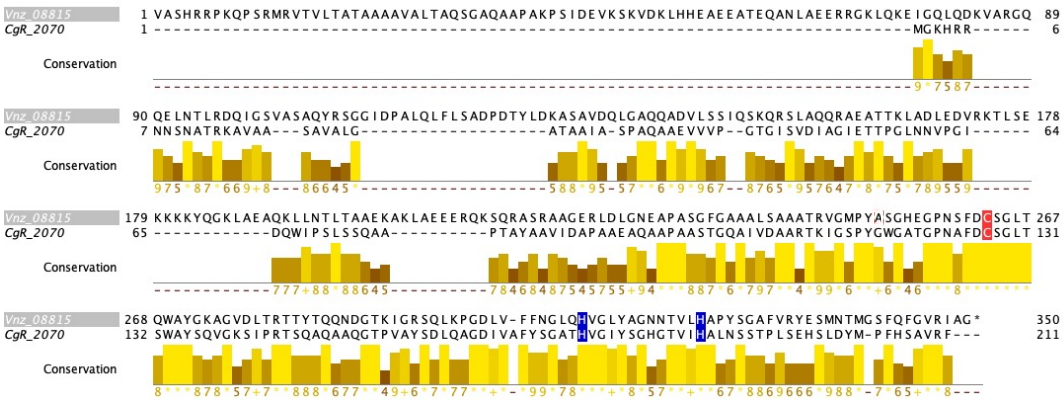

Figure 4.3. Visualisation of Vnz_08815 and CgR_2070 residue alignment. The conserved catalytic triad is highlighted: Cysteine – Red; Histidines – Blue.

The gene *vnz_18430* was identified as coding for the serine protease HtrA3, of the HtrA family previously discussed in relation to the CssRS TCS (**Chapter 1.7.1.5**). In fact, HtrA3 was the only HtrA-like protein not controlled by CssR in *S. lividans* (Vicente *et al.*, 2016). HtrA proteases are involved in protein quality control, capable of degrading misfolded proteins and acting as chaperones for protein stabilisation. Additionally, they can cleave or sequester regulatory proteins, modulating signalling pathways. In contrast to classical serine proteases, the catalytic activity of HtrA proteases can be switched on and off and finely tuned to the requirement of the cell. Generally, they are found extracytoplasmically, so in the extracellular space of Gram-positive bacteria such as *Streptomyces* spp. which could be considered a periplasm (Clausen *et al.*, 2011). HtrA3 is predicted to contain a single TM helix between residues 144-166, indicating the C-terminal catalytic and PDZ (postsynaptic density of 95 kDa, Discs large and zonula occludens 1) domains are likely exposed to the extracellular space. It has also been proposed that autocleavage of HtrA proteases can result in release from the bacterial membrane resulting in a potentially novel mechanism of extracellular transport (Backert *et al.*, 2018). HtrA proteases display a remarkable functional and structural plasticity due to the combination of the catalytic serine protease domain and the target peptide-binding PDZ domain. In prokaryotes this function is predominantly targeted in response to protein-folding stress however little is known about the specific role of HtrA3 in streptomycetes (Clausen, Southan and Ehrmann, 2002). Divergently encoded from *vnz_18430* is *vnz_18425*. Data presented later in this thesis explains why we consider *vnz_18425* to not be a target of CutR regulation and as such was not taken forward to the GUS assays or DNA-binding experiments of **Chapter 4.3**.

The enrichment of CutR-binding to its own promoter was present in both the YP and YPD samples, suggesting binding occurs regardless of glucose supplementation. This is slightly perplexing considering the glucose-responsive binding we see for the other two targets. There are a few hypotheses which could explain this discrepancy. It is possible that the two glucose responsive binding sites are protected by another regulator or by DNA-folding under YP conditions. This would suggest that CutR is active under both YP and YPD conditions but can only access the promoters of

vnz_08815 and *htrA3* when protection is released in the presence of glucose. Secondly it is possible for RRs to form heterodimers rather than homodimers and it could be that either the two glucose-responsive promoters, or the *cutRS* promoter, are bound by a CutR-RR heterodimer (Al-Bassam *et al.*, 2014). Finally, the *cutRS* promoter could contain a different CutR binding site, requiring low concentrations of activated CutR. This could occur in the absence of CutS activation due to nonspecific phosphorylation of CutR through noncognate SKs or small molecule phosphodonors (Barbieri, Wu and Stock, 2013). The first hypothesis would be strengthened by the identification of identical binding sites in all three promoter regions. However, MEME analysis (meme-suite.org) was unable to identify any binding sites present in all three promoter regions which resembled RR binding sites. This weakens the first hypothesis whilst the Co-IP data presented below reveals evidence in support of the second hypothesis.

4.2. Co-IP

Similar to ChIP-seq, co-immunoprecipitation can be used to identify interactions between proteins of interest, *in vivo*. However, Co-IP reveals protein-protein interactions rather than the protein-DNA interactions identified by ChIP-seq. For example, it was used to show that two atypical RRs, BldM and WhiI, form a functional heterodimer which was subsequently shown to bind promoters distinct to the BldM homodimer (Al-Bassam *et al.*, 2014). Co-IP was performed similarly to the ChIP-seq experiment described above, with enriched protein, rather than DNA, extracted and analysed. 213 proteins were found to be at least 2-fold more abundant in the CutR-3xFLAG samples compared to the WT control on YPD. In contrast there were only 22 proteins similarly enriched in the YP samples. These were then filtered for significance with the most enriched proteins (>5-fold enrichment) detailed in **Table 4.1**.

The most abundant protein was CutR itself. As both the specific target of the antibodies, via the FLAG-tag, and probable homodimer this was expected and encouraging to observe. It was 85-fold more abundant in the FLAG-tagged samples on YPD compared to WT and 32-fold on YP. This change in enrichment on YPD to YP could suggest two things: that CutR is more abundant on YPD and/or CutR is forming a homodimer on YPD. Both of these things are expected so it is likely both, however the discrimination between these two facts is impossible with this Co-IP experimental setup because CutR was the FLAG-tagged bait.

In the YPD samples there were 28 proteins >5-fold more abundant, and three of those were 20-fold or greater. One of these was CutR itself as previously mentioned, whilst the other two were Vnz_01460 and Vnz_08945, identified as a L-threonine 3-hydrogenase and phage shock protein A (PspA) respectively. PspA is part of the phage shock protein response induced by extracytoplasmic stress. Whilst in *E. coli* the phage shock response consists of seven genes, (*pspA-G)* most bacterial genomes, including *Streptomyces* spp. encode only *pspA*. In *S. lividans* the *pspA* gene is strongly induced under membrane integrity stress, most notably alkaline stress, and essential for survival and growth under these conditions. Interestingly the *B. subtilis* homologue

of PspA is called LiaH and is involved in the LiaSR TCS homologous itself to the streptomycete EsrSR homologues described in **Chapter 1.7.1.8**. Expression of LiaH is activated by phosphorylated LiaR and counteracts membrane stress. It has also been postulated that LiaH could directly interact with LiaR, repressing its activity in a negative-feedback loop (Jordan *et al.*, 2006). If this was the case, and this remains unconfirmed, there are two possibilities resulting from the PspA-CutR Co-IP enrichment. The first is PspA directly interacts with CutR in a LiaH-LiaR-like manner. The alternative option comes from another part of the Co-IP results. The RR Vnz_22095, homologous to *C. glutamicum* EsrR, was found to be 11-fold more abundant in the YPD FLAG-tagged samples than the WT controls. In the second possibility PspA could interact with EsrR, a system directly homologous to *B. subtilis*, with EsrR also binding CutR creating a PspA-EsrR-CutR complex. Of course, it could also be the opposite with a PspA-CutR-EsrR complex a viable possibility. These Co-IP results require confirmation via targeted protein-protein binding experiments and complementary Co-IP experiments performed with targets such as PspA and EsrR before any further conclusions can be made.

Table 4.1. Proteins significantly enriched from co-immunoprecipitation of CutR-3xFLAG from *S. venezuelae* colonies cultured on YP and YPD for 2 days. A cut-off of > 5.0 protein abundance ratio for FLAG_YPD / WT_YPD and FLAG_YP / WT_YP was used. Where peptides were not detected in a sample, ratios were excluded (-).

Accession	Description	Protein Abundance ratio		
		Flag_YPD / WT_YPD	Flag_YP / WT_YP	Flag_YPD / Flag_YP
Vnz_27390	DNA-binding response regulator; CutR	84.685	32.259	1.568
Vnz_01460	L-threonine 3-dehydrogenase	57.664	1.613	0.980
Vnz_08945	Phage shock protein A	20.263	-	-
Vnz_08915	Iron-sulphur cluster insertion protein; ErpA	15.087	10.033	1.199
Vnz_14500	50S ribosomal protein L25/general stress protein; Ctc	13.919	-	-
Vnz_19420	Folate-binding protein; YgfZ	11.355	0.154	62.345
Vnz_22095	DNA-binding response regulator; EsrR	11.242	-	-
Vnz_13735	Membrane dipeptidase	10.684	1.001	1.952
Vnz_08495	Cell division protein; DivIVA	10.621	-	-
Vnz_07620	Fe-S cluster assembly ATPase; SufC	10.116	0.356	11.989
Vnz_12940	Hypothetical protein	9.490	-	-
Vnz_23725	MgtE family magnesium transporter	8.505	-	-
Vnz_24060	3-phosphoshikimate 1-carboxyvinyltransferase	8.405	-	-
Vnz_17705	Ion channel protein	8.005	4.079	1.306
Vnz_11365	Phosphate starvation-inducible protein; PhoH	7.626	-	-
Vnz_15850	DNA-binding response regulator; CseB	7.589	-	-

Vnz_18835	Phosphoribosylaminoimidazolesuccinocarboxamide synthase	7.295	-	-
Vnz_26675	4-hydroxy-tetrahydrodipicolinate synthase	7.139	1.040	3.255
Vnz_05960	NADPH-dependent ferric siderophore reductase	7.071	-	-
Vnz_24955	Hypothetical protein	6.855	1.035	7.167
Vnz_09595	DNA primase	6.678	-	-
Vnz_18925	Phosphoribosylformylglycinamidine cyclo-ligase	6.562	-	-
Vnz_28790	1-deoxy-D-xylulose-5-phosphate synthase	6.368	0.554	0.789
Vnz_06655	Bifunctional acetaldehyde-CoA/alcohol dehydrogenase	5.360	-	-
Vnz_26710	Hybrid sensor histidine kinase/response regulator; OsaB	5.004	-	7.839
Vnz_11650	Ribonuclease E/G	4.894	18.723	2.397

There was one protein which was significantly more enriched in the YP FLAG/WT comparisons compared to the YPD samples, Vnz_11650, an endonuclease of the RNase E/G family which was found to be roughly 19-fold enriched. Vnz_11650 is 1,291 amino acids in length and contains an arginine rich central domain categorising it as a type III RNaseE/G enzyme involved in stable-RNA processing and mRNA decay (Mackie, 2013). This is similar to the Rns RNaseE/G described in *S. coelicolor* which, whilst non-essential, is capable of forming degradosomes. The ratio of Vnz_11650 when comparing FLAG YPD to FLAG YP is roughly 2-fold higher when glucose is present but is only 5-fold enriched compared to the YPD WT control. This suggests the protein is more abundant when glucose is present but binds CutR less often under those conditions, perhaps preferring the dephosphorylated CutR. Hypothetically, activation of CutR could release it from RNase E/G binding, allowing the formation of active RNA degradosomes. However, with current evidence this is a large theoretical leap and purely presented to encourage discussion.

Whilst many of the interactions presented here warrant further investigation, the overall consensus was that there was no clear and obvious CutR binding partner that could explain the observed phenotype. Thus it was considered more important to define the binding site of homodimeric CutR, discussed below. Further work on these protein-protein interactions would involve *in vitro* binding experiments, requiring heterologous expression and purification of each target protein. This was deemed unfeasible given the remaining time and focus was shifted to further investigating the CutR ChIP-seq results.

4.3. Binding site identification

Reporter genes are commonly used to identify and measure promoter activities. We opted to use the β-glucuronidase (GUS) reporter enzyme encoded by a *gusA* gene that has been optimised for streptomycete research in the pMF96 vector system (Myronovskyi *et al.*, 2011; Feeney *et al.*, 2017). Promoter fusion constructs were generated using conservative estimates of the *cutRS, vnz_08815* and *htrA3* promoter regions informed by the centre of peak enrichment in the ChIP-seq and previous *S. venezuelae* transcript start site mapping (Munnoch *et al.*, 2016). Using GUS assays, optimised for high-throughput using 96-well plates, we tested the activity of all three promoters alongside the empty plasmid as a negative control. These were tested in the WT and Δ*cutRS* strains on both YP and YPD with the glucuronidase activity normalised using cell lysate protein concentration (**Chapter 2.49**).

As can be observed in **Figure 4.4** the *cutRS* operon promoter was observed to have very little activity but was more active than the control plasmid. There was no significant difference between the activity on YP and YPD in the WT strain which matches the glucose-independent CutR binding to *cutRSp* previously observed in the ChIP-seq data. In the *ΔcutRS* mutant, *cutRSp* activity on YP was similar to the WT on YP and YPD however on YPD the activity was almost undetectable, suggesting a lack of *cutRSp* activation on YPD in the absence of CutRS, despite the detectable ChIP-seq enrichment. This likely suggests another regulator is activating the expression of *cutRS* on YP, with CutR taking over that role on YPD. However, the level of expression of all *cutRSp* samples, whilst reliably repeatable, is ultimately so low that it is difficult to be confident in making any conclusions. The glucuronidase activity of *vnz_08815p* and *htrA3p* was observed to be within a better range. The activity of *vnz_08815p* driven glucuronidase expression was approximately 4-fold higher than that of *cutRSp* and did not significantly vary between YP and YPD in the WT samples. Whilst activity was similar to the WT in the Δ*cutRS* YP samples, there was a slight increase in the YPD samples. Together it would appear that the presence of CutRS on YP is irrelevant to promoter activity and actually reduces promoter activity when glucose is abundant. The opposite was found in the *htrA3p* activity assays. Whilst there was a small reduction in glucuronidase activity when comparing the WT and Δ*cutRS* mutant

on YP, this was insignificant compared to the effect on YPD. The addition of glucose increased activity almost 10-fold in the WT *htrA3p* samples but from there fell almost 300-fold to near undetectable levels in the Δ*cutRS* YPD samples. This would suggest CutRS is likely indispensable for *htrA3* expression on YPD and is induced by glucose.

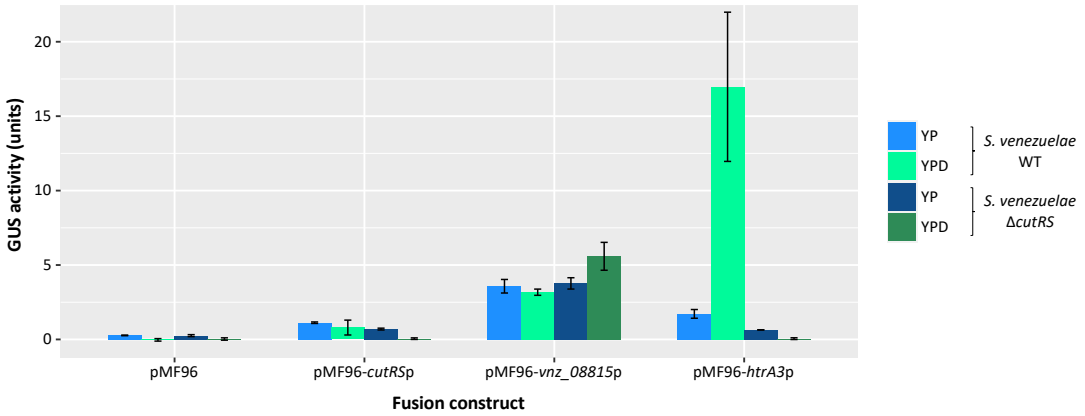

Figure 4.4. Glucuronidase activity of *S. venezuelae* WT and Δ*cutRS* strain cell lysates containing pMF96 fusion constructs or empty pMF96 vector. Glucuronidase activity was measured after 2 days incubation on YP and YPD agar.

The promoter regions chosen for the original pMF96 constructs were quite large, generally around 200 bp but up to 550 bp for the *cutRSp* and this, combined with the relatively wide ChIP-seq peaks, did not allow for the identification of a putative CutR binding site. Attempts were undertaken to define the binding site *in vivo* using variations of the pMF96 constructs with incremental truncations however this proved unsuccessful due to technical issues. Instead, the focus was switched to *in vitro* binding assays using ReDCaT SPR. This technique combines the protein of interest and biotin-labelled double stranded oligo probes to identify and footprint DNA-binding proteins in a manner far more high-throughput than the optimised GUS assay protocol. It does however require considerable amounts of purified protein (Stevenson *et al.*, 2013). RRs are generally amenable to heterologous expression and purification from *E. coli*, often proving non-toxic, soluble and expressed at high concentrations even without codon optimisation. This proved to be the case with CutR, using a N-terminal 6xHis tagged fusion protein it was possible to produce and purify large quantities of soluble protein as detailed in **Chapter 2.30** and **Chapter 2.31**.

Native mass spectrometry was used to confirm the mass of the purified 6xHis-CutR (25,949 Da with a cleaved N-terminal methionine group) with a minor peak present of an additional 178 Da, equivalent to two phosphoryl groups with a neutral loss of a water molecule (**Figure 4.5**). Additional peptide fragmentation was used in an attempt to determine the location of these groups however this was unsuccessful as there were multiple precursor peptides with indistinguishable masses, proving too complex to deconvolute. However, the presence of phosphoryl groups on the purified peptide suggests a proportion of heterologously expressed CutR has been phosphorylated by non-specific kinases in *E. coli*. Unfortunately, this native MS was a targeted ion search and as such unable to confirm the presence of any dimerization within the purified sample.

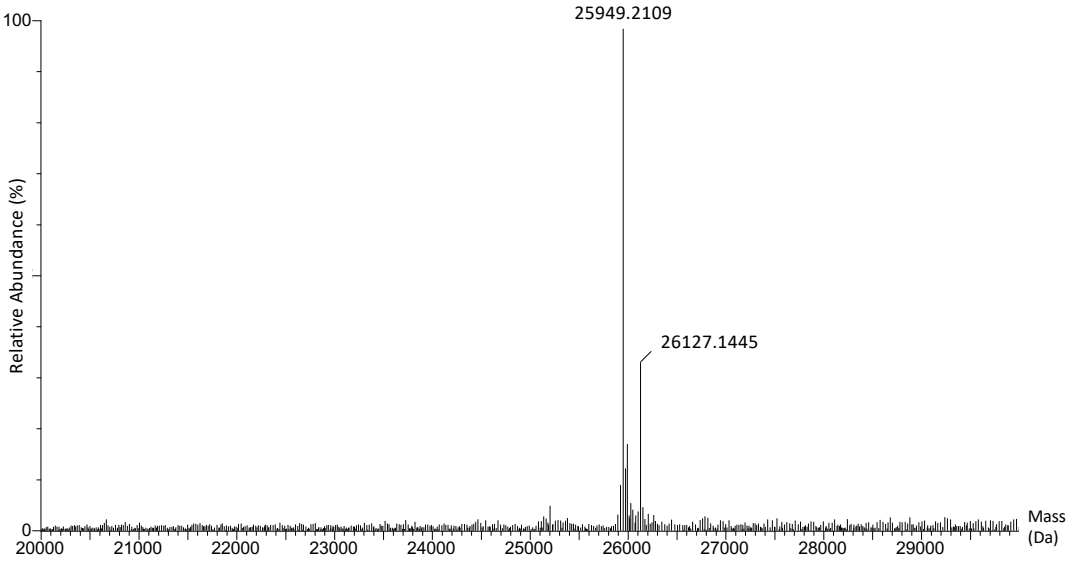

Figure 4.5. Native mass spectrometry analysis of heterologously produced 6xHis-CutR. The peak present at 25,949 Da is equivalent to 6xHis-CutR lacking the N-terminal methionine group. The peak present at 26, 127 Da is equivalent to 6xHis-CutR with the addition of two phosphoryl groups and the neutral loss of a water molecule.

For ReDCaT SPR the three promoters of interest were each divided into a series of overlapping fragments *in silico* as described in **Chapter 2.35***,* resulting in 22 *cutRSp*, 10 *vnz_08815p* and eight *htrA3p* fragments. Using a range of 6xHis-CutR concentrations, a preliminary scan was performed on all 40 fragments to identify putative CutR binding fragments (**Figure 4.6A**). Ligand-binding activity was measured

in $\%R_{MAX}$ of CutR binding to DNA ligand normalised by relative capture level and molecular weight (Stevenson *et al.*, 2013). The molecular weight of CutR for the calculations was that of a single monomer, rather than a dimer, as we had not been able to absolutely confirm the presence of a homodimer with native MS as explained above.

No obvious CutR binding to any *cutRSp* fragments was detected at any of the assayed concentrations which was curious given the obvious CutR enrichments detected in the ChIP-seq data. Binding was however detected in *vnz_08815p* and *htrA3p* fragments with *vnz_08815p* #4 and *htrA3p* #3 observed to have the greatest $\%R_{MAX}$ (**Figure 4.6B**). As the $\%R_{MAX}$ of *htrA3p* #3 was relatively low compared to *vnz_08815p* #4, and was only roughly $20\%R_{MAX}$, the screening was repeated with higher concentrations of CutR to determine if there was concentration-dependant binding indicative of real CutR-DNA interactions, which proved to be the case (**Figure 4.7A**). Two additional fragments centred on the overlaps upstream and downstream of *htrA3p* #3 were included, with the upstream fragment, *htrA3p* #2.5 revealing the binding site was likely towards the 5' end of *htrA3p* #3.

In order to further define the putative CutR binding region both *vnz_08815p* #4 and *htrA3p* #3 were truncated in 2 bp increments from the 3' end, termed "right hand" (RH) truncations for footprinting. Additionally, both fragments were reverse complemented and similarly truncated from the 3' end, termed "left hand" (LH) truncations. This bidirectional approach allows for a more accurate identification of the putative CutR binding site whilst ensuring that there is enough structural support for protein-DNA interaction at all times. Generated fragments were screened as before with the results presented in **Figure 4.7B** (*vnz_08815p*) and **Figure 4.7C** (*htrA3p*). Loss of CutR binding activity was apparent at RH_-24 and RH_-20 for *vnz_08815p* and *htrA3p* respectively whilst truncations from the LH direction were ineffective until LH_-6 for *vnz_08815p* and LH_-12 for *htrA3p* (**Table 4.2**).

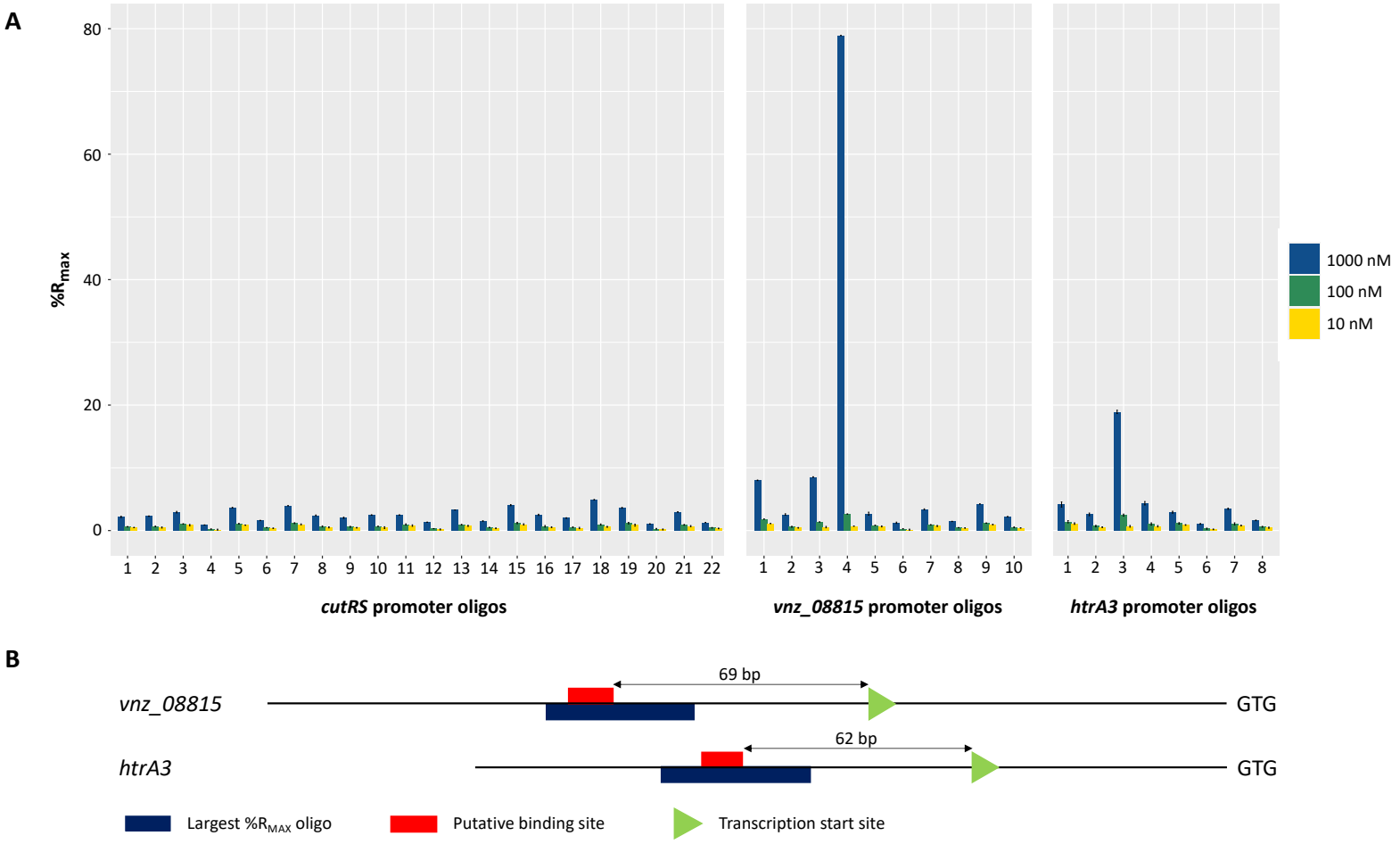

Figure 4.6. A) ReDCaT SPR scanning of the *cutRS, vnz_08815* and *htrA3* promoter region fragments. Three concentrations of 6xHis-CutR were used: 1000, 100 and 10 nM. The $\%R_{MAX}$ was determined using the molecular masses of the annealed oligo duplex and monomeric 6xHis-CutR. **B)** Schematic representations of the promoter regions of *vnz_08815* and *htrA3* including the highest $\%R_{MAX}$ oligo, putative CutR binding site and TSS.

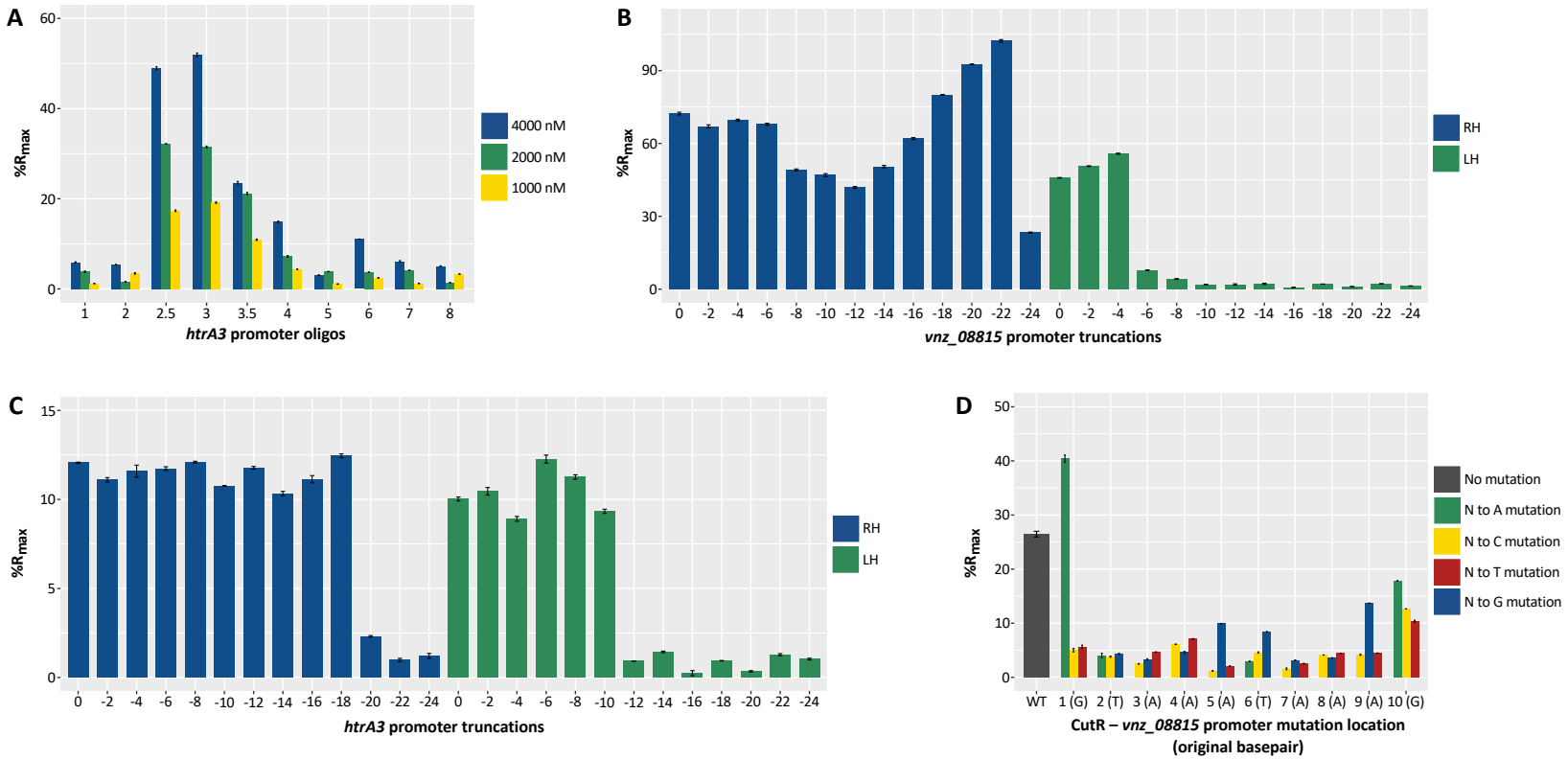

Figure 4.7. A) ReDCaT SPR scanning of the *htrA3* promoter region fragments at 4000, 2000 and 1000 nM. Three concentrations of 6xHis-CutR were used: 1000, 100 and 10 nM. **B)** ReDCaT SPR footprinting of *vnz_08815p* using serially truncated DNA fragments to define the extent of the CutR binding site using 1000 nM 6xHis-CutR. RH: right hand borders; LH: left hand borders. **C)** ReDCaT SPR footprinting of *vnz_08815p* using serially truncated DNA fragments to define the extent of the CutR binding site using 1000 nM 6xHis-CutR. RH: right hand borders; LH: left hand borders. **D)** Further ReDCaT SPR footprinting of *vnz_08815p* using single base pair mutations within the putative binding site. The number indicates location with original nucleotide in brackets. WT represents the unaltered binding site. The $\%R_{MAX}$ for all experiments was determined using the molecular masses of the annealed oligo duplex and monomeric 6xHis-CutR.

Table 4.2. Overview of information derived from ReDCaT SPR experiments and *in silico* analysis of *vnz_08815* and *htrA3* putative promoter regions. RH: "right hand"; LH: "left hand" truncation direction.

	Gene promoter	
	vnz_08815p	***htrA3p***
Largest %R_{MAX} ReDCaT fragment	#3	#4
RH boundary	-24	-20
LH boundary	-6	-12
Truncation refined CutR binding site	GTGTAAATAAAGTG	TATATAAAGGTG
Truncation consensus site	TAWATAAAG	
Distance to TSS	69 bp	62 bp

Finally, to determine the relative importance of each nucleotide within the putative CutR binding site a series of mutations were made to the *vnz_08815p* RH_-22 fragment, specifically to nucleotides within the GTAAATAAAG motif (**Figure 4.7D**). In comparison to the control fragment, almost every single mutation resulted in significant loss of CutR binding. Whilst the first base, G, was not considered part of the truncation-defined consensus binding site, mutation of this position resulted in both increased affinity (G to A) or decreased affinity (G to C or T). Indeed, there is a guanine present at the same position in *htrA3p* but was dispensable for CutR binding during truncation. Whilst position 5 could somewhat tolerate an A to G mutation, both A to C and A to T mutations had the strongest negative effect on CutR binding.

A similar effect was present for the adenine at location 9. Mutation of the final G at location 10 had the weakest effect, with only small reductions in binding affinity for any substituted base. Together this suggests that the core CutR binding site is relatively specific with only a few tolerated substitutions capable of sustaining significant CutR binding *in vitro*, with these mainly present at the extremities. The identified *htrA3p* CutR binding site has a thymine instead of an adenine at location 4. This thymine was not tolerated well in the analysis of *vnz_08815p* mutations resulting in an $\%R_{MAX}$ of about 5, roughly half that of the similar truncated *htrA3p* fragment, suggesting that perhaps other bases outside of the core sequence can help stabilise binding to less preferential sites. Ideally similar mutations would be made to the GUS constructs discussed earlier and promoter activity further examined *in vivo* in the future to determine the true biological tolerance, especially within the core of the binding site. This is further discussed in **Chapter 4.7**. however the identification of a CutR binding site is a big step towards defining the CutRS regulon (**Figure 4.8**).

It is possible that CutR binding could be non-specific due to the AT-rich nature of the suggested consensus sequence. Indeed, the introduction of the G-to-A mutation at position one increased CutR binding (**Figure 4.7D**) which may suggest this to be the case. Further scrambling experiments would be prudent to confirm or deny this possibility.

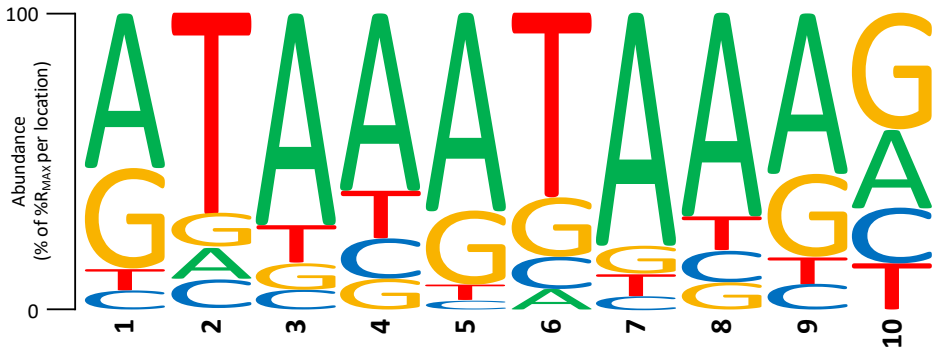

Figure 4.8. CutR-binding consensus sequence logo. The relative abundance of $\%R_{MAX}$ for each location was calculated from the ReDCaT SPR mutagenesis.

4.4. Tandem Mass Tagging proteomics

In general, ChIP-seq experiments are combined with some form of transcriptomics, such as RNA-seq, to identify differential gene expression in mutant strains and confirm putative regulons. Whilst this is often successful, it is important to remember it is, in general, a change in protein, not RNA, abundance which causes a phenotype. There is a complex relationship between mRNA levels and protein abundance which is currently impossible to predict for large datasets (McManus, Cheng and Vogel, 2015). Beyond transcript concentration the final abundance of a protein can be influenced by sequence-dependant translation rates, protein synthesis delay and protein half-life, among other modulators (Liu, Beyer and Aebersold, 2016). The obvious solution to this issue is to measure protein abundance, and ideally activity, rather than mRNA abundance. The recent improvements in LC-MS/MS technologies, alongside the introduction of isobaric tags, has made large-scale proteome comparison achievable and reliable, with one of these techniques termed tandem mass tagging (Thompson *et al.*, 2003). TMT proteomics uses isobaric chemical tags to label isolated peptides via an amine-reactive NHS-ester group. Additionally, the tags allow for multiple samples to be combined and multiplexed before analysis by LC-MS/MS. All differentially tagged peptides of the same mass will appear identical during the MS1 scan however these reporter ions then become distinguishable following fragmentation of the precursor ion during MS2 (Rauniyar and Yates, 2014). With this new technology available, TMT proteomics was chosen over RNA-seq to confirm the CutR regulon identified by ChIP-seq along with providing valuable information in the molecular differences between the *S. venezuelae* WT and Δ*cutRS* mutant.

The proteome comparison between the *S. venezuelae* WT and the Δ*cutRS* strains grown on YPD agar was of primary interest as this is where the phenotype is observed, however the comparison between WT grown on YP and YPD was also of interest and can be seen in **Figure 4.9A**. In regard to the latter, only 347 proteins were 2-fold more abundant in the presence of glucose whilst, when *S. venezuelae* was deprived of glucose on YP and thus exploring, 1,285 proteins were similarly affected. This highlights both the proteins expressed during explorative growth and

the generally repressive nature of glucose on gene expression, also known as carbon catabolite repression (Romero-Rodríguez *et al.*, 2016).

Whilst there is a huge amount of useful data in the above comparison, and indeed the other comparisons not noted here, the full data set, along with full data sets for all the other proteomics experiments detailed in this work, can be accessed within the Supplementary data (**Table S1 – Table S4**). Importantly we can observe the effects of glucose on the abundance of proteins described earlier in this chapter. Both Vnz_08815 and HtrA3 were >15-fold more abundant in the wild-type strain grown on YPD agar in comparison to the samples obtained from YP agar. CutR and CutS were affected but less so, only showing an increase of 2.9- and 2.2-fold respectively. The GDPD Vnz_18425 was less than 2-fold affected. This would suggest that both Vnz_08815 and HtrA3 were important in the response to glucose, and Vnz_18425 less so, if at all. A large change in abundance of TCS proteins, such as CutR and CutS, would not necessarily be expected. Overexpression of large membrane proteins, such as SKs, can reduce membrane stability and induce stress whilst RRs rely on phosphorylation and dimerization more than concentration to affect gene transcription. Indeed, the results of the previous studies discussed in this chapter would suggest expression of the *cutRS* operon is either under exceedingly tight control, or with no apparent CutR-homodimer binding, is simply unresponsive to the presence of glucose.

Of more interest are the results of the WT/Δ*cutRS* comparison on YPD displayed in **Figure 4.9B** with large (>4, <0.25) changes highlighted in **Table 4.3**. Whilst you would expect the fold change for the deleted protein, CutR and CutS, to be infinitely large as no unique CutR or CutS-derived peptides should be detected in the Δ*cutRS* samples, this is not the case due to false positives caused by systematic errors, including miscalling from modified peptides (Bogdanow, Zauber and Selbach, 2016). However, CutR and CutS are the two most differentially abundant proteins in the WT samples in comparison to the mutant.

There were 312 proteins found to increase >2-fold in the Δ*cutRS* samples, whilst only 42 decreased. Whilst Vnz_18425 remains relatively unchanged (1.3-fold reduced) in

the Δ*cutRS* mutant, both HtrA3 and Vnz_08815 are significantly more affected, 8- and 3-fold reduced, respectively. Two other proteins of note are Vnz_23735 (20-fold depleted) and Vnz_02160 (6.8-fold depleted). Vnz_23735 is a conserved MgtE-family $Mg^{2+}/Co^{2+}/Ni^{2+}$ transporter whilst Vnz_02160 is annotated as a hypothetical protein. Further investigation using the NCBI conserved domain search function (www.ncbi.nlm.nih.gov) reveal a N-terminal peptidoglycan binding domain and a C-terminal VanW superfamily domain of unknown function.

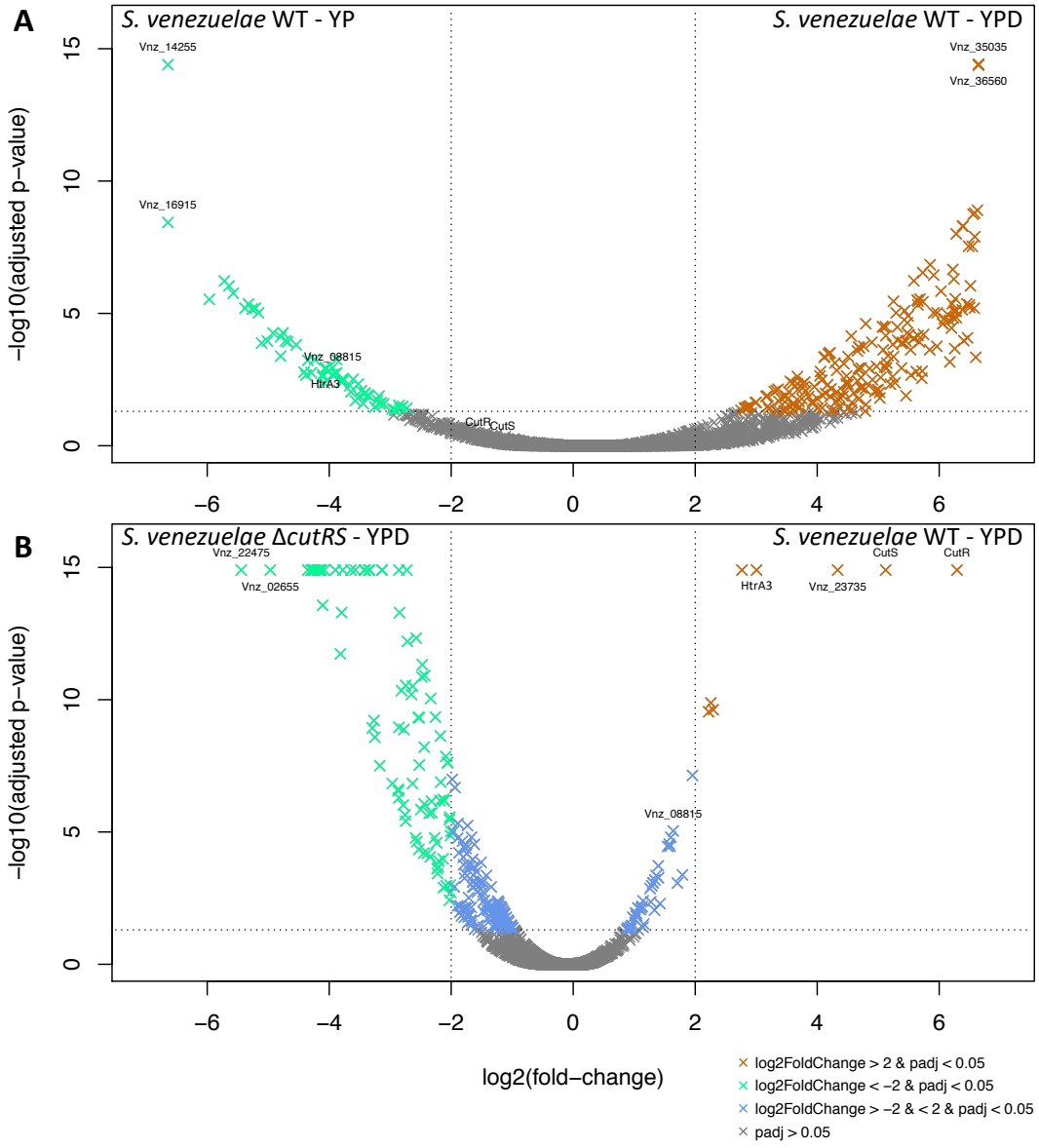

Figure 4.9. Volcano plot of log_2(fold-change) protein abundance against -log_{10}(adjusted p-value between: **A)** *S. venezuelae* WT grown on YP and YPD agar; **B)** *S. venezuelae* WT and Δ*cutRS* strains grown on YPD agar.

With more than 300 proteins differentially more abundant in the Δ*cutRS* YPD samples the data suggests that carbon catabolite repression is less severe than observed in the WT. The decreased abundance of Vnz_08815 and HtrA3 in the Δ*cutRS* mutant grown on YPD, combined with the ChIP-seq data, DNA-binding experiments and increased abundance in the presence of glucose all suggest that CutRS is a direct activator of *vnz_08815* and *htrA3* expression, in response to glucose. However, beyond this fact it becomes difficult to discern other proteins of interest from within the large datasets. Of the proteins identified in **Table 4.3** there are two orphan response regulators which are known to form heterodimers (BldM and WhiI), one TCS RR (CagR) and one SK (CssS) which is discussed later in this chapter.

Table 4.3. Protein abundance ratio between *S. venezuelae* WT and Δ*cutRS* on YPD agar. Filtered to contain significant (p <0.05) hits with a fold-change of >4 or <0.25.

Accession	Description	Protein Abundance Ratio *S. venezuelae* YPD WT / Δ*cutRS*
Vnz_27390	DNA-binding response regulator; CutR	78.38
Vnz_27395	Two-component sensor histidine kinase; CutS	34.835
Vnz_23735	MgtE family magnesium transporter	20.178
Vnz_18430	Protease; HtrA3	8.033
Vnz_02160	Hypothetical protein	6.801
Vnz_25680	Proline dehydrogenase	4.907
Vnz_31560	Acyl-ACP desaturase	4.777
Vnz_25685	1-pyrroline-5-carboxylate dehydrogenase	4.657
Vnz_00400	Mini-circle protein	0.249
Vnz_15810	Hypothetical protein	0.249
Vnz_19085	MFS transporter	0.248
Vnz_11185	ArsR family transcriptional regulator	0.247
Vnz_19320	Hypothetical protein	0.246
Vnz_13465	Peptidase	0.245
Vnz_35455	Oxidoreductase	0.245
Vnz_09560	Biliverdin-producing heme oxygenase	0.24
Vnz_34840	Bifunctional ornithine acetyltransferase/N-acetylglutamate synthase	0.24
Vnz_12285	Potassium-transporting ATPase subunit A	0.236
Vnz_16710	Short-chain dehydrogenase/reductase	0.235
Vnz_14340	Hypothetical protein	0.231
Vnz_16245	Hypothetical protein	0.229
Vnz_36480	YfcE family phosphodiesterase	0.229
Vnz_32470	DUF2470 domain-containing protein	0.228
Vnz_12570	Acyl-CoA dehydrogenase	0.222
Vnz_12205	Hypothetical protein	0.221
Vnz_23115	Septum formation initiator	0.22

Vnz_25290	Hypothetical protein	0.217
Vnz_34720	Hypothetical protein	0.216
Vnz_27940	DNA helicase; UvrD	0.214
Vnz_34830	Acetylornithine aminotransferase	0.213
Vnz_16155	Hypothetical protein	0.212
Vnz_34785	Mon-ribosomal peptide synthetase	0.209
Vnz_29085	Hypothetical protein	0.207
Vnz_09900	Transcriptional regulator	0.201
Vnz_19330	Two-component sensor histidine kinase; CssS	0.2
Vnz_26885	Glutamate ABC transporter ATP-binding protein	0.198
Vnz_11990	Sugar-binding protein	0.197
Vnz_14405	Hypothetical protein	0.195
Vnz_14410	Peptide ABC transporter ATP-binding protein	0.191
Vnz_26880	Glutamate-binding protein	0.185
Vnz_27105	LucA/LucC family protein	0.184
Vnz_34255	Glutamate ABC transporter ATP-binding protein	0.184
Vnz_31930	Histidine kinase	0.183
Vnz_11750	Hypothetical protein	0.18
Vnz_34260	Glutamate-binding protein	0.179
Vnz_18830	Phosphoribosylamine-glycine ligase	0.177
Vnz_12280	Potassium-transporting ATPase subunit B	0.174
Vnz_22005	DNA-binding response regulator; BldM	0.174
Vnz_29080	Transcriptional regulator	0.173
Vnz_18555	DNA-binding response regulator; CagR	0.172
Vnz_22480	Transferase	0.169
Vnz_13900	Hypothetical protein	0.168
Vnz_08075	Lysine 6-monooxygenase	0.167
Vnz_34690	Branched-chain amino acid aminotransferase	0.161
Vnz_10425	Hypothetical protein	0.161
Vnz_25605	Hypothetical protein	0.159
Vnz_24915	Hypothetical protein	0.152

Vnz_09580	Peroxidase	0.151
Vnz_23160	Hypothetical protein	0.149
Vnz_29910	Hypothetical protein	0.149
Vnz_34695	Ligase	0.148
Vnz_02660	Hypothetical protein	0.146
Vnz_36840	Hypothetical protein	0.145
Vnz_37170	Hypothetical protein	0.142
Vnz_23450	GntR family transcriptional regulator	0.139
Vnz_34775	L-lysine 6-monooxygenase	0.138
Vnz_12275	Potassium-transporting ATPase subunit C	0.138
Vnz_34710	Bacilysin biosynthesis protein; BacA	0.138
Vnz_27205	GntR family transcriptional regulator	0.137
Vnz_23130	Secretion protein	0.137
Vnz_01275	N-acetylmuramoyl-L-alanine amidase	0.128
Vnz_34680	Radical SAM protein	0.114
Vnz_26870	Amino acid ABC transporter permease	0.114
Vnz_28820	DNA-binding response regulator; WhiI	0.111
Vnz_26105	Hypothetical protein	0.105
Vnz_16495	WhiB family transcriptional regulator; WblA	0.104
Vnz_06785	Hypothetical protein	0.102
Vnz_36560	Serine protease	0.099
Vnz_27645	Hypothetical protein	0.098
Vnz_23155	Hypothetical protein	0.094
Vnz_08080	Aspartate aminotransferase family protein	0.093
Vnz_15140	Transcriptional regulator	0.084
Vnz_30865	Hypothetical protein	0.08
Vnz_02640	Cytochrome P450	0.073
Vnz_02645	ATP-binding protein	0.072
Vnz_26875	Glutamate ABC transporter permease	0.071
Vnz_31740	ATP-binding protein	0.067
Vnz_15655	RNA polymerase subunit sigma-24	0.059

Vnz_23860	Reductase	0.059
Vnz_35830	Hypothetical protein	0.058
Vnz_22485	N-acetylneuraminate synthase	0.057
Vnz_28050	Cation/H^+ antiporter	0.056
Vnz_22680	DeoR family transcriptional regulator	0.055
Vnz_19340	Serine protease; HtrB	0.053
Vnz_01265	Hypothetical protein	0.052
Vnz_07365	Hypothetical protein	0.051
Vnz_18230	LacI family transcriptional regulator	0.051
Vnz_35045	SAM-dependent methyltransferase	0.049
Vnz_02655	Dynein regulation protein LC7	0.032
Vnz_22475	Hypothetical protein	0.023

As discussed in **Chapter 3.3** the Δ*cutRS* mutant overproduces the antibiotic chloramphenicol. With no evidence of CutR directly regulating the expression of known chloramphenicol regulators, such as *cmlR* or *jadR1* (Sekurova *et al.*, 2016), in the ChIP-seq dataset, it was prudent to investigate the abundance of chloramphenicol biosynthetic proteins, and relevant shikimate pathway enzymes, in the Δ*cutRS* mutant in comparison to the WT samples on YPD (**Table 4.4**). Overall, the chloramphenicol biosynthetic proteins were slightly more abundant in the Δ*cutRS* mutant, on average 1.38-fold increased (s.d. ± 0.200), with the efflux pump CmlF showing the largest increase (1.85-fold). The pathway specific activator CmlR showed the smallest (1.06-fold) change between wild-type and *cutRS* mutant. In comparison, the shikimate pathway enzymes were unchanged with an average 1.03-fold change with some marginally more abundant in the WT samples, but insignificantly so. We were unable to detect the phosphopantetheinyl transferase Vnz_04405 (CmlL) or three shikimate pathway enzymes (Vnz_30840/845/850). The reaction catalysed by Vnz_04405 and Vnz_30850 is also catalysed by Vnz_08705 which was 1.29-fold more abundant in the mutant samples. The reaction catalysed by Vnz_30840 and Vnz_30845 can also be catalysed by CmlB (Vnz_04425) which was 1.25-fold more abundant in the Δ*cutRS* samples (Bibb *et al.*, 2014). This would suggest that the conversion of chorismic acid to 4-amino-4-deoxy chorismic acid is possibly reliant on CmlB which is encoded within the chloramphenicol BGC. However, deletion of the chloramphenicol BGC does not disturb growth or development and so is unlikely to have disrupted the shikimate pathway. It is likely that in the absence of the chloramphenicol BGC, Vnz_30840 and/or Vnz_30845 could be produced to catalyse that same reaction. The Δ*cutRS* mutant produces twice as much chloramphenicol as the WT strain (1649 vs. 725 ng/ml), detectable in the underlying agar. Whilst most of the biosynthetic proteins are only slightly more abundant in the mutant, the CmlF efflux pump has the largest change and the CmlN pump also increases 1.585-fold in the mutant, so it is possible that whilst intracellular production of chloramphenicol does not change much between the WT and Δ*cutRS* mutant, the export of the antibiotic increases in the mutant. This is consistent with the agar plate bioassays and HPLC extraction analysis of the growth medium (**Figure 3.12**and **Figure 3.15**).

Table 4.4. Protein abundance ratio between *S. venezuelae* WT and Δ*cutRS* on YPD agar of chloramphenicol biosynthetic proteins (CHL) and shikimate pathway enzymes (SHI). Proteins not detected indicated with (-). Chloramphenicol BGC protein descriptions adapted from Bibb *et al.*, 2014.

Accession	Description	Protein Abundance Ratio *S. venezuelae* YPD Δ*cutRS* / WT	Pathway
Vnz_04400	Transcriptional regulator; CmlR	1.063	CHL
Vnz_04405	Phosphopantetheinyl transferase; CmlL	-	CHL
Vnz_04410	Cation/H^+ antiporter; CmlN	1.585	CHL
Vnz_04415	Chloramphenicol efflux pump; CmlF	1.848	CHL
Vnz_04420	DAHP synthase; CmlE	1.536	CHL
Vnz_04425	4-amino-4-deoxychorismate mutase; CmlD	1.248	CHL
Vnz_04430	4-amino-4-deoxyprephenate dehydrogenase; CmlC	1.340	CHL
Vnz_04435	4-amino-4-deoxychorismate synthase; CmlB	1.236	CHL
Vnz_04440	L-PAPA β-hydroxylase; CmlA	1.277	CHL
Vnz_04445	Adenylation, PCP and reductase domains; CmlP	1.387	CHL
Vnz_04450	Amidase; CmlH	1.294	CHL
Vnz_04455	N-oxygenase; CmlI	1.314	CHL
Vnz_04460	Putative acyl carrier protein; CmlM	1.563	CHL
Vnz_04465	Short-chain dehydrogenase - CmlJ	1.645	CHL
Vnz_04470	Acyl-CoA-ACP synthase, AMP ligase; CmlK	1.475	CHL
Vnz_04475	Flavin-dependant halogenase; CmlS	1.282	CHL

Vnz_04480	Aldo-keto reductase; CmlT	1.393	CHL
Vnz_05315	Type II 3-dehydroquinate dehydratase	0.970	SHI
Vnz_05320	3-dehydroquinate synthase	0.985	SHI
Vnz_05325	Shikimate kinase	0.964	SHI
Vnz_05330	Chorismate synthase	0.911	SHI
Vnz_05335	Shikimate dehydrogenase	1.098	SHI
Vnz_08705	3-deoxy-7-phosphoheptulonate synthase	1.292	SHI
Vnz_24060	3-phosphoshikimate 1-carboxyvinyltransferase	1.019	SHI
Vnz_26450	3-phosphoshikimate 1-carboxyvinyltransferase	0.969	SHI
Vnz_30840	Aminodeoxychorismate/anthranilate synthase component II	-	SHI
Vnz_30845	2-amino-4-deoxychorismate synthase	-	SHI
Vnz_30850	3-deoxy-7-phosphoheptulonate synthase	-	SHI

4.5. TMT phosphoproteomics

Post-translational modifications (PTM) of proteins can range from huge (2-10 kDa) oligosaccharide or polypeptide structures to simple methyl, phosphoryl and acetyl groups. These PTMs can drastically change the function of a protein and allow a cell to rapidly respond to situations without needing to undergo protein synthesis and degradation, which is both energetically expensive and time consuming. One of the most important PTMs, particularly in relation to this work, is the addition and removal of phosphate groups as observed with SKs and RRs. To date phosphorylation has been detected on serine, threonine, tyrosine, histidine, aspartate, arginine, lysine and cysteine residues in bacterial proteins (Macek *et al.*, 2019). With the advances in mass spectrometry technology discussed above, and increased knowledge of cellular PTMs, it is becoming possible to study the phosphoproteome of cells. The results below detail only the phosphorylation of serine, threonine and tyrosine residues due to their relative stability compared to the other phosphorylated residues (Hardman *et al.*, 2019). This does mean we are unable to detect the histidine and aspartate phosphorylation of SKs and RRs which would be desirable in future experiments.

The samples collected and analysed for the TMT-proteomics described in **Chapters 2.40-2.44** were also used for TMT-phosphoproteomics. The samples were separated after isobaric labelling and high pH fractionation to allow for phosphopeptide enrichment before LC-MS analysis. Whilst this does not mean they are unequivocally the same, this methodology does make them as comparable as possible. **Figure 4.10** reveals the phosphoproteome changes between the *S. venezuelae* WT and Δ*cutRS* strains on YPD to be much less drastic than the proteome changes observed in **Figure 4.9B**. However, phosphorylation is only one of many PTMs and detectable S/T/Y phosphorylation is only three of the eight previously described phosphopeptides, so this represents a small snapshot of cellular PTMs. Four phosphopeptides were found to be enriched in the WT samples compared to Δ*cutRS,* and 26 diminished (**Table 4.5**).

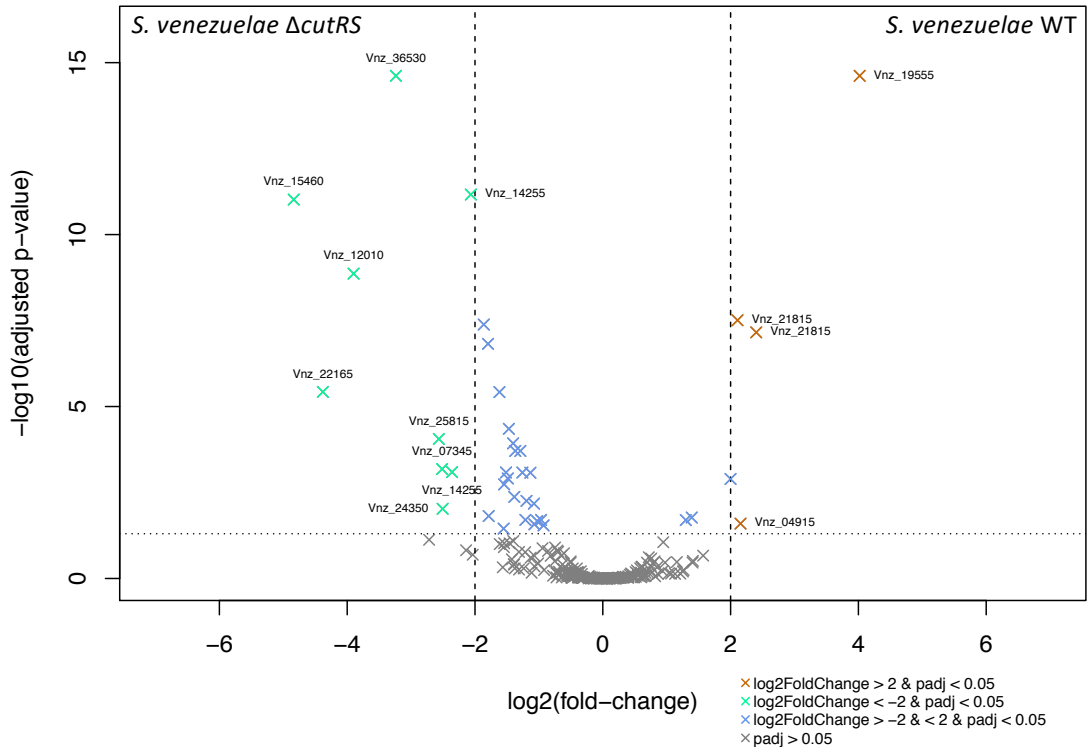

Figure 4.10. Volcano plot of $\log_2$(fold-change) serine/threonine/tyrosine (S/T/Y) protein phosphorylation abundance against -$\log_{10}$(adjusted p-value) between *S. venezuelae* WT and Δ*cutRS* on YPD agar.

Contrastingly, there are far more phosphopeptides found enriched in the mutant strain however many of these are currently annotated as hypothetical proteins. The most enriched phosphopeptide (29-fold) matched to Vnz_15460, annotated as a hypothetical protein. Further investigation reveals Vnz_15460 contains a carbohydrate esterase 4 (CE4) superfamily domain. CE4 superfamily domain proteins are deacetylases catalysing the N- or O-deacetylation of polysaccharides including polymeric GlcNAc, otherwise known as chitin, and bacterial cell wall peptidoglycan, which is formed of alternating β-(1,4) linked GlcNAc and MurNAc residues, also known as murein (Nakamura, Nascimento and Polikarpov, 2017). Whilst little seems to be known about phosphorylation of CE4 deacetylases they share common features with histone deacetylases-8 (HDAC8) including inhibition by the same selective inhibitor ligand, N-hydroxy-4-(naphthalene-1-yl)benzamide, in *Bacillus* spp. (Balomenou *et al.*, 2018). The phosphorylation of HDAC8 at a N-terminal residue

(S39) results in an altered sub-cellular location and a decrease in the rate of deacetylation, despite the PTM being located over 20 Å from the catalytic metal ion (Welker Leng *et al.*, 2019). The identified phosphorylated residue of Vnz_15460 (T47) is similarly N-terminally located which may suggest a similar mechanism of activity modulation in *S. venezuelae* however the modified residue is a tyrosine not serine. HDAC8 is a eukaryotic deacetylase and not directly homologous to CE4s which may explain the residue discrepancy and it is also possible these PTM models are completely incompatible.

In regard to the Δ*cutRS* phenotype, peptidoglycan deacetylation is most likely N-deacetylation with this being preferred over O-deacetylation in Gram-positive bacteria. This modification has been shown to increase resistance to lysozyme and other host defence factors (Vollmer, 2008) and more recently be involved in cell separation, shape, sporulation and cell wall thickness (Balomenou *et al.*, 2013). It is not clear what the role of Vnz_15460 is, beyond a likely CE4 deacetylase, and this would require significant further work. However, it is feasible to believe that the N-terminal phosphorylation of Vnz_15460 could alter the function and/or location of activity and this could be investigated using phospho-mimetic and -depleted mutants to better understand the effect of a N-terminal PMT and its role in the Δ*cutRS* phenotype.

Finally, one chloramphenicol biosynthetic enzyme was found to be significantly differentially phosphorylated in the Δ*cutRS* mutant. The acyl-CoA-ACP synthase / AMP ligase CmlK was phospho-enriched 2.3-fold at Y371. CmlK is thought to adenylate the unidentified aromatic precursor prior to the generation of the dichloroacetylating agent required for the latter stages of chloramphenicol biosynthesis (Piraee, White and Vining, 2004). The effect of this phosphorylation is unknown and whilst there is some precedent for the requirement of tyrosine phosphorylation to enable acyl-CoA synthase activity (Cooke *et al.*, 2011) this does not seem to be a well understood PMT in regards to specialised metabolite biosynthesis but would be worthwhile to investigate.

Table 4.5. Phosphorylation abundance ratio and predicted location of serine/threonine/tyrosine (S/T/Y) phosphorylation between *S. venezuelae* WT and Δ*cutRS* on YPD agar. Filtered to contain significant ($p < 0.05$) hits with a fold-change of >2 or <0.5. Protein abundance from TMT-proteomics also included, except where not available (-).

Accession	Description	Phosphorylation Abundance Ratio YPD *S. venezuelae* WT / Δ*cutRS*	Predicated location of S/T/Y phosphorylation	Protein Abundance
Vnz_19555	Phosphoglyceromutase	16.221	S132	1.025
Vnz_21815	Phosphoglucosamine mutase	5.282	S104	0.944
Vnz_04915	Hypothetical protein	4.455	S108	1.095
Vnz_28550	Tellurite resistance TerB	3.997	S12	2.188
Vnz_15460	Hypothetical protein	0.526	S/T unknown location	1.011
Vnz_13325	Integration host factor	0.512	S77	1.019
Vnz_26610	Hypothetical protein	0.491	S/T unknown location	0.687
Vnz_22660	Phosphomannomutase	0.476	S148	1.095
Vnz_26610	Hypothetical protein	0.456	S102	0.687
Vnz_13410	Hypothetical protein	0.437	S1111	0.737
Vnz_04470	Acyl-CoA-ACP synthase, AMP-ligase; CmlK	0.432	Y371	0.678
Vnz_22165	Succinate-CoA ligase subunit alpha	0.409	S/T unknown location	0.979
Vnz_13410	Hypothetical protein	0.387	S972	0.737
Vnz_13410	Hypothetical protein	0.378	S1143	0.737
Vnz_13410	Hypothetical protein	0.361	S1127	0.737
Vnz_12015	Hypothetical protein	0.357	T413 & T415	0.541
Vnz_22165	Succinate-CoA ligase subunit alpha	0.35	S/T unknown location	0.979

Vnz_26610	Hypothetical protein	0.343	T101	0.687
Vnz_08855	Ubiquinol-cytochrome C reductase	0.341	S154	0.894
Vnz_13410	Hypothetical protein	0.326	S1000 & S1045	0.737
Vnz_37040	Hypothetical protein	0.29	S279	0.379
Vnz_13410	Hypothetical protein	0.275	S920	0.737
Vnz_14255	Transglycosylase	0.195	S96	1.139
Vnz_24350	VOC family virulence protein	0.176	T53 & S59	0.685
Vnz_07345	Cob(I)yrinic acid a,c-diamide adenosyltransferase	0.175	T15	0.808
Vnz_25815	Hypothetical protein	0.169	S398	-
Vnz_36530	ATP-binding protein	0.106	S129	0.269
Vnz_12010	Phosphatase	0.067	S84	0.461
Vnz_22165	Succinate-CoA ligase subunit alpha	0.048	S259	0.979
Vnz_15460	Hypothetical protein	0.035	T47	1.011

4.6. Further investigation of Vnz_08815 and HtrA3

The ChIP-seq, GUS reporter assays and ReDCaT SPR revealed CutR to be interacting with the promoter regions of *vnz_08815* and *htrA3*. Combined with the increased abundance of both of these proteins observed in the *S. venezuelae* WT TMT-proteomics samples, in comparison to the Δ*cutRS* samples, these data were highly suggestive of CutR-induced activation of these genes. Thus, it was decided to investigate these two proteins as part of the molecular mechanism behind the mutant phenotype.

If the expression of these two genes alone is activated by phosphorylated CutR when glucose is present, it was hypothesised that deletion of one, or both genes would recreate the Δ*cutRS* phenotype. Using a targeted CRISPR-Cas9 approach designed by Cobb, Wang and Zhao (2015) it was possible to create scar-less, in-frame deletions of both *vnz_08815* and *htrA3* (**Chapter 2.22**). The deletion efficiency was significantly lower for *vnz_08815* (~1/200 PCR positives), compared with *htrA3* (~1/12 PCR positives) which may indicate a degree of essentiality although this could also be guide-RNA dependant. Both the single mutants, and a double mutant in which Δ*htrA3* was deleted in the Δ*vnz_08815* background, were screened for phenotypes on YP and YPD agar (**Figure 4.11**).

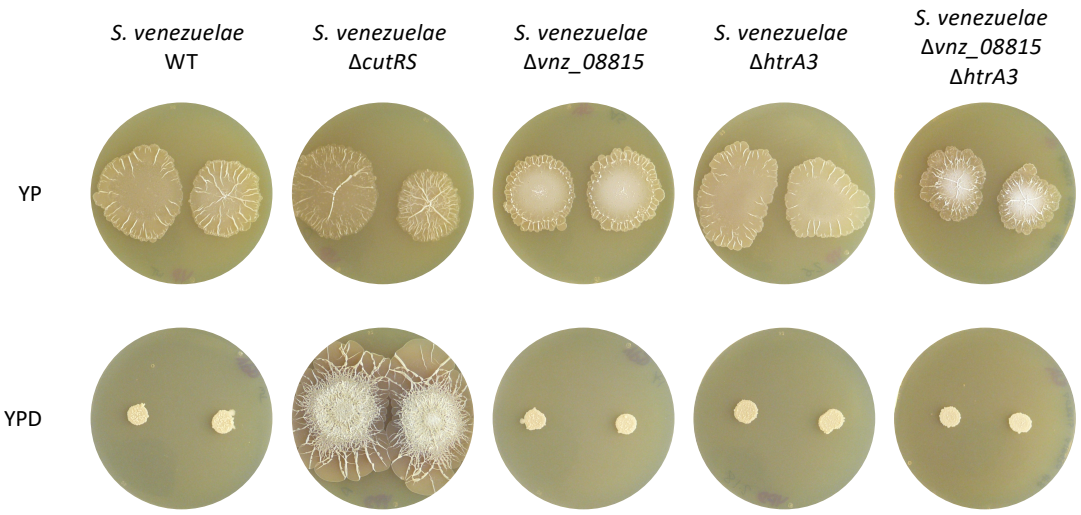

Figure 4.11. Phenotypic comparison of the *S. venezuelae* WT, Δ*cutRS,* Δ*vnz_08815*, Δ*htrA3* and Δ*vnz_08815*Δ*htrA3* strains on both YP and YPD agar.

Neither the single, nor the double mutant strains displayed any altered phenotype in comparison to the *S. venezuelae* WT strain on YPD. There were small phenotypic discrepancies on YP, most prevalent the Δ*vnz_08815*Δ*htrA3* double mutant. The observed colonies were slightly smaller in size with more aerial hyphae production in the centre. Indeed, the same results were also observed on SFM and MYM+TE with and without glucose and the mutant strains showed no growth defects, developing to sporulation normally (data not shown). A number of combinations were attempted to discover if *vnz_08815* and *htrA3* played a role in the Δ*cutRS* phenotype. Using the strong constitutive promoter *ermEp** the genes were overexpressed in the WT, Δ*cutRS,* and single gene deletion strains. This includes the overexpression of *vnz_08815* in both the Δ*vnz_08815* background, and Δ*htrA3* background. None of these combinations could recreate the Δ*cutRS* phenotype.

It is likely that the mutant phenotype is the result of more than just the loss of Vnz_08815 and/or HtrA3 however it is possible these proteins play an important role and thus were deemed worthy of follow-up. One possibility is that in the single deletion strains the strain is capable of activating alternate genes as a counterbalance. To investigate this we used TMT-proteomics, in a similar manner to **Chapter 4.4**, to compare the proteomes of the *S. venezuelae* WT, Δ*vnz_08815* and Δ*htrA3* strains (**Figure 4.12A** and **Figure 4.12B**). As can be observed, there are far fewer significant changes in protein abundance in either single deletion strain in comparison to the changes seen in the *ΔcutRS* mutant (**Figure 4.9**). This could be explained by the fact that neither of these proteins are transcription factors.

What is of interest is the increased abundance of three proteins, encoded in a single operon, in the Δ*htrA3* samples. Vnz_19330 (3-fold increase), Vnz_19335 (2-fold increase) and Vnz_19340 (6-fold increase) are the sensor kinase CssS, partner response regulator CssR and the HtrA-like serine protease HtrB (**Table 4.6**). As discussed in **Chapter 1.7.1.5** the TCS CssRS activates the production of three HtrA-like serine proteases in *S. lividans* as a response to secretion stress but does not regulate the levels of HtrA3, which is homologous to Vnz_18430. The same proteins were also more abundant in the Δ*cutRS* mutant with HtrB 19-fold, CssR 4-fold and CssS 5-fold increased compared to the WT samples. This would suggest that both the

Δ*htrA3* and Δ*cutRS* strains experience some sort of cell envelope stress which requires the expression of CssRS to presumably activate HtrB. The gene *htrB* is encoded upstream of the *cssRS* operon but TSS mapping indicates they are not co-transcribed, but have separate promoters (Munnoch *et al.*, 2016; Bush *et al*., unpublished). Neither of the other two HtrA-like proteins CssRS is reported to activate in *S. lividans* were found to be significantly elevated in either Δ*htrA3* and Δ*cutRS* strains: HtrA1 – Vnz_08960 (not detected) and HtrA2 – Vnz_23710 (1.085-fold and 1.15-fold respectively). This would suggest that either in *S. venezuelae* CssRS only controls the expression of *htrB*, or that in response to the loss of HtrA3, *htrB* expression alone is sufficient compensation. With CutR activating the expression of *htrA3* it is possible that the increase of CssRS and HtrB in the Δ*cutRS* mutant is due to the loss of HtrA3 activity. Data presented below also suggests that CutR represses the expression of *htrB* which may explain the observed changes in HtrB abundance.

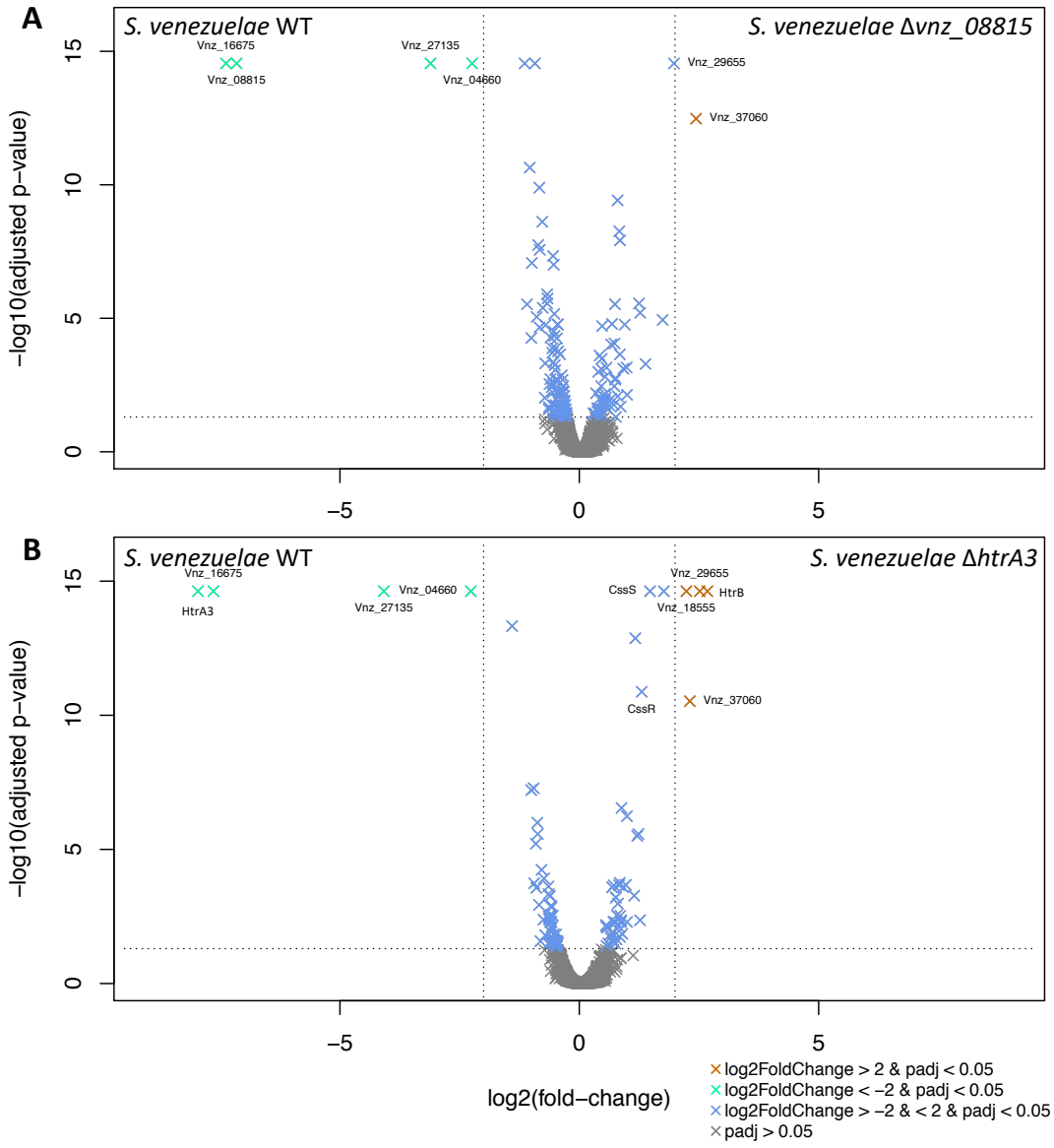

Figure 4.12. Volcano plot of $\log_2$(fold-change) protein abundance against -$\log_{10}$(adjusted p-value) between: **A)** *S. venezuelae* WT and Δ*vnz_08815* on YPD agar; **B)** *S. venezuelae* WT and Δ*htrA3* on YPD agar.

There are no large (>2-fold, <0.5-fold) significant changes in the proteome of Δ*vnz_08815* that are not present in the proteome of Δ*htrA3.* However, the closest homologue to Vnz_08815 is Vnz_08810 (47% identities) which is 1.98-fold more abundant in the Δ*vnz_08815* mutant samples. These genes are sequentially encoded and TSS mapping suggests they are expressed on the same transcript (Munnoch *et al.*, 2016; Bush *et al.,* unpublished). In the proteome of *S. venezuelae* Δ*cutRS*, Vnz_08810 is only 1.25-fold more abundant so whilst it is possible the expression of *vnz_08810* is activated in both mutants, it is more likely that either Vnz_08810 is required less in the Δ*cutRS* mutant, or the deletion of *vnz_08815* has had off-target effects affecting the expression of the downstream gene. Beyond the increased abundance of Vnz_08810 there seems to be no obvious changes to the proteome. As previously mentioned in **Chapter 4.1** Vnz_08815 is homologous to CgR_2070 of *C. glutamicum* which appears to be involved in cell separation but is accessory to CgR_1596. It is possible that a similar situation occurs in *S. venezuelae* where deletion of *vnz_08815* has no phenotypic effect but would exacerbate other cell development defects. Vnz_22100 is the closest homologous protein to CgR_1596 but with only 29% identity and could not be detected in any of the TMT-proteomic samples. Whilst all this deserves further investigation, it appears that the most likely scenario is that HtrA3 is a considerably more important protein in the Δ*cutRS* phenotype than Vnz_08815 and data presented later in **Chapter 5** corroborates this hypothesis.

Table 4.6. Protein abundance ratio between *S. venezuelae* WT and Δ*vnz_08815;* WT and Δ*htrA3* and between Δ*vnz_08815* and Δ*htrA3* on YPD agar. Filtered to contain significant (p <0.05) hits with a fold-change of >2 (highlighted in blue) or <0.5 (highlighted in red).

Accession	Description	Protein Abundance Ratio *S. venezuelae* YPD		
		Δ*vnz_08815* / WT	Δ*htrA3*/ WT	Δ*vnz_08815* / Δ*htrA3*
Vnz_00760	ABC transporter substrate-binding protein	0.885	1.781	0.492
Vnz_04660	MerR family transcriptional regulator	0.212	0.208	1.023
Vnz_07470	Penicillin-binding protein	0.855	2.249	0.371
Vnz_07480	Hypothetical protein	1.145	2.351	0.491
Vnz_08815	Hypothetical protein	0.007	0.933	0.007
Vnz_08840	Cysteine desulfurase	0.453	1.176	0.397
Vnz_09585	Iron transporter	1.613	2.409	0.746
Vnz_12945	Hypothetical protein	0.723	0.498	1.423
Vnz_15870	Peptidase	0.488	0.533	1.07
Vnz_16675	Transcriptional regulator	0.006	0.005	0.727
Vnz_16700	Serine/threonine protein kinase	1.045	2.214	0.458
Vnz_18430	Protease; HtrA3	0.851	0.004	253.469
Vnz_18440	Kanamycin biosynthetic protein	0.499	1.38	0.355
Vnz_18555	DNA-binding response regulator; CagR	0.962	4.714	0.224
Vnz_19330	Two-component sensor histidine kinase; CssS	0.97	2.784	0.341
Vnz_19335	DNA-binding response regulator; CssR	1.139	2.468	0.425
Vnz_19340	Serine protease; HtrB	0.924	6.393	0.132
Vnz_21300	NADH dehydrogenase	1.134	0.669	2.489
Vnz_21505	Hypothetical protein	0.713	1.402	0.495
Vnz_21565	Phage tail protein	0.526	1.043	0.49

Vnz_21570	Hypothetical protein	0.678	1.33	0.457
Vnz_21585	Hypothetical protein	0.469	1.157	0.381
Vnz_22140	Hypothetical protein	0.76	1.692	0.471
Vnz_22170	DNA-directed RNA polymerase sigma-70 factor	3.344	2.181	1.206
Vnz_24930	ABC transporter permease	1.116	2.314	0.79
Vnz_25605	Hypothetical protein	1.014	3.401	0.352
Vnz_26170	Signal peptidase I	0.887	1.863	0.383
Vnz_27135	Acetyltransferase	0.116	0.059	5.311
Vnz_29655	NADPH-dependent FMN reductase	3.937	5.722	1.582
Vnz_29665	Hypothetical protein	2.374	1.609	1.476
Vnz_29910	Hypothetical protein	2.414	1.825	1.449
Vnz_32195	Clp protease	0.564	0.378	1.899
Vnz_36315	GntR family transcriptional regulator	2.611	1.305	1.581
Vnz_37060	Acetaldehyde dehydrogenase (acetylating)	5.423	4.956	1.652

4.7. Expanding the CutR regulon

With the data at our disposal from the above experiments it was prudent to re-analyse the ChIP-seq data using the ReDCaT-identified CutR binding sequence. Using FIMO (Find Individual Motif Occurrences, meme-suite.org/meme/tools/fimo) the *S. venezuelae* genome was scanned for binding sites containing the consensus sequence TAWATAAAG, resulting in 463 motifs with a p-value of <0.0001 (**Table 4.7**). Given the high G/C content of streptomycetes it was unlikely to be a common motif and only two exact matches were found, corresponding to the sites identified in *vnz_08815p* and *htrA3p*. However, the relatively small size of the query sequence resulted in a large number of significant sequences with slight alterations.

Five additional CutR binding sites identified via FIMO were found to be enriched within the ChIP-seq data. As can be seen in **Figure 4.13** normalised binding enrichment varied from only a 1-fold increase to a maximum of 3-fold. Whilst these peaks appear obvious in the displayed data, they were undetected by analysis software or manual scanning of the enrichment data in the original analysis. This may, in part, be due to the size of the peaks in relation to the surrounding noise and highlights the importance of re-analysing old data with new findings.

All new sites detected were within 30 bp of the TSS, suggesting binding of CutR to these newly identified sites occludes the RNA polymerase binding site and represses transcription (**Table 4.8**). The TMT proteomics data supports this, although not entirely. If CutR was acting as a repressor of these genes in the presence of glucose it could be predicted that protein abundance would increase in the YP samples. Of the proteins detected, ignoring Vnz_08815 and HtrA3 which are activated by CutR, all but HtrB followed this trend. Likewise, one could predict a similar increase in the Δ*cutRS* mutant samples on YPD in comparison to the WT, which is indeed observed for all four of the detected proteins

Table 4.7. The most significant FIMO analysis results from a search of the *S. venezuelae* genome using the sequence TAWATAAAG ordered by increasing p-value. Start and Stop refer to genome location of the identified sequence. The p-value of a motif occurrence is defined as the probability of a random sequence of the same length as the motif matching that position of the sequence with as good or better a score. The q-value of a motif occurrence is defined as the false discovery rate if the occurrence is accepted as significant. The presence of a ChIP-seq enrichment peak at the genomic locations is also indicated and highlighted.

Matched Sequence	Start	Stop	Strand	p-value	q-value	ChIP-seq peak
TAAATAAAG	2005139	2005147	-	9.31E-08	0.762	**Yes**
TATATAAAG	4073227	4073235	+	9.31E-08	0.762	**Yes**
TATATAAAT	6304701	6304709	+	2.57E-07	1	No
TACATAAAG	2806732	2806740	-	5.02E-07	1	**Yes**
TAAATAACG	2485650	2485658	-	4.59E-06	1	No
TATATACAG	6304698	6304706	-	4.59E-06	1	No
CAAATAAAG	6495004	6495012	-	4.59E-06	1	**Yes**
TATGTAAAG	7637337	7637345	-	4.59E-06	1	No
TAAATCAAG	7723751	7723759	-	4.59E-06	1	No
TAAATTAAG	724013	724021	+	4.59E-06	1	No
TAAACAAAG	816479	816487	+	4.59E-06	1	No
TATGTAAAG	2536582	2536590	+	4.59E-06	1	No
TCAATAAAG	2705096	2705104	+	4.59E-06	1	No
GATATAAAG	4262120	4262128	+	4.59E-06	1	**Yes**
CAAATAAAG	4343509	4343517	+	4.59E-06	1	No
GAAATAAAG	5346486	5346494	+	4.59E-06	1	No
TACATAAAA	7249387	7249395	-	5.02E-06	1	No
TAAAGAAAT	795911	795919	-	1.22E-05	1	No
TTAATAAAC	981526	981534	-	1.22E-05	1	No
TAAATAGAC	1189594	1189602	-	1.22E-05	1	No
TAAATAAGC	1419114	1419122	-	1.22E-05	1	No
TAATTAAAC	1465961	1465969	-	1.22E-05	1	**Yes**

TAAATTAAT	1679594	1679602	-	1.22E-05	1	No
GAAATAAAC	3008969	3008977	-	1.22E-05	1	No
TCAATAAAA	3147518	3147526	-	1.22E-05	1	No
TAAATCAAA	3726801	3726809	-	1.22E-05	1	No
TATATGAAC	4295157	4295165	-	1.22E-05	1	No
GAAATAAAA	4521414	4521422	-	1.22E-05	1	No
TAAAGAAAC	5558668	5558676	-	1.22E-05	1	No
TAAATCAAC	5635077	5635085	-	1.22E-05	1	No
GAAATAAAT	6308012	6308020	-	1.22E-05	1	No
GATATAAAC	7012546	7012554	-	1.22E-05	1	No
TATATGAAT	7308148	7308156	-	1.22E-05	1	No
TAAGTAAAT	7545799	7545807	-	1.22E-05	1	**Yes**
TATACAAAA	7764894	7764902	-	1.22E-05	1	No
TCAATAAAA	2681395	2681403	+	1.22E-05	1	No
TCAATAAAC	2705906	2705914	+	1.22E-05	1	No
TAAATACAC	2706531	2706539	+	1.22E-05	1	No
TAAACAAAA	3255913	3255921	+	1.22E-05	1	No
TAAATAAGT	4016542	4016550	+	1.22E-05	1	No
TAAATAACC	4102907	4102915	+	1.22E-05	1	No
AAAATAAAT	4414396	4414404	+	1.22E-05	1	No
CAAATAAAC	5215128	5215136	+	1.22E-05	1	No
TAAATCAAT	5619808	5619816	+	1.22E-05	1	No
TATATACAT	5674583	5674591	+	1.22E-05	1	No
GAAATAAAA	6150667	6150675	+	1.22E-05	1	No
TAAATCAAA	7550550	7550558	+	1.22E-05	1	No
TAAATAGAC	7556155	7556163	+	1.22E-05	1	No
TATAGAAAC	7611159	7611167	+	1.22E-05	1	No

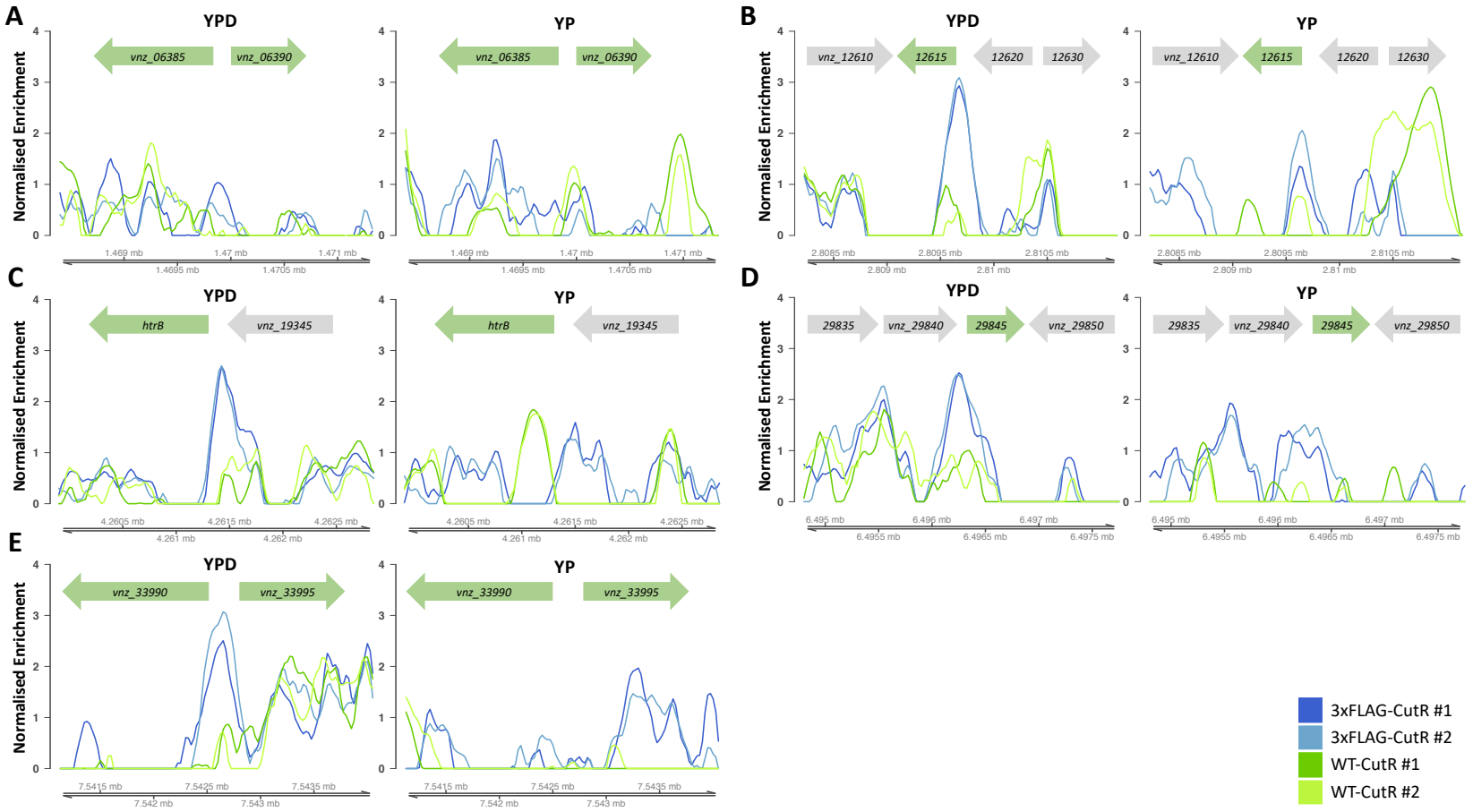

Figure 4.13. Additional CutR binding locations within the *S. venezuelae* genome: **A)** Between the divergent genes *vnz_06385* and *vnz_06390.* **B)** Upstream of the gene *vnz_12615*. **C)** Upstream of the gene *htrB*. **D)** Upstream of the gene *vnz_29845*. **E)** Between the divergent genes *vnz_33990* and *vnz_33995*. The coloured lines show ChIP-seq data for CutR-3xFLAG (dark blue and light blue) and the WT control (green and yellow) at 5 days on YPD and YP. Genome locations are displayed below the relevant graphs with gene schematics above. Genes of interest are highlighted in green.

Table 4.8. Overview of CutR target genes identified through ChIP-seq re-analysis using FIMO results. Transcription regulatory function predicted by location relative to TSS. TMT proteomics data included from previously described experiments. Proteins not detected indicated with (-).

Downstream Gene	Description	Orientation Relative to TSS	Distance to TSS (bp)	CutR Predicted Transcriptional Function	Protein Abundance Ratio *S. venezuelae*	
					WT YPD / Δ*cutRS* YPD	WT YP / WT YPD
vnz_06385	Acyl-CoA dehydrogenase	Coding	-21	Repressor	0.79	3.949
vnz_06390	TetR family transcriptional regulator	Reverse	-28	Repressor	-	-
vnz_08815	Cell wall amidase	Coding	69	Activator	3.115	0.065
vnz_12615	YaaH family transporter	Coding	4	Repressor	-	-
vnz_18430	Serine protease; *htrA3*	Coding	62	Activator	8.033	0.06
vnz_19340	Serine protease; *htrB*	Reverse	17	Repressor	0.053	0.11
vnz_29485	Conserved hypothetical protein	Reverse	28	Repressor	-	-
vnz_33990	Beta-mannosidase	Coding	21	Repressor	0.806	8.334
vnz_33985	LacI family transcriptional regulator	Operon (*vnz_33990*)	Operon (*vnz_33990*)	Repressor	-	-
vnz_33995	Sugar ABC transporter substrate-binding protein	Reverse	0	Repressor	0.769	15.418

This suggests that expression of the *vnz_06385*, *vnz_12615*, *vnz_33990* and *vnz_33995* genes is repressed by CutR while *htrB* is also repressed by CutR but not in a glucose-dependent manner. TSS mapping suggests that *vnz_33985* is likely encoded in the same operon as *vnz_33990* and as such would follow the same trend (Munnoch *et al.*, 2016; Bush *et al*., unpublished). The TSSs of the divergently encoded *vnz_06390* and *vnz_06385* both appear to be upstream of the putative binding site and would be expected to be similarly repressed by CutR (**Figure 4.14**). Some of the binding sites were found on the non-coding strand, with the site in the reverse complement confirmation relative to the TSS suggesting directionality is not essential. Whilst there is no evidence to support promoter orientation affecting gene expression (Lis and Walther, 2016), it is possible such orientation may be correlated with location relative to the TSS, which does determine gene expression. Further MEME analysis was run using all 8 promoter regions in an attempt to detect a wider conserved consensus sequence, however TAWATAAA was still considered the most significant binding motif.

Of these newly identified sites there were three single genes found: *vnz_12615, htrB* and *vnz_29485* encoding a putative YaaH family transporter, the serine protease HtrB and a conserved hypothetical protein, respectively. Neither Vnz_12615 nor Vnz_29485 could be detected in any of the proteomics samples under any tested conditions. HtrB, however, was consistently detected and this has already been discussed.

Two CutR-binding sites were identified within divergent promoters and CutR likely represses the transcription of the divergent genes *vnz_06385* and *vnz_06390*, encoding an acetyl-CoA dehydrogenase and TetR-family transcriptional regulator respectively. However, proteomics data was only found for Vnz_06385 (**Table 4.8**). The *S. venezuelae* homologue of *soxR,* discussed in **Chapter 3**, is *vnz_06365* but genomic proximity is no clear indication of functional link. The divergent genes *vnz_33995* and the putative operon *vnz_33990/895* appear to all be involved in saccharide transport, breakdown and regulation. Whilst Vnz_33895 was not detectable, it appears to belong to the LacI-family of regulators. The activity of these regulators is modulated by small metabolites which are usually monosaccharides, including arabinose, glucose and lactose (Swint-Kruse and Matthews, 2009). The increased abundance of Vnz_33990 and Vnz_33995 on YP, in comparison to YPD, would suggest these could target an alternate carbon source to glucose and, whilst the annotation of beta-mannosidase would suggest this is mannose, further biochemical investigation is needed to confirm this.

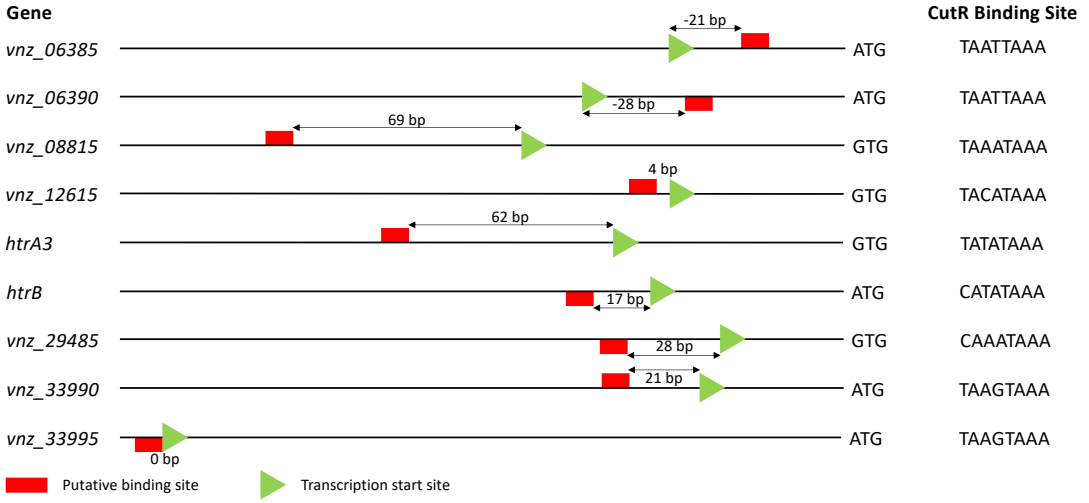

Figure 4.14. Schematic representations of the promoter regions of FIMO-identified genes. The location and strand of the 5'-3' putative CutR binding site has been indicated in red with the TSS in green. The binding site sequence is displayed on the right of each schematic.

4.8. Discussion

The work reported in this chapter was aimed at identifying the CutR regulon, CutR DNA binding site and to investigate any potential CutR-protein interactions. A combination of ChIP-seq, GUS assays and ReDCaT SPR identified a consensus CutR binding site, which, following further *in silico* analysis, allowed for the expansion of the *S. venezuelae* CutR regulon. Proteomics using tandem mass tagging allowed for the accurate quantification and comparison of the *S. venezuelae* proteomes of the WT and Δ*cutRS* strains cultured on YP and YPD agar. Whilst limited in scope, the TMT phosphoproteomic analysis highlighted the potential of whole cell protein PMT detection and comparison. Finally, further investigation of single gene deletion mutants in two key members of the CutR regulon, *vnz_08815* and *htrA3,* revealed there is likely an intricate balance of HtrA-like serine proteases within *S. venezuelae*.

The data described above are significant starting points to defining the role of CutRS in *S. venezuelae* and other streptomycetes. However, future work is required to confirm the observations and to better understand the cellular function of CutRS in the genus *Streptomyces*. Additionally, given the base variations in these putative CutR binding sites ReDCaT SPR would confirm binding *in vitro* and, given the larger sample size, give a better overview of the base pair substitutions tolerated *in vivo* resulting in a more realistic binding site consensus sequence. **Chapter 5** focuses on characterising CutRS in *S. coelicolor* and investigates potential streptomycete-conserved CutR binding locations. These data may further inform and expand the *S. venezuelae* CutR regulon, helping to identify more sites of enrichment within the ChIP-seq data set which can be corroborated with TMT proteomics, a continuous refinement procedure that is overlooked in many studies.

The cell wall amidase, Vnz_08815, and the HtrA3 serine protease are key members of the CutRS regulon and activated by CutR in the presence of glucose. Whilst the GUS reporter data corroborates this for *htrA3p* it suggests the opposite with *vnz_08815p*. However, promoter activity does not directly equate to transcription or translation. The final abundance and activity of the encoded proteins are the key effectors of phenotype. Vnz_08815 levels are increased on YPD compared to YP, and

in the WT samples in comparison to the Δ*cutRS* mutant (Vogel and Marcotte, 2012). Whilst it was possible to define a putative CutR binding motif (TAWATAAAG) this is considerably shorter than previously reported binding sites for homodimeric RRs. For OmpR-family RRs (which includes CutR) these often consist of short (6-7 bp) direct or palindromic repeat sequences separated by a single short spacer sequence positioning the two RR molecules on the same side of the DNA helix (Narayanan *et al.*, 2014; Yan *et al.*, 2019). It is possible that CutR is forming a heterodimer, and this is indicated by the Co-IP results and also because of the discrepancy with regard to the lack of binding to *cutRSp in vitro* despite clear ChIP-seq enrichment. Whilst it would have been beneficial to know the proportion of purified 6xHis-CutR present as a homodimer, it does not prevent the identification of binding sites via ReDCaT SPR as long as some phosphorylation is present, which was confirmed by native MS. A 'prime-and-lock' model has been suggested whereby the first DBD of an OmpR dimer binds to the upstream half-site of the binding sequence 'priming' the first DBD for interaction with the second DBD. Increased flexibility in the dimer allows the second DBD to bind the downstream half-site and 'locks' the complex. Whilst phosphorylation is required to increase the affinity for the upstream half-site, *in vitro* a monomeric RR can still bind that single half-site (Li *et al.*, 2014). This might explain the discrepancy with the binding site identified with SPR as we are likely missing the second half-site. However, if CutR is forming a heterodimer then the second half-site would never be identified without knowledge of the partner protein. The biophysical dynamics of RR-DNA binding is a fascinating field of study, but the complexity caused by variations in phosphorylation state, and not only dimerisation state but also dimerisation partner makes it a very challenging prospect for *in vitro* characterisation without concomitant *in vivo* work. The logical first step would be to test for CutR-protein interactions with the RRs enriched in the Co-IP data (EsrR/OsaB/CseB) *in vitro* using SPR and isothermal calorimetry (ITC) before attempting heterodimer-DNA binding assays.

The serine protease HtrB is increased in the proteomics data for both the Δ*cutRS* mutant and the Δ*htrA3* single mutant relative to wild type. Whilst not immediately apparent in the ChIP-seq data, it was found post-FIMO re-analysis. It appears that

CutR represses the production of this protein, but the protein abundance of HtrB does not follow the expected glucose-dependant response. The increase in HtrB and CssRS levels in the Δ*htrA3* and *ΔcutRS* mutants suggests loss of the encoded HtrA3 protein activity in these strains triggers the cell envelope stress response and that CutRS and CssRS functions overlap. The cell appears to recognise and counteract the lack of *htrA3* expression with increased *htrB* expression independently of CutRS. It would be intriguing to investigate the molecular phenotype of a Δ*htrA3*Δ*htrB* double mutant, and if other HtrA-like proteases are similarly upregulated to negate the loss of these two serine proteases. Evidence from *S. lividans* suggests that deletion mutants in each single *htrA*-like protease gene (*htrA1, htrA2, htrB*) can only be complemented by the specific gene and not by any of the others. However, *htrA3* was not investigated in the published *S. lividans* study as it is not regulated by CssRS, thus it is unknown how it fits into this model (Darmon *et al.*, 2002; Vicente *et al.*, 2016). Understanding the function of HtrA3 will be crucial to understanding the role of CutRS but clearly it has a cell envelope function.

HtrB was found to be 18.9-fold more abundant in the Δ*cutRS* mutant in comparison to the WT, whilst only 6.4-fold more abundant in the Δ*htrA3* single deletion. Similarly, CssR and CssS were 3.7- and 5.0-fold increased in the Δ*cutRS* samples and only 2.3- and 2.8-fold in the Δ*htrA3* samples. This suggests that the loss of *htrA3* is less disruptive to *S. venezuelae* than the loss of *cutRS*. This is corroborated by the colony phenotype which is unchanged in the Δ*htrA3* strain but disparate in the Δ*cutRS* strain, as previously discussed. The TCS CssRS responds to secretion and misfolded protein stress, which must be disrupted to a greater degree in the Δ*cutRS* mutant in comparison to the Δ*htrA3* single deletion. A considerable number of proteins highlighted in the TMT proteomics and phosphoproteomics results are involved in cell wall homeostasis. These include the UDP-N-acetylglucosamine 2-epimerase Vnz_22475, the CE4 deacetylase Vnz_15460 and the Mg^{2+} transporter Vnz_23735. The gene encoding a putative cell wall amidase, *vnz_08815*, was also identified as a target of CutR. Combining these data with the observed HtrB/CssRS response indicates the possible disruption of cell wall homeostasis in the Δ*cutRS* mutant in the presence of glucose.

As with any ‘omics-based approaches, there can be a huge amount of data to deconvolute in order to identify the key results. Whilst describing and understanding the molecular mechanism behind the *S. venezuelae* Δ*cutRS* phenotype is one of the ultimate aims of this work, the conservation of CutRS and its regulatory mechanisms is also of significant interest. The investigation into mechanistic conservation of CutRS regulation in distantly related species of *Streptomyces*, such as *S. coelicolor*, could help reveal the principal genes and proteins involved in potentially all *Streptomyces* spp. and further assist in the understanding of the data described above. Such an investigation is described in the following chapter.

Chapter 5. Molecular characterisation of CutRS in *S. coelicolor*

CutRS is one of 15 TCSs identified as being highly conserved among *Streptomyces* spp. (Mclean *et al.*, 2019). The work presented thus far has focused on the characterisation of CutRS in *S. venezuelae,* a new model streptomycete. Data presented in **Chapter 3** and **Chapter 4** indicate that this system is involved in glucose uptake, exploration and cell envelope homeostasis. However, it remains to be seen if CutRS is functionally conserved. To achieve this we opted to use *S. coelicolor,* a model organism which has been studied genetically for over 65 years (Hopwood, 2007). This chapter aims to determine if the function of CutRS is conserved at both a phenotypic and molecular level. Replicating experiments detailed in **Chapter 4** the work described below compares and contrasts the role of CutRS in *S. coelicolor* with *S. venezuelae* in order to better understand this TCS.

5.1. Conservation of CutRS

With a considerable amount of work done on CutRS in *S. venezuelae* it seemed prudent to preliminarily confirm conservation of function using the *S. venezuelae* Δ*cutRS* strain. To achieve this the *cutRS* operons from *S. coelicolor* and *S. formicae* KY5 were cloned into the vector pIJ10257 downstream of the *ermE** promoter to ensure expression. *S. formicae* KY5 was chosen as the third strain due to its compatibility with genetic tools such as pCRISPomyces-2 and our experience working with the strain. These vectors, pIJ10257-SCO_*cutRS* and pIJ10257-KY5_*cutRS*, were conjugated into *S. venezuelae* WT and Δ*cutRS* and the strains cultured on YP and YPD agar (**Figure 5.1**). Overexpression of either operon had no discernible effect on WT colony morphology on either media. Both vectors in the Δ*cutRS* strain grown on YP agar similarly had no effect. Full complementation of the *S. venezuelae* Δ*cutRS* mutant phenotype was achieved on YPD with both vectors and this confirms that, at least in *S. venezuelae*, CutRS is functionally conserved among streptomycetes. With regard to homology, the *S. coelicolor* and *S. formicae* KY5 CutR homologues both share 98% amino acid identity with *S. venezuelae* CutR. Residues in SKs are less

conserved in comparison to RRs and CutS is no exception. The *S. coelicolor* and the *S. formicae* KY5 CutS homologues share 79% and 82% amino acid identity, respectively, with *S. venezuelae* CutS.

To characterise the CutRS TCS in *S. coelicolor* an in-frame *cutRS* deletion mutant was generated using the pCRISPomyces-2 system. The *S. coelicolor* WT and Δ*cutRS* strains were then cultured on YP and YPD agar as well as MYM+TE and SFM agar, both with and without glucose (**Figure 5.2**). There are conflicting reports regarding the development of *S. coelicolor* on YP agar, and whether it can exhibit the exploration phenotype. Jones *et al.* (2017) report that *S. coelicolor* is incapable of exploring in the presence of *S. cerevisiae* or alkaline mVOCs. However, in **Figure 5.2** *S. coelicolor* WT appears to be, at least mildly, exploring. This observation has been confirmed from independent groups (unpublished data) but requires follow up to define the phenotype as exploratory. It is possible that *S. coelicolor* is incapable of exploring through yeast-driven glucose deprivation and TMA, but exploration can be induced abiotically by the YP medium alone. Regardless of whether it is truly exploring or not, there were only mild phenotypic deviations observed in the *S. coelicolor* Δ*cutRS* mutant in comparison to the WT on the tested media. On YP agar the colonies appear to spread less whilst on MYM+TE agar they appear greyer in colour, likely due to the presence of the grey spore pigment. A similar phenotype can be seen on SFM agar with and without glucose. At this timepoint (14 days) *S. coelicolor* has likely completed its lifecycle on MYM+TE and SFM and regerminated, resulting in the presence of white aerial hyphae again whilst the mutant is delayed, or the spores possibly do not regerminate. Spores collected from the mutant sporulate normally, so this second hypothesis seems unlikely. In contrast to *S. venezuelae*, there is no distinct glucose-dependant phenotype nor significant variations in biomass on the tested media.

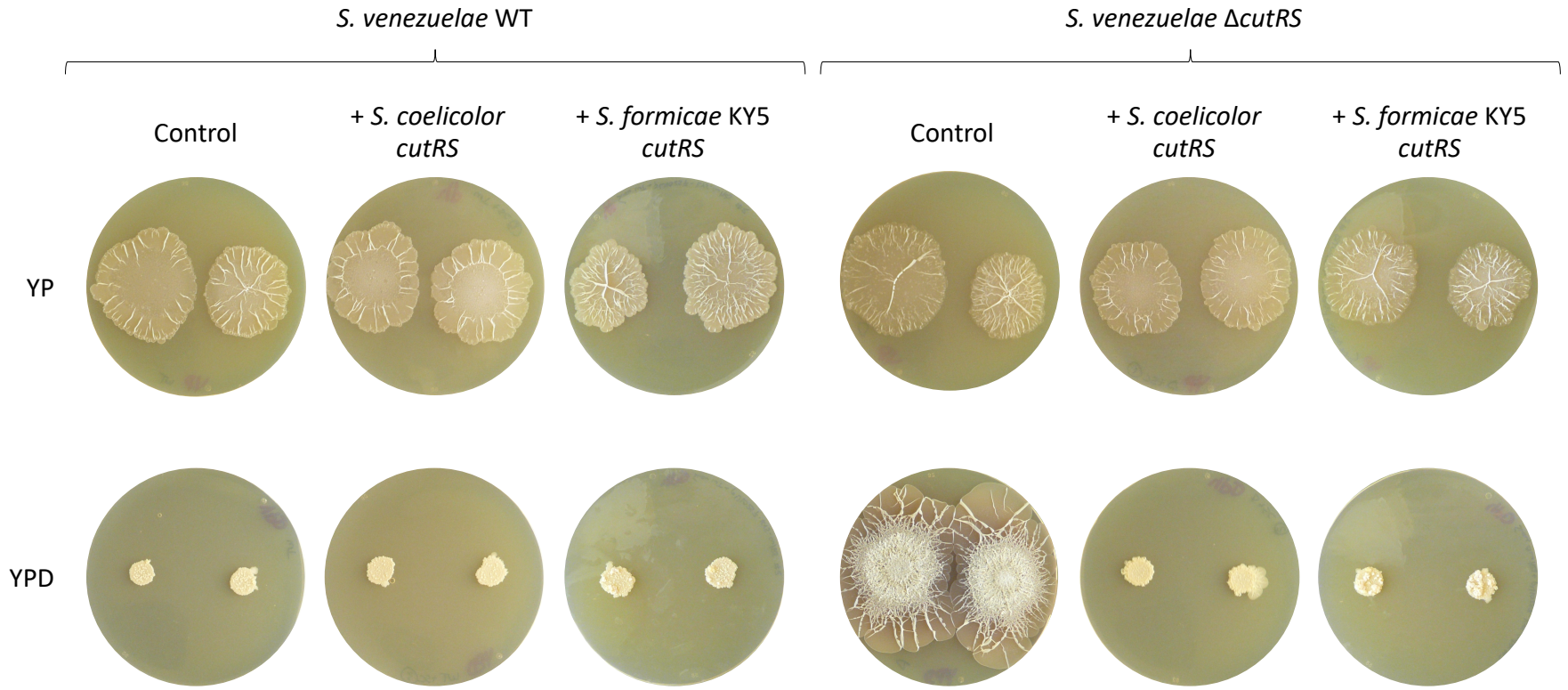

Figure 5.1. Overexpression of the *S. coelicolor* and *S. formicae* KY5 *cutRS* operons in *S. venezuelae* WT and Δ*cutRS* strains cultured on YP and YPD agar.

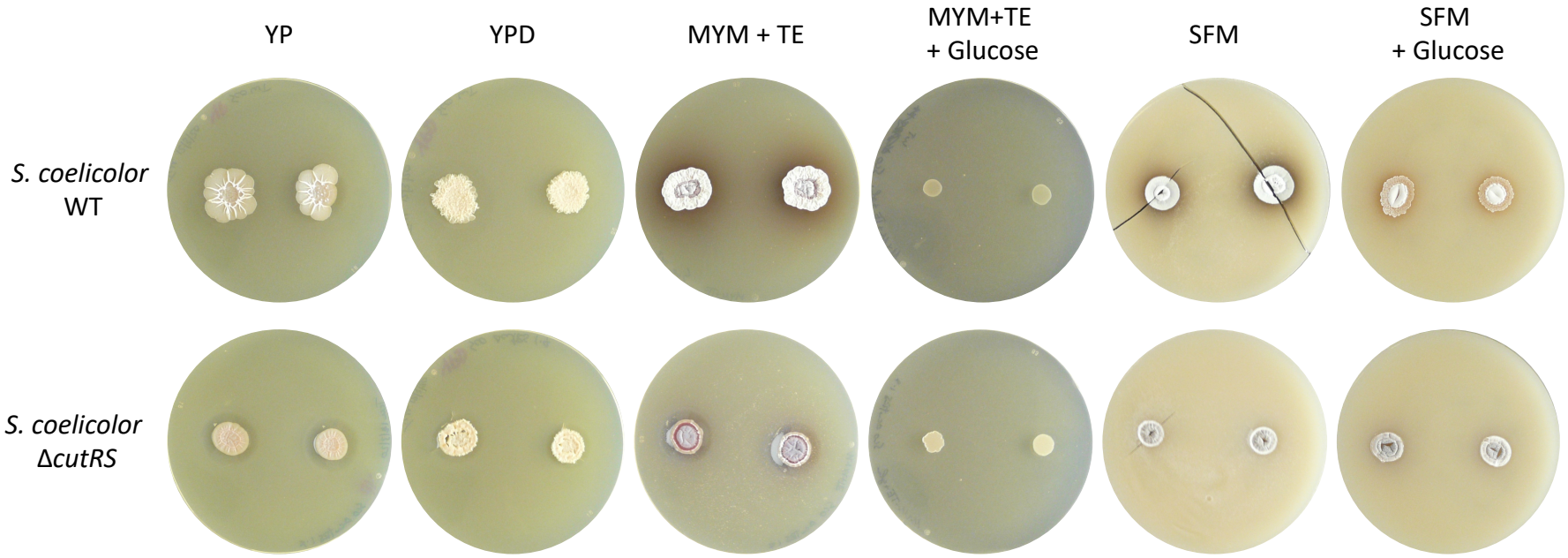

Figure 5.2. *S. coelicolor* WT and Δ*cutRS* cultured on solid culture media YP, MYM+TE and SFM with and without glucose.

Whilst the majority of the original CutRS research was performed in *S. lividans* some preliminary work was presented on *S. coelicolor* CutRS. Disruption of *cutS* in *S. coelicolor* M145 resulted in the overproduction of the blue-pigmented antibiotic ACT on solid media (Chang *et al.*, 1996). During the process of confirming our *S. coelicolor* Δ*cutRS* deletion strains potential mutants were streaked on solid DNA medium. This medium encourages rapid streptomycete growth and severely delays the production of aerial hyphae resulting in mycelium suitable for colony PCR. WT strains cultured on DNA agar produced the typical cream-coloured colonies whilst the colonies later confirmed as Δ*cutRS* mutants overproduced ACT similarly to that described by Chang *et al.* (1996).

To confirm these observations, the *S. coelicolor* WT, Δ*cutRS* and complement strains were plated on DNA agar and DNA agar supplemented with glucose (DNAD)(**Figure 5.3**). As expected both the WT and complemented strains exhibited no ACT production whilst the Δ*cutRS* strain displayed considerable ACT overproduction on both DNA and DNAD agars. Whilst different to the phenotype observed in *S. venezuelae*, deletion of the *cutRS* operon in *S. coelicolor* has a similarly pronounced effect on specialised metabolism. The overproduction of ACT matches the reports by Chang *et al.* (1996) and DNA agar with and without glucose provides suitable conditions for regulon identification via ChIP-seq and comparative proteomics, the results of which are detailed below.

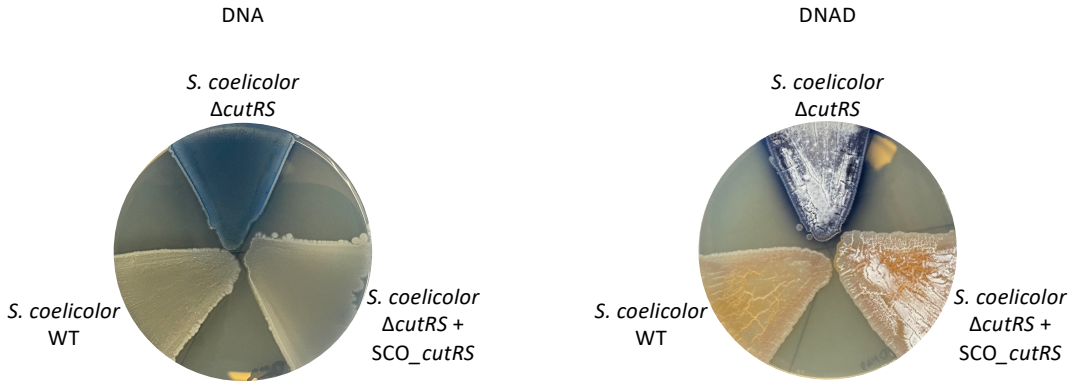

Figure 5.3. *S. coelicolor* WT, Δ*cutRS* and mutant complemented strain cultured on solid DNA and DNA with glucose (DNAD).

5.2. ChIP-seq

As with ChIP-seq in *S. venezuelae* a FLAG-tagged CutR construct was required in *S. coelicolor* to enable isolation of CutR-bound DNA. A vector was designed, similar to the *S. venezuelae* C-terminal 3x-FLAG plasmid, using the *S. coelicolor cutRS* and native promoter. This construct was synthesised by Genewiz (UK) and, once conjugated into the *S. coelicolor* Δ*cutRS* strain, confirmed to complement the mutant phenotype. Despite being highly conserved, there remains the possibility that the CutR regulon expands within each individual species beyond the conserved regulon. To define the conserved regulon, it was decided to also perform ChIP-seq using *S. venezuelae* CutR-3xFLAG in *S. coelicolor*, in addition to *S. coelicolor* CutR-3xFLAG. ChIP-seq was performed and analysed as described in **Chapter 2.45** and **Chapter 2.46** on both DNA and DNAD agar after 3 days of growth on cellophanes.

For the purpose of this work the *S. venezuelae* CutR expressed in *S. coelicolor* will be referred to as *sv*CutR whilst the native *S. coelicolor* CutR in *S. coelicolor* will be called *sc*CutR. The conserved regulon is defined as the target genes regulated by both *sc*CutR and *sv*CutR in *S. coelicolor*. The core regulon is those genes regulated by CutR in both *S. venezuelae* and *S. coelicolor*.

The analysis revealed that, in the absence of glucose (DNA agar), *sc*CutR only bound upstream of its own operon this was, however, less than 2-fold enriched (**Table 5.1**). Contrastingly, in the presence of glucose (DNAD agar) there were 86 sites of enrichment detected (**Table S5**). However only 15 sites were found >2-fold enriched in the analysis of the *sv*CutR DNAD ChIP-seq samples. All 15 of these sites were also enriched within the *sc*CutR data with no binding sites unique to *sv*CutR within the *S. coelicolor* genome (**Table 5.1**). This potentially highlights the extent to which the *sc*CutR regulon has expanded within *S. coelicolor* relative to *S. venezuelae.* Conversely it may have shrunk within *S. venezuelae* relative to *S. coelicolor*, however expansion makes most sense. Every single site of enrichment from the *sv*CutR DNAD agar samples was also enriched in *sv*CutR samples from DNA agar. This suggests that *sv*CutR in *S. coelicolor* is constitutively activated on DNA agar irrespective of glucose supplementation although this requires further confirmation. With the *S. venezuelae*

CutRS capable of complementing the *S. coelicolor* Δ*cutRS* phenotype we can assume that the regulon controlled by *sv*CutR is responsible for the ACT overexpression phenotype and the additional 71 *sc*CutR binding sites are extraneous to this specific observable phenotype but could play important roles in other situations. Thus, whilst the full 86 *sc*CutR binding sites are of interest for the full characterisation of CutRS in *S. coelicolor*, for the purpose of this work the focus centres on the 15 targets bound by both *sv*CutR and *sc*CutR in *S. coelicolor*.

As previously mentioned, CutR binds to its own promoter in both the presence and absence of glucose in *S. coelicolor*. This was also observed for CutR in *S. venezuelae*. However, whilst there were some other targets in *S. venezuelae* which were not glucose responsive, it appears that all the other targets of *sc*CutR are reliant on the presence of glucose. With the same enrichment sites present in DNA and DNAD for *sv*CutR it is likely that activation of *sv*CutRS in *S. coelicolor* is reliant on a different signal, one which is present in both DNA and DNAD. This makes it less likely that the specific ligand for CutS activation is glucose, but it could be a response to the presence of glucose which differs between *S. venezuelae* and *S. coelicolor*. It is also possible that there are kinases present in *S. coelicolor* which are capable of phosphorylating *sv*CutR in a non-specific manner but are unable to activate the native *sc*CutR in a similar manner. However, this is highly unlikely given their 98% identity. The *S. coelicolor* genes homologous to the *S. venezuelae* regulon (**Table 4.8**) were checked for upstream enrichment. As highlighted in **Table 5.1**, significant enrichment was found upstream of *SCO3977* which encodes the serine protease HtrA3. Enrichment was also found upstream of the *SCO4157* which encodes HtrB, discussed at length previously. Enrichment was slightly less than 2-fold (1.92-fold), but the peaks are likely indicative of true binding in comparison to the untagged control samples. This takes the total number of conserved locations up to 16. These two targets, *htrA3* and *htrB*, alongside its own promoter, appear to form the core regulon conserved across both genomes (**Figure 5.4**).

It is worth noting there is an anomalous peak present in the *cutRS* promoter region visible in **Figure 5.4.** This has been excluded from the analysis and likely represents a sequencing artifact from the inclusion of a heterologous copy of the *cutRS* operon as

it is only present in the *sv*CutR samples. The peak present just upstream of the anomalous peak is much more indicative of true protein-DNA binding. Many of the genes in the *sc*CutR/*sv*CutR conserved regulon are annotated as membrane proteins and this seems unlikely to be coincidental. This supports the working hypothesis that the CutRS TCS responds to stress which might affect the integrity of the cell envelope or require extracellular-acting proteins, similar to CssRS. The roles of the significant targets identified from ChIP-seq will be discussed below. In lieu of *in vitro* protein-DNA binding assays such as ReDCaT SPR, *in silico* analysis using MEME was performed. MEME was unable to detect any conserved binding sites across the 16 *sc*CutR/*sv*CutR conserved binding enrichment locations in *S. coelicolor*. Likewise, a FIMO scan of 200 bp centred on each peak of enrichment was unable to find any hits for the TAWATAAA consensus sequence from *S. venezuelae.* Another FIMO scan, this time of the entire genome for TAWATAAA, returned 200 motif occurrences with a p-value <0.0001. However, these did not correspond to any of the 16 locations identified by ChIP-seq. It appears that the CutR binding site identified in *S. venezuelae* is not in use in *S. coelicolor*, at least under the studied conditions. With *S. coelicolor* CutRS able to complement the *S. venezuelae* Δ*cutRS* strain it must be able to bind at the TAWATAAA site as the native CutR does. This may be a result of CutR binding other RRs to form homodimers. However, ChIP-seq alone is not able to discern homodimeric and heterodimeric binding sites. This requires considerable further effort including Co-IP and also *in vitro* binding assays using multiple purified RRs. The data gained from such experiments would be invaluable and efforts should be made in the future to undertake this work. Of course, it is important to consider that the TAWATAAA binding site is incorrect, and this data should not bias any approaches designed to identify the conserved CutR binding site.

Finally, efforts were made to map the peak of enrichment to the predicted TSS for each target gene as was achieved for *S. venezuelae*. However, the quality of dRNA-seq data currently available for *S. coelicolor* TSSs is subpar. This, combined with the broad ChIP-seq enrichment peaks, made the mapping inaccurate and unreliable. As such, without higher quality data this analysis and visualisation cannot be achieved.

Table 5.1. Analysis data from *S. coelicolor* ChIP-seq. The location and relative enrichment of the conserved binding sites of both *S. coelicolor* (*sc*CutR) and *S. venezuelae* CutR-3xFLAG (*sv*CutR) in *S. coelicolor* with >2-fold enrichment. The locus of *htrB* has also been included. The downstream gene target was predicted using peak location and TSS data (Jeong *et al.,* 2016). Multiple gene targets indicate divergently encoded genes with equal likelihood of transcriptional regulation, with the exception of CutRS included for visibility.

Location of Enrichment Peak	**Relative Enrichment (Fold Change vs. Control)**				**Predicted Downstream Target**	**Description**	**Predicted *S. venezuelae* Homologue**
	*sc*CutR DNAD	*sc*CutR DNA	*sv*CutR DNAD	*sv*CutR DNA			
776415	5.53	1.17	4.19	3.44	*SCO0733*	Hypothetical protein	*None*
1518450	5.24	1.07	3.71	2.63	*SCO1422*	Membrane protein	*vnz_04920*
1612020	4.54	0.99	2.76	1.26	*SCO1507*	Integral membrane protein	*vnz_05380*
1876320	3.97	1.19	2.31	1.84	*SCO1754*	Hypothetical protein	*vnz_06735*
2271015	4.10	1.26	2.14	2.38	*SCO2112* *SCO2113*	Hypothetical protein Bacterioferrin	*vnz_08690* *vnz_08695*
3447120	3.72	0.98	2.09	1.81	*SCO3146*	Secreted protein	*vnz_14580*
3985875	3.98	1.11	2.06	2.00	*SCO3608* *SCO3609*	Hypothetical protein Membrane protein	*vnz_28535* *vnz_02005*

4064625	5.66	1.35	4.46	4.37	*SCO3681*	Hypothetical protein	*vnz_16535*
4379205	4.71	0.94	2.67	2.04	*SCO3976*	Phosphodiesterase	*vnz_18425*
					SCO3977	Serine protease; *htrA3*	*vnz_18430*
4575075	3.21	0.94	1.92	1.77	*SCO4157*	Serine protease; *htrB*	*Vnz_19340*
4710390	2.92	0.96	1.81	2.09	*SCO4295*	Cold shock protein	*vnz_19990*
5415990	4.74	1.09	3.43	3.47	*SCO4978*	Integral membrane protein	*vnz_23015*
					SCO4979	Phosphoenolpyruvate carboxykinase	*vnz_23020*
5593545	5.43	0.90	3.26	3.63	*SCO5146*	Methyltransferase	*vnz_23695*
					SCO5147	ECF-subfamily sigma factor	*vnz_23700*
6025335	4.88	0.98	3.05	2.79	*SCO5530*	Membrane protein; *scoF4*	*vnz_25755*
6419205	4.22	1.56	5.13	3.97	*SCO5862*	Two-component regulator; c*utR*	*vnz_27390*
					SCO5863	Two-component sensor kinase; c*utS*	*vnz_23795*
8072745	4.08	0.93	2.29	2.35	*SCO7261*	Membrane protein	*vnz_01215*
					SCO7262	Hypothetical protein	*None*

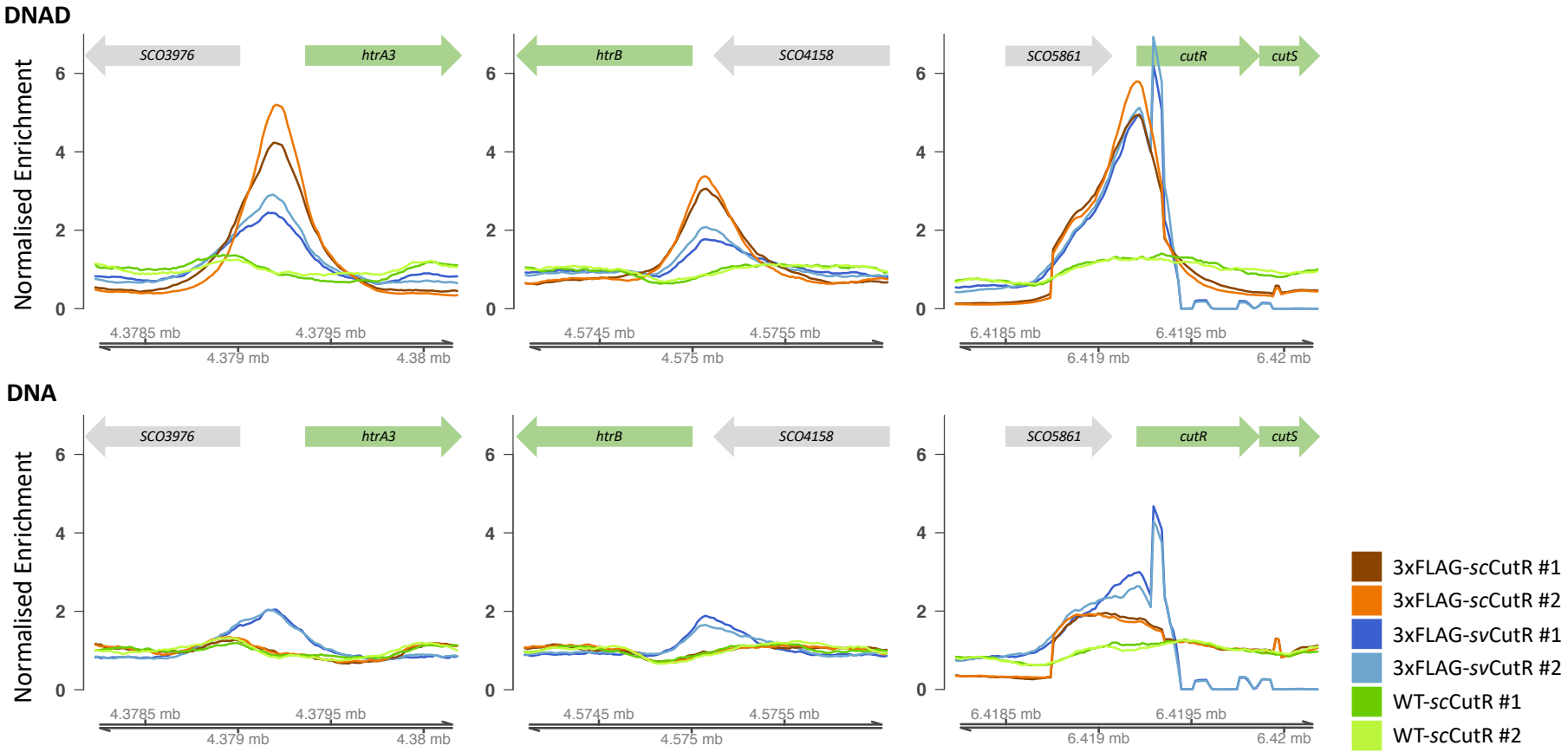

Figure 5.4. ChIP-seq analysis of 3xFLAG-tagged *sc*CutR (dark and light orange) and *sv*CutR (dark and light blue) in *S. coelicolor* with the WT control (green and yellow) at 3 days on DNAD and DNA agar. Genome locations are displayed below the relevant graphs with gene schematics above. Genes of interest are highlighted in green.

5.3. TMT proteomics

TMT proteomics was carried out on *S. coelicolor* WT and Δ*cutRS* cultured on DNA and DNAD media. As with the *S. venezuelae* TMT proteomics the key dataset is the comparison between the WT and mutant on the media containing glucose (DNAD). However, the proteome response to glucose in the *S. coelicolor* WT was also of interest (**Figure 5.5A**). Whilst we observed a large-scale repression of protein production in *S. venezuelae* WT in the presence of glucose (**Chapter 4.4**), no such effect was detected in *S. coelicolor*. On DNA agar 126 proteins were found to be significantly more abundant whilst 137 were similarly affected on DNAD agar. This could suggest that the addition of glucose has less of a carbon catabolite repressive effect on *S. coelicolor.* As has been previously discussed the preferred carbon source, and subsequent bias of primary metabolism routes, varies between *Streptomyces* spp. which may explain the difference between *S. venezuelae* and *S. coelicolor* responses to glucose. These comparisons were also not performed on the same media so are not directly comparable, especially with the *S. venezuelae* explorer phenotype present on YP. However, it does appear that glucose is less repressive to *S. coelicolor* protein production. In contrast to *S. venezuelae*, there was no significant change to CutR or CutS which were 1.457- and 0.80-fold changed in the WT grown on DNA samples compared to WT on DNAD. HtrA3 was 1.99-fold increased which suggest a small increase in abundance but not comparable to that observed in WT *S. venezuelae* in the YPD/YP comparison. The most abundant proteins of the *S. coelicolor* WT on DNA include SCO3487, SCO3480 and SCO3475 which are annotated as a putative hydrolase, racemase and isomerase respectively. The secreted sugar-binding lipoprotein, SCO3484, was found to be 20-fold more abundant in the absence of glucose (Widdick *et al.*, 2011). This has previously been described as a glycerol-3-phosphate binding protein (Schrempf *et al.*, 2011) and the neoagarobiose internalization transporter (Romero-Rodríguez *et al.*, 2016). Neoagarobiose results from the sequential hydrolysis of agarose, a component of agar, to neoagarooligosaccharides finally to neoagarobiose. This would suggest that *S. coelicolor* works to break down agar to galactose as a carbon source in the absence of glucose. This hypothesis is strengthened by the 4.7-fold increased abundance of

the extracellular agarase enzyme DagA (SCO3471) under the same conditions (Buttner, Fearnley and Bibb, 1987). Whilst we can observe increased agarose activity in the plates, it would be desirable to develop an experiment designed solely to quantify and compare agarase activity to confirm these findings.

The proteome changes between *S. coelicolor* WT and Δ*cutRS* on DNAD was more striking with 152 proteins significantly more abundant in the mutant compared to just 50 in the WT (**Figure 5.5B**). CutR and CutS were absent as expected but were not the two most differentially abundant proteins in the WT as they were in *S. venezuelae.* This is likely due to the slightly lower constitutive expression in the WT on DNAD and a different peptide error calling rate resulting from slightly different amino acid compositions. HtrA3 was found to be 3.2-fold more abundant in the WT than the mutant suggesting that CutR activates *htrA3* expression in *S. coelicolor* as it does in *S. venezuelae*. Also following the same pattern observed in *S. venezuelae* was HtrB, with a 12.6-fold increase detected in the Δ*cutRS* mutant. In contrast to the observations in *S. venezuelae* the CssRS TCS remained relatively unchanged in the absence of CutRS; the RR CssR was only 1.04-fold more abundant in the Δ*cutRS* mutant whilst the SK CssS was reduced 1.64-fold.

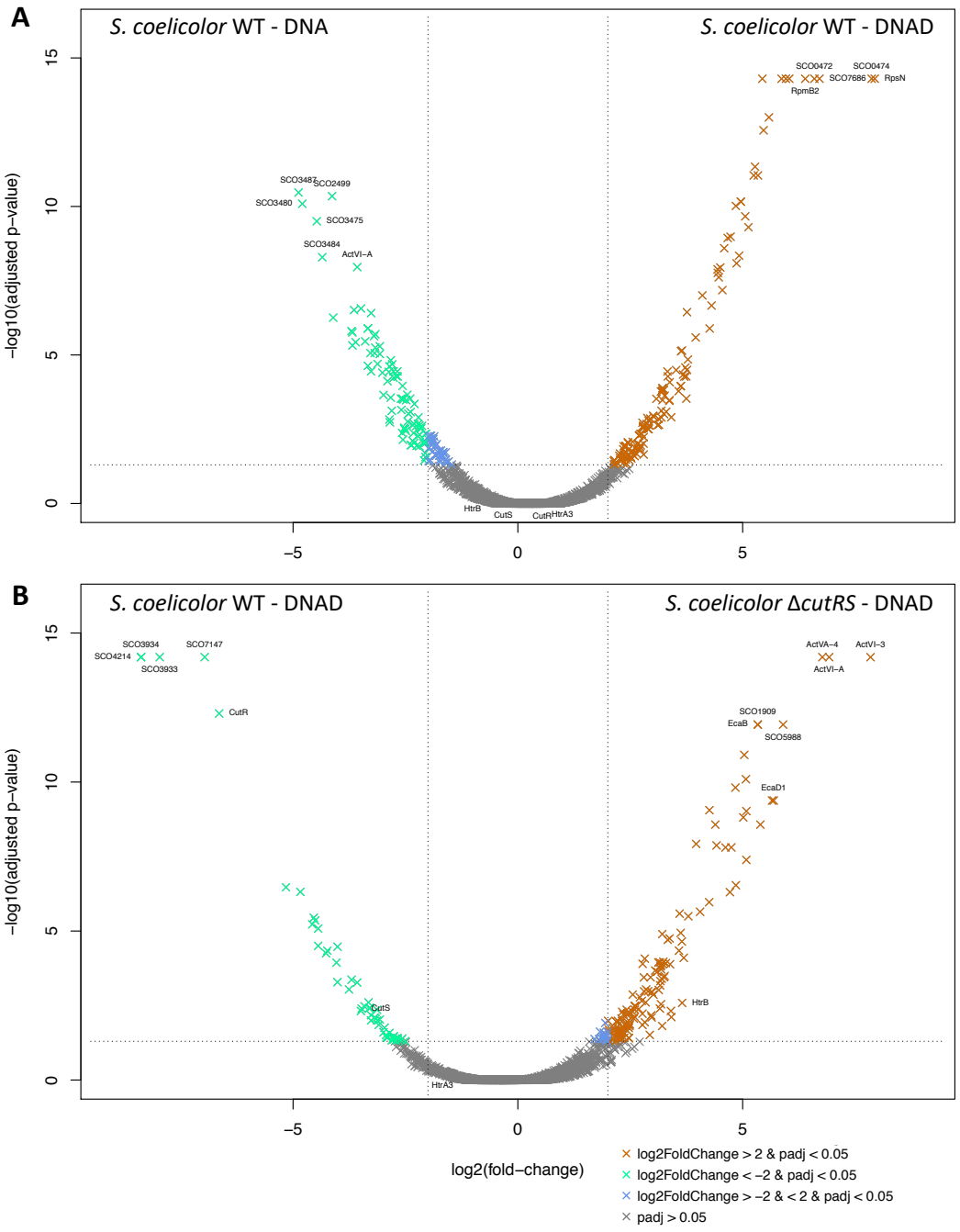

Figure 5.5. Volcano plot of $\log_2$(fold-change) protein abundance against -$\log_{10}$(adjusted p-value between: **A)** *S. coelicolor* WT grown on DNA and DNAD agar; **B)** *S. coelicolor* WT and Δ*cutRS* strains grown on DNAD agar.

The *S. coelicolor* Δ*cutRS* mutant samples on DNAD show a huge increase in the abundance of the ACT biosynthetic proteins which will be discussed separately below. A significant proportion of the proteins found to be >10-fold increased (**Table 5.2**) are annotated as secreted proteins, almost 20%, with even more than this likely to be acting extracellularly. This suggests that the loss of CutRS necessitates a significant shift in the secretome in *S. coelicolor* when grown on DNAD agar. The uncharacterised protein SCO5988 is the most differentially abundant protein in the mutant, excluding ACT-related proteins, being found 58.8-fold increased. No information can be found on SCO5988, and no conserved domains could be identified. SCO5988 does appear to be conserved amongst *Streptomyces* spp. so is worth further investigation. Two proteins, the oxidoreductase EcaD1 SCO4266 and the monooxygenase EcaB SCO1909, are 51.6- and 40.0-fold more abundant in the Δ*cutRS* mutant on DNAD. The genes encoding these two proteins are part of the conserved regulon of the transcription factor SoxR discussed in **Chapter 3.5**. As previously mentioned in **Chapter 1** the WT *S. coelicolor* strain, M145, produces pigmented antibiotics including ACT and RED whilst the strain M512 does not. *S. coelicolor* M512 is a modified heterologous host strain based on M145 which contains deletions of the ACT and RED transcriptional activators *redD* and *actII-ORF4* (Floriano and Bibb, 1996). In a comparison between the two strains, it was found that the expression of *ecaD1* (*ecaD* – used interchangeably) increased 250-fold in the WT compared to the pigment null mutant. Expression of another SoxR-regulated gene, *SCO2478*, encoding a flavoprotein reductase, also increased, although this time 6,000-fold (Dietrich *et al.*, 2008). Further study expanded the SoxR regulon to include *ecaA* (*SCO7008*)*, ecaB* (*SCO1909*) and *ecaC* (*SCO1178*)*;* an ABC-type transporter, a monooxygenase and a protein of nonpredictable function respectively*.* It was also shown that ACT was the key driver of SoxR activation, with transcription of the five SoxR regulation genes occurring only at the same time that the blue pigmented antibiotic was produced (Shin *et al.*, 2011). There is, however, a difference between intracellular ACT and extracellular ACT, with export being coupled to the modification of ACT to its lactone form (γ-ACT)(Bystrykh *et al.*, 1996). Expression of the SoxR regulon genes at WT levels in a Δ*actII*-4 mutant (deficient in ACT production) could be achieved by supplementation of ACT however it took more than 10 times the

amount of intracellular ACT as it did γ-ACT. This suggests that SoxR is tuned to respond to the extracellular γ-ACT compared to the intracellular counterpart (Shin *et al.*, 2011). In contrast ActR, the ACT-sensing repressor, is more sensitive to the three-ringed ACT intermediates than the completed six-ringed ACT suggesting that ActR is an intracellular sensor of ACT (Tahlan *et al.*, 2007, 2008). SoxR itself was found to be decreased 1.49-fold in the *S. coelicolor* Δ*cutRS* proteome, however the precise levels of SoxR are irrelevant, the activation state (via ACT) defines the transcriptional activation ability of SoxR (Dela Cruz *et al.*, 2010). Together these proteins work to neutralise the stress caused by toxic redox-active compounds, such as keto-acids and quinones rather than react to nitric oxides or superoxides (Shin *et al.*, 2011). Changes to SoxR and SoxR-related proteins have consistently been found in *S. venezuelae* and *S. coelicolor* during this work. It is possible these changes are unrelated to the CutRS phenotype but the pattern is striking and worthy of further investigation.

Table 5.2. Protein abundance ratio between *S. coelicolor* WT and Δ*cutRS* on DNAD agar. Filtered to contain significant (p <0.05) hits with a fold change of >10 or <0.1.

SCO Accession	Description	Protein Abundance Ratio *S. coelicolor* DNAD WT / Δ*cutRS*
SCO3934	FtsK/SpoIIIE family protein	333.3
SCO4214	Putative AbaA-like regulatory protein	333.3
SCO3933	Putative regulatory protein	250.0
SCO7147	Putative ketoreductase	125.0
SCO5862	Transcriptional regulatory protein; CutR	100.0
SCO3930	Uncharacterized protein	35.71
SCO3484	Putative secreted sugar-binding protein	28.57
SCO5448	Putative ABC transporter	23.81
SCO2864	HATPase_c domain-containing protein	23.26
SCO3936	Putative plasmid replication initiator protein	22.73
SCO3471	Extracellular agarase; DagA	21.74
SCO3487	Putative hydrolase	21.74
SCO3486	Putative aldehyde dehydrogenase	19.23
SCO6529	Putative ATP/GTP binding protein	18.87
SCO0475	ABC transporter protein, integral membrane subunit	16.39
SCO1148	Putative ABC transporter	16.13
SCO3481	Uncharacterized protein	16.13

SCO0630	Putative acetyltransferase	13.51
SCO1150	50S ribosomal protein L31 type B 2; RpmE2-2	12.99
SCO4610	Putative integral membrane protein	11.90
SCO4670	Putative serine protease	11.24
SCO5863	Sensor protein; CutS	11.11
SCO6646	Putative transport system permease protein	10.64
SCO5447	Neutral metalloproteinase	0.099
SCO7700	2-methylisoborneol synthase	0.096
SCO3229	Putative 4-hydroxyphenylpyruvic acid dioxygenase	0.096
SCO3973	Putative membrane protein	0.094
SCO4818	Uncharacterized protein	0.094
SCO5985	Uncharacterized protein	0.083
SCO5091	Cyclase-thioesterase; ActIV	0.083
SCO6483	Alpha-amylase	0.081
SCO3607	Putative secreted protein	0.080
SCO4157	Putative protease	0.079
SCO6569	Putative secreted solute binding protein	0.077
SCO5984	Putative acyl-CoA dehydrogenase	0.072
SCO5819	Sporulation transcription factor; WhiH	0.064
SCO5087	Actinorhodin polyketide putative beta-ketoacyl synthase 1; ActI-1	0.060
SCO7453	Putative secreted protein	0.052

SCO5084	Putative membrane protein; ActII-3	0.052
SCO1746	Secreted serine protease	0.048
SCO5110	Putative lipoprotein	0.047
SCO3561	Putative secreted protein	0.041
SCO2153	Putative secreted protein	0.038
SCO3244	Putative secreted protein	0.037
SCO5088	Actinorhodin polyketide putative beta-ketoacyl synthase 2; ActI-2	0.035
SCO5089	Actinorhodin polyketide synthase acyl carrier protein; ActI-3	0.035
SCO5072	Hydroxylacyl-CoA dehydrogenase; ActVI-1	0.031
SCO5078	Uncharacterized protein; ActVA-3	0.030
SCO5083	Probable actinorhodin transporter; ActII-2	0.030
SCO5080	Putative hydrolase; ActVA-5	0.030
SCO5086	Putative ketoacyl reductase; ActIII	0.029
SCO1909	Monooxygenase; EcaB	0.025
SCO5073	Putative oxidoreductase; ActVI-2	0.024
SCO5075	Putative oxidoreductase; ActVI-4	0.020
SCO4266	Putative oxidoreductase; EcaD1	0.019
SCO5988	Uncharacterized protein	0.017
SCO5079	Uncharacterized protein; ActVA-4	0.009
SCO5071	Hydroxylacyl-CoA dehydrogenase; ActVI-A	0.008
SCO5074	Putative dehydratase; ActVI-3	0.004

In the absence of RNA-seq or other transcriptomic methods we can use the TMT proteomics to help understand the regulatory effect CutR has on its regulon in *S. coelicolor*, with a focus on those targets conserved between *sc*CutR and *sv*CutR (**Table 5.3**). The majority of the target proteins were found to increase in abundance in the *S. coelicolor* WT samples with the addition of glucose. As previously discussed, the SK CutS is the only protein to reduce in abundance (1.25-fold). On average the other 14 proteins increase 1.79-fold. The three with the greatest abundance change are SCO5530 (4.13-fold), SCO4295 (2.75-fold) and SCO3146 (2.24-fold). These are annotated as a putative membrane protein, the cold shock protein ScoF4 and a secreted protein, respectively. Cold shock proteins (CSP) are interesting. They can be found in almost every organism except yeast and contain at least one cold shock domain. They are multifunctional DNA/RNA binding proteins produced in response to stress, generally a rapid drop in temperature. Cold shock decreases membrane fluidity, enzyme activity and hampers protein folding and CSPs are thought to act as nucleic acid chaperones, preventing secondary structure formation and facilitating translational initiation. More recently have some CSPs have been shown to be involved in homeostasis and more general stress responses (Keto-Timonen *et al.*, 2016).

In the comparison between *S. coelicolor* WT and Δ*cutRS* on DNAD (**Table 5.3**) the conserved CutR targets are on average 2.26-fold more abundant in the WT samples than the mutant samples. Only the aforementioned secreted SCO3146 is more abundant (1.39-fold) in the *S. coelicolor* Δ*cutRS* proteome. Combined with the average increase in the presence of glucose, this drop in protein abundance in the mutant samples would suggest CutR is transcriptionally activating the expression of its regulon. Three membrane proteins are the least abundant proteins among these target proteins: SCO1422 (0.12-fold), SCO5530 (0.18-fold) and SCO1507 (0.27-fold). The integral membrane protein SCO5530 has previously been discussed as the most abundant protein in the presence of glucose within the putative CutR regulon subset. SCO1422 is also a membrane protein, with a FxsA domain. SCO1507 is homologous to the eukaryotic vitamin K epoxide reductase (VKOR). In humans, VKOR is involved in maintaining vitamin K in a reduced state. It achieves this through the re-oxidization

of protein disulphide isomerases (PDI), transferring electrons from PDIs to quinone (Capstick, 2011). VKOR homologues in Gram-positive bacteria are of particular interest in regard to the formation of cell surface disulphide bonds and this will be discussed in greater detail in **Chapter 5.4**.

The change in HtrA3 abundance has previously been discussed, as has HtrB abundance. In contrast to *S. venezuelae,* the phosphodiesterase divergently encoded to *htrA3*, *SCO3976*, is affected by the loss of CutRS, being almost 2.5-fold less abundant. It was found to be 1.34-fold more abundant in the *S. venezuelae* Δ*cutRS* samples on YPD compared to the WT. Although it requires confirmation with transcriptomic experimentation, it appears that CutR plays a general transcriptionally activating role for the genes regulated by both *sc*CutR and *sv*CutR in *S. coelicolor*.

Table 5.3. Protein abundance ratio of the conserved *S. coelicolor* ChIP-seq-identified gene targets between *S. coelicolor* WT on DNA and DNAD agar and between *S. coelicolor* WT and Δ*cutRS* on DNAD agar. Proteins not detected indicated with (-). Filtered to contain significant ($p < 0.05$) hits with a fold-change of >2 (highlighted in blue) or <0.5 (highlighted in red).

SCO Accession	Description	Protein Abundance Ratio *S. coelicolor*	
		WT DNAD / WT DNA	Δ*cutRS* DNAD / WT DNAD
SCO0733	Hypothetical protein	-	-
SCO1422	Membrane protein	1.318	0.119
SCO1507	Integral membrane protein	1.274	0.266
SCO1754	Hypothetical protein	1.311	0.777
SCO2112	Hypothetical protein	1.071	1.023
SCO2113	Bacterioferrin	-	-
SCO3146	Secreted protein	2.244	1.392
SCO3608	Hypothetical protein	-	-
SCO3609	Membrane protein	1.435	0.684
SCO3681	Hypothetical protein	-	-
SCO3976	Phosphodiesterase	1.461	0.406
SCO3977	Serine protease; HtrA3	1.988	0.313
SCO4157	Serine protease; HtrB	0.498	12.60
SCO4295	Cold shock protein; ScoF4	2.748	0.330
SCO4978	Integral membrane protein	-	-
SCO4979	Phosphoenolpyruvate carboxykinase	-	-
SCO5146	Methyltransferase	1.403	0.439
SCO5147	ECF-subfamily sigma factor	1.170	0.531
SCO5530	Membrane protein	4.126	0.178
SCO5862	Two-component regulator; CutR	1.457	0.010
SCO5863	Two-component sensor kinase; CutS	0.800	0.090
SCO7261	Membrane protein	-	-
SCO7262	Hypothetical protein	-	-

We have yet to accurately quantify ACT concentration however the extent of overproduction in the *S. coelicolor* Δ*cutRS* strain on DNAD is clearly observable by eye. It has been previously reported that high levels of glucose have a repressive effect on ACT production in the WT strain (Kang *et al.*, 1998). This repression can be observed in the proteome comparison between *S. coelicolor* WT on DNA and DNAD detailed in **Table 5.4**. With the exception of ActII-1 and ActVA-2, every ACT protein was less abundant in the presence of glucose. The production of the hydroxylacyl-CoA dehydrogenase ActVI-A (0.084-fold), the putative dehydratase ActVI-3 (0.137-fold) and ActVA-4 (0.154-fold), an enzyme proposed to be involved in ACT dimerization (Taguchi *et al.*, 2015), were found to be most affected. The juxtaposing increase in abundance of ActII-1 (2.552-fold) is unsurprising given its suggested role as a transcriptional repressor of the genes encoding for the ACT exporter, *actII-2*, and also *actII-3* (Fernández-Moreno *et al.*, 1991). The role of ActVA-2 does not appear to have been determined, but, according to a NCBI conserved domain search, it is a redox reaction-catalysing enzyme of the PNPOx-like superfamily.

The deletion of *cutRS* from *S. coelicolor* had the opposite effect on ACT BGC protein production on DNAD medium with every detectable ACT BGC protein found at an increased abundance in the mutant in comparison to the WT samples. On average abundance increased 44.5-fold with the dehydratase ActVI-2 229.9-fold more abundant. The aforementioned ActVA-4 was 121.4-fold increased whilst the oxidoreductase ActVI-4 was also over 100-fold (109.4-fold) more abundant. There was no evidence in the ChIP-seq data of CutR binding within the ACT BGC including the promoter region of the transcriptional activator *actII-4* which is an extremely common binding site for regulatory proteins, including TCS RRs (McLean *et al.*, 2019). This is similar to the overproduction of chloramphenicol observed in the *S. venezuelae* Δ*cutRS* mutant with no direct CutR regulation detected. Thus, the regulatory effect on the expression of these BGCs must be indirect, either through secondary regulators or as a side-effect of the phenotype caused by the deletion of *cutRS*. Whilst there was no evidence of CutR binding directly to chloramphenicol BGC proteins and repressing production via protein-protein interaction, CutR Co-IP is yet to be performed in *S. coelicolor* so this cannot be ruled out for ACT yet.

Table 5.4. Protein abundance ratio of the actinorhodin (ACT) biosynthetic proteins between *S. coelicolor* WT on DNA and DNAD agar and between *S. coelicolor* WT and Δ*cutRS* on DNAD agar. Proteins not detected indicated with (-). Filtered to contain significant ($p < 0.05$) hits with a fold-change of >2 (highlighted in blue) or <0.5 (highlighted in red). Hits with a fold change of >100 are highlighted in dark blue.

SCO Accession	Description	Protein Abundance Ratio *S. coelicolor*	
		WT DNAD / WT DNA	Δ*cutRS* DNAD / WT DNAD
SCO5071	Hydroxylacyl-CoA dehydrogenase; ActVI-A	0.084	121.379
SCO5072	Hydroxylacyl-CoA dehydrogenase; ActVI-1	0.392	32.309
SCO5073	Putative oxidoreductase; ActVI-2	0.220	42.035
SCO5074	Putative dehydratase; ActVI-3	0.137	229.893
SCO5075	Putative oxidoreductase; ActVI-4	0.282	50.349
SCO5076	H+ antiporter membrane protein; ActVA-1	-	-
SCO5077	Uncharacterized protein; ActVA-2	1.223	7.076
SCO5078	Uncharacterized protein; ActVA-3	0.361	32.796
SCO5079	Uncharacterized protein; ActVA-4	0.154	109.357
SCO5080	Putative hydrolase; ActVA-5	0.388	33.865
SCO5081	Actinorhodin monooxygenase; ActVA-6	-	-
SCO5082	Putative transcriptional regulatory protein; ActII-1	2.552	2.440
SCO5083	Probable actinorhodin transporter; ActII-2	0.481	33.641
SCO5084	Putative membrane protein; ActII-3	0.785	19.166

SCO5085	Probable actinorhodin operon activatory protein; ActII-4	0.769	4.905
SCO5086	Putative ketoacyl reductase; ActIII	0.197	33.907
SCO5087	Actinorhodin polyketide putative beta-ketoacyl synthase 1; ActI-1	0.547	16.604
SCO5088	Actinorhodin polyketide putative beta-ketoacyl synthase 2; ActI-2	0.252	28.613
SCO5089	Actinorhodin polyketide synthase acyl carrier protein; ActI-3	0.334	28.817
SCO5090	Actinorhodin polyketide synthase bifunctional cyclase/dehydratase; ActVII	0.877	6.044
SCO5091	Cyclase-thioesterase; ActIV	0.462	12.106
SCO5092	Actinorhodin polyketide dimerase; ActVB	-	-

5.4. Discussion

S. venezuelae and *S. coelicolor* are both well-established model streptomycetes. With a relatively different physiology and considerable historic data, *S. coelicolor* was therefore the logical choice for comparative characterisation of the highly conserved TCS CutRS. The *S. venezuelae, S. coelicolor* and *S. formicae* KY5 *cutRS* operons all complemented both the *S. venezuelae* and *S. coelicolor* Δ*cutRS* mutants. A distinct ACT overproduction phenotype, matching previous reports by Chang *et al.* (1996), was observable on DNA agar and the same medium supplemented with glucose (DNAD). No distinct phenotype was detectable on YP, MYM+TE and SFM agars with and without glucose. ChIP-seq analysis with *sc*CutR revealed 86 sites of significant enrichment, with 16 of these sites proving conserved when compared with the *sv*CutR targets in *S. coelicolor*. This core regulon included its own *cutRS* promoter, and those belonging to the serine proteases *htrA3* and *htrB*. Beyond this the regulon was distinct from the regulon identified in *S. venezuelae*. Further work is required to characterise the *sc*CutR binding site *in vitro* and identify any possible CutR-RR heterodimers. The binding site with the consensus sequence TAWATAAAG does not appear to be applicable to the *S. coelicolor* CutR, at least under the studied conditions. This does appear to be at odds with the observed cross-species complementation and should be followed up in future work.

TMT quantitative proteomic analysis revealed far fewer significant changes between the *S. coelicolor* WT proteome on media with and without glucose than observed in the *S. venezuelae* WT, although the base medium was different, which is an important caveat. A similar correlation was seen with the comparison between *S. coelicolor* WT and Δ*cutRS* on DNAD with only 202 total changes. The detected abundance changes were, however, much larger with some proteins found to be over 300-fold changed. Many of these were ACT biosynthetic proteins which were hugely overproduced in the mutant strain, corroborating the phenotypic change detected. Accurate ACT concentration evaluation was not undertaken however the antibiotic is readily observable due to the blue pigmentation.

The role of the core regulon gene *SCO1507*, encoding a putative VKOR homologue, is worthy of future investigation due to its links with extracellular protein folding. There are two homologues in *S. venezuelae*: *vnz_05380* and *vnz_23005,* but no other copies within *S. coelicolor* itself. Whilst Vnz_05380 was not detected in the TMT proteomics, Vnz_23005 was found to be 72.2-fold more abundant in the absence of glucose (YP) in the WT in comparison to YPD samples. Vnz_23005 was also 3.19-fold more abundant in the *S. venezuelae* Δ*cutRS* YPD samples compared to the WT YPD samples. This is opposite to the trend observed with SCO1507, but the stark abundance change in the absence of CutRS is significant. As previously discussed, it appears the CutRS TCS is involved in the response to protein folding / secretion stress, with transcriptional regulation of the serine proteases *htrA3* and *htrB* being key to this function. One obstacle that must be overcome in the proper folding and maturation of some proteins is protection of the cysteine residues. These residues contain reactive thiol side chains which have a wide range of roles including enzyme catalysis, metal binding and redox sensing. Cysteine residues are also vital in the formation of disulphide bonds (Daniels *et al.*, 2010).

Gram-negative bacteria, such as *E. coli*, encode for Dsb-family periplasmic disulphide oxidoreductases. These include the soluble enzyme DsbA which catalyses the formation of disulphide bonds in proteins immediately following translocation to the periplasm. DsbA contains a redox active Cys-X-X-Cys active site which must be re-oxidised by DsbB, which spans the membrane. Meanwhile DsbC works to correct any incorrectly formed disulphide bonds and is maintained by the thiol:disulphide interchange protein DsbD (Capstick, 2011). However, Gram-positive bacteria lack the outer membrane which encompasses the periplasm. Subsequently, secreted proteins must fold in an extracellular environment dominated by a thick, negatively charged cell wall (Daniels *et al.*, 2010). Some Gram-positives, such as Firmicutes, appear to avoid encoding secreted proteins which form disulphide bonds. Actinobacteria however do not exclude cysteines from their exported proteins. As such Actinobacteria have been found to be much more susceptible to reductants than Firmicutes (Daniels *et al.*, 2010). Whilst *S. coelicolor* encodes a *dsbA* homologue, *SCO2634*, it does not encode for the partner *dsbB.* This is where SCO1507 becomes

relevant. It is thought that VKOR homologues can act to re-oxidise DsbA in bacteria lacking DsbB homologues (Capstick, 2011) and it is likely that the CutR regulated protein SCO1507, and its *S. venezuelae* homologue Vnz_23005 (and probably Vnz_05280), perform this role in their respective species.

Increased SCO1507 activity in *S. coelicolor* potentially has significant implications. Not only does it corroborate the working hypothesis of secretion / protein folding stress but also links to development. The escape from the aqueous environment through the formation of aerial hyphae in *Streptomyces* spp. is dependent on chaplin proteins. Chaplins create a hydrophobic coating on the cell surface and deletion of the chaplin-encoding genes results in severely delayed aerial hyphae formation (Elliot *et al.*, 2003). There are eight chaplins of which ChpD-H are short chaplins. All short chaplins, except ChpE, contain two cysteine residues which form intramolecular disulphide bonds, providing structural rigidity (Christina *et al.*, 2008). It is thought that DsbA is likely responsible for the formation of these chaplin disulphide bonds (Capstick, 2011). It would be interesting to investigate the development of *S. coelicolor* and *S. venezuelae* in the absence of SCO1507 and Vnz_23005 respectively. Indeed, we see considerably more aerial hyphae production in the *S. venezuelae* Δ*cutRS* mutant on YPD in comparison to the WT strain with Vnz_23005 more abundant in the mutant. This abundance becomes more pronounced as time progresses with 22.2-fold more Vnz_23005 present in the *S. venezuelae* mutant YPD samples after 9 days compared to the 2-day samples. This matches the abundance of aerial hyphae detected by SEM (**Chapter 3.4**).

Whilst the trend with Vnz_23005 appears to contradict the changes observed with SCO1507, this does not necessarily damage the hypothesis. The proteomic samples were collected from different media (DNA[D] and YP[D]). It is also abundantly clear that *S. coelicolor* and *S. venezuelae* have very different phenotypic responses to glucose and a different glycolytic bias. The shift in abundance between *S. venezuelae* WT cultured in the presence and absence of glucose is opposite that detected between the Δ*cutRS* mutant and WT. Thus, the trend in expression is the same between *S. coelicolor* and *S. venezuelae* but the outcomes opposite. This suggests that the two species could be encountering conditions which affect the redox state

of their extracellular domain in different ways, or that secreted protein folding is optimised to different conditions in the strains. In reality it is likely a combination of both factors with much more nuance involved.

As previously discussed, VKORs use quinones as electron acceptors during the re-oxidation of PDIs. Structurally, the antibiotic ACT is a homodimeric benzoisochromanequinone (**Figure 5.6**) (Taguchi *et al.*, 2012). These quinones within ACT could, conceivably, be used by VKORs such as SCO1507. It is generally agreed that specialised metabolites with antimicrobial activity have functions other than competition. The overproduction of ACT, as well as RED, is a common stress response in *S. coelicolor*. It was always considered that abiotic stress or genetic manipulation might be misperceived by the cell as the effect of competing microorganisms, and this resulted in mechanisms of self-protection such as antibiotics. In many cases this may be correct, but perhaps ACT also functions as an extracellular electron acceptor to assist in key extracellular processes involved in other stress responses. It would be worthwhile to investigate the phenotype of an ACT BGC-disrupted *S. coelicolor* Δ*cutRS* on DNAD to better understand this hypothesis. Likewise, would *S. coelicolor* Δ*cutRS* need to overproduce ACT if the medium was supplemented with quinones or other electron acceptors?

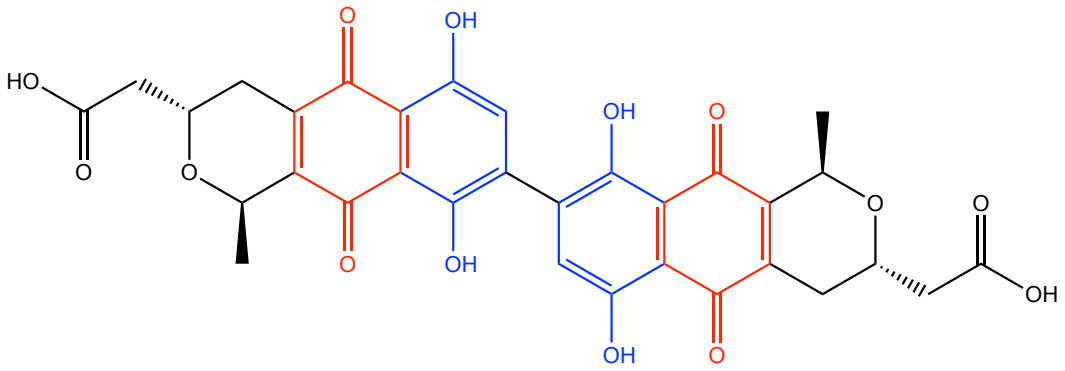

Figure 5.6. The structure of homodimeric benzoisochromanequinone antibiotic actinorhodin. Quinone groups are highlighted in red and hydroquinone groups in blue.

However, chloramphenicol does not contain quinone groups. We have observed that abolishment of chloramphenicol production in *S. venezuelae* has no effect on the Δ*cutRS* phenotype and it is unlikely to be performing a similar role as ACT might be

in *S. coelicolor*. Whilst the addition of pyocyanin was capable of rescuing the mutant phenotype on YPD, it similarly is not a quinone. However, as previously discussed pyocyanin and other redox-active phenazines function as electron shuttles in *Pseudomonas* spp. biofilm colonies. Thus, it is conceivable that they could act as electron acceptors for streptomycete VKORs. It is also possible that these compounds directly create an oxidising environment suitable for disulphide bond formation in secreted proteins.

Finally, the extracellular-facing domain of CutS itself has two cysteine residues. This appears to be highly unusual for TCS SKs and this will be discussed in considerably more detail in **Chapter 6**. Together, with the other data presented in this chapter, it appears that whilst the CutRS TCS may play the same role in *S. coelicolor* as it does in *S. venezuelae* the results are different. This is likely due to the different physiologies of these *Streptomyces* species and their inherent bias towards certain carbon sources and secretion stress responses. The above work constitutes the start of work on the characterisation of CutRS in *S. coelicolor*, and other streptomycetes. With time the intricacies of both the similarities and differences of the role played by CutRS in *S. venezuelae* and *S. coelicolor* will be further explored.

Chapter 6. Characterisation of the CutS extracellular ligand-binding domain

The work presented in this thesis, until this point, has focussed primarily on the response regulator CutR. Characterising the role of the RR is pivotal to defining the regulon and, in general, the molecular mechanism. However, the role of the sensor kinase (SK) is often overlooked, perhaps due to the inherent difficulties associated with working on membrane proteins. Nevertheless, it is equally important to understand. This chapter aims to characterise the SK CutS in *S. venezuelae* and discuss its conservation within the family *Streptomycetaceae*. Specifically, this work focusses on the extracellular ligand-binding domain. By describing the development of a high throughput ligand screening method, based on SPR technology, we hope to encourage further investigation of SK-ligand interactions.

6.1. The CutS sensor kinase

As previously discussed, the *S. coelicolor* and the *S. formicae* KY5 CutS homologues share 79% and 82% amino acid identity with *S. venezuelae* CutS, respectively. However, the extracellular domain, the sensory domain of prototypical SKs with two TM domains, is far less conserved. The *S. venezuelae* CutS extracellular domain (EcCutS) shares only 38% and 36% amino acid identity with its *S. coelicolor* and *S. formicae* KY5 homologues, respectively. This lack of sensory domain conservation in CutS appears to be relatively unusual for SKs containing two TM domains. **Table 6.1** displays a percentage identity comparison of the extracellular domains of TCS SKs conserved between *S. venezuelae*, *S. coelicolor* and *S. formicae* KY5 limited to those with two TM domains. We can observe that, in general, extracellular domain % identity is higher than observed in CutS. The sensory domain of the *S. venezuelae* glutamate binding SK GluK sensory domain, for example, shares 61% amino acid identity with its *S. coelicolor* and *S. formicae* KY5 homologues. Similarly, the sensory domain of *S. venezuelae* AfsQ2 shares 54% amino acid identity with its *S. coelicolor*

counterpart and 60% with the *S. formicae* KY5 homologue. The only other TCS SK with a similarly unconserved sensory domain is CssS which has been previously discussed at length.

The CutS homologues from 93 high-quality streptomycete whole genome sequences were identified and the extracellular domain amino acid sequences aligned (**Figure 6.1**). From this alignment it is clear this domain is even less conserved than original described. Of the 62 amino acids present in *S. venezuelae* EcCutS, only 11 of these (17.74%) are even weakly conserved. Of these, four residues are fully conserved, two C-terminal leucines and two more centrally located cysteines. Leucines are non-polar aliphatic amino acids and the most common residue in TM helixes (Baker *et al.*, 2017). It is possible these two residues are also part of the C-terminal TM domain or important in positioning the TM domain correctly in the membrane playing a structural role. The two cysteines are of more interest as these are highly unusual residues to find in the extracellular domain of SKs. **Table 6.2** shows the results of an analysis of SKs in *S. venezuelae*, *S. coelicolor* and *S. formicae* KY5. Using the Predicted Prokaryotic Regulatory Proteins software (P2RP, www.p2rp.org) all putative SKs, belonging to TCS or otherwise, were identified within these genomes. The number of proteins identified ranged from 163 in *S. venezuelae* to 210 in *S. formicae* KY5. These proteins were then analysed using TMHMM v2.0 (www.cbs.dtu.dk/services/TMHMM/) to detect putative TM domains. On average 12% of these proteins contained exactly two TM domains, an architecture similar to CutS. Proteins lacking any cysteine residues were removed and the remaining protein sequences trimmed to just their extracellular domains. Of the 163 putative SKs originally identified in *S. venezuelae*, only two were determined to contain two TM domains and cysteines within their extracellular domains. These were CutS and CssS. In *S. coelicolor* the same proteins were detected, as they were in *S. formicae* KY5 along with KY5_3157c. KY5_3157c is the SK of a TCS that has no homologue in *S. coelicolor*. A homologue can be found in *S. venezuelae*, Vnz_16275. Not only is Vnz_16275 predicted to contain three TM domains, but the corresponding extracellular domain does not contain any cysteine residues. As described in **Table 6.2** the extracellular domain of KY5_3157c also contains just a single cysteine residue

whilst both CutS and CssS contain two such residues. In *S. venezuelae* the extracellular domain of CssS (EcCssS) is predicted to be 123 amino acids in length whilst EcCutS is only 62 amino acids. However, the two cysteines are similarly spaced in both. In EcCutS they are separated by 17 residues whilst the gap in EcCssS is 24 residues.

Table 6.1. Comparison of two-component system sensor kinase extracellular domains predicted using TMHMM v2.0. Only those SKs with two transmembrane domains have been included. Percentage identity was calculated using the NCBI BLAST tool.

Sensor Kinase Name	Protein Accession	Extracellular Domain	Length (a.a.)	% Identity to *S. venezuelae* copy
MtrB	Vnz_13520	60-222	163	100
	SCO3012	96-263	168	51.50
	KY5_3176c	99-266	168	58.68
DraK	Vnz_13755	28-125	98	100
	SCO3062	28-125	98	64.29
	KY5_3224c	28-125	98	64.29
CssS	Vnz_19330	54-176	122	100
	SCO4155	40-166	127	33.33
	KY5_3798	40-173	134	40.74
AfsQ2	Vnz_22600	41-184	144	100
	SCO4906	55-199	145	54.48
	KY5_5035c	54-197	144	60.42
None	Vnz_24545	39-44	6	100
	SCO5282	55-60	6	None
	KY5_5414c	38-43	6	None
GluK	Vnz_26895	28-168	140	100
	SCO5779	28-172	145	60.69
	KY5_5912	28-172	145	61.38
CutS	Vnz_27395	58-119	62	100
	SCO5863	58-121	64	37.88
	KY5_5992	59-121	63	35.94
VanS	Vnz_33690	30-51	22	100
	SCO3589	36-63	28	None
	KY5_0087	38-56	18	None

This page is blank

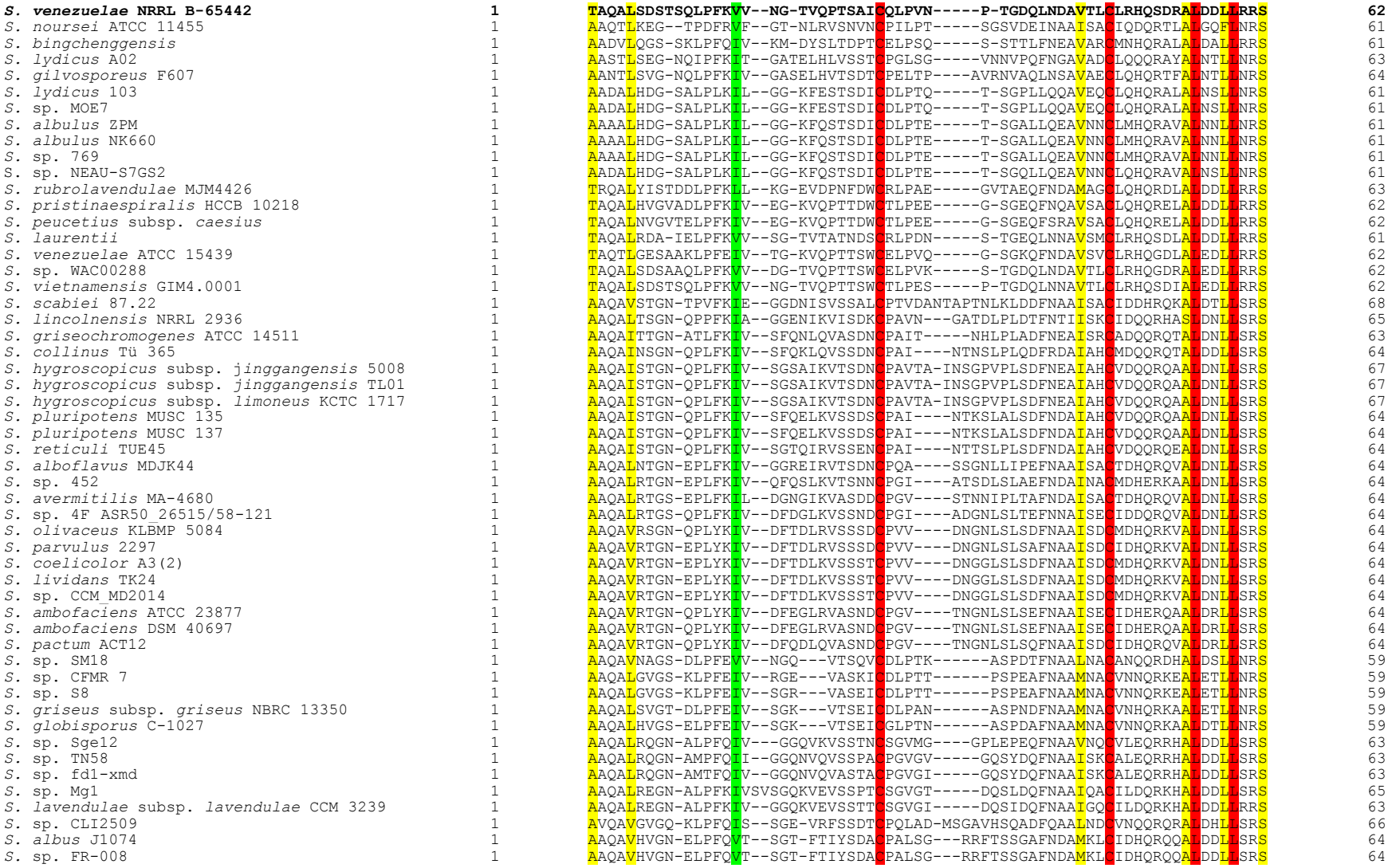
S. venezuelae NRRL B-65442 1 **TAQALSDSTSQLPFKVV--NG-TVQPTSAICQLPVN-----P-TGDQLNDAVTLCLRHQSDRALDDLLRRS** 62
S. noursei ATCC 11455 1 AAQTLKEG--TPDFRVF--GT-NLRVSNVNCPILPT-----SGSVDEINAAISACIQDQRTLALGQFLNRS 61
S. bingchenggensis 1 AADVLQGS-SKLPFQIV--KM-DYSLTDPTCELPSQ-----S-STTLFNEAVARCMNHQRALALDALLRRS 61
S. lydicus A02 1 AASTLSEG-NQIPFKIT--GATELHLVSSTCPGLSG-----VNNVPQFNGAVADCLQQQRAYALNTLLNRS 63
S. gilvosporeus F607 1 AANTLSVG-NQLPFKIV--GASELHVTSDTCPELTP----AVRNVAQLNSAVAECLQHQRTFALNTLLNRS 64
S. lydicus 103 1 AADALHDG-SALPLKIL--GG-KFESTSDICDLPTQ-----T-SGPLLQQAVEQCLQHQRALALNSLLNRS 61
S. sp. MOE7 1 AADALHDG-SALPLKIL--GG-KFESTSDICDLPTQ-----T-SGPLLQQAVEQCLQHQRALALNSLLNRS 61
S. albulus ZPM 1 AAAALHDG-SALPLKIL--GG-KFQSTSDICDLPTE-----T-SGALLQEAVNNCLMHQRAVALNNLLNRS 61
S. albulus NK660 1 AAAALHDG-SALPLKIL--GG-KFQSTSDICDLPTE-----T-SGALLQEAVNNCLMHQRAVALNNLLNRS 61
S. sp. 769 1 AAAALHDG-SALPLKIL--GG-KFQSTSDICDLPTE-----T-SGALLQEAVNNCLMHQRAVALNNLLNRS 61
S. sp. NEAU-S7GS2 1 AADALHDG-SALPLKIL--GG-KFQSTSDICDLPTE-----T-SGQLLQEAVNNCLQHQRAVALNSLLNRS 61
S. rubrolavendulae MJM4426 1 TRQALYISTDDLPFKLL--KG-EVDPNFDWCRLPAE-----GVTAEQFNDAMAGCLQHQRDLALDDLLRRS 63
S. pristinaespiralis HCCB 10218 1 TAQALHVGVADLPFKIV--EG-KVQPTTDWCTLPEE-----G-SGEQFNQAVSACLQHQRELALDDLLRRS 62
S. peucetius subsp. caesius 1 TAQALNVGVTELPFKIV--EG-KVQPTTDWCTLPEE-----G-SGEQFSRAVSACLQHQRELALDDLLRRS 62
S. laurentii 1 TAQALRDA-IELPFKVV--SG-TVTATNDSCRLPDN-----S-TGEQLNNAVSMCLRHQSDLALDDLLRRS 61
S. venezuelae ATCC 15439 1 TAQTLGESAAKLPFEIV--TG-KVQPTTSWCELPVQ-----G-SGKQFNDAVSVCLRHQGDLALEDLLRRS 62
S. sp. WAC00288 1 TAQALSDSAAQLPFKVV--DG-TVQPTTSWCELPVK-----S-TGDQLNDAVTLCLRHQGDRALEDLLRRS 62
S. vietnamensis GIM4.0001 1 TAQALSDSTSQLPFKVV--NG-TVQPTTSWCTLPES-----P-TGDQLNNAVTLCLRHQSDIALEDLLRRS 62
S. scabiei 87.22 1 AAQAVSTGN-TPVFKIE--GGDNISVSSALCPTVDANTAPTNLKLDDFNAAISACIDDHRQKALDTLLSRS 68
S. lincolnensis NRRL 2936 1 AAQALTSGN-QPPFKIA--GGENIKVISDKCPAVN---GATDLPLDTFNTIISKCIDQQRHASLDNLLSRS 65
S. griseochromogenes ATCC 14511 1 AAQAITTGN-ATLFKIV--SFQNLQVASDNCPAIT-----NHLPLADFNEAISRCADQQRQTALDNLLSRS 63
S. collinus Tü 365 1 AAQAINSGN-QPLFKIV--SFQKLQVSSDNCPAI----NTNSLPLQDFRDAIAHCMDQQRQTALDDLLSRS 64
S. hygroscopicus subsp. jinggangensis 5008 1 AAQAISTGN-QPLFKIV--SGSAIKVTSDNCPAVTA-INSGPVPLSDFNEAIAHCVDQQRQAALDNLLSRS 67
S. hygroscopicus subsp. jinggangensis TL01 1 AAQAISTGN-QPLFKIV--SGSAIKVTSDNCPAVTA-INSGPVPLSDFNEAIAHCVDQQRQAALDNLLSRS 67
S. hygroscopicus subsp. limoneus KCTC 1717 1 AAQAISTGN-QPLFKIV--SGSAIKVTSDNCPAVTA-INSGPVPLSDFNEAIAHCVDQQRQAALDNLLSRS 67
S. pluripotens MUSC 135 1 AAQAISTGN-QPLFKIV--SFQELKVSSDSCPAI----NTKSLALSDFNDAIAHCVDQQRQAALDNLLSRS 64
S. pluripotens MUSC 137 1 AAQAISTGN-QPLFKIV--SFQELKVSSDSCPAI----NTKSLALSDFNDAIAHCVDQQRQAALDNLLSRS 64
S. reticuli TUE45 1 AAQAISTGN-QPLFKIV--SGTQIRVSSENCPAI----NTTSLPLSDFNDAIAHCVDQQRQEALDNLLSRS 64
S. alboflavus MDJK44 1 AAQALNTGN-EPLFKIV--GGREIRVTSDNCPQA----SSGNLLIPEFNAAISACTDHQRQVALDNLLSRS 64
S. sp. 452 1 AAQALRTGN-EPLFKIV--QFQSLKVTSNNCPGI----ATSDLSLAEFNDAINACMDHERKAALDNLLSRS 64
S. avermitilis MA-4680 1 AAQALRTGS-EPLFKIL--DGNGIKVASDDCPGV----STNNIPLTAFNDAISACTDHQRQVALDNLLSRS 64
S. sp. 4F ASR50_26515/58-121 1 AAQALRTGS-QPLFKIV--DFDGLKVSSNDCPGI----ADGNLSLTEFNNAISECIDDQRQVALDNLLSRS 64
S. olivaceus KLBMP 5084 1 AAQAVRSGN-QPLYKIV--DFTDLRVSSSDCPVV----DNGNLSLSDFNAAISDCMDHQRKVALDNLLSRS 64
S. parvulus 2297 1 AAQAVRTGN-EPLYKIV--DFTDLRVSSSDCPVV----DNGNLSLSAFNAAISDCIDHQRKVALDNLLSRS 64
S. coelicolor A3(2) 1 AAQAVRTGN-EPLYKIV--DFTDLKVSSSTCPVV----DNGGLSLSDFNAAISDCMDHQRKVALDNLLSRS 64
S. lividans TK24 1 AAQAVRTGN-EPLYKIV--DFTDLKVSSSTCPVV----DNGGLSLSDFNAAISDCMDHQRKVALDNLLSRS 64
S. sp. CCM_MD2014 1 AAQAVRTGN-EPLYKIV--DFTDLKVSSSTCPVV----DNGGLSLSDFNAAISDCMDHQRKVALDNLLSRS 64
S. ambofaciens ATCC 23877 1 AAQAVRTGN-QPLYKIV--DFEGLRVASNDCPGV----TNGNLSLSEFNAAISECIDHERQAALDRLLSRS 64
S. ambofaciens DSM 40697 1 AAQAVRTGN-QPLYKIV--DFEGLRVASNDCPGV----TNGNLSLSEFNAAISECIDHERQAALDRLLSRS 64
S. pactum ACT12 1 AAQAVRTGN-QPLYKIV--DFQDLQVASNDCPGV----TNGNLSLSQFNAAISDCIDHQRQVALDRLLSRS 64
S. sp. SM18 1 AAQAVNAGS-DLPFEVV--NGQ---VTSQVCDLPTK------ASPDTFNAALNACANQQRDHALDSLLNRS 59
S. sp. CFMR 7 1 AAQALGVGS-KLPFEIV--RGE---VASKICDLPTT------PSPEAFNAAMNACVNNQRKEALETLLNRS 59
S. sp. S8 1 AAQALGVGS-KLPFEIV--SGR---VASEICDLPTT------PSPEAFNAAMNACVNNQRKEALETLLNRS 59
S. griseus subsp. griseus NBRC 13350 1 AAQALSVGT-DLPFEIV--SGK---VTSEICDLPAN------ASPNDFNAAMNACVNHQRKAALETLLNRS 59
S. globisporus C-1027 1 AAQALHVGS-ELPFEIV--SGK---VTSEICGLPTN------ASPDAFNAAMNACVNNQRKAALDTLLNRS 59
S. sp. Sge12 1 AAQALRQGN-ALPFQIV---GGQVKVSSTNCSGVMG----GPLEPEQFNAAVNQCVLEQRRHALDDLLSRS 63
S. sp. TN58 1 AAQALRQGN-AMPFQII--GGQNVQVSSPACPGVGV-----GQSYDQFNAAISKCALEQRRHALDDLLSRS 63
S. sp. fd1-xmd 1 AAQALRQGN-AMTFQIV--GGQNVQVASTACPGVGI-----GQSYDQFNAAISKCALEQRRHALDDLLSRS 63
S. sp. Mg1 1 AAQALREGN-ALPFKIVSVSGQKVEVSSPTCSGVGT-----DQSLDQFNAAIQACILDQRKHALDDLLSRS 65
S. lavendulae subsp. lavendulae CCM 3239 1 AAQALREGN-ALPFKIV--GGQKVEVSSTTCSGVGI-----DQSIDQFNAAIGQCILDQRKHALDDLLRRS 63
S. sp. CLI2509 1 AVQAVGVGQ-KLPFQIS--SGE-VRFSSDTCPQLAD-MSGAVHSQADFQAALNDCVNQQRQRALDHLLSRS 66
S. albus J1074 1 AAQAVHVGN-ELPFQVT--SGT-FTIYSDACPALSG---RRFTSSGAFNDAMKLCIDHQRQQALDDLLSRS 64
S. sp. FR-008 1 AAQAVHVGN-ELPFQVT--SGT-FTIYSDACPALSG---RRFTSSGAFNDAMKLCIDHQRQQALDDLLSRS 64

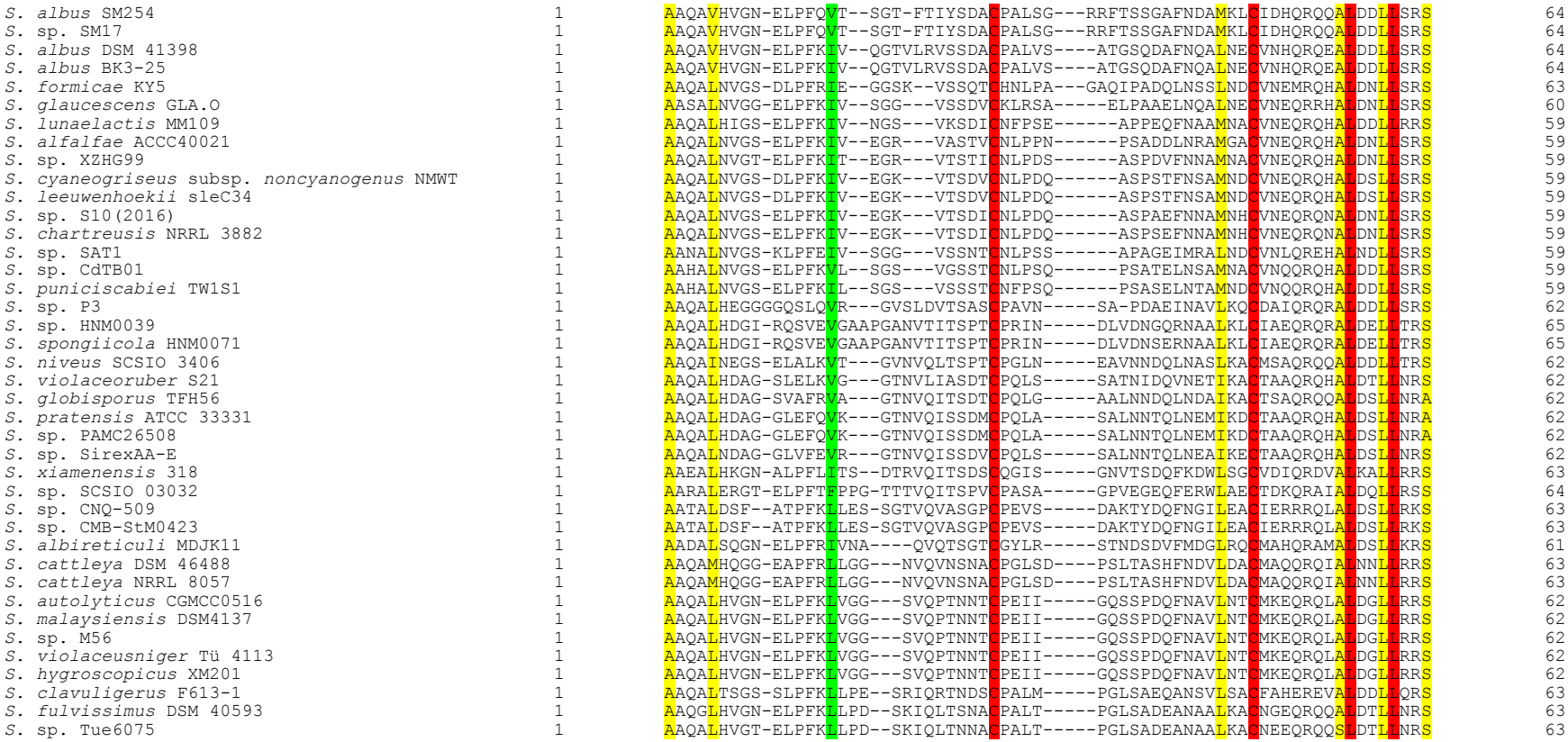

Figure 6.1. Alignment of the extracellular domains of CutS homologues from 93 high-quality *Streptomyces* genome sequences. Residues highlighted in red indicate positions which have a fully conserved residue. Residues highlighted in yellow indicate conservation between groups of strongly similar properties. Residues highlighted in green indicate conservation between groups of weakly similar properties.

Table 6.2. Analysis of the cysteine residue content of sensor kinase (SK) extracellular domains in *S. venezuelae*, *S. coelicolor* and *S. formicae* KY5. The total number of SKs was predicted using P2RP which includes orphan and other non-TCS SKs. Number of transmembrane domains was predicted using TMHMM v2.0.

	S. venezuelae	***S. coelicolor***	***S. formicae* KY5**
Total SKs detected by P2RP	163	196	210
SKs with two TM domains	20	27	21
SKs with any cysteines	13	17	12
SKs with any cysteines within extracellular domain	2	2	3
Detected proteins	CutS (2)	CutS (2)	CutS (2)
(Number of cysteine residues within extracellular domain)	CssS (2)	CssS (2)	CssS (2) KY5_3157c (1)

Figure 6.2A and **Figure 6.2A** depict the structures of the full-length CutS monomer and EcCutS of *S. venezuelae* as predicted by I-TASSER (https://zhanglab.dcmb.med.umich.edu/I-TASSER/). Whilst the CutS model is based on previously reported structures of SK partial structures, EcCutS is more reliant upon primary amino acid sequence. The *in vivo* CutS structure is likely to be dictated by the presence and location of the TM domains and the anchoring of these in the cell membrane and as such the true confirmation is somewhere in-between the two models. This is not accounted for in **Figure 6.2B** whilst **Figure 6.2A** likely underestimates the extracellular domain structure. The location of the two cysteine residues is important, however. **Figure 6.2B** predicts them to be relatively close to each other, possible capable of forming an intramolecular disulphide bond, whilst **Figure 6.2A** would suggest they are too far apart to form such a bond, making intermolecular disulphide bonds more likely. Intermolecular disulphide bonding could be between two CutS monomers, or between a CutS monomer and another protein. These interactions will be discussed further in **Chapter 6.4** but the above data clearly reveals that the extracellular sensory domain of CutS shares significant similarity with CssS and strengthens the hypothesis that these TCSs likely play similar roles in *Streptomyces* spp.

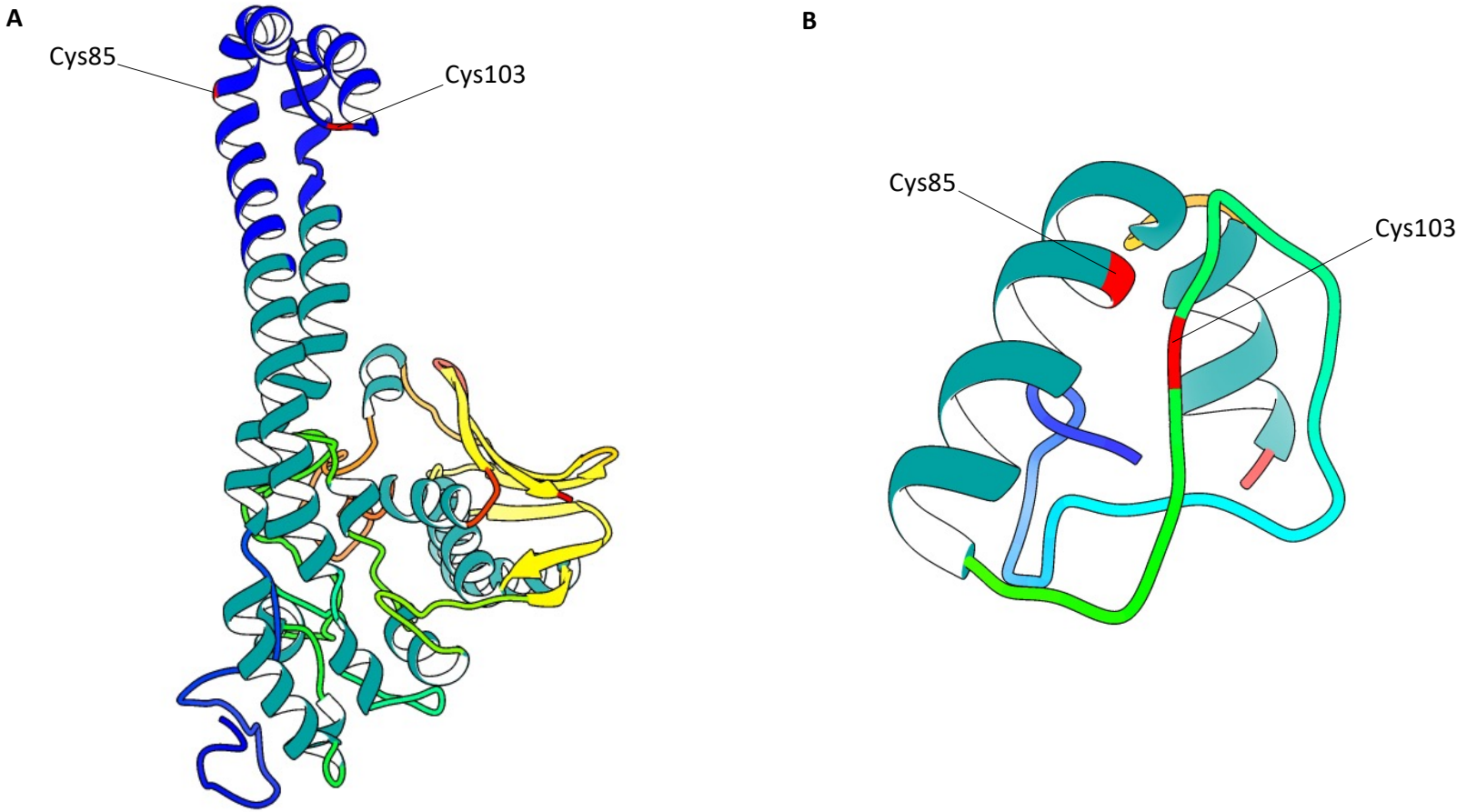

Figure 6.2. The structures of *S. venezuelae*: **A.** CutS as predicted by I-TASSER with the EcCutS region of CutS coloured blue. **B.** The isolated EcCutS region as predicted by I-TASSER. The two cysteine residues have been coloured red and labelled.

6.2. Heterologous expression and purification of EcCutS

In order to characterise EcCutS further heterologous expression and purification was required. The coding region for *S. venezuelae* EcCutS was cloned into the pET28a expression vector to create a fusion construct with a N-terminal 6xHis tag. This was expressed in *E. coli* BL21 pLysS and small-scale purification was carried out as described in **Chapter 2.30**. Soluble expression was confirmed, and expression conditions optimised before large scale purification was performed as described in **Chapter 2.31**.

The expected size of the purified 6xHis-EcCutS was 9,085 Da, a size which proved difficult to accurately confirm using SDS-PAGE. We also wished to detect the presence of any EcCutS dimerisation, an interaction which would likely be broken by the reducing conditions of SDS-PAGE. Whilst native-PAGE was an option, native MS was deemed more suitable and was performed by Dr Jason Crack at UEA (**Figure 6.3**). From this we can see that the main peak present is 8,951 Da representing the tagged EcCutS with N-terminal methionine excision (-134 Da), a common post-translational modification (Bonissone *et al.*, 2013). Three other relevant peaks were identified. The peak with a mass of 5,014 Da was identified to be a breakdown product lacking the 6xHis tag and first 15 residues of EcCutS. A 6x-His EcCutS homodimer was observed with a mass of 17,903 Da as well as a 13,966 Da heterodimer consisting of the 8,951 Da full protein combined with the 5,014 Da breakdown product. The presence of natively forming homodimers is suggestive of a correctly folding SK extracellular domain and this information is important for the SPR experiments described later in this chapter.

Concurrently to native MS, dynamic light scattering was performed to confirm the size of the purified protein (**Table 6.3**). DLS is a simple and rapid biophysical method which uses light scattering to determine the homogeneity and size of macromolecules within solution (Stetefeld, McKenna and Patel, 2016). Whilst DLS was unable to detect the presence of the homodimer it did confirm the most abundant (97.4%) particle by mass correlated to a 9 kDa protein. The accuracy of DLS mass estimation is dependent on the shape of the protein as this determines the

hydrodynamic radius measured through light scattering (Borgstahl, 2007). EcCutS is predicted to form a small globular protein which makes this estimation more accurate than that of, for example, fibrous proteins and this is reflected in the similarity between the predicted size by DLS and that measured by native MS.

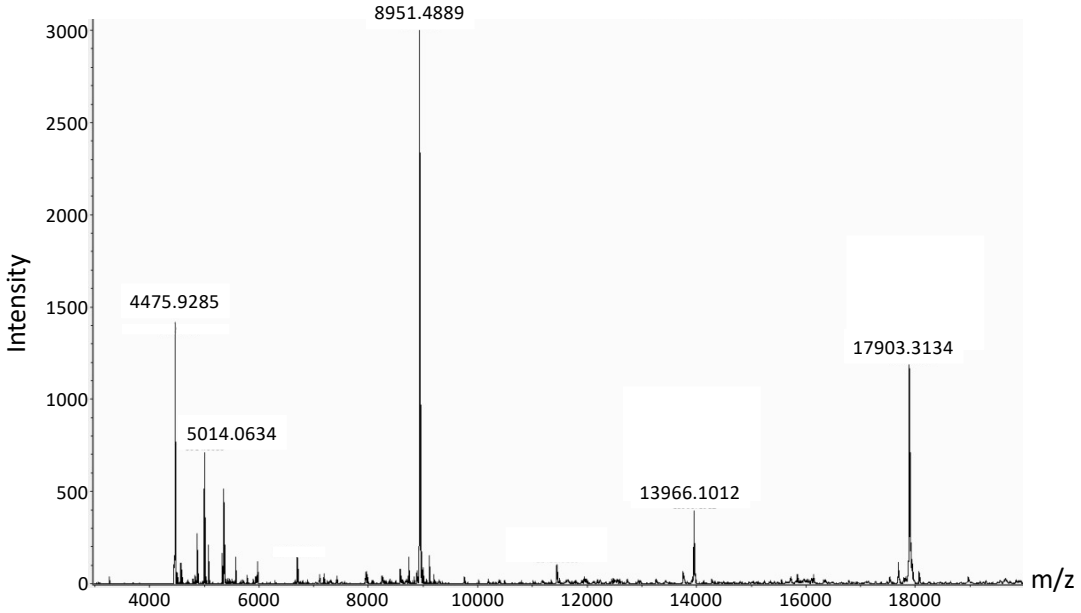

Figure 6.3. Native mass spectrometry analysis of heterologously produced 6xHis-EcCutS. Peaks for the full length (8,951 Da), breakdown (5,014 Da), heterodimer (13,966 Da) and homodimer (17,903) can be identified.

Table 6.3. Table of DLS results for EcCutS in 10 mM phosphate buffer. MW-R: the weight-averaged molecular weight estimated from the measured hydrodynamic radius.

DLS Peak	Radius (nm)	Polydispersity (%)	MW-R (kDa)	Intensity (%)	Mass (%)
1	1.5	11.4	9	5	97.4
2	3.3	0	56	1.3	2.5
3	54.5	14.4	38834	85.8	0
4	3619.4	0	713950000	7.9	0

CD spectroscopy was also used to confirm folding of EcCutS (**Figure 6.4**). Structure prediction from CD spectroscopy data utilises algorithms reliant on curated databases. Because of this the outputs can be biased, especially in the prediction of proteins rich in β-sheets. For the purpose of this work CD spectroscopy was solely performed to confirm folding and presence of secondary structure in EcCutS rather than to estimate the structure itself. Within these limitations we can observe a spectrum at least indicative of protein folding.

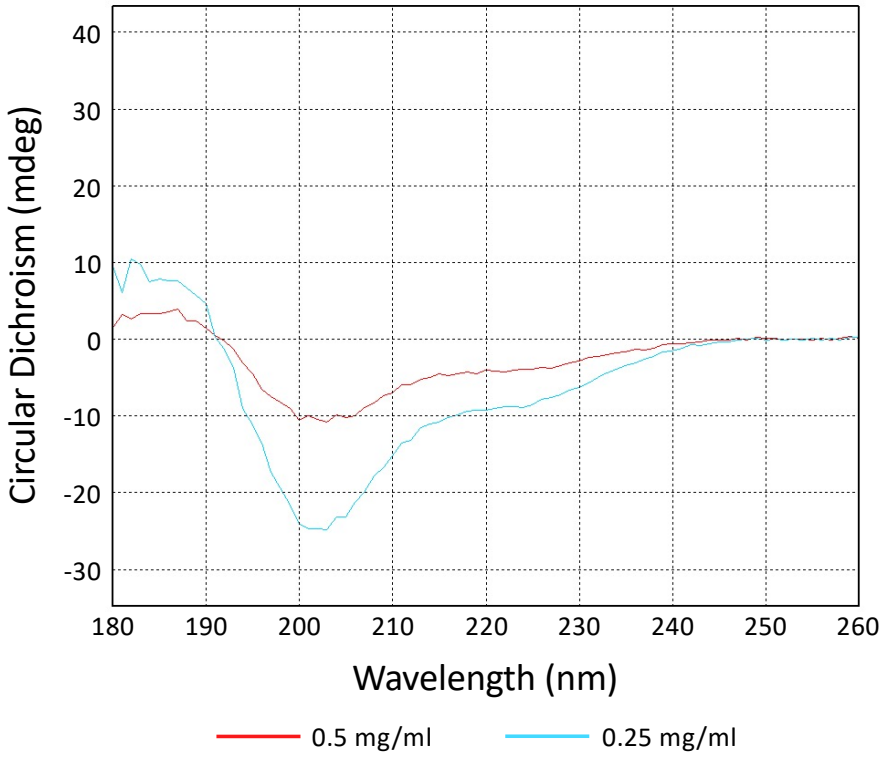

Figure 6.4. Circular dichroism spectroscopy results of heterologously produced 6xHis-EcCutS at concentrations of 0.5 mg/ml and 0.25 mg/ml.

During purification it was noted that, following immobilized metal affinity chromatography (IMAC), the fractions containing 6xHis-EcCutS were pale yellow in colour. Further investigation was performed by Dr Jason Crack using inductively coupled plasma MS (ICP-MS) to check for metal ion binding (data not shown). This did not detect any metal ions associated with 6xHis-EcCutS, consistent with the absence of peaks in the native MS. However, these experiments were both performed on samples post size exclusion where the colour had been lost. Future native MS and ICP-MS would be performed on samples immediately following IMAC to identify any bound metal ions which may be lost during the latter stages of purification.

Combining the above data, we can confidently confirm successful heterologous expression and purification of 6xHis-EcCutS from *E. coli*. DLS confirms the majority of the purified protein is present as a monomer whilst native MS corroborates this and reveals the presence of a breakdown product, heterodimer and most importantly a EcCutS homodimer. The CD spectra suggests EcCutS is folding, but further structural interpretation would be speculative at best. Finally, no metal ion binding was detected with ICP-MS although this data comes with an important caveat explained above. This was unlikely to be the ligand but was worth investigating given the sample colouration. With the CutS ligand still unknown the following work focuses on the development of a ligand screening assay.

6.3. Protein-ligand SPR screening

Historically SK ligand determination has been achieved through a mixture of methods. Generally, the ligand is putatively identified through media supplementation and observation of phenotypic change. As previously discussed in **Chapter 1.7.1.6**, the PhoPR TCS has been shown to co-ordinate phosphate control in response to changes in phosphate availability. This was achieved through numerous transcriptomic studies using phosphate depletion and supplementation of the growth medium but how the SK PhoR detects phosphate levels is not yet known (Martín, Rodríguez-García and Liras, 2017). The GluRK sensor kinase GluK was shown to bind glutamate directly using biolayer interferometry (Li, Jiang and Lu, 2017) whilst a biotin labelled vancomycin probe was used to show that the *S. coelicolor* SK VanS directly binds the glycopeptide antibiotic. This binding correlated to vancomycin resistance through the expression of *vanH*, *vanA* and *vanX* (Koteva *et al.*, 2010). Thus, to date, SK ligand determination has relied on a wide range of techniques which require prior knowledge of the putative ligand, and these techniques are unsuitable for high-throughput screening.

More recently work on chemoreceptor ligand determination has turned to using differential scanning fluorimetry (DSF) (Brewster *et al.*, 2016; Ehrhardt, Warring and Gerth, 2018; Martín-Mora *et al.*, 2019). Whilst DSF is relatively quick and inexpensive it is labour intensive, requires significant amounts of purified protein and reproducibility between experiments can be difficult to achieve. As such we aimed to develop a SPR-based ligand screening method which is less labour intensive, more amenable to scaling up, requires little purified protein and most importantly is reproducible. Whilst a comprehensive protocol can be found in **Chapter 2.34** the key points are shown in **Figure 6.5**.

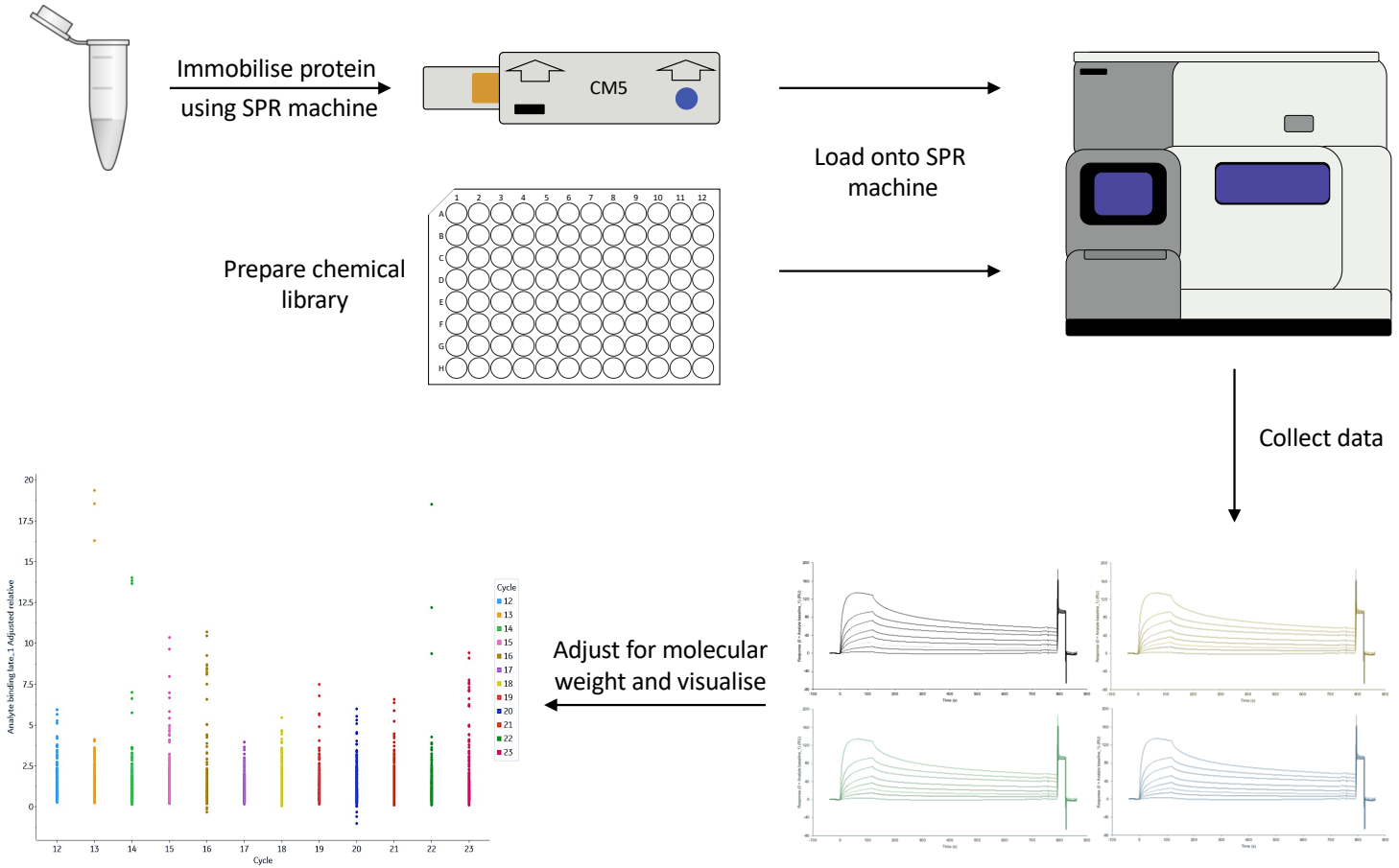

Figure 6.5. Schematic representation of the high throughput protein-ligand SPR screening workflow. Protein of interest is immobilised on a CM5 chip via amine coupling. Meanwhile the chemical library is prepared in 96-well plates. Both the chip and the chemical library are loaded onto the SPR machine and analysed. Data is collected for each individual protein-ligand interaction in triplicate. Finally binding interactions are adjusted for ligand molecular weight and visualised.

The library of ligands chosen for screening was the Biolog Phenotype Microarray (PM) plates. These plates have previously been used as a chemical library for similar purposes in DSF-based studies (Brautigam *et al.*, 2016; Fernández *et al.*, 2016). The 10 plates used (PM1-PM10) contain over 900 compounds including carbon and nitrogen sources, osmolytes, ions, and common nutrient supplements.

Purified 6xHis-EcCutS was immobilised on a CM5 sensor chip. CM5 chips contain a matrix of carboxymethylated dextran covalently attached to a gold surface which can be activated with a combination of NHS and EDC. Attachment occurs through coupling of the primary amine groups on the protein of interest. The excess activated surface is then blocked with ethanolamine to prevent unwanted ligand-chip surface interactions. The reference surface is activated and blocked as above but without protein immobilisation. The amount of protein required is dependent on the protein, efficacy of binding to the activated chip, and the response levels needed for the experiment. However, once this protein is covalently attached it is regenerated between each binding cycle. Thus, the amount needed for chip binding, often in the microgram range, is the only protein required for the entire experiment.

Once the chip is prepared and the chemical library is ready, they are loaded into the SPR machine and protein-ligand binding tested with the methodology described in **Chapter 2.34**. The SPR machine used for this work was a Biacore 8k (Cytiva, UK) which contains 16 flow cells in eight channels allowing for automated high-throughput screening. Once a sufficient binding response is confirmed the screening can commence. With a large enough external pool of SPR running buffer and NaCl, for surface regeneration, the limitation for throughput is the plate storage capabilities of the SPR machine of choice. Preparation and dilution of the chemical library into 2 ml 96-deep well plates allowed for each plate to be screened in triplicate without interruption with each replicate taking around two hours to complete. As such, with a small amount of prior setup, all 10 plates were screened over the course of three days with almost no manual labour required during that time. Once data collection

was completed the results were collated and adjusted for the molecular weight of the ligand to normalise the analyte binding response (**Figure 6.6**).

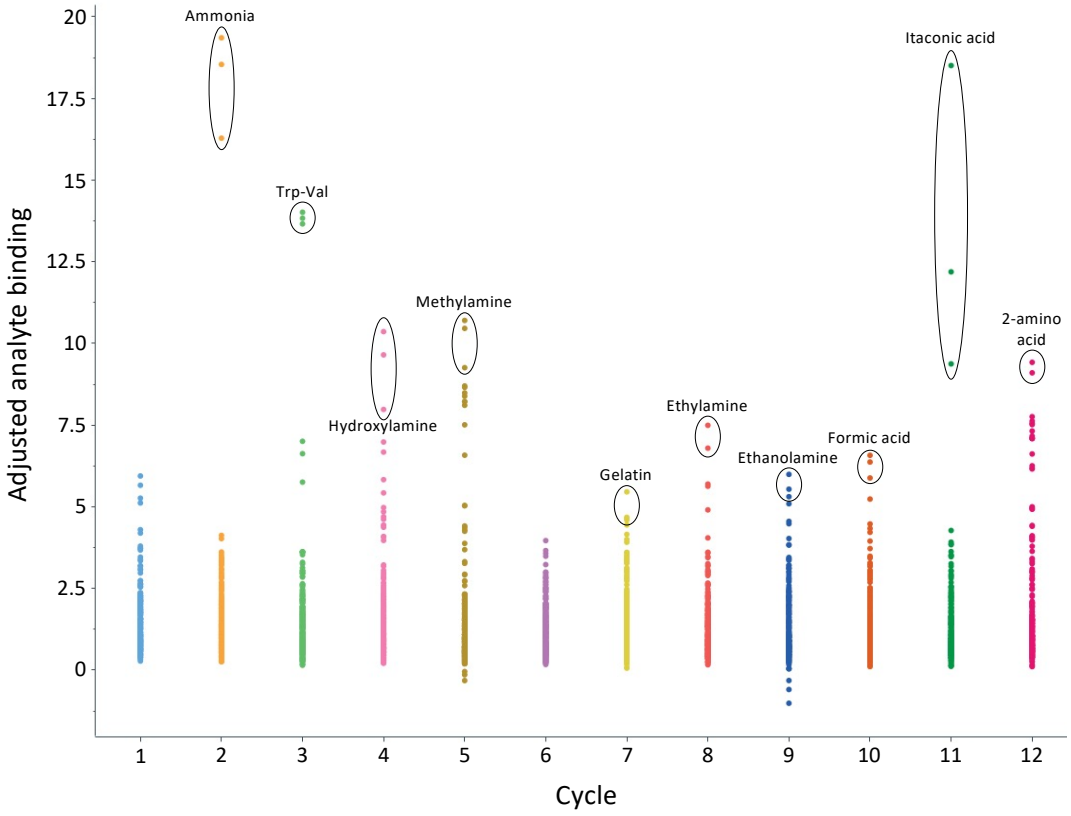

Figure 6.6. The analyte binding response for EcCutS – chemical library SPR screening adjusted for ligand molecular weight. Ligands with increased adjusted analyte binding are encircled and labelled.

As can be seen in **Figure 6.6** the vast majority of screened ligands gave a response below 5 response units (RU). Using the median molecular weight of the ligands (209.6 Da), EcCutS (8,951 Da) and the stable response rate of immobilised protein (~1,000 RU) we can calculate a theoretical R_{max} of 23.42. This would suggest that the responses detected were within an expected range for the experimental conditions. With the exception of itaconic acid, all the ligands of interest (those encircled in **Figure 6.6**) contain amine groups. At first it was thought this was likely cross-reaction with the CM5 chip, given amine coupling is the method of protein attachment. However, there were other amine group containing ligands within the chemical library that did not bind. The recorded analyte response is relative to the empty reference flow cell which also makes this unlikely. Additional consultation with the

manufacturers also suggested this would be highly unlikely given the ethanolamine blocking. Consequently, it was considered that EcCutS was involved in nitrogen sensing. Gelatin, being cheap and easily available, was chosen for follow up SPR experiments. These appeared promising, with a dose-dependent response being observed, indicative of real binding (**Figure 6.7**). Whilst it is technically possible to calculate a steady state affinity KD for the plot displayed in **Figure 6.7** it would be inaccurate. Gelatin is the product of collagen hydrolysis and as such has no accurate molecular mass. A stock solution was created and used for serial two-fold dilutions to detect a dose-dependent response but beyond this it is difficult to calculate affinity or kinetics. The choice of gelatin for follow-up experiments was likely a mistake given these shortcomings. Further investigation was inconclusive on the general amine binding properties of EcCutS, and it is possibly still an artefact of the methodology that requires further refinement. Itaconic acid remains a possible ligand worthy of follow-up.

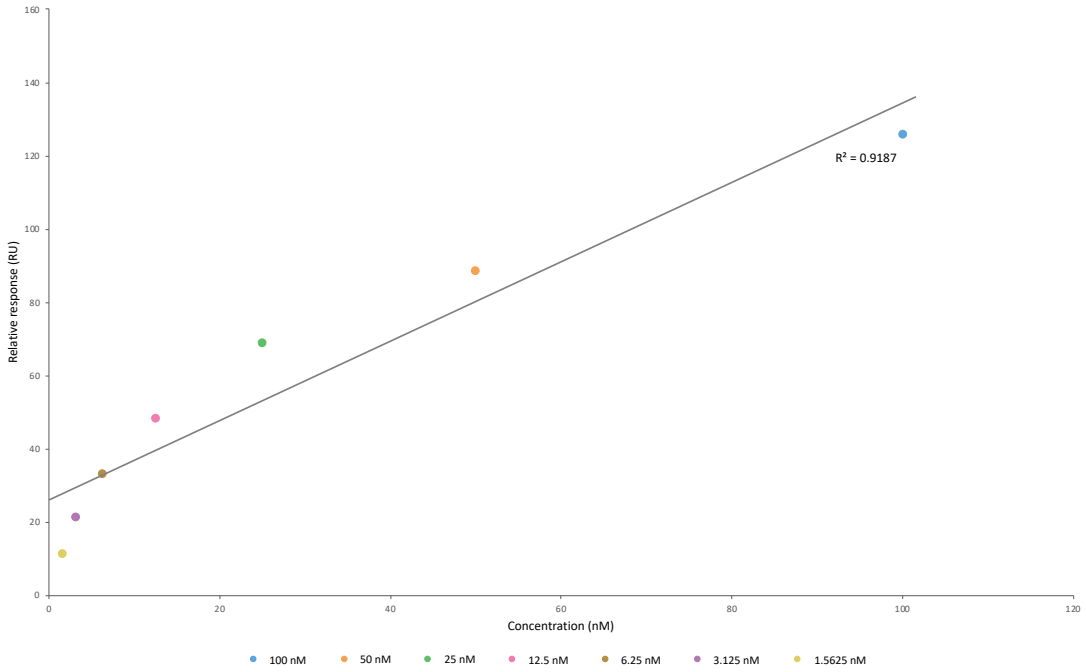

Figure 6.7. Response versus concentration plot for immobilised EcCutS and gelatin assayed at seven concentrations of gelatin. Due to gelatin composition the displayed concentrations are estimates and an accurate steady state affinity cannot be determined.

The work described above is the first attempt at method development for a high-throughput SK extracellular domain – ligand screen using SPR. Whilst further work is required to validate its efficacy, the power of this methodology is clear. With relatively simple setup and small amounts of protein a huge library of chemical ligands can be screened rapidly with high reproducibility and little manual labour. SPR machines are expensive and, without access to one, other methods would be far more cost effective. However, where accessible, this methodology has the potential to accelerate the discovery of SK ligands, a technically difficult and neglected area of study within TCS research.

6.4. Discussion

The work in this chapter switches focus from CutR to the SK CutS and, more specifically, the extracellular sensory domain termed EcCutS. This domain lacks conservation between homologues relative to similar comparisons of other SK extracellular domains. The same trend is apparent with the extracellular domain of the SK CssS. Both EcCutS and EcCssS contain two highly conserved cysteine residues separated by a similar number of amino acids. This dual cysteine structure appears to be unique among the extracellular domains of SKs with a similar two-TM architecture. Homology modelling of EcCutS suggests these two cysteines could be close enough to form an intramolecular disulphide bond whilst similar modelling of the full-length CutS would oppose this hypothesis (**Figure 6.2**). Attempts have been made to determine the structure of EcCutS with X-ray crystallography. To date these efforts have been unsuccessful. It would also be prudent to perform mutagenesis of these cysteines to identify their role in signal detection and reveal if they are forming inter- or intra-molecular disulphide bonds.

Heterologous expression and purification of 6xHis-EcCutS was successful and a number of techniques were used to characterise the purified protein. Native MS identified the full-length protein along with a breakdown product. It also confirmed the presence of both a EcCutS homodimer and EcCutS-breakdown product heterodimer. This suggests that EcCutS is capable of forming a homodimer, the assumed *in situ* conformation, during heterologous expression and under buffered conditions. DLS was not capable of detecting the homodimer but could confirm the sample was >90% monomer by mass. CD spectroscopy confirmed *in vitro* folding whilst ICP-MS was unable detect any metals bound to EcCutS although this still remains a possibility. Finally, a new SPR method was developed using the Biolog PM plates as a chemical library to screen for SK ligands *in vitro*. Whilst further development and validation is required, it was appears to be a methodology worth further development. It revealed the possibility that itaconic acid is a potential EcCutS ligand and this could be followed up using further SPR and ITC.

Itaconic acid, or itaconate, is an organic dicarboxylic acid produced by fungi and lichens. It is also produced by macrophages as an antibacterial; preventing bacterial survival through the inhibition of isocitrate lyase, a glyoxylate shunt enzyme (Cordes, Michelucci and Hiller, 2015). Recently itaconic acid has also been shown to inhibit other key glycolytic enzymes including fructose-bisphosphate aldolase A and L-lactate dehydrogenase A. This inhibition occurs due to the covalent modification of cysteine residues within these enzymes. The electrophilic α, β-unsaturated carboxylic acid of itaconate reacts with the reactive cysteine via Michael addition resulting in 2,3-dicarboxypropyl adducts (Qin *et al.*, 2019). Itaconate has also been shown to increase the alkylation of cysteines within the Kelch-like ECH associated protein 1 (KEAP1), reducing KEAP1 interactions with the transcription factor nuclear factor erythroid 2-related 2 (NRF2) in macrophages. Under normal conditions KEAP1 binds to NRF2 preventing translocation from the cytoplasm to the nucleus. Upon detection of certain stimuli KEAP1 dislocates allowing NRF2 to activate the transcription of multiple genes encoding anti-inflammatory and anti-oxidative stress proteins (Li *et al.*, 2020). As a result of this selective cysteine targeting, synthetic itaconic acid hybrids have been investigated as potential anticancer and antiviral agents (Perković *et al.*, 2020). It is a significant possibility that the EcCutS-itaconic acid interaction detected by SPR screening is due to its reaction with free cysteine residues. Future mass spectrometry experiments would reveal the presence of 2,3-dicarboxypropyl adducts resulting from this interaction. Detection of such adducts would suggest that the cysteine residues of purified EcCutS are reduced as itaconate reacts with S-H not S-S, and that these residues are accessible to ligands.

Whether the alkylation occurs *in vitro* or not it is likely that the *in vivo* purpose of EcCutS is to sense changes to the state of its cysteine sulfhydryl groups, perhaps through oxidation to form intra- or inter-molecular disulphide bonds to EcCutS or other extracellular proteins. As mentioned in **Chapter 5.4**, Actinobacteria are unusual among Gram-positive bacteria in that their secretome includes a significant number of proteins which require disulphide bond formation for correct folding. Other Gram-positive bacteria, including Firmicutes, avoid this due to the complexities involved in ensuring correct folding (Daniels *et al.*, 2010). Whilst the CssS homologues in *Bacillus*

spp. and *Streptomyces* spp. share functionality the *B. subtilis* CssS lacks the sensor domain cysteines found in the streptomycete CssS. This is likely related to the lack of cysteine-containing secreted proteins in Firmicutes and leads us to speculate that CssS is specialised for the actinobacterial secretome. It will be fascinating to investigate the roles of the dual cysteines in the CssS and CutS sensor domains in streptomycetes and ponder the lack of cysteines in the Firmicute CssS.

The highly reactive thiol groups in cysteines make them excellent residues for both reversible and irreversible modifications including not only the aforementioned disulphide bond formation and alkylation but also nitrosylation, oxidation and glutathionylation. These modifications and the reversibility makes them ideally suited for detecting changes to the redox state and regulating changes to the oxidative stress response (Cremers and Jakob, 2013). Sometimes this involves metal centres, such as Zn^{2+}, to stabilise the reactive thiol groups under nominal conditions as is the case with Hsp33, a molecular chaperone (Jakob, Eser and Bardwell, 2000). However other systems rely on thiol-disulphide switches. The transcription factor OxyR contains two cysteine residues 17 Å apart which are reduced in the inactive OxyR conformation. Cys^{199} is first oxidized by H_2O_2 which releases it from its hydrophobic pocket with the extrusion then allowing the formation of a disulphide bond with Cys^{208}. This locks the system into the active state allowing for transcription to occur and a cellular response induced (Choi *et al.*, 2001; Cremers and Jakob, 2013).

Thus, one possibility is that disruption of intramolecular disulphide bonds within each EcCutS monomer is induced by a change in the extracellular redox state, resulting in a conformational change leading to CutS autophosphorylation and CutR activation (**Figure 6.8A**). The same change could also result in the opposite response with CutS constitutively active until disulphide bonds are formed. It is possible that mutation of the dual cysteines might reveal which conformation is the active state however there are numerous confounders to this experiment. Likewise, the disulphide bonds may be inter-molecular between two CutS monomers rather than intra-molecular, and disruption of these bonds could induce SK activation (**Figure 6.8B**). Another possibility is that these reduced cysteine residues are capable of disulphide bonding to exposed cysteines in unfolded secreted proteins. This could be cysteines of any

unfolded peptides or specific proteins the cell considers indicative of extracellular folding status (**Figure 6.8C**). It is possible that CutS and CssS detect different proteins, or groups of proteins, with each group requiring a different secretion stress response and protease. Perhaps it is more complicated, with the CutS / CssS cysteines requiring constant oxidation by thioredoxin-like proteins, such as DsbA, to signal that protein folding mechanism are still functional. The oxidised cysteines would then be reduced to their base state by proteins similar to the VKOR homologue SCO1507 (**Figure 6.8D**). This continuous oxidation and reduction may be complicated but would ensure such systems are active rather than reacting to changes in the extracellular redox state or misfolded protein levels which may be caused by other factors not suitable for a CutRS-driven response.

In summary, whilst the role of these cysteine residues in the sensor domains of CutS and CssS remains unknown, they are likely to be the key to signal detection and subsequent activation of the partner RRs of these two-component systems. The mechanisms proposed above are purely speculation based on the current evidence and it is possible that the real mechanism is vastly different to those hypothesised. Considerable further work is required to better understand EcCutS and CutS in its entirety. This work would also inform on the CssRS system and indeed investigation of CssS could likewise aid CutRS characterisation. In the next chapter the work of this thesis is concluded and a model for CutRS activity in *Streptomyces* spp. is proposed.

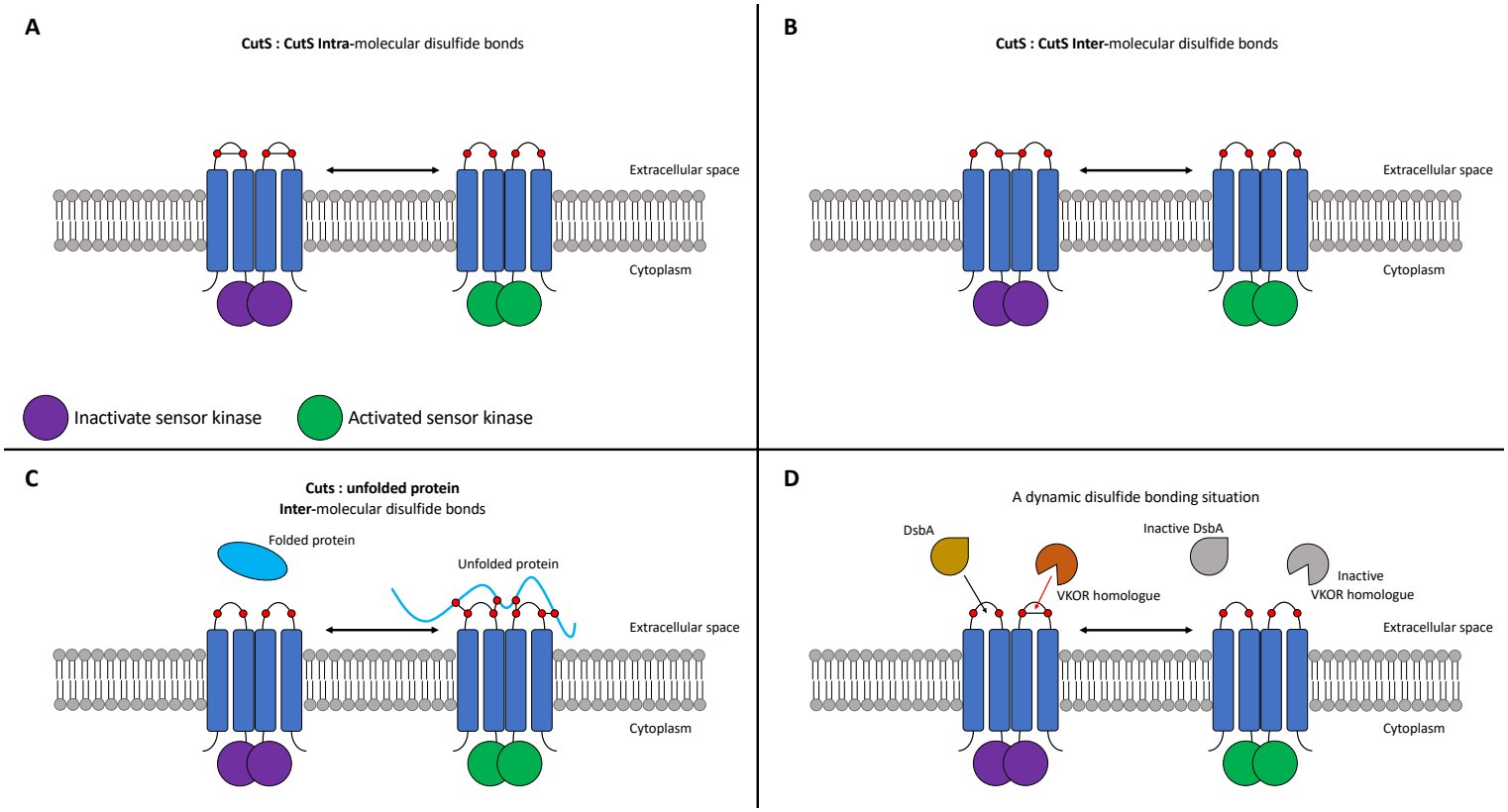

Figure 6.8. Schematic diagram depicting possible scenarios of CutS activation through EcCutS cysteines and disulphide bond formation. **A.** Altered extracellular space redox state results in the reduction of intramolecular disulphide bonds in the extracellular domain of CutS leading to activation of the sensor kinase. **B.** The same change results in the reduction of intermolecular disulphide bonds between the extracellular domain of two CutS monomers leading to activation of the sensor kinase. **C.** Accumulation of misfolded or unfolded protein results in disulphide bonding between exposed cysteines and the extracellular domain of CutS leading to activation of the sensor kinase. **D.** DsbA and VKOR homologue systems dynamically maintain the correct state of cysteines within the extracellular domain of CutS. Disruption to their activity, indicative of a state incapable of properly folding secreted proteins, leads to activation of the sensor kinase.

Chapter 7. Conclusions, model and further work

7.1. Characterisation of the CutRS two-component system in *Streptomyces* spp.

The aim of this work was to improve our understanding of TCSs in *Streptomyces* spp. Consisting of a membrane-bound SK and a cognate RR these systems play pivotal roles in the detection and response to a wide array of signals which are typically extracellular. Previous bioinformatic analysis revealed 15 TCSs to be highly conserved among *Streptomycetaceae* and, prior to the start of this project, a library of TCS operon deletion mutants was generated in the model streptomycete *S. venezuelae.* The work described in this thesis began with phenotypic screening of these 15 mutants, cultured under multiple conditions. This revealed the highly conserved CutRS TCS to be of further interest because on YPD agar it displays a phenotype distinct from the wild-type strain with an appearance similar to that of wild-type colonies undergoing exploratory development. Despite being the first TCS described within the genus *Streptomyces*, little was known about the role of CutRS or its activating signal. Indeed, whilst it was originally proposed to regulate cupric ion transport, hence the name, this was later disproved by the same authors (Tseng and Chen, 1991; Chang *et al.*, 1996). Using a combination of microbiological techniques, molecular manipulation and cutting-edge multi-omics approaches we began to characterise CutRS in both *S. venezuelae* and *S. coelicolor.* We also describe a novel SPR-based methodology for high throughput SK ligand screening and reveal potential biochemical similarities between CutRS and another highly conserved TCS, CssRS.

Phenotypic investigation of the *S. venezuelae* Δ*cutRS* mutant reveals that, whilst identical to the WT strain on YP agar, there are distinct changes on solid media with the addition of glucose. On YPD agar, we believe that the Δ*cutRS* mutant colonies overcome glucose-induced repression of exploratory behaviour by using all the glucose available. This induces, or is induced by, a significant increase in biomass. This same phenotype is observed on MYM+TE+glucose agar and MM+glucose agar. Phenotype screening with a range of saccharides revealed that glucose is the only

sugar tested capable of inducing a phenotype in the *S. venezuelae* Δ*cutRS* mutant. Glycerol was shown to exacerbate exploration in both the WT and mutant strains, and this is under investigation by other groups. The exploratory phenotype, first described by Jones *et al.* in 2017, is defined by a number of hallmarks. These include the presence of elongated, hydrophilic, low-branch number exploratory hyphae, rapid horizontal growth and the production of mVOCs. Our work shows that the *S. venezuelae* Δ*cutRS* mutant exhibits all these characteristics despite being cultured on YPD agar, a growth medium generally repressive to exploratory behaviour. Whilst GC-MS was not able to detect TMA, induction of the exploratory phenotype in physically disconnected streptomycete colonies was observed but onset was delayed significantly. With further experimentation it is likely that the mVOC produced by the mutant could be determined and preliminary evidence suggests it is an amine compound similar to TMA. The mutant strain was capable of being complemented fully *in trans* by the *cutRS* operon under both the native promoter and a strong constitutive promoter, *ermEp**. Complementation was also achieved through overexpression of the *cutRS* operons from *S. coelicolor* and *S. formicae* KY5 confirming the functional conservation of this TCS. A 3xFLAG-tag was fused to the C-terminus of the response regulator CutR without disrupting activity and this allowed for downstream applications including ChIP-seq and Co-IP.

Streptomyces spp. Are prodigious producers of specialised metabolites including molecules with antimicrobial, antiviral and antioncogenic activity. *S. venezuelae* is known to produce chloramphenicol which displays bactericidal activity against Gram-positive bacteria. On YPD agar the mutant was shown to overproduce chloramphenicol, and this was not linked to any direct regulatory effects. Production of chloramphenicol in *S. venezuelae* appears to be constitutive at a basal level but is normally undetectable by traditional overlay assays. We propose that the observed overproduction of chloramphenicol in the Δ*cutRS* mutant is the result of both a metabolic shunt and increased export via the efflux pump CmlF. The shikimate pathway is used to produce aromatic amino acids and parts of this pathway are used in chloramphenicol biosynthesis. With the increased growth observed on YPD agar the cells of the mutant colony must increase proteinogenesis, requiring more amino

acids and shifting metabolic flux through to pathways such as the shikimate pathway. We hypothesise that excess metabolites continue through to chloramphenicol biosynthesis, and this is observed as increased bioactivity in overlay assays.

The addition of redox-active antibiotics including pyocyanin and phenazine-1-carboxylate reverted the *S. venezuelae* Δ*cutRS* phenotype, at a colony level, to that of the WT on YPD agar. These compounds have been investigated in *P. aeruginosa* biofilm colonies in which they act as alternate electron shuttles to balance the intracellular redox state (Dietrich *et al.*, 2006; Ramos *et al.*, 2010). In this case it is possible they are acting as oxidising agents, rebalancing the intracellular redox state caused by excessive glycolysis and NAD(P)H generation. Another possibility is they act in the extracellular space, re-oxidising important enzymes, such as DsbA, which are involved in the formation of disulphide bonds required for the correct folding of secreted proteins.

In addition to *S. venezuelae*, the role of CutRS was also investigated in *S. coelicolor.* Using CRISPR-Cas9 mediated genome editing an in-frame deletion of the *cutRS* operon was made in *S. coelicolor* M145. The *S. coelicolor* Δ*cutRS* mutant was shown to overproduce the blue-pigmented antibiotic on DNA agar and this effect was exacerbated by the supplementation of glucose. Complementation was achieved through the addition of the native *cutRS* operon *in trans*. The *cutRS* operon cloned from *S. venezuelae* and *S. formicae* KY5, under strong constitutive expression, was also capable of phenotypic complementation. Additionally, the *S. venezuelae cutRS* operon under native promoter expression was capable of complementation as was a construct encoding a C-terminally 3xFLAG-tagged CutR and native CutS, similar to that used in *S. venezuelae.*

From colony-level phenotyping we progressed onto more complex molecular characterisation including identification of the CutR regulon in both *S. venezuelae* and *S. coelicolor*. ChIP-seq revealed species-specific regulons but two targets were also conserved cross-species, that of two genes encoding for HtrA-like serine proteases: *htrB* and *htrA3*, with CutR shown to repress the expression of the former and activate the expression of the latter. The other targets appear to be primarily

involved in extracellular activities with the expression of genes encoding for multiple secreted, and membrane-bound proteins, being modulated by CutR. HtrA-like serine proteases are generally found extracytoplasmically, where they degrade misfolded proteins or act as chaperones to ensure correct folding (Clausen *et al.*, 2011). Due to this activity, and their ability to be switched both on and off, they have been implicated in the secretion stress response. CutRS is not the only streptomycete TCS shown to regulate HtrA-like serine proteases. The highly conserved CssRS activates the expression of three genes encoding proteins of the same family: *htrA1, htrA2* and the previously mentioned *htrB* in response to secretion stress (Gullón, Vicente and Mellado, 2012). The overlap between CutRS and CssRS is not just limited to their regulon. TMT proteomics reveals that deletion of *cutRS* or *htrA3* in *S. venezuelae* results in the increased production of CssRS likely responding to the signal-response void created through the absence of CutRS, or an important constituent of its regulon. This is most likely *htrA3*, with deletion of *htrA3* in *S. venezuelae* also resulting in increased production of CssRS and HtrB.

β-glucuronidase reporter assays were used to identify the promoter activity of *cutRSp*, *htrA3p* and also the promoter of *vnz_08815* which encodes for a putative cell wall amidase regulated by CutR in *S. venezuelae*. The activity of the *htrA3p* fusion construct was completely reliant on the presence of both CutRS and growth media supplemented with glucose fitting the model of CutR activation. Results from the *cutRSp* and *vnz_08815p* assays revealed little significant variation between the WT and Δ*cutRS* mutant, or between YP and YPD with further experiments confounded by technical difficulties. To overcome this roadblock a hexahistidine-tagged CutR was heterologously expressed and purified for use in SPR-based ReDCaT experiments. This identified a consensus binding sequence of TAWATAAAG which proved useful in the confirmation of putative CutR targets identified using ChIP-seq. The location of CutR binding at the promoters of *vnz_08815* and *htrA3* relative to the TSSs (-69/-62 bp) is highly suggestive of transcriptional activation which matches with the increased protein abundance in WT versus *ΔcutRS* detected by the TMT-proteomics as well as the aforementioned β-glucuronidase results. The location of the CutR binding site within *htrBp,* 17 bp upstream of the TSS, correlates to a transcriptional

repressor which again matches to protein abundance changes between the *S. venezuelae* WT and Δ*cutRS* mutant.

PTMs are capable of radically altering the activity of a protein and as such we investigated whole cell proteome PTM changes, focussing on phosphorylations. Whilst currently limited to a small number of acid-stable phosphorylated residues the results revealed distinct changes to the *S. venezuelae* Δ*cutRS* phosphoproteome relative to WT. Many of these changes are in proteins linked to cell wall homeostasis and primary metabolism. The integrity of the cell wall is vital in maintaining an extracellular space environment conducive to protein folding, as discussed in **Chapter 4**. These PTM-altered proteins include the CE4 deacetylase Vnz_15460, the GlmM-like phosphoglucosamine mutase Vnz_21815 and the Acyl-CoA-ACP synthase / AMP ligase CmlK. Further investigation into the effects of the detected C-terminal phosphorylation of the chloramphenicol biosynthetic enzyme CmlK in the Δ*cutRS* mutant may increase our understanding of the observed chloramphenicol overproduction in *S. venezuelae* Δ*cutRS*.

The SK CutS, and in particular the extracellular sensor domain termed EcCutS, was also subject to investigation in this work. Using bioinformatics approaches, curious similarities were discovered between EcCutS and EcCssS. In comparison to other related SK sensor domains the amino acid composition of both these peptides was relatively unconserved between homologues from different species. However, both EcCutS and EcCssS contain two cysteine residues separated by a similar number of amino acids. These cysteines are fully conserved among streptomycete CutS homologues and the same is likely to be true for CssS but has yet to be confirmed. Cysteine residues contain highly reactive thiol groups and the presence of two cysteines is generally indicative of disulphide bond formation in mature proteins. Actinobacteria are unusual among Gram-positive bacteria in that they produce secreted proteins which require disulphide bond formation for correct folding outside the cell. In contrast to this, Firmicutes avoid any cysteines in their secreted proteins and cysteines are not present in the *B. subtilis* CssS homologue suggesting these residues are Actinobacteria-specific adaptions (Daniels *et al.*, 2010). We

propose these groups are vital in the detection of change to the redox state of the extracellular space of *Streptomyces* spp.

Finally, hexahistidine-tagged EcCutS was heterologously produced and purified with the presence of both monomeric and homodimeric complexes confirmed by native MS. The determination of SK activating ligands has lagged behind RR regulon research due to the technical difficulties involved working with membrane-bound proteins. The total number of unique SKs produced throughout *Streptomycetaceae* is difficult to determine accurately but would likely be in the hundreds, if not thousands. However, as discussed in **Chapter 6.3**, only a handful of ligands for these have been identified. Additionally, the methodologies used to determine these are variable and often not suitable for high-throughput screening. We describe the development of an SPR-based screening method using a commercially available chemical library to screen SK-ligand interactions in a highly scalable and reproducible manner which, importantly, requires very little sample. Using this method EcCutS was shown to interact with itaconic acid, likely through alkylation of the cysteine residues by nucleophilic addition, forming 2,3-dicarboxypropyl adducts. Future experiments including native MS and ITC will further characterise this interaction. We believe that, with iteration, this methodology could vastly improve detection of SK ligands and accelerate research in this area. It also has potential for use with other families of proteins having already successfully been used on an unrelated transcriptional activator and thus could replace DSF-based techniques.

There is still a considerable amount of work to be done to full characterise CutRS in *S. venezeulae* let alone throughout *Streptomycetaceae.* The conserved binding site is still unclear and whilst we have proposed mechanisms of signal detection these are mainly based upon bioinformatic and *in silico* research and inference from downstream proteomics data. The TMT-proteomics and phosphoproteomics are both incredibly powerful techniques but the hypothesises built upon their results in this work are unsubstantial without further work. Whilst the new SPR methodology shows promise it was inconclusive and would be unable to detect changes in cysteine-bond structural changes although the itaconic acid response may give us some clues to work off.

7.2. Proposed model of CutRS activation in *Streptomyces* spp.

From the work presented in this thesis, and with historical knowledge of TCSs, we can begin to build a hypothetical model of CutRS activity in *Streptomyces* spp**. Figure 7.1** depicts this model. *Streptomyces* spp. secrete unfolded proteins into the extracellular space, which require chaperones to help them fold. These chaperones include enzymes such as DsbA, which catalyses the correct formation of disulphide bonds, a process complicated by the lack of periplasm and the presence of the thick negatively charged peptidoglycan cell wall. Under normal, oxidising conditions the intramolecular disulphide bonds of the CutS remain formed and the CutRS system is inactive. However, changes in the redox state of the extracellular space could prevent the correct folding of secreted proteins and subject the cell to secretion stress. Thus, it is vital the cell can detect and respond to redox stress and CutRS plays a pivotal role in this. CutS detects incorrect protein folding conditions through reduction of the cysteine sulfhydryl groups and the subsequent breakage of its extracellular intramolecular disulphide bond(s), resulting in a conformational change and autophosphorylation of the cytosolic DHp domain. Subsequently this phosphate group is transferred to the partner RR, CutR, inducing homodimerization and DNA-binding. CutR activates transcription of *htrA3* and represses the expression of *htrB.* It also appears to modulate the expression of species-specific CutR target genes. Together this response counteracts secretion stress and restores homeostasis. To this end the HtrA-like serine protease HtrA3 degrades the accumulated misfolded protein in the extracellular space allowing for recycling of amino acids to occur. Meanwhile HtrA3 also acts as a chaperone, aiding the successful folding of newly synthesised secreted proteins. Accessory proteins, such as the cell wall amidase Vnz_08815, alter the cell to remove the source of the stress and restore homeostasis.

CssRS appears to be related to CutRS in both biochemical structure and function, being involved in the detection of secretion stress and containing a similar dual cysteine motif in its extracellular sensor domain. In this model CssS detects secretion stress caused by the accumulation of misfolded protein. In this there is an important distinction between CssRS and CutRS. We hypothesize that CutRS detects conditions conducive to protein folding, whilst CssRS detects unconducive conditions but using

a similar biochemical sensor: the dual cysteines. Activation of CssRS can be induced through the loss of HtrA3 activity resulting in the expression of *htrB*, *htrA1* and *htrA2* which degrade misfolded protein in the extracellular space. Ultimately both CutRS and CssRS respond to changes in the extracellular space which would otherwise impede the successful folding of secreted proteins.

This page is blank

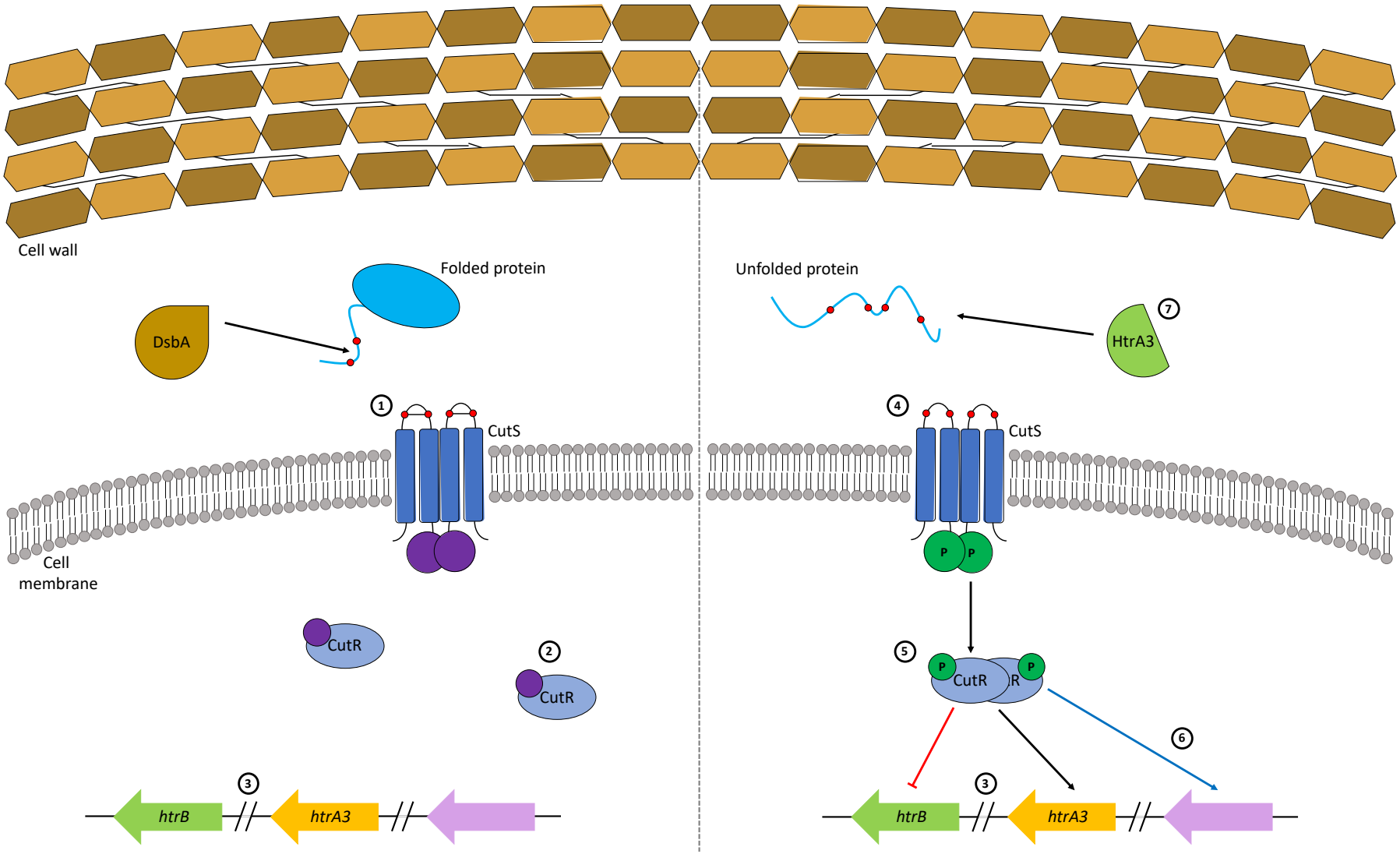
Cell wall
Folded protein
DsbA
Unfolded protein
HtrA3
7
1
CutS
4
CutS
Cell
membrane
P
P
CutR
2
CutR
5
P
CutR
R
P
6
3
htrB
htrA3
3
htrB
htrA3

Figure 7.1. A schematic representation of the CutRS model of activity in *Streptomyces* spp. **1.** Under normal conditions secreted protein folding occurs conventionally. Enzymes including DsbA catalyse the formation of disulphide bonds within folding proteins in the extracellular space of the cell. Under these conditions the extracellular domain of the homodimeric sensor kinase CutS (EcCutS) contains intramolecular disulphide bonds. Whilst these bonds remain formed, the SK remains inactive. **2.** With its partner SK inactive the response regulator CutR remains unphosphorylated and subsequently in its monomeric form. **3.** Members of the CutR regulon, including the two genes encoding for HtrA-like serine proteins *htrA3* and *htrB*, are not affected by CutR regulation and cellular processes continue undisturbed. **4.** Conditions detrimental to extracellular protein folding, such as an imbalanced redox state, cause secretion stress due to the accumulation of misfolded protein and impairment to homeostasis. Under these conditions the disulphide bonds within EcCutS break or are not able to fold in the first place. This causes a conformational change in CutS resulting in autophosphorylation of the DHp domain. **5.** Subsequent transfer of this phosphate group to CutR results in activation and homodimerization of the RR. CutR activates the expression of *htrA3* whilst repressing the transcription of *htrB*. **6.** A subset of the CutR regulon is specialised to each *Streptomyces* spp. with the response effected by these genes adapted to the specific metabolic and developmental bias of each strain. In *S. venezuelae* this would include the putative cell wall hydrolase *vnz_08815* and the sugar-responsive divergent operon *vnz_33985/990/995*. In *S. coelicolor* this includes a series of membrane and secreted proteins-encoding genes and *SCO4295* which encodes for the cold shock protein. **7.** The response effected by the expression of these proteins counteracts the secretion stress with HtrA3 degrading misfolded protein and acting as a chaperone to aid in the successful folding of newly synthesised and secreted proteins. Meanwhile other proteins, such as Vnz_08815, alter the cell to remove the source of the stress, return homeostasis and restore normal cellular functioning.

7.3. Future work and potential applications of CutRS manipulation

The work presented in this thesis dramatically improves our understanding of the CutRS TCS in *Streptomyces* spp. at both a colony and molecular level. There is, however, key areas of this work that remain incomplete and other areas that are worthy of further investigation. Many of these follow up experiments have been described in the relevant preceding chapters but key questions and strategies to answer them will be outlined below.

Streptomyces exploration is a fascinating discovery and fundamentally changes our understanding of the life cycle these spore-forming filamentous bacteria undergo. Our work corroborates findings by other groups investigating exploration, especially in regard to carbon source hierarchy and colony development. How the disruption of *cutRS* in *S. venezuelae* leads to exploration on YPD agar is still not fully understood. Clearly it is the result of glucose depletion in the growth medium but how this is linked to secretion stress requires further investigation. Does the uncontrolled glucose uptake result in rapid colony growth, or vice versa, and why would this seemingly beneficial phenotype be repressed under regular conditions? Detailed mapping of the primary metabolome using LC-MS could help us understand the change in carbon catabolism and which bottlenecks are changing driving the glucose uptake.

The potential identification of CutR-RR heterodimers from the Co-IP results presented in **Chapter 4.2** is not completely novel, but to our knowledge represents the first instance of "typical" RRs forming such interactions. Similar Co-IP experiments in *S. coelicolor* would reveal whether the CutR-EsrR/CseB interactions are a common occurrence or unique to *S. venezuelae.* RRs prove relatively easy to express and purify in heterologous hosts. To confirm and characterise the interactions between CutR and other RRs these target proteins must be purified and subjugated to SPR and ITC experimentation. The same could be performed with other proteins identified through Co-IP, including PspA and RNase E/G which may reveal a novel form of direct RR-protein regulation.

Our data suggests that the conserved CutR targets are *htrB* and *htrA3* and, whilst identified as serine proteases, little is known about their cellular targets or roles. One way to investigate this would be to create fusion constructs to produce 3xFLAG-tagged HtrB and HtrA3 within *S. venezuelae* and *S. coelicolor*. Co-IP could then be performed to identify potential targets of these proteases whilst *in vitro* enzymatic assays could be used to determine if they act to degrade or assist in the folding of the targets. Deletion of multiple HtrA-like serine proteases within a single strain might inform of any redundancy with *S. venezuelae* also encoding *htrA1* and *htrA2* in addition to *htrB* and *htrA3*. This may also help us understand why streptomycetes produce two TCSs, CutRS and CssRS, which appear to carry out similar functions and regulate similar genes in a, potentially, hierarchical manner.

One of the most challenging problems faced in TCS research is the identification of active TCS components. It is possible to deduce the phosphorylation state of proteins *in vitro* using techniques such as Pro-Q Diamond, Quercetin staining (Wang *et al.*, 2014) or native MS. Mutagenesis to create phosphomimetic or non-phosphorylatable version of TCS RRs has also been achieved (Rapun-Araiz *et al.*, 2020) but, in our practical experience, is not possible with some RRs, even canonical RRs. An ideal scenario would be to identify the phosphorylation state of both the SK and RR *in vivo* under conditions with and without the putative activating signal. It is now possible to identify the phosphorylation state of noncanonical amino acids including histidine and aspartate, the key residues of SK and RR signal transduction, through strong anion exchange (Hardman *et al.*, 2019). Repetition of the TMT phosphoproteomics using this new methodology should allow us to determine which conditions CutRS is active under, and at which developmental stages. It is also generally assumed that dimerisation of RRs requires phosphorylation. Using the data gained from this new phosphoproteomics it would be possible to determine which RRs are phosphorylated and thus possible partners for CutR-RR heterodimerisation. Detecting phosphorylated EsrR/CseB would add credence to the possibility of interaction with CutR, as discussed previously.

The most pressing question relating to CutS is to determine the role of the two cysteine residues in the extracellular sensor domain. Mutagenesis of these residues

and subsequent phenotypic screening would give an insight into the essentiality of these residues for signal detection. If this resulted in complementation of the Δ*cutRS* phenotype it could be concluded that these residues were indeed essential for signal detection however further experiments would be required. To confirm the altered CutS was still localising to the membrane the protein would be tagged, and subcellular localisation determine with immunoblotting. Alternatively, polyclonal antibodies could be raised if it was not possible to tag CutS without disrupting function or localisation. Previously the full length *Rhodobacter sphaeroides* SK RegB was purified using a C-terminal hexahistidine tag (Potter *et al.*, 2002) whilst the *E. coli* SKs TorS and EvgS were demonstrated to be functionally active fused with C-terminal mYFP tags (Sommer *et al.*, 2013). This suggests that a C-terminal tag to determine subcellular localisation should not disrupt SK activity and would be an ideal method to use with CutS. This work would likely also work for CssS, and the same experiments could be performed with CssS to better characterise these unusual dual cysteine-containing SKs.

Finally, in regard to SPR SK-ligand screening method development. The next step would be to repeat the process with the sensory domains of TCSs with known ligands, e.g., GluK and VanS. The Biolog plate PM01 contains glutamate and PM12B (not used in the original study) contains vancomycin which would be positive controls for the screening method. Further confirmation of hits would be achieved using SPR kinetics analysis and ITC as a secondary methodology for interaction detection. The ideal final step would be to co-crystalise the identified ligand with the sensory domain and, using X-ray crystallography, generate a structure.

This work, and work on TCS in general, has the potential for broader applications beyond furthering our understanding of complex regulatory systems. These are more ambitious and conceptual; presented below to raise discussion on possible future directions for TCS research.

Deletion of the *cutRS* operon in both *S. venezuelae* and *S. coelicolor* has led to the overproduction of specialised metabolites. Neither chloramphenicol or ACT are of significant interest having been studied for decades and whilst chloramphenicol is

used clinically, it is mass produced synthetically. However, the ability to induce specialised metabolite production in any strain would be a powerful tool in the search for new antibiotics and, given that CutRS is conserved among all streptomycetes, could form the basis of a universal screening strategy. If a conserved genomic region of *cutR* or *cutS* was identified, distinct from the sequences of other TCSs, this could be targeted by a double-strand break (DSB) free editing system such as CRISPR-BEST (Tong *et al.*, 2019). These systems create a single C:G-T:A or T:A-C:G substitution targeted by a sgRNA and, unlike the pCRISPomyces-2 system used in this work, do not require large editing templates for homologous recombination (Cobb, Wang and Zhao, 2015; Tong *et al.*, 2019). Using this system, it would be possible to create a single construct which scarlessly disrupts *cutRS* expression in any streptomycete with the only limitation being the ability of the strain to accept and maintain the plasmid. Large scale bioactivity screening of *cutRS*-disrupted *Streptomyces* spp. linked to metabolomic profiling could expand our chemical libraries and aid in antibiotic discovery from new, and historical, strains.

In the same vein we have managed to significantly increase the biomass of *S. venezuelae* by 20-fold through the deletion of Δ*cutRS* and supplementation of glucose on a few common streptomycete growth media. At the same time rather than reducing specialised metabolism, it actually increases. In the development of industrial strains this would be considered a huge success, increasing biomass and production of a desired compound with the addition of a cheap and readily available carbon source often takes multiple rounds of mutagenesis and years of iterative research. This stems from increasing carbon uptake whilst maintaining a steady stream of metabolites through to specialised metabolism, a balance often difficult to achieve as often growth and primary metabolism will be prioritised by the organism through CCR. If the benefits gained here could be understood and reconstituted in strains of industrial interest, and under fermentation conditions, it could aid in the efficient production of streptomycete specialised metabolites impossible to express in a more amenable heterologous host.

The development of new molecular switches and regulatory systems is a cornerstone of the emerging discipline of synthetic biology. Likewise, such systems are in constant

demand for use in gene expression and the activation of silent genes, including the expression of BGCs in heterologous hosts. However such tools are relatively scare for use in *Streptomyces* spp. (Prudence *et al.*, 2020). There is huge potential in the development of TCSs for use as inducible switches with progress being made including the repurposing of the light-switchable CcaSR in *E. coli* (Schmidl *et al.*, 2014). It has been demonstrated that due to their modular nature TCSs can rewired; replacing the sensor domains of SKs and the DBDs of RRs to create chimeric TCSs with specific functions (Schmidl *et al.*, 2019). One major limitation is the lack of confirmed activating signals however methodologies such as our SPR-based screening system described in **Chapter 6.3** will aid in uncovering these signals. Further potential lies in possibility of RR heterodimerisation. With a small pool of fully characterised TCS capable of forming both RR homo- and hetero-dimers you can generate exponentially more complex responses. As demonstrated in **Figure 7.2** it is also possible to create the seven basic logic gates modern electronics relies upon using just two TCSs capable of heterodimerisation.

The benefits of using TCSs as biological switches extend beyond their modular nature. With the SK being extracellular facing you increase the range of ligands, not restricted by those capable of crossing the cell membrane or those produced through cellular metabolism. Bacteria have already been shown capable of encoding tens of TCS at a single time reducing the probability such switches would prove toxic. In a more practical aspect regarding vector creation the genes encoding TCSs are well-defined operons allowing for simple cloning whilst the RR DNA-binding sequence is longer than many regulators due to the dimeric nature and this reduces the chance of off-target effects through random consensus sequence occurrence.

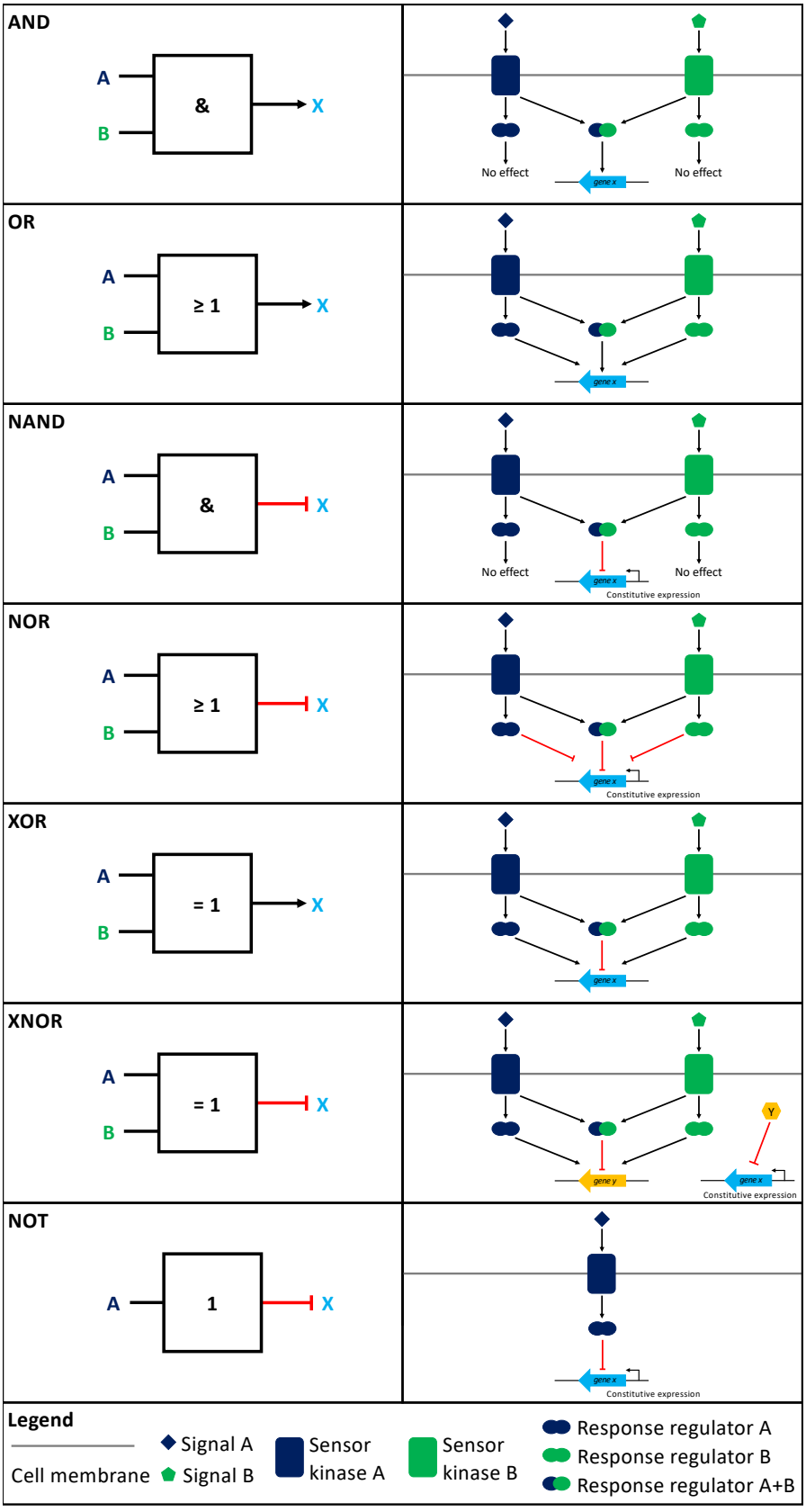

Figure 7.2. Diagrammatic depiction of the seven electronic logic gates and *in vivo* reconstitution using two two-component systems capable of forming both homo- and hetero- response regulator dimers.

7.4. Final conclusions

Streptomyces spp. are a genus of bacteria with the propensity to produce specialised metabolites with applications in the treatment of human disease. Biosynthesis of these compounds is intricately linked to the complex spore-based lifecycle of these filamentous Actinobacteria and response to a diverse array of signals we are currently unable to identify or replicate under laboratory conditions. Despite having the capacity to produce a plethora of novel compounds our understanding of this lifecycle and signal response must improve in order to discover, purify and develop new antibiotics. The work presented in this thesis describes the highly conserved CutRS two-component system which is involved in the secretion stress response, linking primary and specialised metabolism with development, including *Streptomyces* exploration. In *S. venezuelae* and *S. coelicolor* we have begun to characterise the role of CutRS at both the colony and molecular level, described the CutR regulon and theorised on the biochemical aspects of CutS signal detection. Our data suggest that CutR regulates the expression of *htrB* and *htrA3* which encode HtrA-like serine proteases, along with species specific genes, to counter the accumulation of misfolded protein in the extracellular space and / or cell envelope of these bacteria. Signal detection is possibly achieved through the disruption of intramolecular disulphide bonds in a potentially novel extracellular sensory system which contains two fully conserved extracellular cysteine residues.

TCS are complex and our work, and that of others, suggests there is cross-TCS communication and the possibility of RR heterodimerization, convoluting the cellular response to certain signals. Additionally, our work highlights the possibility of regulation through RR-protein interactions, further increasing the potential of these systems. We propose a series of future experiments to continue the work presented in this thesis and speculate on potential applications for the knowledge gained from this system. Increasing our understanding of TCS in *Streptomyces* spp. may prove invaluable in the search for new antimicrobial compounds. Manipulation of the signals these bacteria receive could imitate growth conditions we are unable to generate in the laboratory setting, creating stressors which disrupt development and induce the production of specialised metabolites. At first this may be achieved simply

through the deletion and disruption of TCS operons, or individual SK/RR genes, but could progress to the creation of chimeric or novel TCSs designed to trick strains into the biosynthesis of novel antibiotics. In a time where researchers are desperately searching for an answer to antimicrobial resistance deception may be the solution.

In my opinion, TCS are chronically underappreciated tools with the potential to dramatically accelerate antibiotic discovery and my hope is the work presented in this thesis will contribute to the global knowledge base used to tackle antimicrobial resistance, one of the greatest threats faced by modern humanity.

Chapter 8. Appendix

Table 8.1. Strains used and generated during this thesis.

Strain	Description	Plasmid	Resistance	Source/Reference
E. coli				
Top10	F– *mcr*A Δ(*mrr-hsd*RMS-*mcr*BC) Φ80*lac*ZΔM15 Δ*lac*X74 *rec*A1 *ara*D139 Δ(*ara leu*) 7697 *gal*U *gal*K *rps*L (StrR) *end*A1 *nup*G			Invitrogen™
ET12567	*dam*$^{-}$ *dcm*$^{-}$ *hsdS*$^{-}$	pUZ8002	Cml^{R}, Tet^{R}	(MacNeil *et al.*, 1992)
BL21	*fhuA2 [lon] ompT gal (λ DE3) [dcm] ΔhsdSλ DE3 = λ sBamHIo ΔEcoRI-B int::(lacI::PlacUV5::T7 gene1) i21 Δnin5*			(Studier and Moffatt, 1986)
ECO001-003	BL21 6XHIS *vnz_cutR*	pTCM015, pLysS	Kan^{R}, Cml^{R}	This work
ECO004-006	BL21 6XHIS *vnz_Ec_cutS*	pTCM016	Kan^{R}	This work
Bioassay strains				
E. coli	Wild-type			Lab stock

C. albicans	Clinical isolate			Gift from Neil Gow, University of Exeter
B. subtilis	Wild-type strain 168			Gift from Nicola Stanley Wall, University of Dundee
B. subtilis	JH642 - *trpc2 pheA1 amyE::gfp-cm*		Cml^R	(Stanley *et al.*, 2003)
S. venezuelae				
NRRL B-65442	*S. venezuelae* wild-type strain			(Bush *et al.*, 2019)
M1702	*S. venezuelae* Δ*JAD* Δ*CHL*			Gift from Neil Holmes, JIC, Unpublished
S. venezuelae Δ*cutRS*	*vnz_cutRS::apr oriT*		Apr^R	This work, MM Al-Bassam
VNZ001-003	*S. venezuelae*	pSS170	Hyg^R	This work
VNZ004-006	*S. venezuelae*	pIJ10257	Hyg^R	This work
VNZ007-009	*S. venezuelae*	pMF96	Hyg^R	This work
VNZ010-012	*S. venezuelae ΦBT1 vnz_cutRSp vnz_cutRS*	pTCM001	Hyg^R	This work
VNZ013-015	*S. venezuelae ΦBT1 ermE*p vnz_cutRS*	pTCM002	Hyg^R	This work

VNZ016-018	*S. venezuelae ΦBT1 ermE*p sco_cutRS*	pTCM003	Hyg^R	This work
VNZ019-021	*S. venezuelae ΦBT1 ermE*p KY5_cutRS*	pTCM004	Hyg^R	This work
VNZ022-024	*S. venezuelae ΦBT1 ermE*p vnz_08815*	pTCM005	Hyg^R	This work
VNZ025-027	*S. venezuelae ΦBT1 ermE*p sco_18430*	pTCM006	Hyg^R	This work
VNZ028-030	*S. venezuelae ΦBT1 vnz_cutRSp* GUS	PTCM009	Hyg^R	This work
VNZ031-033	*S. venezuelae ΦBT1 vnz_08815p* GUS	PTCM010	Hyg^R	This work
VNZ034-036	*S. venezuelae ΦBT1 vnz_18430p* GUS	PTCM011	Hyg^R	This work
VNZ037-039	*S. venezuelae ΦBT1 vnz_cutRSp vnz_cutRS cutS_DEL*	PTCM017	Hyg^R	This work
VNZ040-042	*S. venezuelae vnz_cutRS::apr oriT*	pSS170	Apr^R, Hyg^R	This work
VNZ043-045	*S. venezuelae vnz_cutRS::apr oriT*	pIJ10257	Apr^R, Hyg^R	This work
VNZ046-048	*S. venezuelae vnz_cutRS::apr oriT*	pMF96	Apr^R, Hyg^R	This work
VNZ049-051	*S. venezuelae vnz_cutRS::apr oriT ΦBT1 vnz_cutRSp vnz_cutRS*	pTCM001	Apr^R, Hyg^R	This work
VNZ052-054	*S. venezuelae vnz_cutRS::apr oriT ΦBT1 ermE*p vnz_cutRS*	pTCM002	Apr^R, Hyg^R	This work
VNZ055-057	*S. venezuelae vnz_cutRS::apr oriT ΦBT1 ermE*p sco_cutRS*	pTCM003	Apr^R, Hyg^R	This work

VNZ058-060	*S. venezuelae vnz_cutRS::apr oriT ΦBT1 ermE*p KY5_cutRS*	pTCM004	Apr^R, Hyg^R	This work
VNZ061-063	*S. venezuelae vnz_cutRS::apr oriT ΦBT1 ermE*p vnz_08815*	pTCM005	Apr^R, Hyg^R	This work
VNZ064-066	*S. venezuelae vnz_cutRS::apr oriT ΦBT1 ermE*p sco_18430*	pTCM006	Apr^R, Hyg^R	This work
VNZ067-069	*S. venezuelae vnz_cutRS::apr oriT ΦBT1 vnz_cutRSp vnz_cutRS 3xFLAG*	pTCM008	Apr^R, Hyg^R	This work
VNZ070-072	*S. venezuelae vnz_cutRS::apr oriT ΦBT1 vnz_cutRSp* GUS	PTCM009	Apr^R, Hyg^R	This work
VNZ073-074	*S. venezuelae vnz_cutRS::apr oriT ΦBT1 vnz_08815p* GUS	PTCM010	Apr^R, Hyg^R	This work
VNZ076-078	*S. venezuelae vnz_cutRS::apr oriT ΦBT1 vnz_18430p* GUS	PTCM011	Apr^R, Hyg^R	This work
VNZ079-081	*S. venezuelae vnz_cutRS::apr oriT ΦBT1 vnz_cutRSp vnz_cutRS cutS_DEL*	PTCM017	Apr^R, Hyg^R	This work
VNZ082-084	*S. venezuelae ΔJAD ΔCHL vnz_cutRS::apr oriT*		Apr^R	This work
VNZ085-087	*S. venezuelae Δvnz_08815*			This work
VNZ088-090	*S. venezuelae Δvnz_18430*			This work
VNZ091-093	*S. venezuelae Δvnz_08815 Δvnz_18430*			This work
VNZ094-096	*S. venezuelae Δvnz_08815 vnz_cutRS::apr oriT*		Apr^R	This work
VNZ097-099	*S. venezuelae Δvnz_18430 vnz_cutRS::apr oriT*		Apr^R	This work

VNZ100-102	*S. venezuelae* Δ*vnz_08815 ΦBT1 ermE*p vnz_08815*	pTCM005	Hyg^R	This work
VNZ103-105	*S. venezuelae* Δ*vnz_18430 ΦBT1 ermE*p vnz_08815*	pTCM005	Hyg^R	This work
VNZ106-108	*S. venezuelae* Δ*vnz_08815 ΦBT1 ermE*p vnz_18430*	pTCM006	Hyg^R	This work
VNZ109-111	*S. venezuelae* Δ*vnz_18430 ΦBT1 ermE*p vnz_18430*	pTCM006	Hyg^R	This work
S. coelicolor				
M145	*S. coelicolor* wild-type strain, SCP1-, SCP2-			(Kieser *et al.*, 2000)
SCO001-003	*S. coelicolor* Δ*cutRS*			This work
SCO004-006	*S. coelicolor* Δ*cutRS*	pSS170	Hyg^R	This work
SCO007-009	*S. coelicolor* Δ*cutRS*	pIJ10257	Hyg^R	This work
SCO010-012	*S. coelicolor* Δ*cutRS ΦBT1 ermE*p sco_cutRS*	pTCM003	Hyg^R	This work
SCO013-015	*S. coelicolor* Δ*cutRS ΦBT1 ermE*p vnz_cutRS*	pTCM002	Hyg^R	This work
SCO016-018	*S. coelicolor* Δ*cutRS ΦBT1 ermE*p KY5_cutRS*	pTCM004	Hyg^R	This work
SCO019-021	*S. coelicolor* Δ*cutRS ΦBT1 vnz_cutRSp vnz_cutRS*	pTCM001	Hyg^R	This work
SCO022-024	*S. coelicolor* Δ*cutRS ΦBT1 sco_cutRSp sco_cutRS 3xFLAG*	pTCM007	Hyg^R	This work

SCO025-027	*S. coelicolor* Δ*cutRS ΦBT1 vnz_cutRSp vnz_cutRS 3xFLAG*	pTCM008	Hyg^R	This work
SCO028-030	*S. coelicolor*	pSS170	Hyg^R	This work
SCO031-033	*S. coelicolor*	pIJ10257	Hyg^R	This work
SCO034-036	*S. coelicolor ΦBT1 ermE*p sco_cutRS*	pTCM003	Hyg^R	This work
SCO037-039	*S. coelicolor ΦBT1 ermE*p vnz_cutRS*	pTCM002	Hyg^R	This work
SCO040-042	*S. coelicolor ΦBT1 ermE*p KY5_cutRS*	pTCM004	Hyg^R	This work
SCO043-045	*S. coelicolor ΦBT1 vnz_cutRSp vnz_cutRS*	pTCM001	Hyg^R	This work
***S. formicae* KY5**				
Wild-type	*S. formicae* KY5 wild-type strain			Lab stock

Table 8.2. Plasmids used and generated during this thesis.

Plasmid	Description	Resistance	Reference
pSS170	*oriT*, ΦBT1 *attB-int*, *hyg*^{R},	Hyg^{R}	Gift from Susan Schlimpert, JIC.
pIJ10257	*oriT*, ΦBT1 *attB-int, hyg*^{R}, *ermEp**	Hyg^{R}	(Hong *et al.*, 2005)
pET28a	pBR322 origin and fI origin, *Km*^{R}, expression vector	Kan^{R}	Novagen®
pMF96	*ΦBT1 attB-int, hyg*^{R}*, uidA CDS*	Hyg^{R}	(Feeney *et al.*, 2017)
pCRISPomyces-2	*Apr*^{R}*, oriT, rep*$^{pSG5(ts)}$*, ori*^{ColE1}*, sSpcas9,* synthetic guide RNA cassette	Apr^{R}	(Cobb, Wang and Zhao, 2015)
St1Δ*cutRS*	Supercos-1-cosmid containing *vnz_cutRS::apr oriT* with flanking DNA	Kan^{R}, Amp^{R}, Apr^{R}	This work, MM Al-Bassam
pTCM001	pSS170 *vnz_cutRSp vnz_cutRS*	Hyg^{R}	This work, Genewiz®
pTCM002	pIJ10257 *vnz_cutRS*	Hyg^{R}	This work

pTCM003	pIJ10257 sco_*cutRS*	Hyg^R	This work
pTCM004	pIJ10257 *KY5_cutRS*	Hyg^R	This work
pTCM005	pIJ10257 *vnz_08815*	Hyg^R	This work
pTCM006	pIJ10257 *vnz_18430*	Hyg^R	This work, Genewiz®
pTCM007	pSS170 *sco_cutRSp sco_cutRS 3xFLAG*	Hyg^R	This work, Genewiz®
pTCM008	pSS170 *vnz_cutRSp vnz_cutRS 3xFLAG*	Hyg^R	This work, Genewiz®
pTCM009	pMF96 *vnz_cutRSp* GUS	Hyg^R	This work
pTCM010	pMF96 *vnz_08815p* GUS	Hyg^R	This work
pTCM011	pMF96 *vnz_18430p* GUS	Hyg^R	This work
pTCM012	pCRISPomyces-2 *vnz_18430* flanking DNA and gRNA	Apr^R	This work

pTCM013	pCRISPomyces-2 *vnz_08815* flanking DNA and gRNA	Apr^R	This work
pTCM014	pCRISPomyces-2 *sco_cutRS* flanking DNA and gRNA	Apr^R	This work
pTCM015	pET28a 6xHIS *vnz_cutR*	Kan^R	This work
pTCM016	pET28a 6xHIS *vnz_Ec_cutS*	Kan^R	This work
pTCM017	*pSS170 vnz_cutRSp vnz_cutRS cutS_DEL*	Hyg^R	This work

Table 8.3. Primers used and generated during this thesis.

Name	Description	Sequence
pSS170 Test F	pSS170 Seq F	GGTCTGACGCTCAGTGGAAC
pSS170 Test R	pSS170 Seq R	GCTCAGTATCACCGCCAGTG
pIJ10257 Test F	pIJ10257 Test MCS F	GATCTTGACGGCTGGCGAGAG
pIJ10257 Test R	pIJ10257 Test MCS R	GCGTCAGCATATCATCAGCGAGC
pMF96 Test F	pMF96 Test MCS F	GCTCAATCAATCACCGGATCC
pMF96 Test R	pMF96 Test MCS R	CATGTCCGTACCTCCGTTG
pET28a Test F	pET28a Test MCS F	GGAATTGTGAGCGGATAACAATTCC
pET28a Test R	pET28a Test MCS R	GCTTTGTTAGCAGCCGGATC
pCRISP Test F	pCRISP2 Test XbaI site F	AGGCTAGTCCGTTATCAACTTGAAA
pCRISP Test R	pCRISP2 Test XbaI site R	TCGCCACCTCTGACTTGAGCGTCGA
Spacer Test	pCRISP2 Test BbsI site F	ATACGGCTGCCAGATAAGGC
TCM001	*vnz_cutRSp vnz_cutRS* F1	gagaga*cctagg*GTGCAGGTCTTCCAGCTCCGC
TCM002	*vnz_cutRSp vnz_cutRS* R1	ctctct*aagctt*TCAGATCGGCAGAGTGACGCG
TCM003	*vnz_cutS* F1	ggaatt*catATG*GCCACCACCCCAGCG

TCM004	*vnz_cutS* R1	cacaca*aagctt*TCAGATCGGCAGAGTGACGC
TCM005	*vnz_cutS* Seq F1	cacggacccgttcacgaacg
TCM006	*vnz_Ec_cutS* F1	ggaatt*catatg*ACCGCGCAGGCGCTCAG
TCM007	*vnz_Ec_cutS* R1	cacaca*aagctt*tcaGAGCGAACGGCGCAGGAG
TCM008	*vnz_cutRS cutS* deletion GF1	agctgcccttcaaggtcgtcaacggcacggtcgtcacgctctgcctgcgg
TCM009	*vnz_cutRS cutS* deletion GR1	cggtcgctctggtgccgcaggcagagcgtgacgaccgtgccgttgacgac
TCM010	*vnz_cutRSp* F1B	ggaattc*catatg*GTGGGGACGGGTCAGAC
TCM011	*vnz_cutRSp* R1B	cacaca*ctcgag*GTCGTACATCCTTCCCGTTGAG
TCM012	*vnz_08815p* F1	gagaga*catatg*ACGCATCGGCAACTCCTGG
TCM013	*vnz_08815p* R1	ctctct*ctcgag*GAAGGCGAGCTCCTTCTTCCTC
TCM014	*vnz_18430p* F1	gagaga*catatg*GGCGTCATGGTGCCATTGG
TCM015	*vnz_18430p* R1	ctctct*ctcgag*AGCTCGCTCTCCTCGTTGAC
TCM016	*vnz_08815* deletion F1B	ctcggttgccgccgggcgttttttta*tctaga*GAGATCGACGCCGCGAAGG
TCM017	*vnz_08815* deletion R1B	AGCCGGCGATGCGGACGCCGAACTGGAACGCCACGAAGGCGAGCTCCTTC
TCM018	*vnz_08815* deletion F2	GCTCTGAGGAAGAAGGAGCTCGCCTTCGTGGCGTTCCAGTTCGGCGTCCG
TCM019	*vnz_08815* deletion R2	cggccttttacggttcctggc*ctctaga*GGTACGACCAGACCATCAGGC

TCM020	*vnz_08815* gRNA F	acgcGACCTCGTCTATCGAGGGCT
TCM021	*vnz_08815* gRNA R	aaacAGCCCTCGATAGACGAGGTC
TCM022	*vnz_08815* deletion Seq F	GCCTTATGCCCGAATTCTGG
TCM023	*vnz_08815* deletion Test F	GGAAGCGGAATCGCTTCACC
TCM024	*vnz_08815* deletion Test R	GTCGGACACACAAAGTGACGC
TCM025	*vnz_08815* GF1	aactagagtcgacctgcatagatct*aagctt*GTGGCGTCCCACCGTCGAC
TCM026	*vnz_08815* GR1	tctccgctcatgagaacctaggatcc*aagctt*TCAGCCGGCGATGCGGAC
TCM027	*vnz_18430* deletion F1B	ctcggttgccgccgggcgtttttta*tctaga*CCTGCTTGGGACGGTTGGT
TCM028	*vnz_18430* deletion R1B	CAGCCTAGCCGGTCAGCTGTCGCCGGTGCCGTTCTCGGTGCTCACAGCTC
TCM029	*vnz_18430* deletion F2	ACGAGGAGAGCGAGCTGTGAGCACCGAGAACGGCACCGGCGACAGCTGAC
TCM030	*vnz_18430* deletion R2	acgcggccttttacggttcctggcc*tctaga*CGGTAGCAGGAGGCCAGC
TCM031	*vnz_18430* deletion Seq F	TAGACATCCTGGCCCTCCTA
TCM032	*vnz_18430* deletion Test F	GCAGGTCGGAAGACTCAGTCG
TCM033	*vnz_18430* deletion Test R	GCCTCGACGGTTTTCAAGACC
TCM034	*vnz_18430* gRNA F2	acgcGTGCGCCTGAGAGTGGGGCT
TCM035	*vnz_18430* gRNA R2	aaacAGCCCCACTCTCAGGCGCAC

TCM036	*sco_cutRS* GF1	actagagtcgacctgcatagatct*aagctt*AAAATCTCGCATTCCCGCTC
TCM037	*sco_cutRS* GR1	tccgctcatgagaacctaggatcc*aagctt*GTGAGATGTCGGGGTCATGA
TCM038	*sco_cutRS ermE*p* Seq F	GCAAGATCGTCGAACTGGG
TCM039	*sco_cutRS ermE*p* Seq R	GCTCGCTGCGTTCGTTGG
TCM040	*sco_cutRS* deletion F1B	tcggttgccgccgggcgtttttttatctagaGACGGACTTCGGAGCGTAGG
TCM041	*sco_cutRS* deletion F2	AGGACAAGCGACGTGCGCGTACTCGTCGTCGGGCTCGTGATGCGCGTGAC
TCM042	*sco_cutRS* deletion R1B	CAGACGGGGAGCGTCACGCGCATCACGAGCCCGACGACGAGTACGCGCAC
TCM043	*sco_cutRS* deletion R2	gcggccttttacggttcctggcctctagaCCAGGTCGATGATCCGGTCG
TCM044	*sco_cutRS* gRNA F	acgcCAGCGTGAGCCTTATCCGGA
TCM045	*sco_cutRS* gRNA R	aaacTCCGGATAAGGCTCACGCTG
TCM046	*sco_cutRS* deletion Seq F	AAAATCTCGCATTCCCGCTC
TCM047	*sco_cutRS* deletion Test F	CGTCTTCGAACCCCTCCAGC
TCM048	*sco_cutRS* deletion Test R	CGCTCAAAGCGAACATCCTCG
TCM049	*KY5_cutRS* F1	gagaga*cataTG*CGTGTACTCGTCGTCGAGG
TCM050	*KY5_cutRS* R1	ctctct*aagctt*TCAGAGGGGCAGGGTGACAC
TCM051	*S. venezuelae* Δ*cutRS* ReDIRECT Test F	GCCCAGCTCCACGATCTT

TCM052	*S. venezuelae* Δ*cutRS* ReDIRECT Test R	AGGAACTGGGCGCCTG
TCM101	ReDCaT *vnz_08815p* F1	ACGCATCGGCAACTCCTGGGCCTTATGCCCGAATTCTGGG
TCM102	ReDCaT *vnz_08815p* R1	CCCAGAATTCGGGCATAAGGCCCAGGAGTTGCCGATGCGTcctaccctacgtcctcctgc
TCM103	ReDCaT *vnz_08815p* F2	TGCCCGAATTCTGGGGGGCGCACCGTCAACTGCTCATCAC
TCM104	ReDCaT *vnz_08815p* R2	GTGATGAGCAGTTGACGGTGCGCCCCCCAGAATTCGGGCAcctaccctacgtcctcctgc
TCM105	ReDCaT *vnz_08815p* F3	TCAACTGCTCATCACTGCCCGTGCGGTGCGTGTAAATAAA
TCM106	ReDCaT *vnz_08815p* R3	TTTATTTACACGCACCGCACGGGCAGTGATGAGCAGTTGAcctaccctacgtcctcctgc
TCM107	ReDCaT *vnz_08815p* F4	GTGCGTGTAAATAAAGTGGTGCGTGCGCGATATTTTTGCC
TCM108	ReDCaT *vnz_08815p* R4	GGCAAAAATATCGCGCACGCACCACTTTATTTACACGCACcctaccctacgtcctcctgc
TCM109	ReDCaT *vnz_08815p* F5	CGCGATATTTTTGCCAGTGGGATTTGAACTGATCACAACT
TCM110	ReDCaT *vnz_08815p* R5	AGTTGTGATCAGTTCAAATCCCACTGGCAAAAATATCGCGcctaccctacgtcctcctgc
TCM111	ReDCaT *vnz_08815p* F6	GAACTGATCACAACTTGGTCACTAGGGTCGGGCTTCGAAC
TCM112	ReDCaT *vnz_08815p* R6	GTTCGAAGCCCGACCCTAGTGACCAAGTTGTGATCAGTTCcctaccctacgtcctcctgc
TCM113	ReDCaT *vnz_08815p* F7	GGTCGGGCTTCGAACCTTCGCGCGGTTGATCACCCATCCG
TCM114	ReDCaT *vnz_08815p* R7	CGGATGGGTGATCAACCGCGCGAAGGTTCGAAGCCCGACCcctaccctacgtcctcctgc
TCM115	ReDCaT *vnz_08815p* F8	TTGATCACCCATCCGGGGTGGCGGCGGAGGAACCGCCTGC

TCM116	ReDCaT *vnz_08815p* R8	GCAGGCGGTTCCTCCGCCGCCACCCCGGATGGGTGATCAAcctaccctacgtcctcctgc
TCM117	ReDCaT *vnz_08815p* F9	GGAGGAACCGCCTGCCCCTCACCGGATGGGCGGCTCTGAG
TCM118	ReDCaT *vnz_08815p* R9	CTCAGAGCCGCCCATCCGGTGAGGGGCAGGCGGTTCCTCCcctaccctacgtcctcctgc
TCM119	ReDCaT *vnz_08815p* F10	CACCGGATGGGCGGCTCTGAGGAAGAAGGAGCTCGCCTTC
TCM120	ReDCaT *vnz_08815p* R10	GAAGGCGAGCTCCTTCTTCCTCAGAGCCGCCCATCCGGTGcctaccctacgtcctcctgc
TCM121	ReDCaT *vnz_18430p* F1	GGCGTCATGGTGCCATTGGCGGGGTGGGGCGGGCACACCG
TCM122	ReDCaT *vnz_18430p* R1	CGGTGTGCCCGCCCCACCCCGCCAATGGCACCATGACGCCcctaccctacgtcctcctgc
TCM123	ReDCaT *vnz_18430p* F2	GGGGCGGGCACACCGGAAGGCGTCCGTTCTGTCCGTATAT
TCM124	ReDCaT *vnz_18430p* R2	ATATACGGACAGAACGGACGCCTTCCGGTGTGCCCGCCCCcctaccctacgtcctcctgc
TCM125	ReDCaT *vnz_18430p* F2.5	GAAGGCGTCCGTTCTGTCCGTATATAAAGGTGGGGGTGCG
TCM126	ReDCaT *vnz_18430p* R2.5	CGCACCCCCACCTTTATATACGGACAGAACGGACGCCTTCcctaccctacgtcctcctgc
TCM127	ReDCaT *vnz_18430p* F3	GTTCTGTCCGTATATAAAGGTGGGGGTGCGAACGCACAGC
TCM128	ReDCaT *vnz_18430p* R3	GCTGTGCGTTCGCACCCCCACCTTTATATACGGACAGAACcctaccctacgtcctcctgc
TCM129	ReDCaT *vnz_18430p* F3.5	TATATAAAGGTGGGGGTGCGAACGCACAGCTCCGCCTTAC
TCM130	ReDCaT *vnz_18430p* R3.5	GTAAGGCGGAGCTGTGCGTTCGCACCCCCACCTTTATATAcctaccctacgtcctcctgc
TCM131	ReDCaT *vnz_18430p* F4	GTGCGAACGCACAGCTCCGCCTTACAGCGGTCTGACGTCC

TCM132	ReDCaT *vnz_18430p* R4	GGACGTCAGACCGCTGTAAGGCGGAGCTGTGCGTTCGCACcctaccctacgtcctcctgc
TCM133	ReDCaT *vnz_18430p* F5	AGCGGTCTGACGTCCTGTGGGAAAAGCTTGTGCAGCACCC
TCM134	ReDCaT *vnz_18430p* R5	GGGTGCTGCACAAGCTTTTCCCACAGGACGTCAGACCGCTcctaccctacgtcctcctgc
TCM135	ReDCaT *vnz_18430p* F6	GCTTGTGCAGCACCCTGGAGCCAGGCAGGTGCCCCCGTAG
TCM136	ReDCaT *vnz_18430p* R6	CTACGGGGGCACCTGCCTGGCTCCAGGGTGCTGCACAAGCcctaccctacgtcctcctgc
TCM137	ReDCaT *vnz_18430p* F7	CAGGTGCCCCCGTAGGTACCACCACCCCGCGCAGTCAACG
TCM138	ReDCaT *vnz_18430p* R7	CGTTGACTGCGCGGGGTGGTGGTACCTACGGGGGCACCTGcctaccctacgtcctcctgc
TCM139	ReDCaT *vnz_18430p* F8	AGGTACCACCACCCCGCGCAGTCAACGAGGAGAGCGAGCT
TCM140	ReDCaT *vnz_18430p* R8	AGCTCGCTCTCCTCGTTGACTGCGCGGGGTGGTGGTACCTcctaccctacgtcctcctgc
TCM141	ReDCaT *vnz_cutRSp* F1	GGGACGGGTCAGACGCCCGGCGCGGCAACCTCCACGCCGT
TCM142	ReDCaT *vnz_cutRSp* R1	ACGGCGTGGAGGTTGCCGCGCCGGGCGTCTGACCCGTCCCcctaccctacgtcctcctgc
TCM143	ReDCaT *vnz_cutRSp* F2	CAACCTCCACGCCGTGCTCGGCGGCCAGTCGGTGCAGGTC
TCM144	ReDCaT *vnz_cutRSp* R2	GACCTGCACCGACTGGCCGCCGAGCACGGCGTGGAGGTTGcctaccctacgtcctcctgc
TCM145	ReDCaT *vnz_cutRSp* F3	CAGTCGGTGCAGGTCTTCCAGCTCCGCCTGCTCGACCTCC
TCM146	ReDCaT *vnz_cutRSp* R3	GGAGGTCGAGCAGGCGGAGCTGGAAGACCTGCACCGACTGcctaccctacgtcctcctgc
TCM147	ReDCaT *vnz_cutRSp* F4	GCCTGCTCGACCTCCGCCAGGTAGTCGTCGCCCGTCTCAC

TCM148	ReDCaT *vnz_cutRSp* R4	GTGAGACGGGCGACGACTACCTGGCGGAGGTCGAGCAGGCcctaccctacgtcctcctgc
TCM149	ReDCaT *vnz_cutRSp* F5	CGTCGCCCGTCTCACGAGCCCGCGTGAGGTCGGTCTGCGT
TCM150	ReDCaT *vnz_cutRSp* R5	ACGCAGACCGACCTCACGCGGGCTCGTGAGACGGGCGACGcctaccctacgtcctcctgc
TCM151	ReDCaT *vnz_cutRSp* F6	GAGGTCGGTCTGCGTGGTCCTGATGCGGTGCAGCAGGCCT
TCM152	ReDCaT *vnz_cutRSp* R6	AGGCCTGCTGCACCGCATCAGGACCACGCAGACCGACCTCcctaccctacgtcctcctgc
TCM153	ReDCaT *vnz_cutRSp* F7	CGGTGCAGCAGGCCTGCGGTGAAAGCGTCCATCGTGCGCC
TCM154	ReDCaT *vnz_cutRSp* R7	GGCGCACGATGGACGCTTTCACCGCAGGCCTGCTGCACCGcctaccctacgtcctcctgc
TCM155	ReDCaT *vnz_cutRSp* F8	CGTCCATCGTGCGCCCCCTCGTCATGGGTCCGGTGGCACG
TCM156	ReDCaT *vnz_cutRSp* R8	CGTGCCACCGGACCCATGACGAGGGGGCGCACGATGGACGcctaccctacgtcctcctgc
TCM157	ReDCaT *vnz_cutRSp* F9	GGGTCCGGTGGCACGGGGGTGTGCCGAGGGTGGGTGGATC
TCM158	ReDCaT *vnz_cutRSp* R9	GATCCACCCACCCTCGGCACACCCCCGTGCCACCGGACCCcctaccctacgtcctcctgc
TCM159	ReDCaT *vnz_cutRSp* F10	GAGGGTGGGTGGATCACGCACCGCGGTCCTCCGGGAGCGG
TCM160	ReDCaT *vnz_cutRSp* R10	CCGCTCCCGGAGGACCGCGGTGCGTGATCCACCCACCCTCcctaccctacgtcctcctgc
TCM161	ReDCaT *vnz_cutRSp* F11	GTCCTCCGGGAGCGGAGAGCGGTAGGTGGCGCGCCACATA
TCM162	ReDCaT *vnz_cutRSp* R11	TATGTGGCGCGCCACCTACCGCTCTCCGCTCCCGGAGGACcctaccctacgtcctcctgc
TCM163	ReDCaT *vnz_cutRSp* F12	GTGGCGCGCCACATACAGGGCGTGATCACGGGGTGTGCAG

TCM164	ReDCaT *vnz_cutRSp* R12	CTGCACACCCCGTGATCACGCCCTGTATGTGGCGCGCCACcctaccctacgtcctcctgc
TCM165	ReDCaT *vnz_cutRSp* F13	TCACGGGGTGTGCAGTCGTCCTCCCCAACCGTTTCCTCAG
TCM166	ReDCaT *vnz_cutRSp* R13	CTGAGGAAACGGTTGGGGAGGACGACTGCACACCCCGTGAcctaccctacgtcctcctgc
TCM167	ReDCaT *vnz_cutRSp* F14	CAACCGTTTCCTCAGAGAAACCTCAACTGGCCCGGAATTC
TCM168	ReDCaT *vnz_cutRSp* R14	GAATTCCGGGCCAGTTGAGGTTTCTCTGAGGAAACGGTTGcctaccctacgtcctcctgc
TCM169	ReDCaT *vnz_cutRSp* F15	ACTGGCCCGGAATTCCGGTGAATTCTTCGATCACCGCCCC
TCM170	ReDCaT *vnz_cutRSp* R15	GGGGCGGTGATCGAAGAATTCACCGGAATTCCGGGCCAGTcctaccctacgtcctcctgc
TCM171	ReDCaT *vnz_cutRSp* F16	TTCGATCACCGCCCCGCGCCCCACCGCGCGCCCCCGGTCC
TCM172	ReDCaT *vnz_cutRSp* R16	GGACCGGGGGCGCGCGGTGGGGCGCGGGGCGGTGATCGAAcctaccctacgtcctcctgc
TCM173	ReDCaT *vnz_cutRSp* F17	GCGCGCCCCCGGTCCGCCACCCGCCCGCCCCCGGCCCCGC
TCM174	ReDCaT *vnz_cutRSp* R17	GCGGGGCCGGGGGCGGGCGGGTGGCGGACCGGGGGCGCGCcctaccctacgtcctcctgc
TCM175	ReDCaT *vnz_cutRSp* F18	CGCCCCCGGCCCCGCACCGCCGTCTTACAGCCGGTTTACG
TCM176	ReDCaT *vnz_cutRSp* R18	CGTAAACCGGCTGTAAGACGGCGGTGCGGGGCCGGGGGCGcctaccctacgtcctcctgc
TCM177	ReDCaT *vnz_cutRSp* F19	TACAGCCGGTTTACGCGCGTACGGGGCAGGATGGACACGC
TCM178	ReDCaT *vnz_cutRSp* R19	GCGTGTCCATCCTGCCCCGTACGCGCGTAAACCGGCTGTAcctaccctacgtcctcctgc
TCM179	ReDCaT *vnz_cutRSp* F20	GCAGGATGGACACGCACAGTCAGTGCTCAGGTTTCAGCCG

TCM180	ReDCaT *vnz_cutRSp* R20	CGGCTGAAACCTGAGCACTGACTGTGCGTGTCCATCCTGCcctaccctacgtcctcctgc
TCM181	ReDCaT *vnz_cutRSp* F21	CTCAGGTTTCAGCCGGTCCCCACCCCGGACAGGGCTCAAC
TCM182	ReDCaT *vnz_cutRSp* R21	GTTGAGCCCTGTCCGGGGTGGGGACCGGCTGAAACCTGAGcctaccctacgtcctcctgc
TCM183	ReDCaT *vnz_cutRSp* F22	TCCCCACCCCGGACAGGGCTCAACGGGAAGGATGTACGAC
TCM184	ReDCaT *vnz_cutRSp* R22	GTCGTACATCCTTCCCGTTGAGCCCTGTCCGGGGTGGGGAcctaccctacgtcctcctgc
TCM185	ReDCaT *vnz_08815p* RH -2 truncation F	GTGCGTGTAAATAAAGTGGTGCGTGCGCGATATTTTTG
TCM186	ReDCaT *vnz_08815p* RH -2 truncation R	CAAAAATATCGCGCACGCACCACTTTATTTACACGCACcctaccctacgtcctcctgc
TCM187	ReDCaT *vnz_08815p* RH -4 truncation F	GTGCGTGTAAATAAAGTGGTGCGTGCGCGATATTTT
TCM188	ReDCaT *vnz_08815p* RH -4 truncation R	AAAATATCGCGCACGCACCACTTTATTTACACGCACcctaccctacgtcctcctgc
TCM189	ReDCaT *vnz_08815p* RH -6 truncation F	GTGCGTGTAAATAAAGTGGTGCGTGCGCGATATT
TCM190	ReDCaT *vnz_08815p* RH -6 truncation R	AATATCGCGCACGCACCACTTTATTTACACGCACcctaccctacgtcctcctgc
TCM191	ReDCaT *vnz_08815p* RH -8 truncation F	GTGCGTGTAAATAAAGTGGTGCGTGCGCGATA
TCM192	ReDCaT *vnz_08815p* RH -8 truncation R	TATCGCGCACGCACCACTTTATTTACACGCACcctaccctacgtcctcctgc
TCM193	ReDCaT *vnz_08815p* RH -10 truncation F	GTGCGTGTAAATAAAGTGGTGCGTGCGCGA
TCM194	ReDCaT *vnz_08815p* RH -10 truncation R	TCGCGCACGCACCACTTTATTTACACGCACcctaccctacgtcctcctgc
TCM195	ReDCaT *vnz_08815p* RH -12 truncation F	GTGCGTGTAAATAAAGTGGTGCGTGCGC

TCM196	ReDCaT *vnz_08815p* RH -12 truncation R	GCGCACGCACCACTTTATTTACACGCACcctaccctacgtcctcctgc
TCM197	ReDCaT *vnz_08815p* RH -14 truncation F	GTGCGTGTAAATAAAGTGGTGCGTGC
TCM198	ReDCaT *vnz_08815p* RH -14 truncation R	GCACGCACCACTTTATTTACACGCACcctaccctacgtcctcctgc
TCM199	ReDCaT *vnz_08815p* RH -16 truncation F	GTGCGTGTAAATAAAGTGGTGCGT
TCM200	ReDCaT *vnz_08815p* RH -16 truncation R	ACGCACCACTTTATTTACACGCACcctaccctacgtcctcctgc
TCM201	ReDCaT *vnz_08815p* RH -18 truncation F	GTGCGTGTAAATAAAGTGGTGC
TCM202	ReDCaT *vnz_08815p* RH -18 truncation R	GCACCACTTTATTTACACGCACcctaccctacgtcctcctgc
TCM203	ReDCaT *vnz_08815p* RH -20 truncation F	GTGCGTGTAAATAAAGTGGT
TCM204	ReDCaT *vnz_08815p* RH -20 truncation R	ACCACTTTATTTACACGCACcctaccctacgtcctcctgc
TCM205	ReDCaT *vnz_08815p* RH -22 truncation F	GTGCGTGTAAATAAAGTG
TCM206	ReDCaT *vnz_08815p* RH -22 truncation R	CACTTTATTTACACGCACcctaccctacgtcctcctgc
TCM207	ReDCaT *vnz_08815p* RH -24 truncation F	GTGCGTGTAAATAAAG
TCM208	ReDCaT *vnz_08815p* RH -24 truncation R	CTTTATTTACACGCACcctaccctacgtcctcctgc
TCM209	ReDCaT *vnz_08815p* LH F	GGCAAAAATATCGCGCACGCACCACTTTATTTACACGCAC
TCM210	ReDCaT *vnz_08815p* LH R	GTGCGTGTAAATAAAGTGGTGCGTGCGCGATATTTTTGCCcctaccctacgtcctcctgc
TCM211	ReDCaT *vnz_08815p* LH -2 truncation F	GGCAAAAATATCGCGCACGCACCACTTTATTTACACGC

TCM212	ReDCaT *vnz_08815p* LH -2 truncation R	GCGTGTAAATAAAGTGGTGCGTGCGCGATATTTTTGCCcctaccctacgtcctcctgc
TCM213	ReDCaT *vnz_08815p* LH -4 truncation F	GGCAAAAATATCGCGCACGCACCACTTTATTTACAC
TCM214	ReDCaT *vnz_08815p* LH -4 truncation R	GTGTAAATAAAGTGGTGCGTGCGCGATATTTTTGCCcctaccctacgtcctcctgc
TCM215	ReDCaT *vnz_08815p* LH -6 truncation F	GGCAAAAATATCGCGCACGCACCACTTTATTTAC
TCM216	ReDCaT *vnz_08815p* LH -6 truncation R	GTAAATAAAGTGGTGCGTGCGCGATATTTTTGCCcctaccctacgtcctcctgc
TCM217	ReDCaT *vnz_08815p* LH -8 truncation F	GGCAAAAATATCGCGCACGCACCACTTTATTT
TCM218	ReDCaT *vnz_08815p* LH -8 truncation R	AAATAAAGTGGTGCGTGCGCGATATTTTTGCCcctaccctacgtcctcctgc
TCM219	ReDCaT *vnz_08815p* LH -10 truncation F	GGCAAAAATATCGCGCACGCACCACTTTAT
TCM220	ReDCaT *vnz_08815p* LH -10 truncation R	ATAAAGTGGTGCGTGCGCGATATTTTTGCCcctaccctacgtcctcctgc
TCM221	ReDCaT *vnz_08815p* LH -12 truncation F	GGCAAAAATATCGCGCACGCACCACTTT
TCM222	ReDCaT *vnz_08815p* LH -12 truncation R	AAAGTGGTGCGTGCGCGATATTTTTGCCcctaccctacgtcctcctgc
TCM223	ReDCaT *vnz_08815p* LH -14 truncation F	GGCAAAAATATCGCGCACGCACCACT
TCM224	ReDCaT *vnz_08815p* LH -14 truncation R	AGTGGTGCGTGCGCGATATTTTTGCCcctaccctacgtcctcctgc
TCM225	ReDCaT *vnz_08815p* LH -16 truncation F	GGCAAAAATATCGCGCACGCACCA
TCM226	ReDCaT *vnz_08815p* LH -16 truncation R	TGGTGCGTGCGCGATATTTTTGCCcctaccctacgtcctcctgc
TCM227	ReDCaT *vnz_08815p* LH -18 truncation F	GGCAAAAATATCGCGCACGCAC

TCM228	ReDCaT *vnz_08815p* LH -18 truncation R	GTGCGTGCGCGATATTTTTGCCcctaccctacgtcctcctgc
TCM229	ReDCaT *vnz_08815p* LH -20 truncation F	GGCAAAAATATCGCGCACGC
TCM230	ReDCaT *vnz_08815p* LH -20 truncation R	GCGTGCGCGATATTTTTGCCcctaccctacgtcctcctgc
TCM231	ReDCaT *vnz_08815p* LH -22 truncation F	GGCAAAAATATCGCGCAC
TCM232	ReDCaT *vnz_08815p* LH -22 truncation R	GTGCGCGATATTTTTGCCcctaccctacgtcctcctgc
TCM233	ReDCaT *vnz_08815p* LH -24 truncation F	GGCAAAAATATCGCGC
TCM234	ReDCaT *vnz_08815p* LH -24 truncation R	GCGCGATATTTTTGCCcctaccctacgtcctcctgc
TCM235	ReDCaT *vnz_18430p* RH -2 truncation F	GTTCTGTCCGTATATAAAGGTGGGGGTGCGAACGCACA
TCM236	ReDCaT *vnz_18430p* RH -2 truncation R	TGTGCGTTCGCACCCCCACCTTTATATACGGACAGAACcctaccctacgtcctcctgc
TCM237	ReDCaT *vnz_18430p* RH -4 truncation F	GTTCTGTCCGTATATAAAGGTGGGGGTGCGAACGCA
TCM238	ReDCaT *vnz_18430p* RH -4 truncation R	TGCGTTCGCACCCCCACCTTTATATACGGACAGAACcctaccctacgtcctcctgc
TCM239	ReDCaT *vnz_18430p* RH -6 truncation F	GTTCTGTCCGTATATAAAGGTGGGGGTGCGAACG
TCM240	ReDCaT *vnz_18430p* RH -6 truncation R	CGTTCGCACCCCCACCTTTATATACGGACAGAACcctaccctacgtcctcctgc
TCM241	ReDCaT *vnz_18430p* RH -8 truncation F	GTTCTGTCCGTATATAAAGGTGGGGGTGCGAA
TCM242	ReDCaT *vnz_18430p* RH -8 truncation R	TTCGCACCCCCACCTTTATATACGGACAGAACcctaccctacgtcctcctgc
TCM243	ReDCaT *vnz_18430p* RH -10 truncation F	GTTCTGTCCGTATATAAAGGTGGGGGTGCG

TCM244	ReDCaT *vnz_18430p* RH -10 truncation R	CGCACCCCCACCTTTATATACGGACAGAACcctaccctacgtcctcctgc
TCM245	ReDCaT *vnz_18430p* RH -12 truncation F	GTTCTGTCCGTATATAAAGGTGGGGGTG
TCM246	ReDCaT *vnz_18430p* RH -12 truncation R	CACCCCCACCTTTATATACGGACAGAACcctaccctacgtcctcctgc
TCM247	ReDCaT *vnz_18430p* RH -14 truncation F	GTTCTGTCCGTATATAAAGGTGGGGG
TCM248	ReDCaT *vnz_18430p* RH -14 truncation R	CCCCCACCTTTATATACGGACAGAACcctaccctacgtcctcctgc
TCM249	ReDCaT *vnz_18430p* RH -16 truncation F	GTTCTGTCCGTATATAAAGGTGGG
TCM250	ReDCaT *vnz_18430p* RH -16 truncation R	CCCACCTTTATATACGGACAGAACcctaccctacgtcctcctgc
TCM251	ReDCaT *vnz_18430p* RH -18 truncation F	GTTCTGTCCGTATATAAAGGTG
TCM252	ReDCaT *vnz_18430p* RH -18 truncation R	CACCTTTATATACGGACAGAACcctaccctacgtcctcctgc
TCM253	ReDCaT *vnz_18430p* RH -20 truncation F	GTTCTGTCCGTATATAAAGG
TCM254	ReDCaT *vnz_18430p* RH -20 truncation R	CCTTTATATACGGACAGAACcctaccctacgtcctcctgc
TCM255	ReDCaT *vnz_18430p* RH -22 truncation F	GTTCTGTCCGTATATAAA
TCM256	ReDCaT *vnz_18430p* RH -22 truncation R	TTTATATACGGACAGAACcctaccctacgtcctcctgc
TCM257	ReDCaT *vnz_18430p* RH -24 truncation F	GTTCTGTCCGTATATA
TCM258	ReDCaT *vnz_18430p* RH -24 truncation R	TATATACGGACAGAACcctaccctacgtcctcctgc
TCM259	ReDCaT *vnz_18430p* LH F	GCTGTGCGTTCGCACCCCCACCTTTATATACGGACAGAAC

TCM260	ReDCaT *vnz_18430p* LH R	GTTCTGTCCGTATATAAAGGTGGGGGTGCGAACGCACAGCcctaccctacgtcctcctgc
TCM261	ReDCaT *vnz_18430p* RH -2 truncation F	GCTGTGCGTTCGCACCCCCACCTTTATATACGGACAGA
TCM262	ReDCaT *vnz_18430p* RH -2 truncation R	TCTGTCCGTATATAAAGGTGGGGGTGCGAACGCACAGCcctaccctacgtcctcctgc
TCM263	ReDCaT *vnz_18430p* RH -4 truncation F	GCTGTGCGTTCGCACCCCCACCTTTATATACGGACA
TCM264	ReDCaT *vnz_18430p* RH -4 truncation R	TGTCCGTATATAAAGGTGGGGGTGCGAACGCACAGCcctaccctacgtcctcctgc
TCM265	ReDCaT *vnz_18430p* RH -6 truncation F	GCTGTGCGTTCGCACCCCCACCTTTATATACGGA
TCM266	ReDCaT *vnz_18430p* RH -6 truncation R	TCCGTATATAAAGGTGGGGGTGCGAACGCACAGCcctaccctacgtcctcctgc
TCM267	ReDCaT *vnz_18430p* RH -8 truncation F	GCTGTGCGTTCGCACCCCCACCTTTATATACG
TCM268	ReDCaT *vnz_18430p* RH -8 truncation R	CGTATATAAAGGTGGGGGTGCGAACGCACAGCcctaccctacgtcctcctgc
TCM269	ReDCaT *vnz_18430p* RH -10 truncation F	GCTGTGCGTTCGCACCCCCACCTTTATATA
TCM270	ReDCaT *vnz_18430p* RH -10 truncation R	TATATAAAGGTGGGGGTGCGAACGCACAGCcctaccctacgtcctcctgc
TCM271	ReDCaT *vnz_18430p* RH -12 truncation F	GCTGTGCGTTCGCACCCCCACCTTTATA
TCM272	ReDCaT *vnz_18430p* RH -12 truncation R	TATAAAGGTGGGGGTGCGAACGCACAGCcctaccctacgtcctcctgc
TCM273	ReDCaT *vnz_18430p* RH -14 truncation F	GCTGTGCGTTCGCACCCCCACCTTTA
TCM274	ReDCaT *vnz_18430p* RH -14 truncation R	TAAAGGTGGGGGTGCGAACGCACAGCcctaccctacgtcctcctgc
TCM275	ReDCaT *vnz_18430p* RH -16 truncation F	GCTGTGCGTTCGCACCCCCACCTT

TCM276	ReDCaT *vnz_18430p* RH -16 truncation R	AAGGTGGGGGTGCGAACGCACAGCcctaccctacgtcctcctgc
TCM277	ReDCaT *vnz_18430p* RH -18 truncation F	GCTGTGCGTTCGCACCCCCACC
TCM278	ReDCaT *vnz_18430p* RH -18 truncation R	GGTGGGGGTGCGAACGCACAGCcctaccctacgtcctcctgc
TCM279	ReDCaT *vnz_18430p* RH -20 truncation F	GCTGTGCGTTCGCACCCCCA
TCM280	ReDCaT *vnz_18430p* RH -20 truncation R	TGGGGGTGCGAACGCACAGCcctaccctacgtcctcctgc
TCM281	ReDCaT *vnz_18430p* RH -22 truncation F	GCTGTGCGTTCGCACCCC
TCM282	ReDCaT *vnz_18430p* RH -22 truncation R	GGGGTGCGAACGCACAGCcctaccctacgtcctcctgc
TCM283	ReDCaT *vnz_18430p* RH -24 truncation F	GCTGTGCGTTCGCACC
TCM284	ReDCaT *vnz_18430p* RH -24 truncation R	GGTGCGAACGCACAGCcctaccctacgtcctcctgc
TCM285	ReDCaT *vnz_08815p* RH -22 7a mutation F	GTGCGTaTAAATAAAGTG
TCM286	ReDCaT *vnz_08815p* RH -22 7a mutation R	CACTTTATTTAtACGCACcctaccctacgtcctcctgc
TCM287	ReDCaT *vnz_08815p* RH -22 7c mutation F	GTGCGTcTAAATAAAGTG
TCM288	ReDCaT *vnz_08815p* RH -22 7c mutation R	CACTTTATTTAgACGCACcctaccctacgtcctcctgc
TCM289	ReDCaT *vnz_08815p* RH -22 7t mutation F	GTGCGTtTAAATAAAGTG
TCM290	ReDCaT *vnz_08815p* RH -22 7t mutation R	CACTTTATTTAaACGCACcctaccctacgtcctcctgc
TCM291	ReDCaT *vnz_08815p* RH -22 8a mutation F	GTGCGTGaAAATAAAGTG

TCM292	ReDCaT *vnz_08815p* RH -22 8a mutation R	CACTTTATTTtCACGCACcctaccctacgtcctcctgc
TCM293	ReDCaT *vnz_08815p* RH -22 8c mutation F	GTGCGTGcAAATAAAGTG
TCM294	ReDCaT *vnz_08815p* RH -22 8c mutation R	CACTTTATTTgCACGCACcctaccctacgtcctcctgc
TCM295	ReDCaT *vnz_08815p* RH -22 8g mutation F	GTGCGTGgAAATAAAGTG
TCM296	ReDCaT *vnz_08815p* RH -22 8g mutation R	CACTTTATTTcCACGCACcctaccctacgtcctcctgc
TCM297	ReDCaT *vnz_08815p* RH -22 9t mutation F	GTGCGTGTtAATAAAGTG
TCM298	ReDCaT *vnz_08815p* RH -22 9t mutation R	CACTTTATTaACACGCACcctaccctacgtcctcctgc
TCM299	ReDCaT *vnz_08815p* RH -22 9c mutation F	GTGCGTGTcAATAAAGTG
TCM300	ReDCaT *vnz_08815p* RH -22 9c mutation R	CACTTTATTgACACGCACcctaccctacgtcctcctgc
TCM301	ReDCaT *vnz_08815p* RH -22 9c mutation F	GTGCGTGTgAATAAAGTG
TCM302	ReDCaT *vnz_08815p* RH -22 9c mutation R	CACTTTATTcACACGCACcctaccctacgtcctcctgc
TCM303	ReDCaT *vnz_08815p* RH -22 10t mutation F	GTGCGTGTAtATAAAGTG
TCM304	ReDCaT *vnz_08815p* RH -22 10t mutation R	CACTTTATaTACACGCACcctaccctacgtcctcctgc
TCM305	ReDCaT *vnz_08815p* RH -22 10c mutation F	GTGCGTGTAcATAAAGTG
TCM306	ReDCaT *vnz_08815p* RH -22 10c mutation R	CACTTTATgTACACGCACcctaccctacgtcctcctgc
TCM307	ReDCaT *vnz_08815p* RH -22 10g mutation F	GTGCGTGTAgATAAAGTG

TCM308	ReDCaT *vnz_08815p* RH -22 10g mutation R	CACTTTATcTACACGCACcctaccctacgtcctcctgc
TCM309	ReDCaT *vnz_08815p* RH -22 11t mutation F	GTGCGTGTAAtTAAAGTG
TCM310	ReDCaT *vnz_08815p* RH -22 11t mutation R	CACTTTAaTTACACGCACcctaccctacgtcctcctgc
TCM311	ReDCaT *vnz_08815p* RH -22 11c mutation F	GTGCGTGTAAcTAAAGTG
TCM312	ReDCaT *vnz_08815p* RH -22 11c mutation R	CACTTTAgTTACACGCACcctaccctacgtcctcctgc
TCM313	ReDCaT *vnz_08815p* RH -22 11g mutation F	GTGCGTGTAAgTAAAGTG
TCM314	ReDCaT *vnz_08815p* RH -22 11g mutation R	CACTTTAcTTACACGCACcctaccctacgtcctcctgc
TCM315	ReDCaT *vnz_08815p* RH -22 12a mutation F	GTGCGTGTAAAaAAAGTG
TCM316	ReDCaT *vnz_08815p* RH -22 12a mutation R	CACTTTtTTTACACGCACcctaccctacgtcctcctgc
TCM317	ReDCaT *vnz_08815p* RH -22 12c mutation F	GTGCGTGTAAAcAAAGTG
TCM318	ReDCaT *vnz_08815p* RH -22 12c mutation R	CACTTTgTTTACACGCACcctaccctacgtcctcctgc
TCM319	ReDCaT *vnz_08815p* RH -22 12g mutation F	GTGCGTGTAAAgAAAGTG
TCM320	ReDCaT *vnz_08815p* RH -22 12g mutation R	CACTTTcTTTACACGCACcctaccctacgtcctcctgc
TCM321	ReDCaT *vnz_08815p* RH -22 13t mutation F	GTGCGTGTAAATtAAGTG
TCM322	ReDCaT *vnz_08815p* RH -22 13t mutation R	CACTTaATTTACACGCACcctaccctacgtcctcctgc
TCM323	ReDCaT *vnz_08815p* RH -22 13c mutation F	GTGCGTGTAAATcAAGTG

TCM324	ReDCaT *vnz_08815p* RH -22 13c mutation R	CACTTgATTTACACGCACcctaccctacgtcctcctgc
TCM325	ReDCaT *vnz_08815p* RH -22 13g mutation F	GTGCGTGTAAATgAAGTG
TCM326	ReDCaT *vnz_08815p* RH -22 13g mutation R	CACTTcATTTACACGCACcctaccctacgtcctcctgc
TCM327	ReDCaT *vnz_08815p* RH -22 14a mutation F	GTGCGTGTAAATAtAGTG
TCM328	ReDCaT *vnz_08815p* RH -22 14a mutation R	CACTaTATTTACACGCACcctaccctacgtcctcctgc
TCM329	ReDCaT *vnz_08815p* RH -22 14c mutation F	GTGCGTGTAAATAcAGTG
TCM330	ReDCaT *vnz_08815p* RH -22 14c mutation R	CACTgTATTTACACGCACcctaccctacgtcctcctgc
TCM331	ReDCaT *vnz_08815p* RH -22 14g mutation F	GTGCGTGTAAATAgAGTG
TCM332	ReDCaT *vnz_08815p* RH -22 14g mutation R	CACTcTATTTACACGCACcctaccctacgtcctcctgc
TCM333	ReDCaT *vnz_08815p* RH -22 15a mutation F	GTGCGTGTAAATAAtGTG
TCM334	ReDCaT *vnz_08815p* RH -22 15a mutation R	CACaTTATTTACACGCACcctaccctacgtcctcctgc
TCM335	ReDCaT *vnz_08815p* RH -22 15c mutation F	GTGCGTGTAAATAAcGTG
TCM336	ReDCaT *vnz_08815p* RH -22 15c mutation R	CACgTTATTTACACGCACcctaccctacgtcctcctgc
TCM337	ReDCaT *vnz_08815p* RH -22 15g mutation F	GTGCGTGTAAATAAgGTG
TCM338	ReDCaT *vnz_08815p* RH -22 15g mutation R	CACcTTATTTACACGCACcctaccctacgtcctcctgc
TCM339	ReDCaT *vnz_08815p* RH -22 16a mutation F	GTGCGTGTAAATAAAaTG

TCM340	ReDCaT *vnz_08815p* RH -22 16aa mutation R	CAtTTTATTTACACGCACcctaccctacgtcctcctgc
TCM341	ReDCaT *vnz_08815p* RH -22 16t mutation F	GTGCGTGTAAATAAAtTG
TCM342	ReDCaT *vnz_08815p* RH -22 16t mutation R	CAaTTTATTTACACGCACcctaccctacgtcctcctgc
TCM343	ReDCaT *vnz_08815p* RH -22 16c mutation F	GTGCGTGTAAATAAAcTG
TCM344	ReDCaT *vnz_08815p* RH -22 16c mutation R	CAgTTTATTTACACGCACcctaccctacgtcctcctgc

Chapter 9. References

Aart, L. T. Van Der, Spijksma, G. K., Harms, A., Vollmer, W., Hankemeier, T. and van Wezel, G. P. (2018) 'High-Resolution Analysis of the Peptidoglycan Composition in *Streptomyces coelicolor*', *Journal of Bacteriology*, 200(20), pp. e00290-18.

Abraham, E. P., Chain, E., Fletcher, C. M., Gardner, A. D., Heatley, N. G., Jennings, M. A. and Florey, H. W. (1941) 'Futher observations on penicillin', *The Lancet*, 238(6155), pp. 177–189.

Ahmed, E. and Holmström, S. J. M. (2014) 'Siderophores in environmental research: roles and applications.', *Microbial biotechnology*, 7(3), pp. 196–208.

Aínsa, J. A., Parry, H. D. and Chater, K. F. (1999) 'A response regulator-like protein that functions at an intermediate stage of sporulation in *Streptomyces coelicolor* A3(2)', *Molecular Microbiology*, 34(3), pp. 607–619.

Al-Bassam, M. M., Bibb, M. J., Bush, M. J., Chandra, G. and Buttner, M. J. (2014) 'Response regulator heterodimer formation controls a key stage in *Streptomyces* development', *PLoS genetics*, 10(8), pp. e1004554–e1004554.

Alduina, R., Tocchetti, A., Costa, S., Ferraro, C., Cancemi, P., Sosio, M. and Donadio, S. (2020) 'A Two-Component regulatory system with opposite effects on glycopeptide antibiotic biosynthesis and resistance', *Scientific Reports*, 10(1), p. 6200.

Allenby, N. E. E., Laing, E., Bucca, G., Kierzek, A. M. and Smith, C. P. (2012) 'Diverse control of metabolism and other cellular processes in *Streptomyces coelicolor* by the PhoP transcription factor: genome-wide identification of *in vivo* targets', *Nucleic acids research*, 40(19), pp. 9543–9556.

Álvarez-Álvarez, R., Rodríguez-García, A., Santamarta, I., Pérez-Redondo, R., Prieto-Domínguez, A., Martínez-Burgo, Y. and Liras, P. (2014) 'Transcriptomic analysis of *Streptomyces clavuligerus* Δ*ccaR*::*tsr*: effects of the cephamycin C-clavulanic acid cluster regulator CcaR on global regulation', *Microbial Biotechnology*, 7(3), pp. 221–231.

Amábile-Cuevas, C. F. and Demple, B. (1991) 'Molecular characterization of the soxRS genes of *Escherichia coli*: two genes control a superoxide stress regulon.', *Nucleic acids research*, 19(16), pp. 4479–4484.

Anantharaman, V. and Aravind, L. (2003) 'Evolutionary history, structural features and biochemical diversity of the NlpC/P60 superfamily of enzymes', *Genome biology*, 4(2), pp. R11–R11.

Antoraz, S., Santamaría, R. I., Díaz, M., Sanz, D. and Rodríguez, H. (2015) 'Toward a new focus in antibiotic and drug discovery from the *Streptomyces* arsenal', *Frontiers in microbiology*, 6, p. 461.

Apel, A. K., Sola-Landa, A., Rodríguez-García, A. and Martín, J. F. (2007) 'Phosphate control of *phoA*, *phoC* and *phoD* gene expression in *Streptomyces coelicolor* reveals significant differences in binding of PhoP to their promoter regions', *Microbiology*,

153(10), pp. 3527–3537.

Aslam, B., Wang, W., Arshad, M. I., Khurshid, M., Muzammil, S., Rasool, M. H., Nisar, M. A., Alvi, R. F., Aslam, M. A., Qamar, M. U., Salamat, M. K. F. and Baloch, Z. (2018) 'Antibiotic resistance: a rundown of a global crisis', *Infection and drug resistance*, 11, pp. 1645–1658.

Audrain, B., Farag, M. A., Ryu, C.-M. and Ghigo, J.-M. (2015) 'Role of bacterial volatile compounds in bacterial biology', *FEMS Microbiology Reviews*, 39(2), pp. 222–233.

Ayer, S. W., McInnes, A. G., Thibault, P., Walter, J. A., Doull, J. L., Parnell, T. and Vining, L. C. (1991) 'Jadomycin, a novel 8H-benz[b]oxazolo[3,2-f]phenanthridine antibiotic from from *Streptomyces venezuelae* ISP5230.', *Tetrahedron Letters*, 32(44), pp. 6301–6304.

Backert, S., Bernegger, S., Skórko-Glonek, J. and Wessler, S. (2018) 'Extracellular HtrA serine proteases: An emerging new strategy in bacterial pathogenesis', *Cellular Microbiology*, 20(6), p. e12845.

Baker, J. A., Wong, W.-C., Eisenhaber, B., Warwicker, J. and Eisenhaber, F. (2017) 'Charged residues next to transmembrane regions revisited: "Positive-inside rule" is complemented by the "negative inside depletion/outside enrichment rule"', *BMC Biology*, 15(1), p. 66.

Balomenou, S., Fouet, A., Tzanodaskalaki, M., Couture-Tosi, E., Bouriotis, V. and Boneca, I. G. (2013) 'Distinct functions of polysaccharide deacetylases in cell shape, neutral polysaccharide synthesis and virulence of *Bacillus anthracis*', *Molecular Microbiology*, 87(4), pp. 867–883.

Balomenou, S., Koutsioulis, D., Tomatsidou, A., Tzanodaskalaki, M., Petratos, K. and Bouriotis, V. (2018) 'Polysaccharide deacetylases serve as new targets for the design of inhibitors against *Bacillus anthracis* and *Bacillus cereus*', *Bioorganic & Medicinal Chemistry*, 26(13), pp. 3845–3851.

Barabás, G. and Szabó, G. (1968) 'Role of streptomycin in the life of *Streptomyces griseus*: streptidine-containing fractions in the cell walls of *Streptomyces griseus* strains.', *Canadian journal of microbiology*, 14(12), pp. 1325–1331.

Baral, B., Akhgari, A. and Metsä-Ketelä, M. (2018) 'Activation of microbial secondary metabolic pathways: Avenues and challenges', *Synthetic and systems biotechnology*, 3(3), pp. 163–178.

Barbieri, C. M., Wu, T. and Stock, A. M. (2013) 'Comprehensive analysis of OmpR phosphorylation, dimerization, and DNA binding supports a canonical model for activation', *Journal of molecular biology*, 425(10), pp. 1612–1626.

Barka, E. A., Vatsa, P., Sanchez, L., Gaveau-Vaillant, N., Jacquard, C., Meier-Kolthoff, J. P., Klenk, H.-P., Clément, C., Ouhdouch, Y. and van Wezel, G. P. (2015) 'Taxonomy, Physiology, and Natural Products of Actinobacteria', *Microbiology and molecular biology reviews : MMBR*, 80(1), pp. 1–43.

Baron, S. (1996) *Medical Microbiology*. Edited by S. Baron. Galveston (TX).

Barona-Gómez, F., Wong, U., Giannakopulos, A. E., Derrick, P. J. and Challis, G. L. (2004) 'Identification of a cluster of genes that directs desferrioxamine biosynthesis

in *Streptomyces coelicolor* M145.', *Journal of the American Chemical Society*, 126(50), pp. 16282–16283.

Belknap, K. C., Park, C. J., Barth, B. M. and Andam, C. P. (2020) 'Genome mining of biosynthetic and chemotherapeutic gene clusters in *Streptomyces* bacteria', *Scientific Reports*, 10(1), p. 2003.

Bentley, R. and Haslam, E. (1990) 'The Shikimate Pathway — A Metabolic Tree with Many Branches', *Critical Reviews in Biochemistry and Molecular Biology*, 25(5), pp. 307–384.

Bentley, S. D. *et al.* (2002) 'Complete genome sequence of the model actinomycete *Streptomyces coelicolor* A3(2)', *Nature*, 417, p. 141.

Bibb, L. A., Kunkle, C. A. and Schmitt, M. P. (2007) 'The ChrA-ChrS and HrrA-HrrS signal transduction systems are required for activation of the *hmuO* promoter and repression of the *hemA* promoter in *Corynebacterium diphtheriae*', *Infection and Immunity*, 75(5), pp. 2421–2431.

Bibb, M. (2005) 'Regulation of secondary metabolism in *Streptomyces*', *Current Opinion in Microbiology*, 8, pp. 208–215.

Bibb, Mervyn J., Fernández-Martínez, L. T., Borsetto, C., Gomez-Escribano, J. P., Bibb, Maureen J., Al-Bassam, M. M. and Chandra, G. (2014) 'New insights into chloramphenicol biosynthesis in *Streptomyces venezuelae* ATCC 10712', *Antimicrobial Agents and Chemotherapy*, 58(12), pp. 7441–7450.

Bihlmaier, C., Welle, E., Hofmann, C., Welzel, K., Vente, A., Breitling, E., Müller, M., Glaser, S. and Bechthold, A. (2006) 'Biosynthetic Gene Cluster for the Polyenoyltetramic Acid α-Lipomycin', *Antimicrobial Agents and Chemotherapy*, 50(6), pp. 2113 LP – 2121.

Bishop, A., Fielding, S., Dyson, P. and Herron, P. (2004) 'Systematic insertional mutagenesis of a streptomycete genome: A link between osmoadaptation and antibiotic production', *Genome Res.*, 14(5), pp. 893–900.

Bobek, J., Šmídová, K. and Čihák, M. (2017) 'A Waking Review: Old and Novel Insights into the Spore Germination in *Streptomyces*', *Frontiers in microbiology*, 8, p. 2205.

Bogdanow, B., Zauber, H. and Selbach, M. (2016) 'Systematic Errors in Peptide and Protein Identification and Quantification by Modified Peptides', *Molecular & cellular proteomics : MCP*, 15(8), pp. 2791–2801.

Bonissone, S., Gupta, N., Romine, M., Bradshaw, R. A. and Pevzner, P. A. (2013) 'N-terminal protein processing: a comparative proteogenomic analysis', *Molecular & cellular proteomics : MCP*, 12(1), pp. 14–28.

Borgstahl, G. E. O. (2007) 'How to Use Dynamic Light Scattering to Improve the Likelihood of Growing Macromolecular Crystals BT - Macromolecular Crystallography Protocols: Volume 1, Preparation and Crystallization of Macromolecules', in Walker, J. M. and Doublié, S. (eds). Totowa, NJ: Humana Press, pp. 109–130.

Borodina, I., Schöller, C., Eliasson, A. and Nielsen, J. (2005) 'Metabolic network analysis of *Streptomyces tenebrarius*, a *Streptomyces* species with an active entner-doudoroff pathway.', *Applied and environmental microbiology*, 71(5), pp. 2294–

2302.

Boukhris, I., Dulermo, T., Chouayekh, H. and Virolle, M.-J. (2016) 'Evidence for the negative regulation of phytase gene expression in *Streptomyces lividans* and *Streptomyces coelicolor*', *Journal of Basic Microbiology*, 56(1), pp. 59–66.

Brautigam, C. A., Deka, R. K., Liu, W. Z. and Norgard, M. V (2016) 'The Tp0684 (MglB-2) Lipoprotein of *Treponema pallidum*: A Glucose-Binding Protein with Divergent Topology', *PLOS ONE*, 11(8), p. e0161022.

Brenes, A., Hukelmann, J., Bensaddek, D. and Lamond, A. I. (2019) 'Multibatch TMT Reveals False Positives, Batch Effects and Missing Values', *Molecular & Cellular Proteomics*, 18(10), pp. 1967–1980.

Brewster, J. L., McKellar, J. L. O., Finn, T. J., Newman, J., Peat, T. S. and Gerth, M. L. (2016) 'Structural basis for ligand recognition by a Cache chemosensory domain that mediates carboxylate sensing in *Pseudomonas syringae*', *Scientific Reports*, 6(1), p. 35198.

Brian, P., Riggle, P. J., Santos, R. A. and Champness, W. C. (1996) 'Global negative regulation of *Streptomyces coelicolor* antibiotic synthesis mediated by an *absA*-encoded putative signal transduction system', *Journal of Bacteriology*, 178(11), pp. 3221–3231.

Brocker, M. and Bott, M. (2006) 'Evidence for activator and repressor functions of the response regulator MtrA from *Corynebacterium glutamicum*', *FEMS Microbiology Letters*, 264(2), pp. 205–212.

Brzoska, P. and Boos, W. (1989) 'The *ugp*-encoded glycerophosphoryldiester phosphodiesterase, a transport-related enzyme of *Escherichia coli*', *FEMS Microbiology Reviews*, 5(1–2), pp. 115–124.

Burns, W. H., Saral, R., Santos, G. W., Laskin, O. L., Lietman, P. S., McLaren, C. and Barry, D. W. (1982) 'Isolation and characterisation of resistant Herpes simplex virus after acyclovir therapy.', *Lancet (London, England)*, 1(8269), pp. 421–423.

Bush, K. (2013) 'Proliferation and significance of clinically relevant β-lactamases.', *Annals of the New York Academy of Sciences*, 1277, pp. 84–90.

Bush, M., Tschowri, N., Schlimpert, S., Flärdh, K. and Buttner, M. (2015) 'c-di-GMP signalling and the regulation of developmental transitions in streptomycetes', *Nature Reviews Microbiology*, 13(12), pp. 749–760.

Bush, M. J., Bibb, M. J., Chandra, G., Findlay, K. C. and Buttner, M. J. (2013) 'Genes required for aerial growth, cell division, and chromosome segregation are targets of WhiA before sporulation in *Streptomyces venezuelae*', *mBio*, 4(5), pp. e00684-13.

Bush, M. J., Chandra, G., Al-Bassam, M. M., Findlay, K. C. and Buttner, M. J. (2019) 'BldC Delays Entry into Development To Produce a Sustained Period of Vegetative Growth in *Streptomyces venezuelae*.', *mBio*, 10(1).

Buttner, M. J., Fearnley, I. M. and Bibb, M. J. (1987) 'The agarase gene (*dagA*) of *Streptomyces coelicolor* A3(2): nucleotide sequence and transcriptional analysis', *Molecular and General Genetics MGG*, 209(1), pp. 101–109.

Bystrykh, L V, Herrema, J. K., Malpartida, F., Hopwood, D., Dijkhuizen, L., Herrema, J. N. K., Bystrykh, Leonid V and Ferna, M. (1996) 'Production of actinorhodin-related "blue pigments" by *Streptomyces coelicolor* A3 (2).', *J. Bacteriol.*, 3(2), pp. 2238–2244.

Cano, R. J. and Borucki, M. K. (1995) 'Revival and identification of bacterial spores in 25- to 40-million-year-old Dominican amber', *Science*, 268(5213), pp. 1060 LP – 1064.

Capstick, D. S., Willey, J. M., Buttner, M. J. and Elliot, M. A. (2007) 'SapB and the chaplins: connections between morphogenetic proteins in *Streptomyces coelicolor*.', *Molecular microbiology*, 64(3), pp. 602–613.

Capstick, D. S. (2011) *Chaplin amyloid fiber formation and the role of the chaplins in the aerial development of* Streptomyces coelicolor. McMaster University.

Carro, L., Castro, J. F., Razmilic, V., Nouioui, I., Pan, C., Igual, J. M., Jaspars, M., Goodfellow, M., Bull, A. T., Asenjo, J. A. and Klenk, H.-P. (2019) 'Uncovering the potential of novel micromonosporae isolated from an extreme hyper-arid Atacama Desert soil', *Scientific Reports*, 9(1), p. 4678.

Chang, H.-M., Chen, M.-Y., Shieh, Y.-T., Bibb, M. J. and Chen, C. W. (1996) 'The cutRS signal transduction system of *Streptomyces lividans* represses the biosynthesis of the polyketide antibiotic actinorhodin', *Molecular Microbiology*, 21(5), pp. 107–108.

Chater, K. (1999) 'David Hopwood and the emergence of *Streptomyces* genetics.', *International microbiology*, 2(2), pp. 61–68.

Chater, K. (2016) 'Recent advances in understanding *Streptomyces*.', *F1000Research*, 5, pp. 2795–2811.

Chen, R., Wong, H. L. and Burns, B. P. (2019) 'New Approaches to Detect Biosynthetic Gene Clusters in the Environment', *Medicines (Basel, Switzerland)*, 6(1), p. 32.

Choi, H.-J., Kim, S.-J., Mukhopadhyay, P., Cho, S., Woo, J.-R., Storz, G. and Ryu, S.-E. (2001) 'Structural Basis of the Redox Switch in the OxyR Transcription Factor', *Cell*, 105(1), pp. 103–113.

Christina, D. B., S., C. D., J., Bibb Maureen, C., F. K., J., Buttner Mark and A., E. M. (2008) 'Function and Redundancy of the Chaplin Cell Surface Proteins in Aerial Hypha Formation, Rodlet Assembly, and Viability in *Streptomyces coelicolor*', *Journal of Bacteriology*, 190(17), pp. 5879–5889.

Clark, L. C., Seipke, R. F., Prieto, P., Willemse, J., van Wezel, G. P., Hutchings, M. I. and Hoskisson, P. a (2013) 'Mammalian cell entry genes in *Streptomyces* may provide clues to the evolution of bacterial virulence.', *Scientific reports*, 3, p. 1109.

Clausen, T., Kaiser, M., Huber, R. and Ehrmann, M. (2011) 'HTRA proteases: regulated proteolysis in protein quality control', *Nature Reviews Molecular Cell Biology*, 12(3), pp. 152–162.

Clausen, T., Southan, C. and Ehrmann, M. (2002) 'The HtrA Family of Proteases: Implications for Protein Composition and Cell Fate', *Molecular Cell*, 10(3), pp. 443–455.

Cobb, R. E., Wang, Y. and Zhao, H. (2015) 'High-Efficiency Multiplex Genome Editing

of *Streptomyces* Species Using an Engineered CRISPR/Cas System', *ACS Synthetic Biology*, 4(6), pp. 723–728.

Cooke, M., Orlando, U., Maloberti, P., Podestá, E. J. and Cornejo Maciel, F. (2011) 'Tyrosine phosphatase SHP2 regulates the expression of acyl-CoA synthetase ACSL4', *Journal of lipid research*, 52(11), pp. 1936–1948.

Cordes, T., Michelucci, A. and Hiller, K. (2015) 'Itaconic Acid: The Surprising Role of an Industrial Compound as a Mammalian Antimicrobial Metabolite', *Annual Review of Nutrition*, 35(1), pp. 451–473.

Cremers, C. M. and Jakob, U. (2013) 'Oxidant sensing by reversible disulfide bond formation', *The Journal of biological chemistry*, 288(37), pp. 26489–26496.

Dela Cruz, R., Gao, Y., Penumetcha, S., Sheplock, R., Weng, K. and Chander, M. (2010) 'Expression of the *Streptomyces coelicolor* SoxR regulon is intimately linked with actinorhodin production', *Journal of bacteriology*, 192(24), pp. 6428–6438.

Daniel-Ivad, M., Hameed, N., Tan, S., Dhanjal, R., Socko, D., Pak, P., Gverzdys, T., Elliot, M. A. and Nodwell, J. R. (2017) 'An Engineered Allele of afsQ1 Facilitates the Discovery and Investigation of Cryptic Natural Products', *ACS Chemical Biology*, 12(3), pp. 628–634.

Daniels, R., Mellroth, P., Bernsel, A., Neiers, F., Normark, S., von Heijne, G. and Henriques-Normark, B. (2010) 'Disulfide bond formation and cysteine exclusion in Gram-positive bacteria', *The Journal of biological chemistry*, 285(5), pp. 3300–3309.

Darmon, E., Noone, D., Masson, A., Bron, S., Kuipers, O. P., Devine, K. M. and Van Dijl, J. M. (2002) 'A novel class of heat and secretion stress-responsive genes is controlled by the autoregulated CssRS two-component system of *Bacillus subtilis*', *Journal of Bacteriology*, 184(20), pp. 5661–5671.

Darwin, A. J. (2005) 'The phage-shock-protein response', *Molecular Microbiology*, 57(3), pp. 621–628.

Demain, A. L. (2009) 'Antibiotics: Natural products essential to human health', *Medicinal Research Reviews*, 29(6), pp. 821–842.

Derouaux, A., Halici, S., Nothaft, H., Neutelings, T., Moutzourelis, G., Dusart, J., Titgemeyer, F. and Rigali, S. (2004) 'Deletion of a Cyclic AMP Receptor Protein Homologue Diminishes Germination and Affects Morphological Development of *Streptomyces coelicolor*', *Journal of Bacteriology*, 186(6), pp. 1893 LP – 1897.

Devine, R., McDonald, H. P., Qin, Z., Arnold, C. J., Noble, K., Chandra, G., Wilkinson, B. and Hutchings, M. I. (2021) 'Re-wiring the regulation of the formicamycin biosynthetic gene cluster to enable the development of promising antibacterial compounds', *Cell Chemical Biology*, 28(4), pp. 515-523.e5.

Diacon, A. H. *et al.* (2009) 'The diarylquinoline TMC207 for multidrug-resistant tuberculosis.', *The New England journal of medicine*, 360(23), pp. 2397–2405.

Dietrich, L. E. P., Price-Whelan, A., Petersen, A., Whiteley, M. and Newman, D. K. (2006) 'The phenazine pyocyanin is a terminal signalling factor in the quorum sensing network of Pseudomonas aeruginosa', *Molecular Microbiology*, 61(5), pp. 1308–1321.

Dietrich, L. E. P., Teal, T. K., Price-whelan, A. and Newman, D. K. (2008) 'Redox-Active Antibiotics Control Gene Expression and Community Behavior in Divergent Bacteria', 321(5893), pp. 1203–1206.

Dietrich, L. E. P., Okegbe, C., Price-Whelan, A., Sakhtah, H., Hunter, R. C. and Newman, D. K. (2013) 'Bacterial community morphogenesis is intimately linked to the intracellular redox state', *Journal of bacteriology*, 195(7), pp. 1371–1380.

Ding, H., Hidalgo, E. and Demple, B. (1996) 'The redox state of the [2Fe-2S] clusters in SoxR protein regulates its activity as a transcription factor.', *The Journal of biological chemistry*, 271(52), pp. 33173–33175.

Doull, J. L., Singh, A. K., Hoare, M. and Ayer, S. W. (1994) 'Conditions for the production of jadomycin B by *Streptomyces venezuelae* ISP5230: Effects of heat shock, ethanol treatment and phage infection', *Journal of Industrial Microbiology*, 13(2), pp. 120–125.

Ehrhardt, M. K. G., Warring, S. L. and Gerth, M. L. (2018) 'Screening Chemoreceptor-Ligand Interactions by High-Throughput Thermal-Shift Assays.', *Methods in molecular biology (Clifton, N.J.)*, 1729, pp. 281–290.

Ehrlich, J., Bartz, Q. R., Smith, R. M., Joslyn, D. A. and Burkholder, P. R. (1947) 'Chloromycetin, a New Antibiotic From a Soil Actinomycete', *Science*, 106(2757), p. 417.

Ehrlich, J., Gottlieb, D., Burkholder, P. R., Anderson, L. E. and Pridham, T. G. (1948) '*Streptomyces venezuelae*, n. sp., the source of chloromycetin', *Journal of bacteriology*, 56(4), pp. 467–477.

Elliot, M. A., Karoonuthaisiri, N., Huang, J., Bibb, M. J., Cohen, S. N., Kao, C. M. and Buttner, M. J. (2003) 'The chaplins: a family of hydrophobic cell-surface proteins involved in aerial mycelium formation in *Streptomyces coelicolor*.', *Genes & development*, 17(14), pp. 1727–1740.

Fairhurst, R. M. and Dondorp, A. M. (2016) 'Artemisinin-Resistant *Plasmodium falciparum* Malaria', *Microbiology spectrum*, 4(3), pp. 10.1128/microbiolspec.EI10-0013–2016.

Feehily, C. and Karatzas, K. A. G. (2013) 'Role of glutamate metabolism in bacterial responses towards acid and other stresses', *Journal of Applied Microbiology*, 114(1), pp. 11–24.

Feeney, M. A., Chandra, G., Findlay, K. C., Paget, M. S. B. and Buttner, M. J. (2017) 'Translational Control of the SigR-Directed Oxidative Stress Response in *Streptomyces* via IF3-Mediated Repression of a Noncanonical GTC Start Codon', *mBio*, 8(3), pp. e00815-17.

Fernández-Martínez, L. T., Santos-Beneit, F. and Martín, J. F. (2012) 'Is PhoR–PhoP partner fidelity strict? PhoR is required for the activation of the *pho* regulon in *Streptomyces coelicolor*', *Molecular Genetics and Genomics*, 287(7), pp. 565–573.

Fernández-Moreno, M. A., Caballero, J., Hopwood, D. A. and Malpartida, F. (1991) 'The act cluster contains regulatory and antibiotic export genes, direct targets for translational control by the bldA tRNA gene of *Streptomyces*', *Cell*, 66(4), pp. 769–

780.

Fernández, M., Morel, B., Corral-Lugo, A. and Krell, T. (2016) 'Identification of a chemoreceptor that specifically mediates chemotaxis toward metabolizable purine derivatives', *Molecular Microbiology*, 99(1), pp. 34–42.

Flärdh, K. and Buttner, M. J. (2009) '*Streptomyces* morphogenetics: dissecting differentiation in a filamentous bacterium', *Nature Reviews Microbiology*, 7(1), pp. 36–49.

Flärdh, K., Findlay, K. C. and Chater, K. F. (1999) 'Association of early sporulation genes with suggested developmental decision points in *Streptomyces coelicolor* A3(2).', *Microbiology (Reading, England)*, 145 (Pt 9, pp. 2229–2243.

Fleming, A. (1929) 'On the Antibacterial Action of Cultures of a *Penicillium*, with Special Reference to their Use in the Isolation of *B. influenzæ*', *British journal of experimental pathology*, 10(3), pp. 226–236.

Fleming, A. (1945) 'Nobel Lecture', *Nobel Media AB 2020*.

Floriano, B. and Bibb, M. (1996) '*afsR* is a pleiotropic but conditionally required regulatory gene for antibiotic production in *Streptomyces coelicolor* A3(2)', *Molecular Microbiology*, 21(2), pp. 385–396.

Fol, M., Chauhan, A., Nair, N. K., Maloney, E., Moomey, M., Jagannath, C., Madiraju, M. V. V. S. and Rajagopalan, M. (2006) 'Modulation of *Mycobacterium tuberculosis* proliferation by MtrA, an essential two-component response regulator', *Molecular Microbiology*, 60(3), pp. 643–657.

Fröjd, M. J. and Flärdh, K. (2019) 'Apical assemblies of intermediate filament-like protein FilP are highly dynamic and affect polar growth determinant DivIVA in *Streptomyces venezuelae*', *Molecular Microbiology*, 112(1), pp. 47–61.

Fu, J., Qin, R., Zong, G., Liu, C., Kang, N., Zhong, C. and Cao, G. (2019) 'The CagRS Two-Component System Regulates Clavulanic Acid Metabolism via Multiple Pathways in *Streptomyces clavuligerus* F613-1', *Frontiers in Microbiology*, p. 244.

Fukuda, I., Hirabayashi-Ishioka, Y., Sakikawa, I., Ota, T., Yokoyama, M., Uchiumi, T. and Morita, A. (2013) 'Optimization of Enrichment Conditions on TiO2 Chromatography Using Glycerol As an Additive Reagent for Effective Phosphoproteomic Analysis', *Journal of Proteome Research*, 12(12), pp. 5587–5597.

Gallagher, K. A., Schumacher, M. A., Bush, M. J., Bibb, M. J., Chandra, G., Holmes, N. A., Zeng, W., Henderson, M., Zhang, H., Findlay, K. C., Brennan, R. G. and Buttner, M. J. (2020) 'c-di-GMP Arms an Anti-σ to Control Progression of Multicellular Differentiation in *Streptomyces*', *Molecular Cell*, 77(3), pp. 586-599.e6.

Galperin, M. Y. (2006) 'Structural Classification of Bacterial Response Regulators: Diversity of Output Domains and Domain Combinations ', *Journal of Bacteriology*, 188(12), pp. 4169–4182.

Gao, B., Paramanathan, R. and Gupta, R. S. (2006) 'Signature proteins that are distinctive characteristics of Actinobacteria and their subgroups', *Antonie van Leeuwenhoek*, 90(1), pp. 69–91.

Gao, C., Hindra, Mulder, D., Yin, C. and Elliot, M. A. (2012) 'Crp Is a Global Regulator of Antibiotic Production in *Streptomyces*', *mBio*. Edited by M. B. Winkler Karen, 3(6), pp. e00407-12.

Gao, R. and Stock, A. M. (2013) 'Probing kinase and phosphatase activities of two-component systems *in vivo* with concentration-dependent phosphorylation profiling', *Proceedings of the National Academy of Sciences*, 110(2), pp. 672 LP – 677.

Gilbert, M., Morosoli, R., Shareck, F. and Kluepfel, D. (1995) 'Production and Secretion of Proteins by streptomycetes', *Critical Reviews in Biotechnology*, 15(1), pp. 13–39.

Glazebrook, M. A., Doull, J. L., Stuttard, C. and Vining, L. C. (1990) 'Sporulation of *Streptomyces venezuelae* in submerged cultures.', *Journal of general microbiology*, 136(3), pp. 581–588.

Glick, R., Gilmour, C., Tremblay, J., Satanower, S., Avidan, O., Déziel, E., Greenberg, E. P., Poole, K. and Banin, E. (2010) 'Increase in Rhamnolipid Synthesis under Iron-Limiting Conditions Influences Surface Motility and Biofilm Formation in *Pseudomonas aeruginosa*', *Journal of Bacteriology*, 192(12), pp. 2973 LP – 2980.

Godinez, O., Dyson, P., del Sol, R., Barrios-Gonzalez, J., Millan-Pacheco, C. and Mejia, A. (2015) 'Targeting the osmotic stress response for strain improvement of an industrial producer of secondary metabolites', *Journal of Microbiology and Biotechnology*, 25(11), pp. 1787–1795.

Gomez-Escribano, J. P., Holmes, N. A., Schlimpert, S., Bibb, Maureen J, Chandra, G., Wilkinson, B., Buttner, M. J. and Bibb, Mervyn J (2021) '*Streptomyces venezuelae* NRRL B-65442: genome sequence of a model strain used to study morphological differentiation in filamentous Actinobacteria', *Journal of Industrial Microbiology and Biotechnology*.

Grantcharova, N., Lustig, U. and Flärdh, K. (2005) 'Dynamics of FtsZ assembly during sporulation in *Streptomyces coelicolor* A3(2).', *Journal of bacteriology*, 187(9), pp. 3227–3237.

Gribskov, M., Devereux, J. and Burgess, R. R. (1984) 'The codon preference plot: graphic analysis of protein coding sequences and prediction of gene expression.', *Nucleic acids research*, 12(1 Pt 2), pp. 539–549.

Groisman, E. A. (2016) 'Feedback Control of Two-Component Regulatory Systems.', *Annual review of microbiology*, 70, pp. 103–124.

Gubbens, J., Janus, M., Florea, B. I., Overkleeft, H. S. and van Wezel, G. P. (2012) 'Identification of glucose kinase-dependent and -independent pathways for carbon control of primary metabolism, development and antibiotic production in *Streptomyces coelicolor* by quantitative proteomics', *Molecular Microbiology*, 86(6), pp. 1490–1507.

Gullón, S., Vicente, R. L. and Mellado, R. P. (2012) 'A novel two-component system involved in secretion stress response in *Streptomyces lividans*', *PloS one*, 7(11), pp. e48987–e48987.

Gunnarsson, N., Mortensen, U. H., Sosio, M. and Nielsen, J. (2004) 'Identification of

the Entner–Doudoroff pathway in an antibiotic-producing actinomycete species', *Molecular Microbiology*, 52(3), pp. 895–902.

Gust, B., Kieser, T. and Chater, K. (2002) 'PCR targeting system in *Streptomyces coelicolor* A3(2)', *John Innes Centre*, 3(2), pp. 1–39.

Haas, L. F. (1999) 'Papyrus of Ebers and Smith', *Journal of Neurology, Neurosurgery & Psychiatry*, 67(5), pp. 578 LP – 578.

Hardman, G., Perkins, S., Brownridge, P. J., Clarke, C. J., Byrne, D. P., Campbell, A. E., Kalyuzhnyy, A., Myall, A., Eyers, P. A., Jones, A. R. and Eyers, C. E. (2019) 'Strong anion exchange-mediated phosphoproteomics reveals extensive human non-canonical phosphorylation', *The EMBO Journal*, 38(21), p. e100847.

Harvey, J. C., Cantrell, J. R. and Fisher, A. M. (1957) 'Actinomycosis: Its recognition and treatment', *Annals of Internal Medicine*, 46(5), pp. 868–885.

Heermann, R., Lippert, M.-L. and Jung, K. (2009) 'Domain swapping reveals that the N-terminal domain of the sensor kinase KdpD in *Escherichia coli* is important for signaling', *BMC Microbiology*, 9(1), p. 133.

Hesketh, A., Hill, C., Mokhtar, J., Novotna, G., Tran, N., Bibb, M. and Hong, H.-J. (2011) 'Genome-wide dynamics of a bacterial response to antibiotics that target the cell envelope', *BMC genomics*, 12, p. 226.

Hirsch, C. F. and Ensign, J. C. (1976) 'Nutritionally defined conditions for germination of *Streptomyces viridochromogenes* spores.', *Journal of bacteriology*, 126(1), pp. 13–23.

Hodgkin, D. C. (1949) 'The X-ray analysis of the structure of penicillin.', *Advancement of science*, 6(22), pp. 85–89.

Hoffman, L. R., D'Argenio, D. A., MacCoss, M. J., Zhang, Z., Jones, R. A. and Miller, S. I. (2005) 'Aminoglycoside antibiotics induce bacterial biofilm formation', *Nature*, 436(7054), pp. 1171–1175.

Hölscher, T. and Kovács, Á. T. (2017) 'Sliding on the surface: bacterial spreading without an active motor', *Environmental Microbiology*, 19(7), pp. 2537–2545.

Hong, H.-J., Hutchings, M. I., Hill, L. M. and Buttner, M. J. (2005) 'The role of the novel Fem protein VanK in vancomycin resistance in *Streptomyces coelicolor*.', *The Journal of biological chemistry*, 280(13), pp. 13055–13061.

Hong, H.-J., Paget, M. S. B. and Buttner, M. J. (2002) 'A signal transduction system in *Streptomyces coelicolor* that activates the expression of a putative cell wall glycan operon in response to vancomycin and other cell wall-specific antibiotics', *Molecular Microbiology*, 44(5), pp. 1199–1211.

Hong, H. J., Hutchings, M. I., Neu, J. M., Wright, G. D., Paget, M. S. B. and Buttner, M. J. (2004) 'Characterization of an inducible vancomycin resistance system in *Streptomyces coelicolor* reveals a novel gene (*vanK*) required for drug resistance', *Molecular Microbiology*, 52(4), pp. 1107–1121.

Hopwood, D. A. (2007) *Streptomyces in Nature and Medicine: The Antibiotic Makers*. New York: Oxford University Press.

Hutchings, M. I., Hoskisson, P. A., Chandra, G. and Buttner, M. J. (2004) 'Sensing and responding to diverse extracellular signals? Analysis of the sensor kinases and response regulators of *Streptomyces coelicolor* A3(2)', *Microbiology*, 150(9), pp. 2795–2806.

Hutchings, M. I., Hong, H. J. and Buttner, M. J. (2006) 'The vancomycin resistance VanRS two-component signal transduction system of *Streptomyces coelicolor*', *Molecular Microbiology*, 59(3), pp. 923–935.

Hutchings, M. I., Truman, A. W. and Wilkinson, B. (2019) 'Antibiotics: past, present and future', *Current opinion in microbiology*, 51, pp. 72–80.

Ishizuka, H., Horinouchi, S., Kieser, H. M., Hopwood, D. A. and Beppu, T. (1992) 'A putative two-component regulatory system involved in secondary metabolism in *Streptomyces* spp.', *Journal of bacteriology*, 174(23), pp. 7585–7594.

Jakob, U., Eser, M. and Bardwell, J. C. (2000) 'Redox switch of *hsp33* has a novel zinc-binding motif.', *The Journal of biological chemistry*, 275(49), pp. 38302–38310.

Jeong, Y., Kim, J.-N., Kim, M. W., Bucca, G., Cho, S., Yoon, Y. J., Kim, B.-G., Roe, J.-H., Kim, S. C., Smith, C. P. and Cho, B.-K. (2016) 'The dynamic transcriptional and translational landscape of the model antibiotic producer *Streptomyces coelicolor* A3(2)', *Nature Communications*, 7, p. 11605.

Joly, N., Engl, C., Jovanovic, G., Huvet, M., Toni, T., Sheng, X., Stumpf, M. P. H. and Buck, M. (2010) 'Managing membrane stress: the phage shock protein (Psp) response, from molecular mechanisms to physiology', *FEMS Microbiology Reviews*, 34(5), pp. 797–827.

Jones, S. E., Ho, L., Rees, C. A., Hill, J. E., Nodwell, J. R. and Elliot, M. A. (2017) '*Streptomyces* exploration is triggered by fungal interactions and volatile signals', *eLife*, 6, pp. 1–21.

Jones, S. E., Pham, C. A., Zambri, M. P., McKillip, J., Carlson, E. E. and Elliot, M. A. (2019) '*Streptomyces* Volatile Compounds Influence Exploration and Microbial Community Dynamics by Altering Iron Availability', *mBio*, 10(2), pp. e00171-19.

Jones, S. E. and Elliot, M. A. (2017) '*Streptomyces* Exploration: Competition, Volatile Communication and New Bacterial Behaviours.', *Trends in microbiology*, 25(7), pp. 522–531.

Jordan, S., Junker, A., Helmann, J. D. and Mascher, T. (2006) 'Regulation of LiaRS-dependent gene expression in *Bacillus subtilis*: identification of inhibitor proteins, regulator binding sites, and target genes of a conserved cell envelope stress-sensing two-component system', *Journal of bacteriology*, 188(14), pp. 5153–5166.

Kang, S. G., Jin, W., Bibb, M. and Lee, K. J. (1998) 'Actinorhodin and undecylprodigiosin production in wild-type and *relA* mutant strains of *Streptomyces coelicolor* A3(2) grown in continuous culture.', *FEMS microbiology letters*, 168(2), pp. 221–226.

Kapadia, M., Rolston, K. V. I. and Han, X. Y. (2007) 'Invasive *Streptomyces* Infections: Six Cases and Literature Review', *American Journal of Clinical Pathology*, 127(4), pp. 619–624.

Keto-Timonen, R., Hietala, N., Palonen, E., Hakakorpi, A., Lindström, M. and Korkeala, H. (2016) 'Cold Shock Proteins: A Minireview with Special Emphasis on Csp-family of Enteropathogenic *Yersinia*', *Frontiers in Microbiology*, 7, p. 1151.

Keulen, G. van, Alderson, J., White, J. and Sawers, R. G. (2007) 'The obligate aerobic actinomycete *Streptomyces coelicolor* A3(2) survives extended periods of anaerobic stress', *Environmental Microbiology*, 9(12), pp. 3143–3149.

Kieser, T., Bibb, M. J., Buttner, M. J., Chater, K. F. and Hopwood, D. A. (2000) *Practical* Streptomyces *Genetics*, *John Innes Centre Ltd.* John Innes Foundation.

Kim, Y. J., Moon, M. H., Song, J. Y., Smith, C. P., Hong, S.-K. and Chang, Y. K. (2008) 'Acidic pH shock induces the expressions of a wide range of stress-response genes', *BMC Genomics*, 9(1), p. 604.

Kleine, B., Chattopadhyay, A., Polen, T., Pinto, D., Mascher, T., Bott, M., Brocker, M. and Freudl, R. (2017) 'The three-component system EsrISR regulates a cell envelope stress response in *Corynebacterium glutamicum*', *Molecular Microbiology*, 106(5), pp. 719–741.

Körner, H., Sofia, H. J. and Zumft, W. G. (2003) 'Phylogeny of the bacterial superfamily of Crp-Fnr transcription regulators: exploiting the metabolic spectrum by controlling alternative gene programs', *FEMS Microbiology Reviews*, 27(5), pp. 559–592.

Koshland, D. E. (2002) 'The Seven Pillars of Life', *Science*, 295(5563), pp. 2215 LP – 2216.

Koteva, K., Hong, H.-J., Wang, X. D., Nazi, I., Hughes, D., Naldrett, M. J., Buttner, M. J. and Wright, G. D. (2010) 'A vancomycin photoprobe identifies the histidine kinase VanSsc as a vancomycin receptor', *Nature Chemical Biology*, 6(5), pp. 327–329.

Kwon, S. Y. and Kwon, H. J. (2013) 'The possible role of SCO3388, a *tmrB*-like gene of *Streptomyces coelicolor*, in germination and stress survival of spores', *Journal of Applied Biological Chemistry*, 56(3), pp. 165–170.

Leu, W. M., Chen, L. Y., Liaw, L. L. and Lee, Y. H. (1992) 'Secretion of the *Streptomyces* tyrosinase is mediated through its trans-activator protein, MelC1.', *The Journal of biological chemistry*, 267(28), pp. 20108–20113.

Levine, D. P. (2006) 'Vancomycin: A History', *Clinical Infectious Diseases*, 42(Supplement_1), pp. S5–S12.

Li, L., Jiang, W. and Lu, Y. (2017) 'A Novel Two-Component System, GluR-GluK, Involved in Glutamate Sensing and Uptake in *Streptomyces coelicolor*', *Journal of bacteriology*, 199(18), pp. e00097-17.

Li, R., Zhang, P., Wang, Y. and Tao, K. (2020) 'Itaconate: A Metabolite Regulates Inflammation Response and Oxidative Stress', *Oxidative medicine and cellular longevity*, 2020, p. 5404780.

Li, Y., Pinto-Tomás, A. A., Rong, X., Cheng, K., Liu, M. and Huang, Y. (2019) 'Population Genomics Insights into Adaptive Evolution and Ecological Differentiation in streptomycetes', *Applied and Environmental Microbiology*. Edited by C. Vieille, 85(7), pp. e02555-18.

Li, Yi-Chuan, Chang, C., Chang, C.-F., Cheng, Y.-H., Fang, P.-J., Yu, T., Chen, S.-C., Li, Yi-Ching, Hsiao, C.-D. and Huang, T. (2014) 'Structural dynamics of the two-component response regulator RstA in recognition of promoter DNA element', *Nucleic Acids Research*, 42(13), pp. 8777–8788.

Lindsay, W. L. (1991) 'Iron oxide solubilization by organic matter and its effect on iron availability', *Plant and Soil*, 130, pp. 27–34.

Liot, Q. and Constant, P. (2016) 'Breathing air to save energy--new insights into the ecophysiological role of high-affinity [NiFe]-hydrogenase in *Streptomyces avermitilis*.', *MicrobiologyOpen*, 5(1), pp. 47–59.

Lis, M. and Walther, D. (2016) 'The orientation of transcription factor binding site motifs in gene promoter regions: does it matter?', *BMC Genomics*, 17(1), p. 185.

Liu, M., Zhang, P., Zhu, Y., Lu, T., Wang, Y., Cao, G., Shi, M., Chen, X.-L., Tao, M. and Pang, X. (2019) 'Novel Two-Component System MacRS Is a Pleiotropic Regulator That Controls Multiple Morphogenic Membrane Protein Genes in *Streptomyces coelicolor*.', *Applied and environmental microbiology*, 85(4), pp. e02178--18.

Liu, Y., Beyer, A. and Aebersold, R. (2016) 'On the Dependency of Cellular Protein Levels on mRNA Abundance.', *Cell*, 165(3), pp. 535–550.

Lobanovska, M. and Pilla, G. (2017) 'Penicillin's Discovery and Antibiotic Resistance: Lessons for the Future?', *The Yale journal of biology and medicine*, 90(1), pp. 135–145.

Long, C. P., Gonzalez, J. E., Feist, A. M., Palsson, B. O. and Antoniewicz, M. R. (2017) 'Fast growth phenotype of E. coli K-12 from adaptive laboratory evolution does not require intracellular flux rewiring', *Metabolic engineering*, 44, pp. 100–107.

Loomba, P. S., Taneja, J. and Mishra, B. (2010) 'Methicillin and Vancomycin Resistant *S. aureus* in Hospitalized Patients', *Journal of global infectious diseases*, 2(3), pp. 275–283.

Lu, Y., He, J., Zhu, H., Yu, Z., Wang, R., Chen, Y., Dang, F., Zhang, W., Yang, S. and Jiang, W. (2011) 'An Orphan Histidine Kinase, OhkA, Regulates Both Secondary Metabolism and Morphological Differentiation in *Streptomyces coelicolor*', *Journal of Bacteriology*, 193(12), pp. 3020–3032.

Ludwig, W., Euzéby, J., Schumann, P., Busse, H.-J., Trujillo, M. E., Kämpfer, P. and Whitman, W. B. (2015) 'Road map of the phylum Actinobacteria', *Bergey's Manual of Systematics of Archaea and Bacteria*. (Major Reference Works), pp. 1–37.

Macek, B., Forchhammer, K., Hardouin, J., Weber-Ban, E., Grangeasse, C. and Mijakovic, I. (2019) 'Protein post-translational modifications in bacteria', *Nature Reviews Microbiology*, 17(11), pp. 651–664.

Mackie, G. A. (2013) 'RNase E: at the interface of bacterial RNA processing and decay', *Nature Reviews Microbiology*, 11(1), pp. 45–57.

MacNeil, D. J., Gewain, K. M., Ruby, C. L., Dezeny, G., Gibbons, P. H. and MacNeil, T. (1992) 'Analysis of *Streptomyces avermitilis* genes required for avermectin biosynthesis utilizing a novel integration vector.', *Gene*, 111(1), pp. 61–68.

Madan Babu, M. and Teichmann, S. A. (2003) 'Evolution of transcription factors and the gene regulatory network in *Escherichia coli*', *Nucleic acids research*, 31(4), pp. 1234–1244.

Martín-Martín, S., Rodríguez-García, A., Santos-Beneit, F., Franco-Domínguez, E., Sola-Landa, A. and Martín, J. F. (2017) 'Self-control of the PHO regulon: the PhoP-dependent protein PhoU controls negatively expression of genes of PHO regulon in *Streptomyces coelicolor*', *The Journal Of Antibiotics*, 71, p. 113.

Martín-Mora, D., Ortega, Á., Matilla, M. A., Martínez-Rodríguez, S., Gavira, J. A. and Krell, T. (2019) 'The Molecular Mechanism of Nitrate Chemotaxis via Direct Ligand Binding to the PilJ Domain of McpN', *mBio*, 10(1), pp. e02334-18.

Martín, J. F., Rodríguez-García, A. and Liras, P. (2017) 'The master regulator PhoP coordinates phosphate and nitrogen metabolism, respiration, cell differentiation and antibiotic biosynthesis: Comparison in *Streptomyces coelicolor* and *Streptomyces avermitilis*', *Journal of Antibiotics*, 70(5), pp. 534–541.

Martinez, L. F., Bishop, A., Parkes, L., Del Sol, R., Salerno, P., Sevcikova, B., Mazurakova, V., Kormanec, J. and Dyson, P. (2009) 'Osmoregulation in *Streptomyces coelicolor*: Modulation of SigB activity by OsaC', *Molecular Microbiology*, 71(5), pp. 1250–1262.

Martínez-Argudo, I., Salinas, P., Maldonaldo, R. and Contreras A. (2002) 'Domain Interactions on the *ntr* Signal Transduction Pathway: Two-Hybrid Analysis of Mutant and Truncated Derivatives of Histidine Kinase NtrB', *Journal of Bacteriology*, 184(1), pp. 200-206.

van der Maten, E., van den Broek, B., de Jonge, M. I., Rensen, K. J. W., Eleveld, M. J., Zomer, A. L., Cremers, A. J. H., Ferwerda, G., de Groot, R., Langereis, J. D. and van der Flier, M. (2018) '*Streptococcus pneumoniae* PspC Subgroup Prevalence in Invasive Disease and Differences in Contribution to Complement Evasion', *Infection and immunity*, 86(4), pp. e00010-18.

McCormick, J. R. and Flärdh, K. (2012) 'Signals and regulators that govern *Streptomyces* development', *FEMS Microbiology Reviews*, 36(1), pp. 206–231.

Mclean, T. C., Lo, R., Tschowri, N., Hoskisson, P. A., Bassam, M. M. Al, Hutchings, I. and Som, N. F. (2019) 'Sensing and responding to diverse extracellular signals : an updated analysis of the sensor kinases and response regulators of *Streptomyces* species', *Microbiology*, 165(9), pp. 1–24.

McLean, T. C., Wilkinson, B., Hutchings, M. I. and Devine, R. (2019) 'Dissolution of the Disparate: Co-ordinate Regulation in Antibiotic Biosynthesis', *Antibiotics (Basel, Switzerland)*, 8(2), p. 83.

McLean, T. C., Hoskisson, P. A. and Seipke, R. F. (2016) 'Coordinate Regulation of Antimycin and Candicidin Biosynthesis', *mSphere*, 1(6), pp. e00305-16.

McManus, J., Cheng, Z. and Vogel, C. (2015) 'Next-generation analysis of gene expression regulation – comparing the roles of synthesis and degradation', *Molecular BioSystems*, 11(10), pp. 2680–2689.

Mendes, M. V, Tunca, S., Antón, N., Recio, E., Sola-Landa, A., Aparicio, J. F. and

Martín, J. F. (2007) 'The two-component *phoR-phoP* system of *Streptomyces natalensis*: Inactivation or deletion of *phoP* reduces the negative phosphate regulation of pimaricin biosynthesis', *Metabolic Engineering*, 9(2), pp. 217–227.

Mika, F. and Hengge, R. (2005) 'A two-component phosphotransfer network involving ArcB, ArcA, and RssB coordinates synthesis and proteolysis of σS (RpoS) in *E. coli*', *Genes & Development*, 19(22), pp. 2770–2781.

Millán-Aguiñaga, N., Soldatou, S., Brozio, S., Munnoch, J. T., Howe, J., Hoskisson, P. A. and Duncan, K. R. (2019) 'Awakening ancient polar Actinobacteria: diversity, evolution and specialized metabolite potential', *Microbiology*, 165(11), pp. 1169–1180.

Möker, N., Brocker, M., Schaffer, S., Krämer, R., Morbach, S. and Bott, M. (2004) 'Deletion of the genes encoding the MtrA-MtrB two-component system of *Corynebacterium glutamicum* has a strong influence on cell morphology, antibiotics susceptibility and expression of genes involved in osmoprotection', *Molecular Microbiology*, 54(2), pp. 420–438.

Munnoch, J. T., Martinez, M. T. P., Svistunenko, D. A., Crack, J. C., Le Brun, N. E. and Hutchings, M. I. (2016) 'Characterization of a putative NsrR homologue in *Streptomyces venezuelae* reveals a new member of the Rrf2 superfamily', *Scientific Reports*, 6, p. 31597.

Murray, T. S. and Kazmierczak, B. I. (2008) '*Pseudomonas aeruginosa* Exhibits Sliding Motility in the Absence of Type IV Pili and Flagella', *Journal of Bacteriology*, 190(8), pp. 2700 LP – 2708.

Myronovskyi, M., Welle, E., Fedorenko, V. and Luzhetskyy, A. (2011) 'β-Glucuronidase as a Sensitive and Versatile Reporter in actinomycetes', *Applied and Environmental Microbiology*, 77(15), pp. 5370–5383.

Nakamura, A. M., Nascimento, A. S. and Polikarpov, I. (2017) 'Structural diversity of carbohydrate esterases', *Biotechnology Research and Innovation*, 1(1), pp. 35–51.

Narayanan, A., Kumar, S., Evrard, A. N., Paul, L. N. and Yernool, D. A. (2014) 'An asymmetric heterodomain interface stabilizes a response regulator–DNA complex', *Nature Communications*, 5(1), p. 3282.

Nelson, M. L., Dinardo, A., Hochberg, J. and Armelagos, G. J. (2010) 'Brief communication: Mass spectroscopic characterization of tetracycline in the skeletal remains of an ancient population from Sudanese Nubia 350–550 CE', *American Journal of Physical Anthropology*, 143(1), pp. 151–154.

Nguyen, K. T., Piastro, K., Gray, T. A. and Derbyshire, K. M. (2010) 'Mycobacterial Biofilms Facilitate Horizontal DNA Transfer between Strains of *Mycobacterium smegmatis*', *Journal of Bacteriology*, 192(19), pp. 5134–5142.

Nixon, B. T., Ronson, C. W. and Ausubel, F. M. (1986) 'Two-component regulatory systems responsive to environmental stimuli share strongly conserved domains with the nitrogen assimilation regulatory genes ntrB and ntrC.', *Proceedings of the National Academy of Sciences of the United States of America*, 83(20), pp. 7850–7854.

Noda, Y., Yoda, K., Takatsuki, A. and Yamasaki, M. (1992) 'TmrB protein, responsible for tunicamycin resistance of *Bacillus subtilis*, is a novel ATP-binding membrane protein', *Journal of bacteriology*, 174(13), pp. 4302–4307.

Nothaft, H., Dresel, D., Willimek, A., Mahr, K., Niederweis, M. and Titgemeyer, F. (2003) 'The phosphotransferase system of *Streptomyces coelicolor* is biased for N-acetylglucosamine metabolism', *Journal of bacteriology*, 185(23), pp. 7019–7023.

O'Neill, J. (2016) 'Tackling drug-resistant infections globally: final report and recommendations', 1(May).

O'Neill, M., Summers, E. and Collins (Firm : Bishopbriggs, S. (2015) *Collins English dictionary*.

Obanye, A. I. C., Hobbs, G., Gardner, D. C. J. and Oliver, S. G. (1996) 'Correlation between carbon flux through the pentose phosphate pathway and production of the antibiotic methylenomycin in *Streptomyces coelicolor* A3(2)', *Microbiology*, 142(1), pp. 133–137.

Ortiz De Orué Lucana, D. and Groves, M. R. (2009) 'The three-component signalling system HbpS-SenS-SenR as an example of a redox sensing pathway in bacteria', *Amino Acids*, 37(3), pp. 479–486.

Osei Sekyere, J. (2018) 'Candida auris: A systematic review and meta-analysis of current updates on an emerging multidrug-resistant pathogen', *MicrobiologyOpen*, 7(4), pp. e00578–e00578.

Otten, H. (1986) 'Domagk and the development of the sulphonamides', *Journal of Antimicrobial Chemotherapy*, 17(6), pp. 689–690.

Paget, M. S., Chamberlin, L., Atrih, A., Foster, S. J. and Buttner, M. J. (1999) 'Evidence that the extracytoplasmic function sigma factor SigmaE is required for normal cell wall structure in *Streptomyces coelicolor* A3(2)', *Journal of bacteriology*, 181(1), pp. 204–211.

Paget, M. S. B., Leibovitz, E. and Buttner, M. J. (1999) 'A putative two-component signal transduction system regulates σ(E), a sigma factor required for normal cell wall integrity in *Streptomyces coelicolor* A3(2)', *Molecular Microbiology*, 33(1), pp. 97–107.

Palleroni, N. J. (1976) 'Chemotaxis in *Actinoplanes*.', *Archives of microbiology*, 110(1), pp. 13–18.

Paolo, S. S., Huang, J., Cohen, S. N. and Thompson, C. J. (2006) '*rag* genes: novel components of the RamR regulon that trigger morphological differentiation in *Streptomyces coelicolor*', *Molecular Microbiology*, 61(5), pp. 1167–1186.

Parche, S., Nothaft, H., Kamionka, A. and Titgemeyer, F. (2000) 'Sugar uptake and utilisation in *Streptomyces coelicolor*: a PTS view to the genome', *Antonie van Leeuwenhoek*, 78(3), pp. 243–251.

Paredes-Sabja, D., Setlow, P. and Sarker, M. R. (2011) 'Germination of spores of *Bacillales* and *Clostridiales* species: mechanisms and proteins involved.', *Trends in microbiology*, 19(2), pp. 85–94.

Perković, I., Beus, M., Schols, D., Persoons, L. and Zorc, B. (2020) 'Itaconic acid hybrids as potential anticancer agents', *Molecular Diversity*.

Piette, A., Derouaux, A., Gerkens, P., Noens, E. E. E., Mazzucchelli, G., Vion, S., Koerten, H. K., Titgemeyer, F., De Pauw, E., Leprince, P., van Wezel, G. P., Galleni, M. and Rigali, S. (2005) 'From Dormant to Germinating Spores of *Streptomyces coelicolor* A3(2): New Perspectives from the *crp* Null Mutant', *Journal of Proteome Research*, 4(5), pp. 1699–1708.

Piraee, M., White, R. L. and Vining, L. C. (2004) 'Biosynthesis of the dichloroacetyl component of chloramphenicol in *Streptomyces venezuelae* ISP5230: genes required for halogenation', *Microbiology*, 150(1), pp. 85–94.

Pomposiello, P. J. and Demple, B. (2001) 'Redox-operated genetic switches: the SoxR and OxyR transcription factors.', *Trends in biotechnology*, 19(3), pp. 109–114.

Potter, C. A., Ward, A., Laguri, C., Williamson, M. P., Henderson, P. J. F. and Phillips-Jones, M. K. (2002) 'Expression, Purification and Characterisation of Full-length Histidine Protein Kinase RegB from *Rhodobacter sphaeroides*', *Journal of Molecular Biology*, 320(2), pp. 201–213.

Prudence, S. M. M., Addington, E., Castaño-Espriu, L., Mark, D. R., Pintor-Escobar, L., Russell, A. H. and McLean, T. C. (2020) 'Advances in actinomycete research: an ActinoBase review of 2019', *Microbiology (Reading, England)*, 166(8), pp. 683–694.

Purushotham, G., Sarva, K. B., Blaszczyk, E., Rajagopalan, M. and Madiraju, M. V (2015) '*Mycobacterium tuberculosis oriC* sequestration by MtrA response regulator', *Molecular microbiology*, 98(3), pp. 586–604.

Qin, W., Qin, K., Zhang, Y., Jia, W., Chen, Y., Cheng, B., Peng, L., Chen, N., Liu, Y., Zhou, W., Wang, Y.-L., Chen, X. and Wang, C. (2019) 'S-glycosylation-based cysteine profiling reveals regulation of glycolysis by itaconate', *Nature Chemical Biology*, 15(10), pp. 983–991.

Qin, Z., Munnoch, J. T., Devine, R., Holmes, N. A., Seipke, R. F., Wilkinson, K. A., Wilkinson, B. and Hutchings, M. I. (2017) 'Formicamycins, antibacterial polyketides produced by *Streptomyces formicae* isolated from African *Tetraponera* plant-ants', *Chemical Science*, 8(4), pp. 3218–3227.

Quon, K. C., Marczynski, G. T. and Shapiro, L. (1996) 'Cell Cycle Control by an Essential Bacterial Two-Component Signal Transduction Protein', *Cell*, 84(1), pp. 83–93.

Ramos, I., Dietrich, L. E. P., Price-Whelan, A. and Newman, D. K. (2010) 'Phenazines affect biofilm formation by Pseudomonas aeruginosa in similar ways at various scales', *Research in microbiology*, 161(3), pp. 187–191.

Rapun-Araiz, B., Haag, A. F., De Cesare, V., Gil, C., Dorado-Morales, P., Penades, J. R. and Lasa, I. (2020) 'Systematic Reconstruction of the Complete Two-Component Sensorial Network in *Staphylococcus aureus*', *mSystems*, 5(4), pp. e00511-20.

Rauniyar, N. and Yates, J. R. (2014) 'Isobaric Labeling-Based Relative Quantification in Shotgun Proteomics', *Journal of Proteome Research*, 13(12), pp. 5293–5309.

Rawlings, N. D., Barrett, A. J., Thomas, P. D., Huang, X., Bateman, A. and Finn, R. D. (2018) 'The MEROPS database of proteolytic enzymes, their substrates and inhibitors

in 2017 and a comparison with peptidases in the PANTHER database', *Nucleic Acids Research*, 46(D1), pp. D624–D632.

Rico, S., Santamaría, R. I., Yepes, A., Rodríguez, H., Laing, E., Bucca, G., Smith, C. P. and Díaz, M. (2014) 'Deciphering the regulon of *Streptomyces coelicolor* AbrC3, a positive response regulator of antibiotic production', *Applied and Environmental Microbiology*, 80(8), pp. 2417–2428.

Risdian, C., Mozef, T. and Wink, J. (2019) 'Biosynthesis of Polyketides in *Streptomyces*', *Microorganisms*, 7(5), p. 124.

Rodríguez, H., Rico, S., Yepes, A., Franco-Echevarría, E., Antoraz, S., Santamaría, R. I. and Díaz, M. (2015) 'The two kinases, AbrC1 and AbrC2, of the atypical two-component system AbrC are needed to regulate antibiotic production and differentiation in *Streptomyces coelicolor*', *Frontiers in Microbiology*, 6(MAY), pp. 1–9.

Roemer, T. and Krysan, D. J. (2014) 'Antifungal drug development: challenges, unmet clinical needs, and new approaches', *Cold Spring Harbor perspectives in medicine*, 4(5), p. a019703.

Rohwer, J. M., Meadow, N. D., Roseman, S., Westerhoff, H. V and Postma, P. W. (2000) 'Understanding glucose transport by the bacterial phosphoenolpyruvate:glycose phosphotransferase system on the basis of kinetic measurements *in vitro*.', *The Journal of biological chemistry*, 275(45), pp. 34909–34921.

Romero-Rodríguez, A., Rocha, D., Ruiz-Villafan, B., Tierrafría, V., Rodríguez-Sanoja, R., Segura-González, D. and Sánchez, S. (2016) 'Transcriptomic analysis of a classical model of carbon catabolite regulation in *Streptomyces coelicolor*', *BMC Microbiology*, 16(1), p. 77.

Romero-Rodríguez, A., Robledo-Casados, I. and Sánchez, S. (2015) 'An overview on transcriptional regulators in *Streptomyces*', *Biochimica et Biophysica Acta - Gene Regulatory Mechanisms*.

Rozas, D., Gullón, S. and Mellado, R. P. (2012) 'A Novel Two-Component System Involved in the Transition to Secondary Metabolism in *Streptomyces coelicolor*', *PLoS ONE*. Edited by M. Polymenis, 7(2), p. e31760.

Ruban-Ośmiałowska, B., Jakimowicz, D., Smulczyk-Krawczyszyn, A., Chater, K. F. and Zakrzewska-Czerwińska, J. (2006) 'Replisome localization in vegetative and aerial hyphae of *Streptomyces coelicolor*.', *Journal of bacteriology*, 188(20), pp. 7311–7316.

Sánchez, L. and Braña, A. F. (1996) 'Cell density influences antibiotic biosynthesis in *Streptomyces clavuligerus*.', *Microbiology (Reading, England)*, 142 (Pt 5, pp. 1209–1220.

Santos-Beneit, F., Rodríguez-García, A., Sola-Landa, A. and Martín, J. F. (2009a) 'Cross-talk between two global regulators in *Streptomyces*: PhoP and AfsR interact in the control of *afsS*, *pstS* and *phoRP* transcription', *Molecular Microbiology*, 72(1), pp. 53–68.

Santos-Beneit, F., Rodríguez-García, A., Apel, A. K. and Martín, J. F. (2009b)

'Phosphate and carbon source regulation of two PhoP-dependent glycerophosphodiester phosphodiesterase genes of *Streptomyces coelicolor*', *Microbiology*, 155(6), pp. 1800–1811.

Sauer, U. and Eikmanns, B. J. (2005) 'The PEP-pyruvate-oxaloacetate node as the switch point for carbon flux distribution in bacteria.', *FEMS microbiology reviews*, 29(4), pp. 765–794.

Schatz, A., Bugle, E. and Waksman, S. A. (1944) 'Streptomycin, a Substance Exhibiting Antibiotic Activity Against Gram-Positive and Gram-Negative Bacteria.', *Proceedings of the Society for Experimental Biology and Medicine*, 55(1), pp. 66–69.

Schmidl, S. R., Sheth, R. U., Wu, A. and Tabor, J. J. (2014) 'Refactoring and Optimization of Light-Switchable *Escherichia coli* Two-Component Systems', *ACS Synthetic Biology*, 3(11), pp. 820–831.

Schmidl, S. R., Ekness, F., Sofjan, K., Daeffler, K. N.-M., Brink, K. R., Landry, B. P., Gerhardt, K. P., Dyulgyarov, N., Sheth, R. U. and Tabor, J. J. (2019) 'Rewiring bacterial two-component systems by modular DNA-binding domain swapping', *Nature Chemical Biology*, 15(7), pp. 690–698.

Schobert, M. and Görisch, H. (2001) 'A soluble two-component regulatory system controls expression of quinoprotein ethanol dehydrogenase (QEDH) but not expression of cytochrome c550 of the ethanol-oxidation system in *Pseudomonas aeruginosa*', *Microbiology*, 147(2), pp. 363–372.

Schrempf, H., Koebsch, I., Walter, S., Engelhardt, H. and Meschke, H. (2011) 'Extracellular *Streptomyces* vesicles: amphorae for survival and defence', *Microbial biotechnology*, 4(2), pp. 286–299.

Schulz-Bohm, K., Martín-Sánchez, L. and Garbeva, P. (2017) 'Microbial Volatiles: Small Molecules with an Important Role in Intra- and Inter-Kingdom Interactions', *Frontiers in microbiology*, 8, p. 2484.

Schumacher, M. A., Zeng, W., Findlay, K. C., Buttner, M. J., Brennan, R. G. and Tschowri, N. (2017) 'The *Streptomyces* master regulator BldD binds c-di-GMP sequentially to create a functional BldD2-(c-di-GMP)4 complex', *Nucleic acids research*, 45(11), pp. 6923–6933.

Seipke, R. F., Kaltenpoth, M. and Hutchings, M. I. (2012) '*Streptomyces* as symbionts: an emerging and widespread theme?', *FEMS microbiology reviews*, 36(4), pp. 862–76.

Sekurova, O. N., Zhang, J., Kristiansen, K. A. and Zotchev, S. B. (2016) 'Activation of chloramphenicol biosynthesis in *Streptomyces venezuelae* ATCC 10712 by ethanol shock: insights from the promoter fusion studies', *Microbial cell factories*, 15, p. 85.

Sexton, D. L., St-Onge, R. J., Haiser, H. J., Yousef, M. R., Brady, L., Gao, C., Leonard, J. and Elliot, M. A. (2015) 'Resuscitation-promoting factors are cell wall-lytic enzymes with important roles in the germination and growth of *Streptomyces coelicolor*.', *Journal of bacteriology*, 197(5), pp. 848–860.

Shah, I. M., Laaberki, M.-H., Popham, D. L. and Dworkin, J. (2008) 'A eukaryotic-like Ser/Thr kinase signals bacteria to exit dormancy in response to peptidoglycan

fragments.', *Cell*, 135(3), pp. 486–496.

Sharif, E. U. and O'Doherty, G. A. (2012) 'Biosynthesis and Total Synthesis Studies on The Jadomycin Family of Natural Products', *European journal of organic chemistry*, 2012(11), p. 10.1002/ejoc.201101609.

Shevchenko, A., Tomas, H., Havli, J., Olsen, J. V and Mann, M. (2006) 'In-gel digestion for mass spectrometric characterization of proteins and proteomes', *Nature Protocols*, 1(6), pp. 2856–2860.

Shin, J.-H., Singh, A. K., Cheon, D.-J. and Roe, J.-H. (2011) 'Activation of the SoxR Regulon in *Streptomyces coelicolor* by the Extracellular Form of the Pigmented Antibiotic Actinorhodin', *Journal of Bacteriology*, 193(1), pp. 75 LP – 81.

Shu, D., Chen, L., Wang, W., Yu, Z., Ren, C., Zhang, W., Yang, S., Lu, Y. and Jiang, W. (2008) '*afsQ1-Q2-sigQ* is a pleiotropic but conditionally required signal transduction system for both secondary metabolism and morphological development in *Streptomyces coelicolor*', *Applied Microbiology and Biotechnology*, 81(6), p. 1149.

Silver, L. L. (2011) 'Challenges of antibacterial discovery', *Clinical microbiology reviews*, 24(1), pp. 71–109.

Sola-Landa, A., Rodríguez-García, A., Franco-Domínguez, E. and Martín, J. F. (2005) 'Binding of PhoP to promoters of phosphate-regulated genes in *Streptomyces coelicolor*: identification of PHO boxes', *Molecular Microbiology*, 56(5), pp. 1373–1385.

Sola-Landa, A., Rodríguez-García, A., Apel, A. K. and Martín, J. F. (2008) 'Target genes and structure of the direct repeats in the DNA-binding sequences of the response regulator PhoP in *Streptomyces coelicolor*', *Nucleic acids research*, 36(4), pp. 1358–1368.

Sola-Landa, A., Moura, R. S. and Martín, J. F. (2003) 'The two-component PhoR-PhoP system controls both primary metabolism and secondary metabolite biosynthesis in *Streptomyces lividans*', *Proceedings of the National Academy of Sciences*, 100(10), pp. 6133 LP – 6138.

Som, N. F., Heine, D., Holmes, N. A., Munnoch, J. T., Chandra, G., Seipke, R. F., Hoskisson, P. A., Wilkinson, B. and Hutchings, M. I. (2017) 'The conserved actinobacterial two-component system MtrAB coordinates chloramphenicol production with sporulation in *Streptomyces venezuelae* NRRL B-65442', *Frontiers in Microbiology*, 8(JUN), pp. 1–11.

Som, N. F., Heine, D., Holmes, N. A., Knowles, F., Chandra, G., Seipke, R. F., Hoskisson, P. A., Wilkinson, B. and Hutchings, M. I. (2017) 'The MtrAB two-component system controls antibiotic production in *Streptomyces coelicolor* A3(2)', *Microbiology (Reading, England)*, 163(10), pp. 1415–1419.

Sommer, E., Koler, M., Frank, V., Sourjik, V. and Vaknin, A. (2013) 'The Sensory Histidine Kinases TorS and EvgS Tend to Form Clusters in *Escherichia coli* Cells', *PLOS ONE*, 8(10), p. e77708.

Song, J. Y., Kim, E. S., Kim, D. W., Jensen, S. E. and Lee, K. J. (2009) 'A gene located downstream of the clavulanic acid gene cluster in *Streptomyces clavuligerus* ATCC

27064 encodes a putative response regulator that affects clavulanic acid production', *Journal of Industrial Microbiology & Biotechnology*, 36(2), pp. 301–311.

Sorsby, A., Ungar, J. and Crick, R. P. (1953) 'Aureomycin, chloramphenicol, and terramycin in ophthalmology', *British medical journal*, 2(4831), pp. 301–304.

Stanley, N. R., Britton, R. A., Grossman, A. D. and Lazazzera, B. A. (2003) 'Identification of catabolite repression as a physiological regulator of biofilm formation by *Bacillus subtilis* by use of DNA microarrays.', *Journal of bacteriology*, 185(6), pp. 1951–1957.

Stapleton, P. D. and Taylor, P. W. (2002) 'Methicillin resistance in *Staphylococcus aureus:* mechanisms and modulation', *Science progress*, 85(Pt 1), pp. 57–72.

Stetefeld, J., McKenna, S. A. and Patel, T. R. (2016) 'Dynamic light scattering: a practical guide and applications in biomedical sciences', *Biophysical reviews*, 8(4), pp. 409–427.

Stevenson, C. E. M., Assaad, A., Chandra, G., Le, T. B. K., Greive, S. J., Bibb, M. J. and Lawson, D. M. (2013) 'Investigation of DNA sequence recognition by a streptomycete MarR family transcriptional regulator through surface plasmon resonance and X-ray crystallography', *Nucleic acids research*, 41(14), pp. 7009–7022.

Stincone, A., Prigione, A., Cramer, T., Wamelink, M. M. C., Campbell, K., Cheung, E., Olin-Sandoval, V., Grüning, N.-M., Krüger, A., Tauqeer Alam, M., Keller, M. A., Breitenbach, M., Brindle, K. M., Rabinowitz, J. D. and Ralser, M. (2015) 'The return of metabolism: biochemistry and physiology of the pentose phosphate pathway.', *Biological reviews of the Cambridge Philosophical Society*, 90(3), pp. 927–963.

Stock, A. M., Robinson, V. L. and Goudreau, P. N. (2000) 'Two-Component Signal Transduction', *Annual Review of Biochemistry*, 69(1), pp. 183–215.

Studier, F. W. and Moffatt, B. A. (1986) 'Use of bacteriophage T7 RNA polymerase to direct selective high-level expression of cloned genes.', *Journal of molecular biology*, 189(1), pp. 113–130.

Süssmuth, R. D. and Mainz, A. (2017) 'Nonribosomal Peptide Synthesis—Principles and Prospects', *Angewandte Chemie International Edition*, 56(14), pp. 3770–3821.

Swint-Kruse, L. and Matthews, K. S. (2009) 'Allostery in the LacI/GalR family: variations on a theme', *Current opinion in microbiology*, 12(2), pp. 129–137.

Taguchi, T., Ebihara, T., Furukawa, A., Hidaka, Y., Ariga, R., Okamoto, S. and Ichinose, K. (2012) 'Identification of the actinorhodin monomer and its related compound from a deletion mutant of the *actVA-ORF4* gene of *Streptomyces coelicolor* A3(2)', *Bioorganic & Medicinal Chemistry Letters*, 22(15), pp. 5041–5045.

Taguchi, T., Maruyama, T., Sawa, R., Igarashi, M., Okamoto, S. and Ichinose, K. (2015) 'Structure and biosynthetic implication of 5R-(N-acetyl-L-cysteinyl)-14S-hydroxy-dihydrokalafungin from a mutant of the *actVA-ORF4* gene for actinorhodin biosynthesis in *Streptomyces coelicolor* A3(2)', *The Journal of Antibiotics*, 68(7), pp. 481–483.

Tahlan, K., Ahn, S. K., Sing, A., Bodnaruk, T. D., Willems, A. R., Davidson, A. R. and Nodwell, J. R. (2007) 'Initiation of actinorhodin export in *Streptomyces coelicolor*.',

Molecular microbiology, 63(4), pp. 951–961.

Tahlan, K., Yu, Z., Xu, Y., Davidson, A. R. and Nodwell, J. R. (2008) 'Ligand recognition by ActR, a TetR-like regulator of actinorhodin export.', *Journal of molecular biology*, 383(4), pp. 753–761.

Tan, S., Tan, H. T. and Chung, M. C. M. (2008) 'Membrane proteins and membrane proteomics', *PROTEOMICS*, 8(19), pp. 3924–3932.

Thompson, A., Schäfer, J., Kuhn, K., Kienle, S., Schwarz, J., Schmidt, G., Neumann, T. and Hamon, C. (2003) 'Tandem Mass Tags: A Novel Quantification Strategy for Comparative Analysis of Complex Protein Mixtures by MS/MS', *Analytical Chemistry*, 75(8), pp. 1895–1904.

Titgemeyer, F., Walkenhorst, J., Reizer, J., Stuiver, M. H., Cui, X. and Saier, M. H. (1995) 'Identification and characterization of phosphoenolpyruvate: fructose phosphotransferase systems in three *Streptomyces* species', *Microbiology*, 141(1), pp. 51–58.

Tong, Y., Whitford, C. M., Robertsen, H. L., Blin, K., Jørgensen, T. S., Klitgaard, A. K., Gren, T., Jiang, X., Weber, T. and Lee, S. Y. (2019) 'Highly efficient DSB-free base editing for streptomycetes with CRISPR-BEST', *Proceedings of the National Academy of Sciences*, 116(41), pp. 20366 LP – 20375.

Tran, N. T., Huang, X., Hong, H.-J., Bush, M. J., Chandra, G., Pinto, D., Bibb, M. J., Hutchings, M. I., Mascher, T. and Buttner, M. J. (2019) 'Defining the regulon of genes controlled by σE, a key regulator of the cell envelope stress response in *Streptomyces coelicolor*', *Molecular Microbiology*, 112(2), pp. 461–481.

Tseng, H. -C and Chen, C. W. (1991) 'A cloned *ompR*-like gene of *Streptomyces lividans* 66 suppresses defective *melC1*, a putative copper-transfer gene', *Molecular Microbiology*, 5(5), pp. 1187–1196.

Tsuge, Y., Ogino, H., Teramoto, H., Inui, M. and Yukawa, H. (2008) 'Deletion of cgR_1596 and cgR_2070, encoding NlpC/P60 proteins, causes a defect in cell separation in Corynebacterium glutamicum R', *Journal of bacteriology*, 190(24), pp. 8204–8214.

Tsujibo, H., Hatano, N., Okamoto, T., Endo, H., Miyamoto, K. and Inamori, Y. (1999) 'Synthesis of chitinase in *Streptomyces thermoviolaceus* is regulated by a two-component sensor-regulator system', *FEMS Microbiology Letters*, 181(1), pp. 83–90.

Tyanova, S., Temu, T. and Cox, J. (2016) 'The MaxQuant computational platform for mass spectrometry-based shotgun proteomics.', *Nature protocols*, 11(12), pp. 2301–2319.

Ueatrongchit, T. and Asano, Y. (2011) 'Highly selective l-threonine 3-dehydrogenase from *Cupriavidus necator* and its use in determination of l-threonine', *Analytical Biochemistry*, 410(1), pp. 44–56.

Ulrich, L. E., Koonin, E. V. and Zhulin, I. B. (2005) 'One-component systems dominate signal transduction in prokaryotes', *Trends in microbiology*, 13(2), pp. 52-56.

Valent, P., Groner, B., Schumacher, U., Superti-Furga, G., Busslinger, M., Kralovics, R., Zielinski, C., Penninger, J. M., Kerjaschki, D., Stingl, G., Smolen, J. S., Valenta, R.,

Lassmann, H., Kovar, H., Jäger, U., Kornek, G., Müller, M. and Sörgel, F. (2016) 'Paul Ehrlich (1854-1915) and His Contributions to the Foundation and Birth of Translational Medicine', *Journal of Innate Immunity*, 8(2), pp. 111–120.

Ventola, C. L. (2015) 'The antibiotic resistance crisis: part 1: causes and threats', *P & T : a peer-reviewed journal for formulary management*, 40(4), pp. 277–283.

Vicente, R. L., Gullón, S., Marín, S. and Mellado, R. P. (2016) 'The Three *Streptomyces lividans* HtrA-Like Proteases Involved in the Secretion Stress Response Act in a Cooperative Manner', *PLOS ONE*, 11(12), p. e0168112.

Vogel, C. and Marcotte, E. M. (2012) 'Insights into the regulation of protein abundance from proteomic and transcriptomic analyses', *Nature reviews. Genetics*, 13(4), pp. 227–232.

Vollmer, W. (2008) 'Structural variation in the glycan strands of bacterial peptidoglycan', *FEMS Microbiology Reviews*, 32(2), pp. 287–306.

Vrancken, K., Van Mellaert, L. and Anné, J. (2008) 'Characterization of the *Streptomyces lividans* PspA response', *Journal of bacteriology*, 190(10), pp. 3475–3481.

Vreeland, R. H., Rosenzweig, W. D. and Powers, D. W. (2000) 'Isolation of a 250 million-year-old halotolerant bacterium from a primary salt crystal', *Nature*, 407(6806), pp. 897–900.

Waksman, S. A. and Henrici, A. T. (1943) 'The Nomenclature and Classification of the actinomycetes', *Journal of Bacteriology*, 46(4), pp. 337 LP – 341.

Waksman, S. A., Schatz, A. and Reynolds, D. M. (1946) 'Production of antibiotic substances by actinomycetes.', *Annals of the New York Academy of Sciences*, 1213, pp. 112–124.

Waksman, S. A. and Woodruff, H. B. (1940) 'Bacteriostatic and Bactericidal Substances Produced by a Soil *Actinomyces*.', *Proceedings of the Society for Experimental Biology and Medicine*, 45(2), pp. 609–614.

Wang, C., Ge, H., Dong, H., Zhu, C., Li, Y., Zheng, J. and Cen, P. (2007) 'A novel pair of two-component signal transduction system *ecrE1/ecrE2* regulating antibiotic biosynthesis in *Streptomyces coelicolor*', *Biologia*, 62(5), pp. 511–516.

Wang, R., Mast, Y., Wang, J., Zhang, W., Zhao, G., Wohlleben, W., Lu, Y. and Jiang, W. (2013) 'Identification of two-component system AfsQ1/Q2 regulon and its cross-regulation with GlnR in *Streptomyces coelicolor*', *Molecular Microbiology*, 87(1), pp. 30–48.

Wang, X., Ni, M., Niu, C., Zhu, X., Zhao, T., Zhu, Z., Xuan, Y. and Cong, W. (2014) 'Simple detection of phosphoproteins in SDS-PAGE by quercetin', *EuPA Open Proteomics*, 4, pp. 156–164.

Welker Leng, K. R., Castañeda, C. A., Decroos, C., Islam, B., Haider, S. M., Christianson, D. W. and Fierke, C. A. (2019) 'Phosphorylation of Histone Deacetylase 8: Structural and Mechanistic Analysis of the Phosphomimetic S39E Mutant', *Biochemistry*, 58(45), pp. 4480–4493.

Wezel, G. P. Van, Mahr, K., König, M., Traag, B. A., Pimentel-Schmitt, E. F., Willimek, A. and Titgemeyer, F. (2005) 'GlcP constitutes the major glucose uptake system of *Streptomyces coelicolor* A3(2)', *Molecular Microbiology*, 55(2), pp. 624–636.

Wezel, G. P. Van, Mahr, K., Nothaft, H., Thomae, A. W., Bibb, M. and Titgemeyer, F. (2007) 'A New Piece of an Old Jigsaw : Glucose Kinase Is Activated Posttranslationally in a Glucose Transport-Dependent Manner in *Streptomyces coelicolor* A3(2)', pp. 67–74.

WHO (2017) *Global priority list of antibiotic-resistant bacteria to guide research, discovery, and development of new antibiotics*.

Widdick, D. A., Hicks, M. G., Thompson, B. J., Tschumi, A., Chandra, G., Sutcliffe, I. C., Brülle, J. K., Sander, P., Palmer, T. and Hutchings, M. I. (2011) 'Dissecting the complete lipoprotein biogenesis pathway in *Streptomyces scabies*', *Molecular Microbiology*, 80(5), pp. 1395–1412.

Wyszynski, F. J., Hesketh, A. R., Bibb, M. J. and Davis, B. G. (2010) 'Dissecting tunicamycin biosynthesis by genome mining: Cloning and heterologous expression of a minimal gene cluster', *Chemical Science*, 1(5), pp. 581–589.

Xu, Z., Wang, Y., Chater, K. F., Ou, H. and Xu, H. H. (2017) 'Large-Scale Transposition Mutagenesis of *Streptomyces coelicolor* Identifies Hundreds of Genes Influencing Antibiotic Biosynthesis', *Appl. Environ. Microbiol.*, 83(6), pp. 1–16.

Xue-Mei, J., Chang, Y.-K., Lee, J. H. and Hong, S.-K. (2017) 'Effects of Increased NADPH Concentration by Metabolic Engineering of the Pentose Phosphate Pathway on Antibiotic Production and Sporulation in *Streptomyces lividans* TK24', *Journal of Microbiology and Biotechnology*, 27(10), pp. 1867–1876.

Yagüe, P., López-García, M. T., Rioseras, B., Sánchez, J. and Manteca, A. (2013) 'Pre-sporulation stages of *Streptomyces* differentiation: state-of-the-art and future perspectives.', *FEMS microbiology letters*, 342(2), pp. 79–88.

Yagüe, P., Rodríguez-García, A., López-García, M. T., Rioseras, B., Martín, J. F., Sánchez, J. and Manteca, A. (2014) 'Transcriptomic Analysis of Liquid Non-Sporulating *Streptomyces coelicolor* Cultures Demonstrates the Existence of a Complex Differentiation Comparable to That Occurring in Solid Sporulating Cultures', *PLOS ONE*, 9(1), p. e86296.

Yamanaka, R., Tabata, S., Shindo, Y., Hotta, K., Suzuki, K., Soga, T. and Oka, K. (2016) 'Mitochondrial Mg(2+) homeostasis decides cellular energy metabolism and vulnerability to stress', *Scientific reports*, 6, p. 30027.

Yan, H., Wang, Q., Teng, M. and Li, X. (2019) 'The DNA-binding mechanism of the TCS response regulator ArlR from *Staphylococcus aureus*', *Journal of Structural Biology*, 208(3), p. 107388.

Yeo, K. J., Han, Y.-H., Eo, Y. and Cheong, H.-K. (2013) 'Expression, purification, crystallization and preliminary X-ray analysis of the extracellular sensory domain of DraK histidine kinase from *Streptomyces coelicolor*', *Acta crystallographica. Section F, Structural biology and crystallization communications*, 69(Pt 8), pp. 909–911.

Yepes, A., Rico, S., Rodríguez-García, A., Santamaría, R. I. and Díaz, M. (2011) 'Novel

Two-component Systems Implied in Antibiotic Production in *Streptomyces coelicolor*', *PLoS ONE*, 6(5).

Yim, G., de la Cruz, F., Spiegelman, G. B. and Davies, J. (2006) 'Transcription modulation of *Salmonella enterica* serovar Typhimurium promoters by sub-MIC levels of rifampin', *Journal of bacteriology*, 188(22), pp. 7988–7991.

Yim, G., Huimi Wang, H. and Davies FRS, J. (2007) 'Antibiotics as signalling molecules', *Philosophical Transactions of the Royal Society B: Biological Sciences*, 362(1483), pp. 1195–1200.

Yu, Z., Zhu, H., Dang, F., Zhang, W., Qin, Z., Yang, S., Tan, H., Lu, Y. and Jiang, W. (2012) 'Differential regulation of antibiotic biosynthesis by DraR-K, a novel two-component system in *Streptomyces coelicolor*.', *Molecular microbiology*, 85(3), pp. 535–556.

Zahrt, T. C. and Deretic, V. (2000) 'An Essential Two-Component Signal Transduction System in *Mycobacterium tuberculosis*', *Journal of Bacteriology*, 182(13), pp. 3832–3838.

Zhang, P., Zhao, Z., Li, H., Chen, X.-L., Deng, Z., Bai, L. and Pang, X. (2015) 'Production of the antibiotic FR-008/candicidin in *Streptomyces* sp. FR-008 is co-regulated by two regulators, FscRI and FscRIV, from different transcription factor families.', *Microbiology (Reading, England)*, 161(Pt 3), pp. 539–52.

Zhang, P., Wu, L., Zhu, Y., Liu, M., Wang, Y., Cao, G., Chen, X.-L., Tao, M. and Pang, X. (2017) 'Deletion of MtrA Inhibits Cellular Development of *Streptomyces coelicolor* and Alters Expression of Developmental Regulatory Genes', *Frontiers in Microbiology*, 8, p. 2013.

Zhu, Y., Zhang, P., Zhang, J., Xu, W., Wang, X., Wu, L., Sheng, D., Ma, W., Cao, G., Chen, X., Lu, Y., Zhang, Y.-Z. and Pang, X. (2019) 'The developmental regulator MtrA binds GlnR boxes and represses nitrogen metabolism genes in *Streptomyces coelicolor*', *Molecular Microbiology*, 112(1), pp. 29–46.

Zhu, Y., Xu, W., Zhang, J., Zhang, P., Zhao, Z., Sheng, D., Ma, W., Zhang, Y.-Z., Bai, L. and Pang, X. (2020) 'A Hierarchical Network of Four Regulatory Genes Controlling Production of the Polyene Antibiotic Candicidin in *Streptomyces* sp. Strain FR-008', *Applied and Environmental Microbiology*. Edited by M. Julia Pettinari, 86(9), pp. e00055-20.

Zhu, Y., Zhang, P., Zhang, J., Wang, J., Lu, Y. and Pang, X. (2020) 'Impact on Multiple Antibiotic Pathways Reveals MtrA as a Master Regulator of Antibiotic Production in *Streptomyces* spp. and Potentially in Other Actinobacteria.', *Applied and environmental microbiology*, 86(20).

Zucko, J., Dunlap, W. C., Shick, J. M., Cullum, J., Cercelet, F., Amin, B., Hammen, L., Lau, T., Williams, J., Hranueli, D. and Long, P. F. (2010) 'Global genome analysis of the shikimic acid pathway reveals greater gene loss in host-associated than in free-living bacteria', *BMC genomics*, 11, p. 628.